Algerian Democratic And Popular Republic

Ministry Of Higher Education And Scientific Research

Echahid Hamma Lakhdar University - El Oued

FACULTY OF TECHNOLOGY

DEPARTMENT OF ELECTRICAL ENGINEERING

Domain: Science and Technology

Field: Electrical Engineering

2nd Year of Master's Degree Specialty: Electrical Networks

Course Material For Teaching The Subject

High Voltage Techniques

Dr. GUIA Talal

Associate Professor "A"

2024

Table Of Contents

Preface

This document is specifically designed for second -year Master 's students in Electrotechnics , specializing in electrical networks (Semester 5). It aims to provide comprehensive knowledge of high voltage techniques , addressing both the theoretical aspects and practical applications required in this field. The content will equip students with the necessary skills for understanding and managing high voltage systems , with a focus on insulation coordination, electric field control, and ionization phenomena.

This material will also serve as a valuable resource for professionals and engineers working in the electrical industry , particularly in the design , maintenance , and optimization of high voltage equipment and networks.

The texts presented in this document are inspired by various technical references and industry guides. Any feedback , suggestions , or constructive criticism for improving the material are highly encouraged and will be greatly appreciated.

Email: guia_talal@yahoo.fr
Email: talal-guia@univ-eloued.dz

Abstract

Abstract
This course provides second -year Master 's students in Electrotechnics , specializing in electrical networks, with an in-depth understanding of high voltage techniques . It covers both theoretical foundations and practical applications , equipping students with the skills needed to analyze, design, and maintain high voltage systems. Topics include insulation coordination, electric field control, and ionization phenomena , with a focus on real -world applications in electrical network optimization and equipment performance. This course also serves as a valuable resource for professionals working in the field of electrical engineering.

Keywords : High Voltage , Insulation Coordination , Electric Field , Ionization , Electrical Networks

Résumé
Ce cours offre aux étudiants de deuxième année de Master en Électrotechnique, spécialisés en réseaux électriques , une compréhension approfondie des techniques de haute tension. Il aborde les fondements théoriques ainsi que les applications pratiques , permettant aux étudiants d'acquérir les compétences nécessaires pour analyser, concevoir et maintenir des systèmes haute tension. Les sujets traités incluent la coordination de l'isolement, le contrôle des champs électriques et les phénomènes d'ionisation , avec un accent particulier sur les applications réelles pour l'optimisation des réseaux électriques et la performance des équipements. Ce cours constitue également une ressource précieuse pour les professionnels du domaine de l'ingénierie électrique.

Mots -clés : Haute Tension , Coordination d'Isolement , Champ Électrique , Ionisation, Réseaux Électriques

Chapter I:
INTRODUCTION

I.1 The Function Of High Voltage Technology

The primary objective of high voltage technology and engineering is to effectively manage elevated electric field strengths. These fields are not only present in equipment that operates or undergoes testing at high voltages, but can also be found in devices with relatively lower voltages and minimal insulation, such as thin capacitors with polymer film insulation. The key factor determining the "breakdown strength" of insulating materials is the electric field strength rather than the voltage itself. Despite this, the field is commonly referred to as "high voltage technology" and "high voltage engineering," which isn't entirely accurate. In essence, the role of high voltage engineering is to ensure that the electric stress, represented by the electric field strength (E), always remains substantially lower than the breakdown strength (E_d), even in all possible conditions.

"Stress"	E	<<	E_d	"Strength"
(Field strength)			(Electric strength)	

The principle of maintaining electric field strength below breakdown strength is simple to state but challenging to implement.

It's important to note that, in theory, the condition $E < E_d$ (where E_d represents breakdown strength) should be sufficient. However, since E_d cannot be precisely determined, it's necessary to apply a significant safety margin, ensuring $E \ll E_d$.

Another point to clarify is the interchangeable use of the terms "electric field intensity," "electric field strength," and "electric field stress." To avoid confusion with "electric strength," which refers to the breakdown strength of insulating materials, the term "electric field intensity" is preferable as it clearly indicates the strength of the field. Nonetheless, "electric field strength" or "electric field stress" are more commonly used in high voltage engineering.

As a result, it's crucial for the reader to consistently differentiate between the intensity or stress of an electric field and the breakdown strength, or dielectric strength, of a material.

I.2 Applications of High Voltage Technology

The primary use of high voltage technology is in equipment and systems designed for the transmission and distribution of electrical energy. In Germany, common rated voltages for three-phase AC systems include 12 kV, 24 kV, 123 kV, 245 kV, and 420 kV. Countries with vast distances between power plants and urban areas, such as North America, Asia, South America, Southern Africa, Eastern Europe, and Russia, often use even higher transmission voltages. For extreme transmission applications, particularly in China and India, voltages around 1 MV are employed. As three-phase high-voltage AC (HVAC) transmission approaches its technological and economic limits, high-voltage DC

(HVDC) transmission is becoming more viable, with voltages exceeding 1000 kV being utilized today.

High-voltage engineering must ensure that power apparatus and systems, such as generators, transformers, switchgear, cables, and transmission lines, are equipped with safe, reliable, and economical insulation systems.

High voltages are essential for power transmission due to the quadratic relationship between transmission line losses (P_L) and the current (I). These losses are expressed for a line-to-ground (phase) voltage (V_{Ph}) as:

$$P_L = 3\,R\,I^2 \qquad \text{and} \qquad S = 3\,V_{Ph}\,I$$

To minimize losses when transmitting large apparent power (S), the most effective strategy is to reduce the current (I) by increasing the voltage (V_{Ph}).

Economic and environmentally-friendly power transmission with minimal losses can only be achieved through the use of higher voltages. However, there are limits to increasing voltage due to the rising cost of insulation. It is often cost-effective to choose a rated voltage (in kV) close to the transmission distance (in km), especially for standard voltage levels. In urban areas, where high transmission power is required, voltages are significantly higher to reduce current and line losses to acceptable levels.

Other applications of high-voltage engineering extend into various technological fields, including:

- Telecommunications (for high-power transmitters),
- X-ray technology (for accelerating electrons using high voltages),
- Laser technology (where electric gas discharges are used to stimulate atoms).
- Medical engineering: for example, lithotripters, which use electro-acoustic shock waves to break down kidney stones.
- Research applications: particle beam acceleration through high-voltage generators.
- Production technology: used in processes like electrostatic lacquering, coating, material treatment, and high-speed shaping via shock waves.
- Electromagnetic compatibility testing: ensuring devices withstand high voltages.
- Lightning and over-voltage protection: safeguarding systems from electrical surges.
- Environmental protection: via electrostatic filters.
- Recycling technology: separating materials through electro-acoustic shock waves.
- Electroporation of biological cells: used for applications such as processing sugar beets, fruits, and wine.
- Electronic components: such as capacitors.
- Electronic tubes and copiers.
- Ignition devices: like spark plugs in motor vehicles.

I.3 Perspectives of High Voltage Engineering

High voltage technology is undeniably a vital component for ensuring reliable, cost-effective, and environmentally friendly power supply systems. In addition to being essential for numerous technological advancements, this field is constantly confronted with new challenges.

The role of high voltage technologies is critical in advancing power engineering, particularly in the integration of combined heat and power (CHP) systems and renewable energy sources. Strong transmission and distribution networks are required to meet these demands. The supply of wind and solar energy is highly variable, while the demand for heat and electricity often doesn't align, highlighting the need for robust grids.

Due to the limited storage options, compensating for energy fluctuations requires the use of peak power plants connected through high-voltage transmission networks.

High voltage engineering faces new challenges, particularly in efforts to reduce CO_2 emissions by harnessing global hydropower potential. Transmission distances of over 1000 km, along with high power requirements, are feasible only with high-voltage direct current (HVDC) technology.

Note: Another option is using solar energy from desert regions to produce hydrogen gas through electrolysis, transporting it via pipelines, and generating electricity again in fuel cells. However, this system has a much lower efficiency compared to an all-electrical system.

In general, high-temperature superconductivity offers potential for reducing current losses and transmission voltages, but it will not eliminate the need for high voltages in energy transmission. New high-voltage equipment will continue to be developed for both existing systems and new applications.

I.4 Overview

This course focuses on the challenges faced by high voltage engineers, with examples drawn from typical insulation systems in power engineering. To introduce the ideas, concepts, and methods of high voltage engineering, we will examine a wall bushing as an example of a common insulation system (see Figure 1-1). The primary function of a wall bushing is to allow a conductor carrying high voltage to pass through a grounded wall with minimal insulation-core diameter, ensuring that no electric discharges occur on the surfaces or electrodes. The conductor passes through the main insulation body, which includes conductive grading layers (such as an oil-impregnated paper core with metallic foils of varying lengths). The insulation core is housed in a casing made of outdoor porcelain, a flange, indoor porcelain, and screening toroids. Additional insulation material, like mineral oil, fills the gaps to form secondary insulation.

In the design process, the electric field strength must first be determined to assess the stress on the insulating materials. While simple analytical calculations and estimates may suffice for initial evaluations, complex insulation systems often require numerical

calculations for accurate results across various dielectric materials. Figure 1-1 illustrates the equipotential lines in 25% increments.

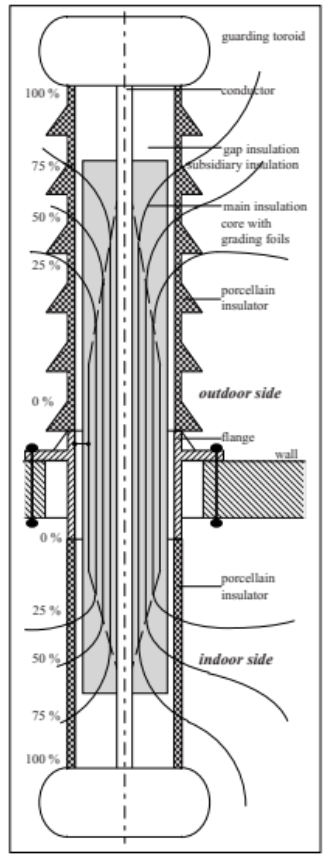

Figure I.1: Wall bushing, example for a typical insulation system in high voltage engineering (schematic).

Once the field strengths are calculated, they must be compared to the electric strengths of the insulating materials, which vary significantly. The lowest strength is typically provided by the ambient air (external strength), while the highest strength is required for the main insulation (internal strength). Particular care must be taken with the electric strengths of interfaces and contaminated surfaces, which can be improved using shed profiles.

If field strengths are too high or electric strengths are insufficient, the design will need to be modified and improved. This often involves an iterative optimization process. The most essential techniques for optimization include potential grading (through grading layers or insulation system geometries like lengths and diameters) and careful contouring of electrodes. Moreover, an appropriate selection of dielectric materials must be made, taking into account technological, economic, and environmental considerations. Factors such as manufacturing quality control and testing also play a significant role.

After production, the quality of a high voltage product is confirmed through high voltage tests, typically involving AC, impulse, and DC voltages. These test and measurement techniques, must meet stringent requirements as per ISO 9000 standards and other international regulations.

Additionally, as operating times for high voltage apparatus often exceed nominal lifetimes, diagnostic methods are crucial for assessing the condition of aging or defective equipment. This makes onsite testing and continuous monitoring (or "online monitoring") of power apparatus increasingly important, alongside laboratory testing. Making decisions about reinvestment, including estimating the remaining lifetime of equipment, is key to maintaining cost-effective and reliable energy systems.

Note: In the context of high voltage engineering, "insulation" refers to the collection of dielectric materials and components that make up a technical system to ensure galvanic separation of electrically conductive parts. While the term "isolation" is sometimes used interchangeably, it generally refers to separation properties or functions in a broader sense. "Insulation" specifically pertains to dielectric materials, components, and systems.

Chapter II:

INSULATION COORDINATION

II.1 Introduction

The term Insulation Co-ordination was originally introduced to arrange the insulation levels of the several components in the transmission system in such a manner that an insulation failure, if it did occur, would be confined to the place on the system where it would result in the least damage, be the least expensive to repair, and cause the least disturbance to the continuity of the supply. The present usage of the term is broader. Insulation co-ordination now comprises the selection of the electric strength of equipment in relation to the voltages which can appear on the system for which the equipment is intended. The overall aim is to reduce to an economically and operationally acceptable level the cost and disturbance caused by insulation failure and resulting system outages.

To keep interruptions to a minimum, the insulation of the various parts of the system must be so graded that flashovers only occur at intended points. With increasing system voltage, the need to reduce the amount of insulation in the system, by proper co-ordination of the insulating levels become more critical.

II.2 Terminology

Nominal System Voltage: It is the r.m.s. phase-to-phase voltage by which a system is designated

Maximum System Voltage: It is the maximum rise of the r.m.s. phase-to-phase system voltage

For the nominal system voltages used in Sri Lanka, the international maximum system voltages are shown in table II.1.

Nominal System Voltage (kV)	11	33	66	132	220
Maximum System Voltage (kV)	12	36	72.5	145	245

Table II.1

Factor of Earthing: This is the ratio of the highest r.m.s. phase-to-earth power frequency voltage on a sound phase during an earth fault to the r.m.s. phase-to-phase power frequency voltage which would be obtained at the selected location without the fault.

This ratio characterises, in general terms, the earthing conditions of a system as viewed from the selected fault location.

Effectively Earthed System : A system is said to be effectively earthed if the factor of earthing does not exceed 80%, and non-effectively earthed if it does.

[Note: Factor of earthing is 100% for an isolated neutral system, while it is 57.7% (corresponding to $1/\sqrt{3}$) for a solidly earthed system. In practice, the effectively earthed condition is obtained when the ratio $x_0/x_1 < 3$ and the ratio $r_0/x_1 < 1$.

Insulation Level: For equipment rated at less than 300 kV, it is a statement of the Lightning impulse withstand voltage and the short duration power frequency withstand voltage.

For equipment rated at greater than 300 kV, it is a statement of the Switching impulse withstand voltage and the power frequency withstand voltage.

Conventional Impulse Withstand Voltages: This is the peak value of the switching or lightning impulse test voltage at which an insulation shall not show any disruptive discharge when subjected to a specified number of applications of this impulse under specified conditions.

Conventional Maximum Impulse Voltage: This is the peak value of the switching or lightning overvoltage which is adopted as the maximum overvoltage in the conventional procedure of insulation co-ordination.

Statistical Impulse Withstand Voltage: This is the peak value of a switching or lightning impulse test voltage at which insulation exhibits, under the specified conditions, a 90% probability of withstand. In practice, there is no 100% probability of withstand voltage. Thus the value chosen is that which has a 10% probability of breakdown.

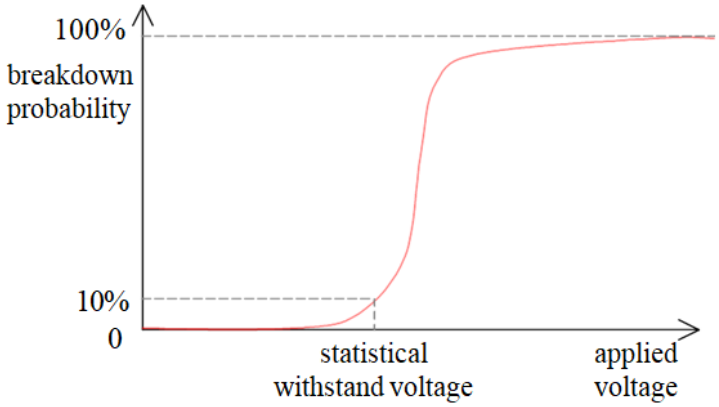

Figure II.1 - Statistical Impulse Withstand Voltage

Statistical Impulse Voltage: This is the switching or lightning overvoltage applied to equipment as a result of an event of one specific type on the system (line energizing, reclosing, fault occurrence, lightning discharge, etc), the peak value of which has a 2% probability of being exceeded.

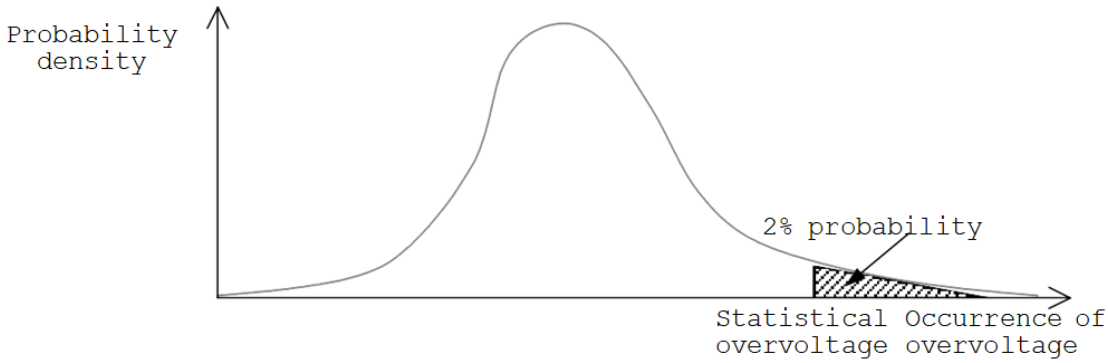

Figure II.2 - Statistical Impulse Voltage

Rated Short Duration Power Frequency Withstand Voltage: This is the prescribed r.m.s. value of sinusoidal power frequency voltage that the equipment shall withstand during tests made under specified conditions and for a specific time, usually not exceeding one minute.

Protective Level of Protective Device: These are the highest peak voltage value which should not be exceeded at the terminals of a protective device when switching impulses and lightning impulses of standard

shape and rate values are applied under specific conditions.

II.3 Conventional method of insulation coordination

In order to avoid insulation failure, the insulation level of different types of equipment connected to the system has to be higher than the magnitude of transient over-voltages that appear on the system. The magnitude of transient over-voltages are usually limited to a protective level by protective devices. Thus the insulation level has to be above the protective level by a safe margin. Normally the impulse insulation level is established at a value 15-25% above the protective level.

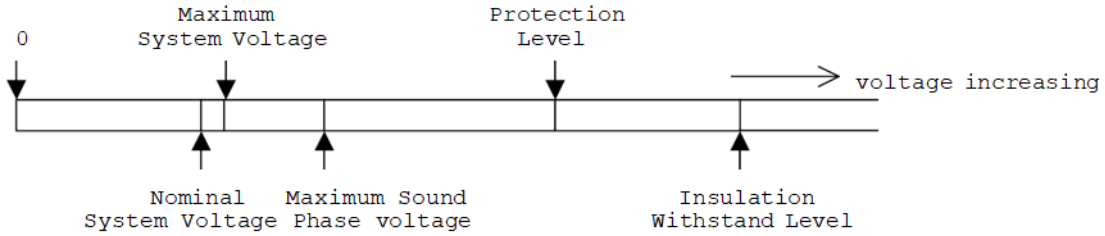

Figure II.3 Different level of insulation coordination

Consider the typical coordination of a 132 kV transmission line between the transformer insulation, a line gap (across an insulator string) and a coordinating gap (across the transformer bushing).

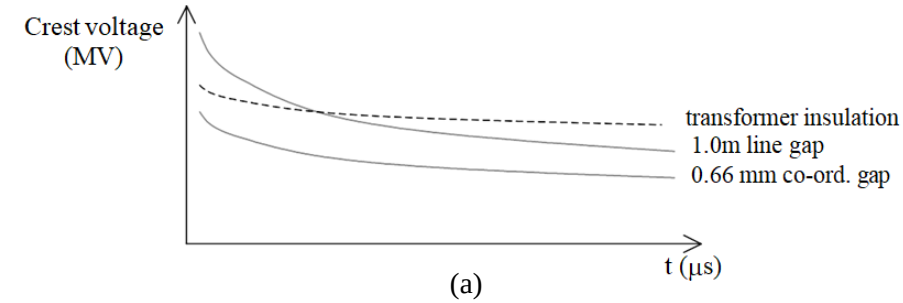

(a)

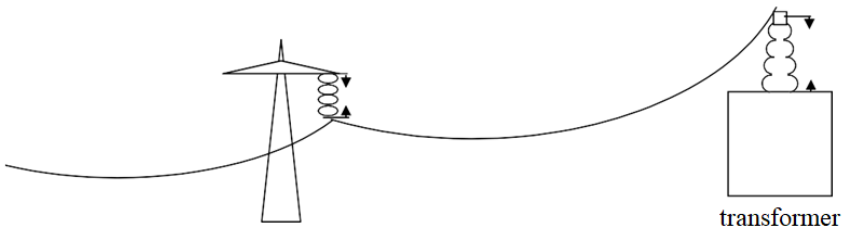

(b)

Figure II.4 - Coordination using gaps

Note: In a rural distribution transformer, a lightning arrester may not be used on account of the high cost and a coordinating gap mounted on the transformer bushing may be the main surge limiting device.

In coordinating the system under consideration, we have to ensure that the equipment used are protected, and that inadvertent interruptions are kept to a minimum. The coordinating gap must be chosen so as to provide protection of the transformer under all conditions. However, the line gaps protecting the line

insulation can be set to a higher characteristic to reduce unnecessary interruptions.

For the higher system voltages, the simple approach used above is inadequate. Also, economic considerations dictate that insulation co-ordination be placed on a more scientific basis.

II.4 Statistical Method of Insulation Coordination

At the higher transmission voltages, the length of insulator strings and the clearances in air do not increase linearly with voltage but approximately to $V^{1.6}$ The required number of suspension units for different overvoltage factors is shown.

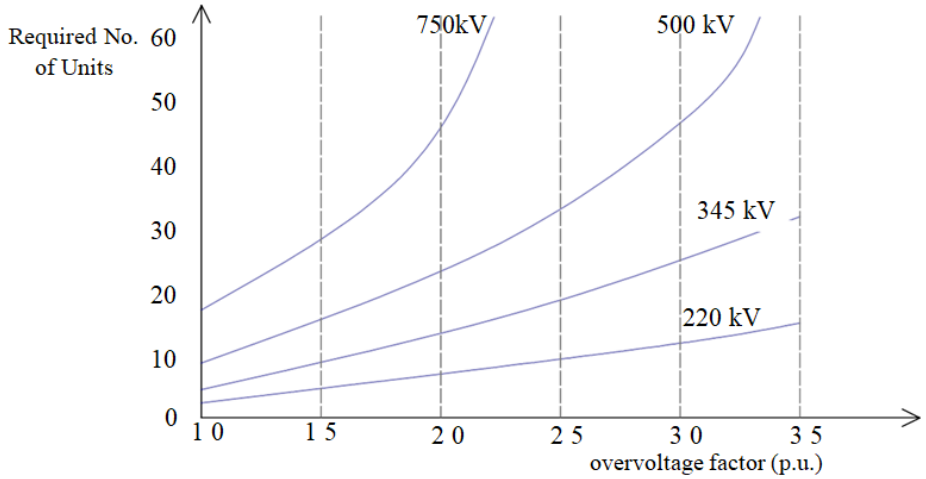

Figure II.6 - Requirement of number of units for different voltages

It is seen that the increase in the number of disc units is only slight for the 220 kV system, with the increase in the overvoltage factor from 2.0 to 3.5, but that there is a rapid increase in the 750 kV system. Thus, while it may be economically feasible to protect the lower voltage lines up to an overvoltage factor of 3.5 (say), it is definitely not economically feasible to have an overvoltage factor of more than about 2.0 or 2.5 on the higher voltage lines. In the higher voltage systems, it is the switching over-voltages that is predominant. However, these may be controlled by proper design of switching devices.

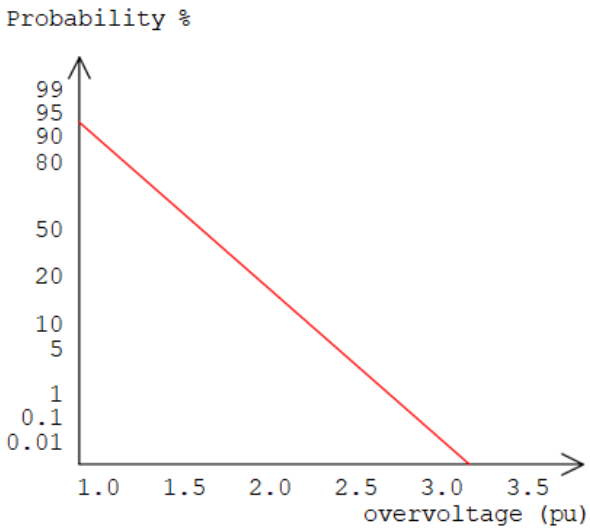

Figure II.6 Probability of overvoltage exceeding abscissae

In a statistical study, what has to be known is not the highest overvoltage possible, but the statistical distribution of over-voltages. The switching overvoltage probability in typical line is shown. It is seen that probability of overvoltage decreases very rapidly. Thus it is not economic to provide insulation above a certain overvoltage value. In practice, the overvoltage distribution characteristic is modified by the use of switching resistors which damp out the switching over-voltages or by the use of surge diverters set to operate on the higher switching over-voltages. In such cases, the failure probability would be extremely low.

II.4.1 Evaluation of Risk Factor

The aim of statistical methods is to quantify the risk of failure of insulation through numerical analysis of the statistical nature of the overvoltage magnitudes and of electrical withstand strength of insulation.

The risk of failure of the insulation is dependant on the integral of the product of the overvoltage density function $f_0(V)$ and the probability of insulation failure P(V). Thus the risk of flashover per switching operation is equal to the area under the curve $f_0(V) * P(V) * dV$.

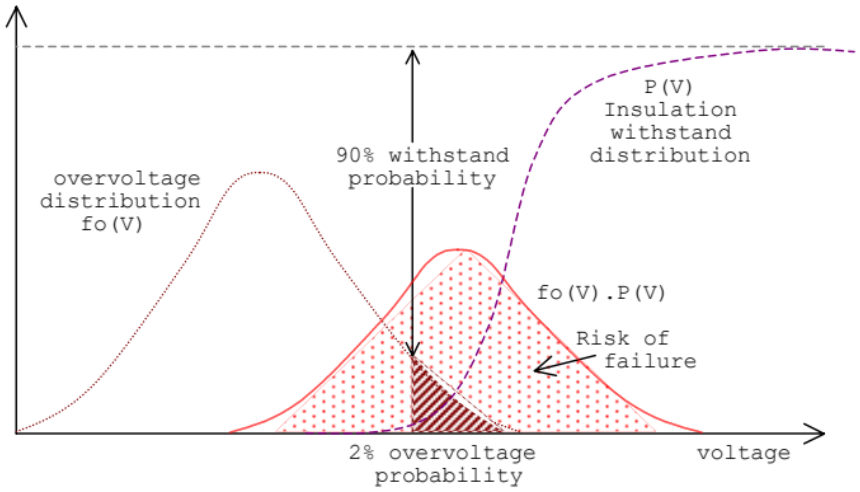

Figure II.7 - Evaluation of risk factor

Since we cannot find suitable insulation such that the withstand distribution does not overlap with the overvoltage distribution, in the statistical method of analysis, the insulation is selected such that the 2% overvoltage probability coincides with the 90% withstand probability as shown.

II.5 Length of Overhead Shielding Wire

For reasons of economics, the same degree of protection is not provided throughout a transmission line. Generally, it is found sufficient to provide complete protection against direct strikes only on a short length of line prior to the substation. This can be calculated as follows.

Consider a surge **e** approaching the terminal equipment. When the surge magnitude exceeds the critical voltage $\mathbf{e_0}$, corona would occur, distorting the surge wavefront, as it travels. The minimum length of earth wire should be chosen such that in traversing that length, all voltage above the maximum surge that can arrive att the terminal has been distorted by corona. [The maximum permissible surge corresponds to the incident voltage that would cause insulation failure at the terminal equipment.]

II.5.1 Modification of Waveshape by Corona

When a surge voltage wave travelling on an overhead line causes an electric field around it exceeding the critical stress of air, corona will be formed. This corona formation obviously extracts the energy required from the surge. Since the power associated with corona increases as the square of the excess voltage, the attenuation of the waveform will not be uniform so that the waveform gets distorted. Further, corona increases the effective radius of the conductor giving rise to a greater capacitance for the outer layers. Since the line inductance remains virtually a constant, the surge associated with the outer layers of corona would have a lower wave velocity than in the conductor itself. These effects in practice give rise to a wavefront distortion and not a wavetail distortion, as shown in figure II.8.

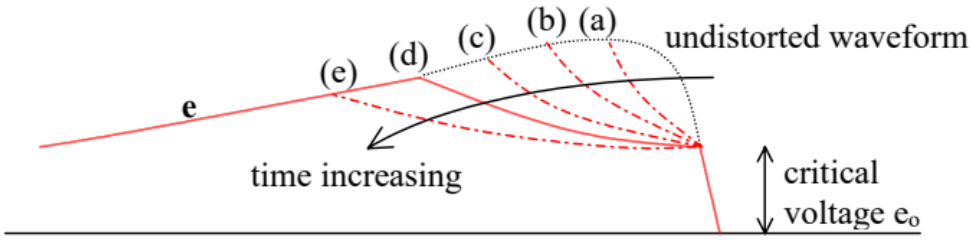

Figure II.8 - Modification of waveshape due to corona

Corona thus reduces the steepness of the wavefront above the critical voltage, as the surge travels down the line. This means that energy is lost to the atmosphere.

Now consider the mathematical derivation.

Energy associated with a surge waveform $= \frac{1}{2}Ce^2 + \frac{1}{2}\ L\ i^2$

But the surge voltage e is related to the surge current i by the equation

$$i = \frac{e}{Z_0} = e\sqrt{\frac{C}{L}}, \text{ i.e. } \frac{l}{2}Li^2 = \frac{l}{2}Ce^2$$

So that the total wave energy $= Ce^2$

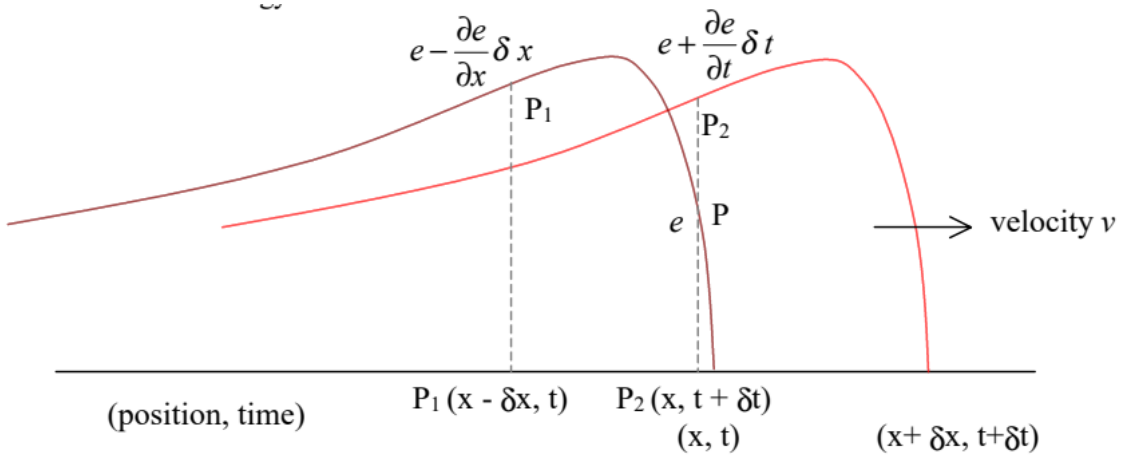

Figure II.9 - Propagation of Surge

Consider the figure II.9. Let the voltage at a point P at position **x** be **e** at time **t**.

Then voltage at point P_1 just behind P would be $e - \frac{\partial e}{\partial x}$ at time t, or $e - \frac{\partial e}{\partial x} v\, \delta t$.

If the voltage is above corona inception, it would not remain at this value but would attain a value $e + \frac{\partial e}{\partial t}\, \delta t$ at P at time t+Δt , when the surge at P_1 moves forward to P_2.

Note : $\frac{\partial e}{\partial x}\ \frac{\partial e}{\partial t}$ would in fact be negative quantities on the wavefront.

Thus corona causes a depression in the voltage from $e - v\frac{\partial e}{\partial x}\, \delta t$ to $e + \frac{\partial e}{\partial t}\, \delta t$, with a corresponding loss of energy of $C\left[\left(e - v\frac{\partial e}{\partial x}\delta t\right)^2 - \left(e + \frac{\partial e}{\partial t}\delta t\right)^2\right]$ or $-2Ce\left[v\frac{\partial e}{\partial x} + \frac{\partial e}{\partial t}\right]\delta t$.

The energy to create a corona field is proportional to the square of the excess voltage. i.e. $k(e - e_0)^2$.

Thus the energy requiredto change the voltage from e to $e + \frac{\partial e}{\partial t}\, \delta t$ is given by

$$k\left[\left(e + \frac{\partial e}{\partial t}\delta t - e_0\right)^2 - (e - e_0)^2\right] \text{ or } 2k(e - e_0)\frac{\partial e}{\partial t}\delta t$$

The loss of energy causing distortion must be equal to the change in energy required. Thus

$$-2Ce\left[v\frac{\partial e}{\partial x} + \frac{\partial e}{\partial t}\right]\delta t = 2k(e - e_0)\frac{\partial e}{\partial t}\cdot \delta t$$

Rearranging and simplifying gives the equation

$$v\frac{\partial e}{\partial x} = -\left[1 + \frac{k}{C}\cdot\frac{(e - e_0)}{e}\right]\frac{\partial e}{\partial t}$$

Wave propagation under ideal conditions is written in the form

$$v\frac{\partial e}{\partial x} = -\frac{\partial e}{\partial t}$$

Thus we see that the wave velocity has decreased below the normal propagation velocity, and that the wave velocity of an increment of voltage at **e** has a magnitude given by

$$v_e = \frac{v}{1 + \frac{k}{c}\left(\frac{e - e_0}{e}\right)}$$

Thus the time of travel for an element at e when it travels a distance x is given by

$$t = \frac{x}{v_e} = \frac{x}{v}\left[1 + \frac{k}{C}\left[\frac{e - e_o}{e}\right]\right]$$

$$\text{i.e. } \left[\frac{x}{v_e} - \frac{x}{v}\right] = \frac{x}{v}\cdot\frac{k}{C}\left[\frac{e - e_o}{e}\right]$$

$\left(\frac{x}{v_e} - \frac{x}{v}\right)$ is the time lag Δt corresponding to the voltage element at e. Thus

$$\frac{\Delta t}{x} = \frac{k}{v.C}\left[1 - \frac{e_0}{e}\right]$$

Example II.1

A transformer has an impulse insulation level of 1050 kV and is to be operated with an insulation margin of **15**% under lightning impulse conditions. The transformer has a surge impedance of 1600 S and is connected to a transmission line having a surge impedance of 400 S . A short length of overhead earth wire is to be used for shielding the line near the transformer from direct strikes. Beyond the shielded length, direct strokes on the phase conductor can give rise to voltage waves of the form $\mathbf{1000e^{-0.05t}kV}$ (where t is expressed in μs).

If the corona distortion in the line is represented by the expression $\frac{\Delta t}{x} = \frac{1}{B}\left[1 - \frac{e_0}{e}\right] \boldsymbol{\mu s/m}$, where B=110m/μs and $\mathbf{e_0 = 200kV}$, determine the minimum length of shielding wire necessary in order that the transformer insulation will not fail due to lightning surges.

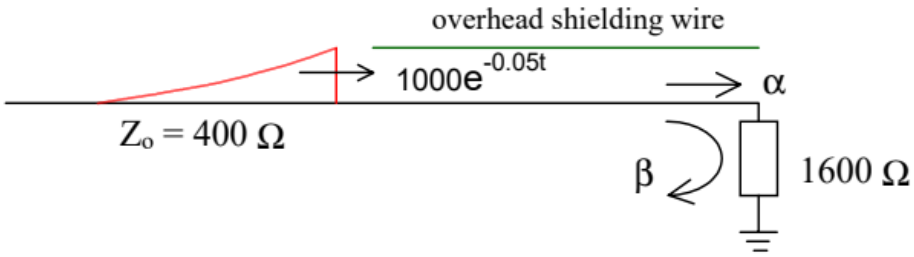

Transmission coefficient $\boldsymbol{\alpha} = \frac{2\times1600}{1600+400} = \mathbf{1.6}$

For a B.I.L of 1050 kV, and an insulation margin of 15%,

Maximum permissible voltage = 1050 x 85/100 = 892.5 kV.

Since the voltage is increased by the transmission coefficient 1.6 at the terminal equipment, the maximum permissible incident voltage must be decreased by this factor.

Thus maximum permissible incident surge = 892.5/ 1.6 = 557.8 kV

Thus for the transformer insulation to be protected by the shielding wire, the distortion caused must reduce the surge to a magnitude of 557.8 kV.

Therefore, $1000e_1^{-0.05t} = 557.8$. This gives the delay time $t_1 = \Delta t = 11.6$ μs.

Substitution in the equation gives 11.67/x = 1/100 . (1 - 200/557.8)

Solution gives x = 2002 m = 2.0 km.

Thus the minimum length of shielding wire required is 2 km.

II.6 Surge Protection

An overhead earth wire provides considerable protection against direct strikes. They also reduce induced overvoltages. However, they do not provide protection against surges that may still reach the terminal equipment. Such protection may either be done by diverting the major part of the energy of the surge to earth (surge diverters), or by modifying the waveform to make it less harmful (surge modifiers). The insertion of a

short length of cable between an overhead line and a terminal equipment is the commonest form of surge modifier.

II.6.1 Spark gaps for surge protection

The simplest and cheapest form of protection is the spark gap. The selected gap spacing should no only be capable of withstanding the highest normal power frequency voltage but should flash-over when overvoltages occur, protecting the equipment.

However, this is not always possible due to the voltage-time characteristics gaps and equipment having different shapes. Also, once a gap flashes over under a surge voltage, the ionised gap allows a power frequency follow through current, leading to a system outage. Thus rod gaps are generally used as a form of back up protection rather than the main form of protection.

Typical values of gap settings for transmission and distribution voltages are as in the following table II.2.

Nominal System Voltage (kV)	66	132	275	400
Gap setting (mm)	380	660	1240	1650

Table II.2

One of the most extensively used protective spark gaps in distribution systems is the **duplex** rod gap, which makes use of 2 rod gaps in series. Typical settings for these gaps are as given in the table.

Nominal System Voltage (kV)	11	33
Gap setting (mm)	2 x 31	2 x 63

Table II.3

When spark over occurs across a simple rod gap, the voltage suddenly collapses giving rise to a chopped wave. This chopped wave may sometimes be more onerous to a transformer than the original wave itself.

Expulsion Tube Lightning Arrestor

An expulsion tube arrestor consists essentially of a spark gap arranged in a fibre tube, and another series external rod gap. A typical arrangement for a 33 kV expulsion tube, with the external gap of the order of 50 mm and the internal gap of about 180 mm is shown in figure II.10.

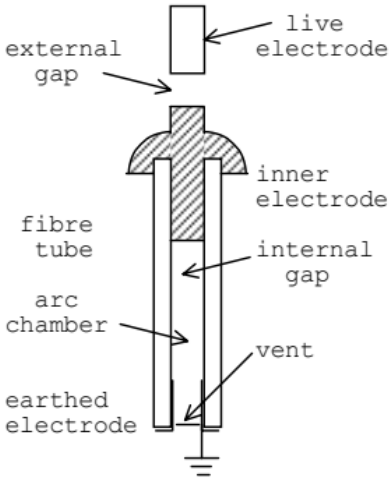

Figure II.10 - Expulsion Tube

The purpose of the external gap is to isolate the fibre tube from normal voltages thus preventing unnecessary deterioration. When an overvoltage occurs, spark over takes place between the electrodes and the follow current arc is constrained within the small volume of the tube. The high temperature of the arc rapidly vaporises the organic materials of the wall of the tube and causes a high gas pressure (up to 7000 p.s.i.) to be built up. The high pressure and the turbulence of the gas extinguishes the arc at a natural current zero, and the hot gasses are expelled through the vent in the earthed electrode. The power frequency follow current is interrupted within one or two half cycles so that protective relays would not operate causing unnecessary interruptions.

The expulsion gaps, which are comparatively cheap, are suitable for the protection of transmission line insulators and for the protection of rural distribution transformers, where other arrestors may be too expensive and rod gaps inadequate. However, they are unsuitable for the protection of expensive terminal equipment on account of their poor voltage-time characteristics.

II.6.2 Surge Diverters

Surge diverters (or lightning arrestors) generally consist of one or more spark gaps in series, together with one or more non-linear resistors in series. Silicon Carbide (SiC) was the material most often used in these non-linear resistor surge diverters. However, Zinc Oxide (ZnO) is being used in most modern day surge diverters on account of its superior volt-ampere characteristic. In fact the ZnO arrestor is often used gapless, as its normal follow current is negligibly small. The volt-ampere characteristics of SiC and of ZnO non-linear elements are shown for comparison with that of a linear resistor in figure II.11.

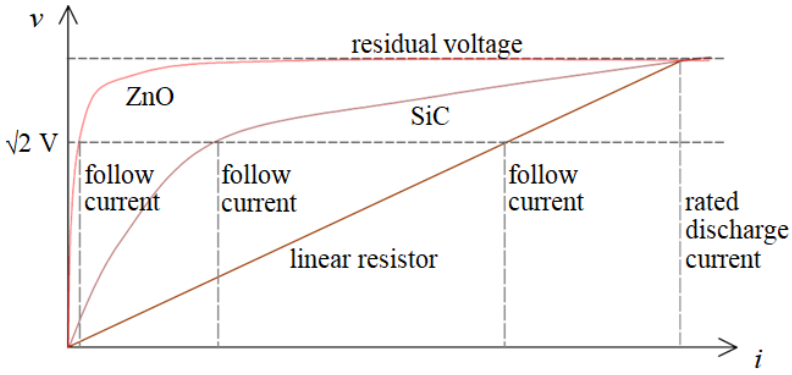

Figure II.11 - Volt-Ampere characteristics of non-linear elements

It is seen that while a large current is drawn under overvoltage condition in all three cases, the follow current is fairly large in the linear resistor, small in the SiC resistor, and negligibly small in the ZnO resistor. Their characteristics may be mathematically expressed as follows.

$v = k_1 i$ for a linear resistor

$v = k_2 i^{0.2}$ for a Silicon Carbide resistor

$v = k_3 i^{0.03}$ for a Zinc Oxide resistor

If the current were to increase a 100 times, the corresponding increase in voltage would be 100 times for the linear resistor, 2.5 times for the SiC resistor, but only 1.15 times for the ZnO resistor. This means that for the same residual voltage and the same discharge current, the follow current would be (in the absence of a series gap) of the **kA** for a linear resistor, **A** for a SiC resistor and just **mA** for a ZnO resistor.

When a series spark gap is required for eliminating the follow current, it is preferable to have a number of small spark gaps in series rather than having a single spark gap having an equivalent breakdown spacing. This is because the rate of rise of the recovery strength of a number of series gaps is faster than that of the single gap. However, when spark gaps are connected in series, it is difficult to ensure an even voltage distribution among them due to leakage paths (Figure II.11)

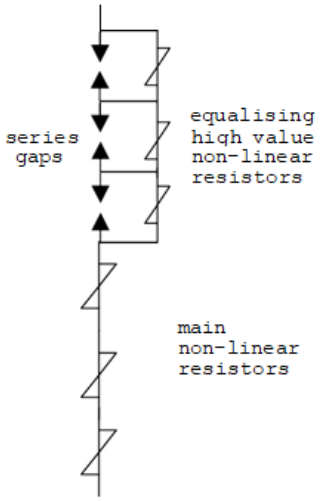

Figure II.11 - Non-linear Arrestor

The problem is generally overcome by having high equal resistances shunting the series gaps, ensuring a uniform distribution.

When a surge appears at a surge diverter terminal, within a short time the breakdown voltage of the series gap is reached, and the arrestor discharges. Unlike in the rod gap, the voltage does not collapse to zero instantly due to the voltage across the non-linear resistor. When the surge voltage increases, there is a corresponding but rapid decrease of the resistance discharging the surge energy to earth. Once the surge passes through, the power frequency voltage remaining is insufficient to maintain a sufficient current for the arc to continue. Thus the arcs extinguish and the gaps reseal. In the case of the ZnO arrestor, due to the negligible continuous power frequency current even in the absence of a series gap, the series gap is sometimes eliminated simplifying construction.

II.6.3 Selection of Surge Diverters

Surge diverters for a particular purpose are selected as follows.

(a) Rated Voltage

The designated maximum permissible r.m.s. value of power frequency voltage between line and earth terminals.

This is generally selected corresponding to 80% of the system phase-to-phase voltage for effectively earthed systems and corresponding to 100% of the system phase-to-phase voltage for non-effectively earthed systems. **Note**: A surge diverter of a higher rating may sometimes have to be chosen if some of the other required criteria are not satisfied by this diverter].

(b) Discharge Current

The surge current that flows through the surge diverter after spark over.

Nominal discharge current: This is the discharge current having a designated crest value and waveshape, which is used to classify a surge diverter with respect to durability and protective characteristics.

The standard waveform for the discharge current is taken as 8/20 μs).

The nominal value of discharge current is selected from the standard values 10 kA (station type), 5 kA (intermediate line type), 2.5 kA (distribution type) and 1.5 kA (secondary type), depending on the application. The highest ratings are used for the protection of major power stations, while the lowest ratings are used in rural distribution systems. The above nominal discharge currents are chosen based on statistical investigations which have shown that surge diverter currents at the station has the following characteristic.

99 % of discharge currents are less than 10 kA
95 % of discharge currents are less than 5 kA
90 % of discharge currents are less than 3 kA
70 % of discharge currents are less than 1 kA
50% of discharge currents are less than 0.5 kA

(c) Discharge Voltage (or Residual voltage)

The Discharge voltage is the voltage that appears between the line and earth terminals of the surge diverter during the passage of discharge currents.

The discharge voltage of the selected arrestor should be below the BIL of the protected equipment by a suitable margin (generally selected between 15% and 25%).

The discharge voltage of an arrestor at nominal discharge current is not a constant, but also depends on the rate of rise of the current and the waveshape. Typically, an increase of the rate of rise from 1 kA/μs to 5 kA/μs would increase the discharge voltage by only about 35 %.

The dependence of the discharge voltage on the discharge current is also small. Typically, an increase of discharge current from 5 kA to 10 kA would increase the discharge voltage by about 15% for Silicon Carbide arrestors and by about 2% for Zinc Oxide arrestors. {The discharge voltage is more often referred to as the residual discharge voltage].Power frequency spark over voltage

The power frequency spark over voltage is the r.m.s. value of the lowest power frequency voltage, applied between the line and earth terminals of a surge diverter, which causes spark-over of all the series gaps.

The power frequency spark over voltage should generally be greater than about 1.5 times the rated voltage of the arrestor, to prevent unnecessary sparkover during normal switching operations.

(d) Impulse spark over voltage

The impulse spark over voltage is the highest value of voltage attained during an impulse of a given waveshape and polarity, applied between the line and earth terminals of a surge diverter prior to the flow of discharge

current.

The impulse spark over voltage is not a constant but is dependant on the duration of application. Thus it is common to define a wavefront impulse sparkover voltage in addition to the impulse spark-over voltage.

Arrestor Rating kV rms	Minimum Power frequency withstand	Maximum Impulse Spark-over voltage (1.2/50 μs) kV crest	Maximum Residual Voltage kV crest	Maximum Wavefront Sparkover Voltage kV crest
36	1.5 times rated voltage	130	133	150
50		180	184	207
60		216	221	250
75		270	276	310

Table II.4

Good designs aim to keep (i) the peak discharge residual voltage, (ii) the maximum impulse sparkover voltage and (iii) the maximum wavefront impulse sparkover voltage reasonably close to each other. Table II.4 gives a typical comparison.

Example II.2

A lightning arrestor is required to protect a 5 MVA, 66/11 kV transformer which is effectively earthed in the system. The transformer is connected to a 66 kV, 3 phase system which has a BIL of 350 kV. Select a suitable lightning arrestor.

For 66 kV, maximum value of system rms voltage = 72.5 kV Therefore, voltage rating for effectively earthed system = 72.5 x 0.8 = 58 kV

The selected voltage rating is usually higher by a margin of about 5%.

Selected voltage rating = 1.05 x 58 = 60.9 = 60 kV

Protective level of selected arrestor (highest of 216, 221 and 250 from table) = 250 kV

Margin of protection (crest value) = 350 - 250 = 100 kV

Which is more than the required margin of 15 to 25%.

= 100/250 x 100 % = 40%

Check the power frequency breakdown voltage.

Power frequency breakdown voltage of arrestor = 60 x 15 = 90 kV

Assuming the dynamic power frequency overvoltage to be limited to 25% above maximum voltage at arrestor location,

Dynamic phase-to-neutral voltage = 1.25 x 72.5 x 0.8 = 72.5 kV

This voltage is less than the withstand voltage of the arrestor. In fact the factor of 1.5 automatically ensures that this requirement is satisfied.

Thus the chosen arrestor is satisfactory.

II.6.4 Separation limit for lightning arrestors

Best protection is obtained for terminal equipment by placing the arrestor as near as possible to that equipment. However, it is not feasible to locate an arrestor adjacent to each piece of equipment. Thus it is usually located adjacent to the transformer. However, where the BIL of the transformer permits, the arrestor may be located at a distance from the transformer to include other substation equipment within the protected zone. Thus it may be worthwhile installing them on the busbars themselves when permissible.

When arrestors must be separated from the protected equipment, additional voltage components are introduced, which add instant by instant to the discharge voltage. The maximum voltage at the terminal of a line as a result of the first reflection of a travelling wave may be expressed mathematically as

$$E_t = E_a + \beta \frac{de}{dt} x \frac{2l}{300}$$

up to a maximum of $2\ \beta\ E_a$. The factor 2 arises from the return length from arrestor to transformer, and the factor 300 is based on a travelling wave velocity of 300 m/μs in the overhead line. l is the separation between the arrestor and the transformer location, β the reflection coefficient at the transformer location, E_a is the discharge voltage at the arrestor, and de/dt is the rate of rise of the wavefront. When the value of β is not known, it may generally be assumed as equal to 1 without much loss of accuracy. Figure II.13 shows how the voltage at the terminal increases with separation for typical rates of rise.

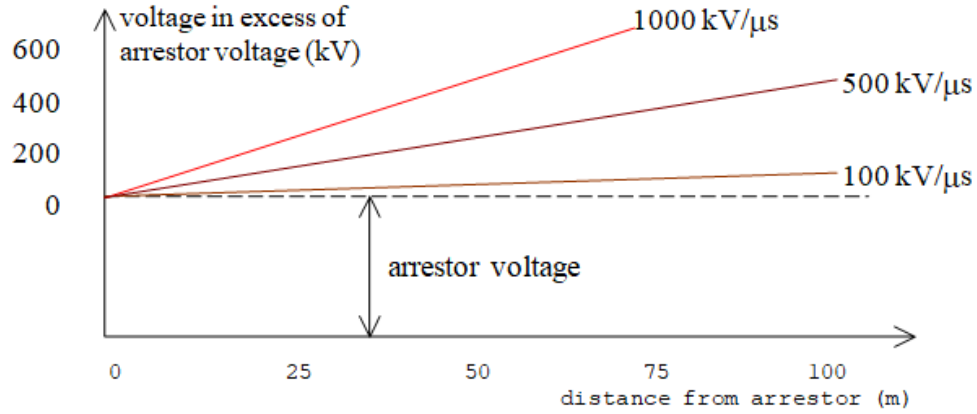

Figure II.13 - Lightning arrestor separation

Example II.3

A 500 kV steep fronted wave (rate of rise 1000 kV/μs) reaches a transformer of surge impedance 1600 Ω through a line of surge impedance 400 Ω and protected by a lightning arrestor with a protective spark-over level of 650 kV, 90 m from the transformer. Sketch the voltage waveforms at the arrestor location and at the transformer location. Sketch also the waveforms if the separation is reduced to 30 m.

If the separation is 90 m, travel time of line τ = 90/300 = 0.3 μs

Transmission coefficient $\alpha = \frac{2\ 1600}{1600+400} = 1.6$

Reflection coefficient β = 1.6 - 1 = 0.6

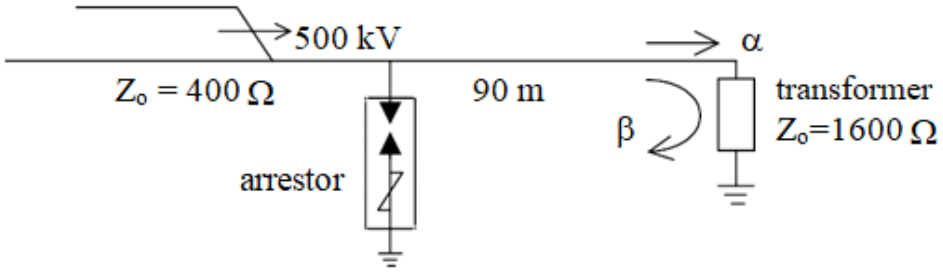

The voltage waveforms at the arrestor location and at the transformer location can be sketched as follows.

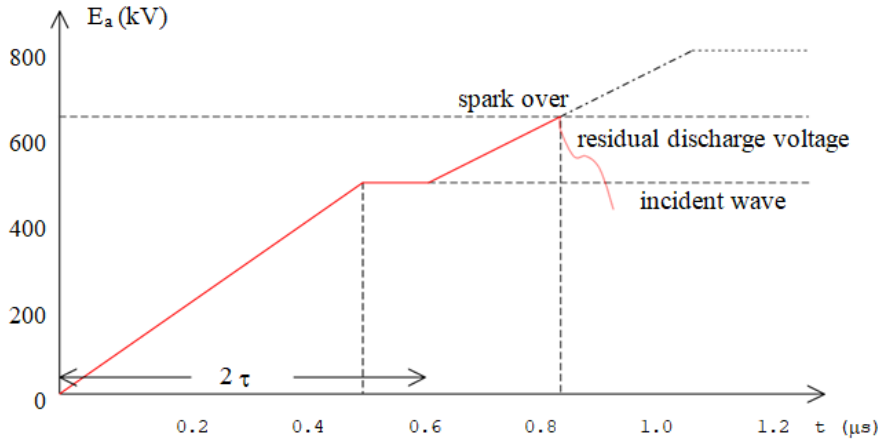

(a)

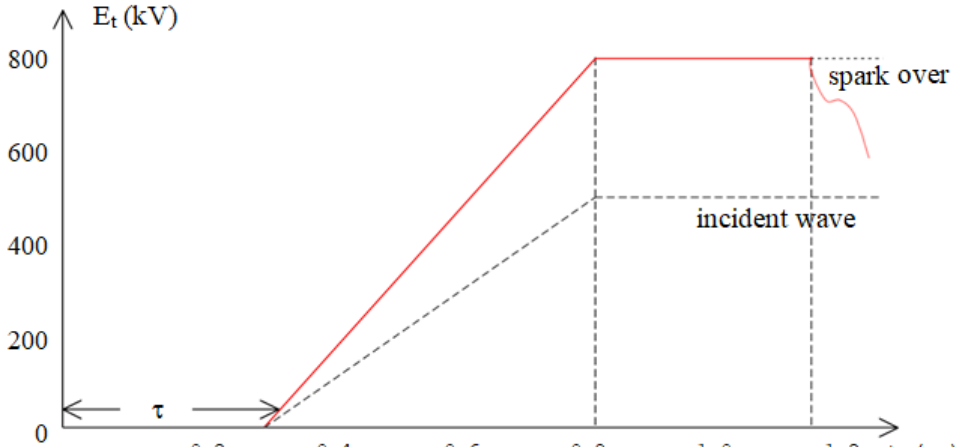

(b)

Figure II.14 Voltage waveforms at the arrestor location and at the transformer location

If the separation is 30 m, travel time of line τ = 30/300 = 0.1 :s

In this case the voltage waveforms at the arrestor and the transformer location are as follows.

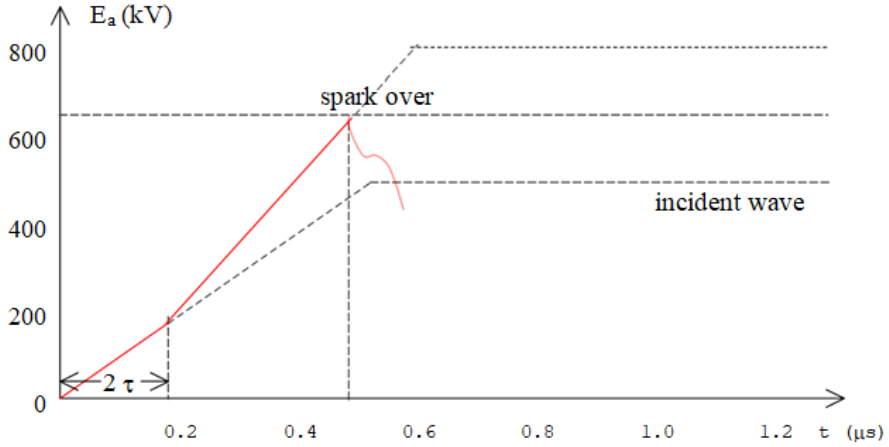

(c)

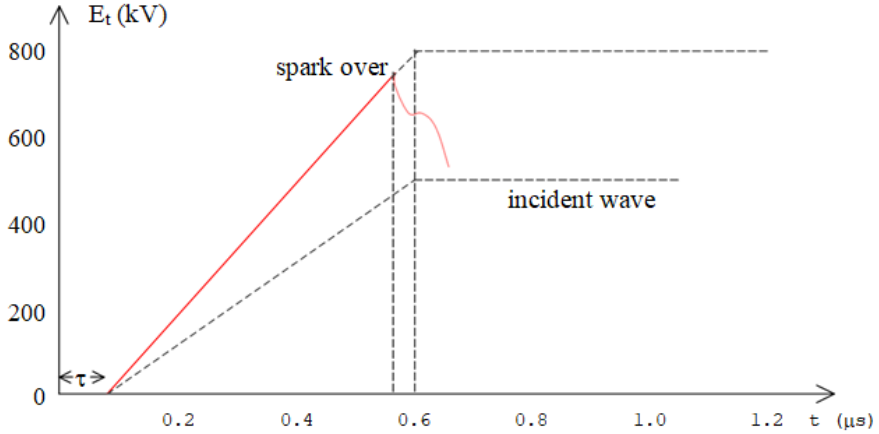

(d)

Figure II.15 Voltage waveforms at the arrestor location and at the transformer location separation is 30 m

The maximum value of the voltage E_t at the terminal for each case can be determined from $E_t = E_a + 0.6\frac{de}{dt} x \frac{2l}{300}$ up to a maximum of 0.6 E_a.

For 90 m, maximum E_t −> 650 + 0.6 x 1000 x 90 x 2 / 300 = 1010 kV > 1.6 x 500

Therefore maximum E_t = 800 kV

For 30 m, maximum E_t −> 650 + 0.6 x 1000 x 30 x 2 / 300 = 770 kV < 1.6 x 500

Therefore maximum E_t = 770 kV

What would have been the maximum separation permissible between the transformer and the lightning arrestor, if the BIL of the transformer was 900 kV and a protective margin of 25 % is required, for the above example ?

For a protective margin of 25 %, maximum permissible surge at transformer = 900/1.25 = 720 kV

Therefore 720 = 650 + 0.6 x 1000 x 2 L / 300

This gives the maximum permissible length L = 17.5 m.

If the maximum rate of rise was taken as 500 kV/∶s, the maximum length would have worked out at 35 m.

Characteristics of lightning arrestors and separation limits

Table II.5 gives the characteristics for station type lightning arrestors and separation distances permissible between arrestor location and power transformer. For line type arrestors, the discharge voltages are about 10 to 20% higher and the corresponding separation distances are roughly half. When multiple lines meet at a busbar, the voltages transmitted are lower (corresponding to 2V/n for n identical lines). It has been suggested that in the presence of multiple lines, the separation distances may be exceeded by about 9% for one additional line, 21 % for two addition lines and 39% for three additional lines for the same degree of protection.

Nominal System Voltage kV	Transformer BIL kV (peak)	Line Construction	Line Insulation kV	Arrestor Rating kV	Discharge Voltage (kV) at			Separation distance m
					5 kA	10 kA	20 kA	
23	150	wood	500	20 25	58 71	65 81	76 94	23 15
34.5	200	wood	600	30 37	88 105	101 121	117 140	27 18
69	350	wood steel	1020 600	60 73 60 73	176 210 176 210	201 241 201 241	232 279 232 279	41 23 47 29
138	550 550 650	steel	930	109 121 145	316 351 420	350 401 481	418 466 558	52 35 47
230	825 900 1050	steel	1440	182 195 242	528 568 700	605 651 800	700 756 930	44 55 58

Table II.5

A typical co-ordination of insulation in station equipment for some system voltages is given in table II.6 together with the corresponding line insulation.

Rated System Voltage (kV)	Impulse Withstand Voltage (kV) peak						
	Transformer	Circuit Breakers CTs,CVTs	Switch & Post Insulation	Bus Insulation		Line Insulation	
				Suspension	Tension	Steel	Wood
22	150	150	225	255	255	-	500
33	200	250	250	320	320	-	600
66	350	350	380	400	470	600	1020
132	550	650	750	700	775	930	-
220	900	1050	1050	1140	1210	1440	-

Table II.6

Example II.4

A lightning arrestor is to be located on the main 132 kV busbar, 30 m away from a 132/33 kV transformer. If the BIL of the transformer on the 132 kV side is 650 kV, and the transformer is effectively earthed, select a suitable lightning arrestor to protect the transformer from a surge rising at 1000 kV/μs on the 132 kV side originating beyond the busbar on a line of surge impedance 375 Ω. (Use the tables given in the text for any required additional data).

No. of discs	Dry f.o.v. kV_{rms}	Wet f.o.v. kV_{rms}	Impulse f.o.v. kV_{crest}
1	80	50	150
2	155	90	255
3	215	130	355
4	270	170	440
5	325	215	525
6	380	255	610
7	435	295	695
8	485	335	780
9	540	375	860
10	590	415	945
11	640	455	1025
12	690	490	1105
13	735	525	1185
14	785	565	1265
16	875	630	1425
18	965	690	1585
20	1055	750	1745
25	1280	900	2145
30	1505	1050	2550

Table II.7

Maximum system voltage for 132 kV = 138 kV

Nominal rating of surge diverter = 138 x 0.8 = 110.4 kV

If this amount is increased by a tolerance of 5%

Nominal rating = 110.4 x 1.05 = 115.9 kV

From these two figures, we can see that either the 109 kV or the 121 kV rated arrestor may be used. Let us

consider the 109 kV arrestor.

Line insulation for 138 kV corresponds to 930 kV. Thus this would be the maximum surge that can be transmitted by the line. Assuming doubling of voltage at the transformer, and an arrestor residual discharge voltage of E_a, the surge current and hence the arrestor discharge current would be given by

$$I_a = \frac{2E - E_a}{Z_0} = \frac{2x930 - E_a}{375}$$

For the 109 kV arrestor, E_a range from 316 kV to 418 kV. For this I_a has the range 4.12 kA to 3.85 kA. Thus the 5 kA rated arrestor is suitable. For this E_a = 315 kV.

Peak value to which the transformer potential would rise on a surge rising at 1000 kV/μs is given by

$$E_t = E_a + \beta \frac{de}{dt} x \frac{2l}{300}, \text{assuming } \beta = 1$$

Thus E_t = 315 + 2 x 1000 x 30 / 300 = 515 kV

This gives a protective margin, for the BIL of 650 kV, of = 100 x (650 - 515)/515 = 26.2%

Thus the arrestor to be selected is the 109 kV, 5 kA one which is found to be completely satisfactory. Flashover voltages of standard discs (254 x 146 mm) is given in the table II.8.

In selecting the number of units, it is common practice to allow one or two more units to allow for a unit becoming defective. Thus for lines up to 220 kV, one additional unit; and for 400 kV, 2 unit may be used.

Rated System Voltage kVrms	Tension Insulators		Suspension Insulators	
	Impulse f.o.v. kV	No. of discs	Impulse f.o.v. kV	No. of discs
33	320	3	320	3
66	470	5	400	4
132	775	9	700	8
220	1210	15	1140	14

Table II.8

Also tension insulator units have their axis more or less horizontal and are more affected by rain. Also a failure of tension insulators are more sever than of suspension insulators. Thus one additional disc is used on tension insulators.

Table II.8 shows the number of disc units (254 x 146 mm) used in Busbar Insulation in a typical substation, for both tension as well as suspension insulators.

Further, for the 132 kV and 220 kV systems, if the lines are provided with proper shielding and low tower footing resistances (say less than 7 S), the number of disc units may be reduced based on a switching surge flashover voltage of 6.5 × (rated phase to neutral system voltage) and a power frequency flash-over voltage of 3 × (rated phase to neutral system voltage).

On this basis, 7 units are recommended for the 132 kV system and 11 units for the 220 kV system.

Chapter III: CONTROL OF ELECTRIC FIELDS

III.1 INTRODUCTION

The potential at a point plays an important role in obtaining any information regarding the electrostatic field at that point. The electric field intensity can be obtained from the potential by gradient operation on the potential

i.e. $$E = -\nabla V \quad (1)$$

which is nothing but differentiation and the electric field intensity can be used to find electric flux density using the relation

$$D = \varepsilon E \quad (2)$$

The divergence of this flux density which is again a differentiation results in volume charge density.

$$\nabla . D = \rho_v \quad (3)$$

Therefore, our objective should be to evaluate potential which of course can be found in terms of, charge configuration. However it is not a simple job as the exact distribution of charges for a particular potential at a point is not readily available. Writing D=εE in equation (3) we have

$$\nabla . \varepsilon E = \rho_v$$

or $$-\nabla . \varepsilon . \nabla V = \rho_v$$

or $$\varepsilon \nabla^2 V = -\rho_v$$

or $$\nabla^2 V = -\frac{\rho_v}{\varepsilon} \quad (4)$$

This is known as Poisson's equation. However, in most of the high voltage equipments, space charges are not present and hence $\rho_v = 0$ and hence equation (4) is written as

$$\nabla^2 V = 0 \quad (5)$$

Equation (5) is known as Laplace's equation

If $\rho_v = 0$, it indicates zero volume charge density but it allows point charges, line charge, ring charge and surface charge density to exist at singular location as sources of the field.

Here ∇ is a vector operator and is termed as del operator and expressed mathematically in cartesian coordinates as

$$\nabla = \frac{\partial}{\partial x}\bar{a}_x + \frac{\partial}{\partial y}\bar{a}_y + \frac{\partial}{\partial z}\bar{a}_z \qquad ...(6)$$

where $\bar{a}_x, \bar{a}_y$ and $\bar{a}_z$ are unit vectors in the respective increasing directions.

Hence Laplace's equation in cartesian coordinates is given

$$\nabla^2 V = \frac{\partial^2 V}{\partial x^2} + \frac{\partial^2 V}{\partial y^2} + \frac{\partial^2 V}{\partial z^2} = 0 \qquad ...(7)$$

Since $\nabla.\nabla$ is a dot produce of two vectors, it is a scalar quantity. Following methods are normally used for determination of the potential distribution

(i) Numerical methods

(ii) Electrolytic tank method.

Some of the numerical methods used are

(a) Finite difference method (FDM)

(b) Finite element method (FEM)

(c) Charge simulation method (CSM)

(d) Surface charge simulation method (SCSM).

III.2 FINITE DIFFERENCE METHOD

Let us assume that voltage variations is a two dimensional problem *i.e.* it varies in *x-y* plane and it does not vary along *z*-co-ordinate and let us divide the interior of a cross section of the region where the potential distribution is required into squares of length *h* on a side as shown in Figure III.1.

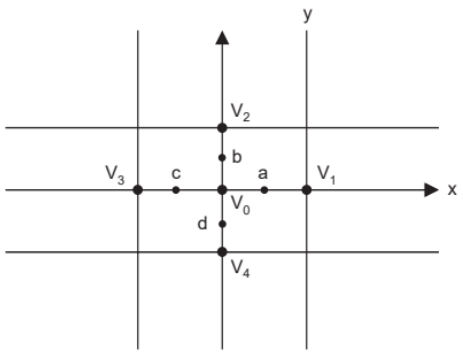

Figure III.1 - A portion of a region containing a two-dimensional potential field divided into square of side h .

Assuming the region to be charge free

$$\nabla . D = 0 \text{ or } \nabla . E = 0$$

and for a two-dimensional situation

$$\frac{\partial E_x}{\partial x} + \frac{\partial E_y}{\partial y} = 0$$

And from equation (7) the Laplace equation is

$$\frac{\partial^2 \mathrm{V}}{\partial \mathrm{x}^2} + \frac{\partial^2 \mathrm{V}}{\partial \mathrm{y}^2} = 0 \qquad \text{...(8)}$$

Approximate values for these partial derivatives may be obtained in terms of the assumed values (Here V_0 is to be obtained when V_1, V_2, V_3 and V_4 are known Figure III.1.

$$\left.\frac{\partial V}{\partial x}\right|_a = \frac{V_1 - V_0}{h} \quad and \quad \left.\frac{\partial V}{\partial x}\right|_c = \frac{V_0 - V_3}{h}$$

From the gradients

$$\left.\frac{\partial^2 V}{\partial x^2}\right|_0 = \frac{\left.\frac{\partial V}{\partial x}\right|_a - \left.\frac{\partial V}{\partial x}\right|_c}{h} = \frac{V_1 - V_0 - V_0 + V_3}{h^2} \qquad \text{...(10)}$$

Similarly $\left.\frac{\partial^2 V}{\partial y^2}\right|_0 = \frac{V_2 - V_0 - V_0 + V_4}{h^2}$

Substituting in equation (8) we have

$$\frac{\partial^2 V}{\partial x^2} + \frac{\partial^2 V}{\partial y^2} = \frac{V_1 + V_2 + V_3 + V_4 - 4V_0}{h^2} = 0$$

or $$V_0 = \frac{1}{4}(V_1 + V_2 + V_3 + V_4) \qquad \text{…(11)}$$

As mentioned earlier the potentials at four corners of the square are either known through computations or at start, these correspond to boundary potentials which are known a priori. From equation (11) it is clear that the potential at point *O* is the average of the potential at the four neighbouring points. The iterative method uses equation (11) to determine the potential at the corner of every square sub- division in turn and then the process is repeated over the entire region until the difference in values is less than a prespecified value.

The method is found suitable only for two dimensional symmetrical field where a direct solution is possible. In order to work for irregular three dimensional field so that these nodes are fixed upon boundaries, becomes extremely difficult. Also to solve for such fields as very large number of *V*(*x*, *y*) values of potential are required which needs very

large computer memory and computation time and hence this method is normally not recommended for a solution of such electrostatic problems.

III.3 FINITE ELEMENT METHOD

This method is not based on seeking the direct solution of Laplace equation as in case of FDM, instead in Finite element method use is made of the fact that in an electrostatic field the total energy enclosed in the whole field region acquires a minimum value. This means that this voltage distribution under given conditions of electrode surface should make the enclosed energy function to be a minimum for a given dielectric volume *v*.

We know that electrostatic energy stored per unit volume is given as

$$W = \frac{1}{2} \in E^2 \qquad \text{...(12)}$$

For a situation where electric field is not uniform, and if it can be assumed uniform for a differential volume δv, the electric energy over the complete volume is given as

$$W = \frac{1}{2} \int_V \frac{1}{2} \in (-\nabla V) dv \qquad \text{...(13)}$$

To obtain voltage distribution, our performance index is to minimise *W* as given in equation

(13).

Let us assume an isotropic dielectric medium and an electrostatic field without any space charge.

The potential *V* would be determined by the boundaries formed by the metal electrode surfaces.

Equation (13) can be rewritten in cartesian coordinates as

$$W = \frac{1}{2} \in \iiint \left[\left(\frac{\partial V}{\partial x}\right)^2 + \left(\frac{\partial V}{\partial y}\right)^2 + \left(\frac{\partial V}{\partial z}\right)^2 \right] dxdydz \qquad \text{...(14)}$$

Assuming that potential distribution is only two-dimensional and there is no change in potential along *z*-direction, then $\frac{\partial V}{\partial z} = 0$ and hence equation (14) reduces to

$$W_A = z\iint \left[\frac{1}{2} \in \left\{\left(\frac{\partial V}{\partial x}\right)^2 + \left(\frac{\partial V}{\partial y}\right)^2\right\}\right] dxdy \qquad ...(15)$$

Here z is constant and W_A represents the energy density per unit area and the quantity within integral sign represents differential energy per elementary area $dA = dxdy$.

In this method also the field between electrodes is divided into discrete elements as in FDM. The shape of these elements is chosen to be triangular for two dimensional representation and tetrahedron for three dimensional field representation Figure III.2 (*a*) and (*b*).

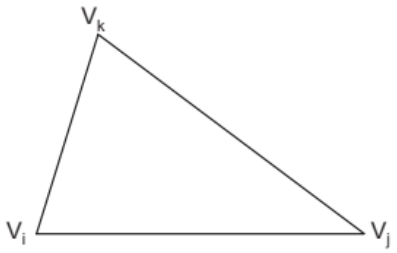

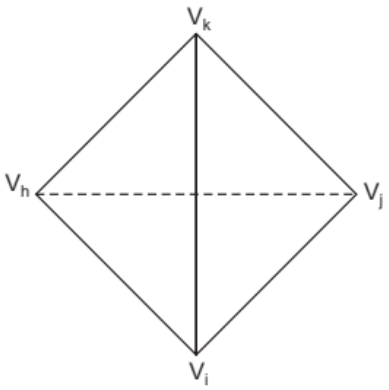

Figure III.2 (a) Triangular finite element (b) Tetrahedron finite element.

The shape and size of these finite elements is suitably chosen and these are irregularly distributed within the field. It is to be noted that wherever within the medium higher electric stresses are expected *e.g.* corners and edges of electrodes, triangles of smaller size should be chosen.

Let us consider an element e_1 as shown in Figure III.2 (*a*) as part of the total field having nodes *i*, *j* and *k* in anti-clockwise direction. There will be a large no. of such elements e_1, e_2 .....e_N . Having obtained the potential of the nodes of these elements, the potential distribution within each elements is required to be obtained. For this normally a linear relations of *V* on *x* and *y* is assumed and hence the first order approximation gives

$$V(x, y) = a_1 + a_2x + a_3\, y \qquad ...(16)$$

It is to be noted that for better accuracy of results higher order approximation *e.g.* square or cubic would be required. Equation (16) implies that electric field intensity within the element is constant and potentials at any point within the element are linearly

distributed. The potentials at nodes *i*, *j* and *k* are given as

$$V_i = a_1 + a_2 x_i + a_3 y_i \quad V_j = a_1 + a_2 x_j + a_3 y_j \quad V_k = a_1 + a_2 x_k + a_3 y_k \qquad ...(17)$$

Equation (17) can be rewritten in matrix form as

$$\begin{bmatrix} V_i \\ V_j \\ V_k \end{bmatrix} = \begin{bmatrix} 1 & x_i & y_i \\ 1 & x_j & y_j \\ 1 & x_k & y_k \end{bmatrix} \begin{bmatrix} a_1 \\ a_2 \\ a_3 \end{bmatrix} \qquad ...(18)$$

By using Cramer's rules, the coefficient a_1, a_2, a_3 can be obtained as follows

$$a_1 = \frac{1}{2\Delta_e}\left(\alpha_i V_i + \alpha_j V_j + \alpha_k V_k\right) \qquad ...(19)$$

$$a_2 = \frac{1}{2\Delta_e}(\beta_i V_i + \beta_j V_j + \beta_k V_k)$$

and $$a_3 = \frac{1}{2\Delta_e}(\gamma_i V_i + \gamma_j V_j + \gamma_k V_k)$$

where $\alpha_i = x_j y_k - x_k y_j$, $\alpha_j = x_k y_i - x_i y_k$, $\alpha_k = x_i y_j - x_j y_i$

$\beta_i = y_i - y_k$, $\beta_j = y_k - y_i$, $\beta_k = y_i - y_j$

$\gamma_i = x_k - x_j$, $\gamma_j = x_i - x_k$, $\gamma_k = x_j - x_i$

and $2\Delta_e = \alpha_i + \alpha_j + \alpha_k = \beta_i \gamma_j - \beta_j \gamma_i$

where Δ_e represents the area of the triangular element under consideration. As mentioned earlier the nodes must be numbered anticlockwise, else Δ_e may turn out to be negative.

From equation (16), the partial derivatives of *V* are

$$\frac{\partial V}{\partial x} = a_2 = f(V_i, V_j, V_k) \quad \text{and} \quad \frac{\partial V}{\partial y} = a_3 = f(V_i, V_j, V_k) \qquad ...(20)$$

We know that for obtaining the voltage at various nodes we have to minimise the energy within the whole system for which derivatives of energies with respect to potential distribution in each element is required. For the element *e* under consideration, let W_e be the energy enclosed in the element, then energy per unit length in the *z*-direction W_e /*z* denoted by $W_{\Delta e}$ can be obtained by using equation (15) as follows

$$W_{\Delta e} = \frac{W_e}{z} = \frac{1}{2} \in \Delta e \left\{ \left(\frac{\partial V}{\partial x}\right)^2 + \left(\frac{\partial V}{\partial y}\right)^2 \right\}_e \quad \text{...(21)}$$

Here $\Delta e = \iint_e dxdy$

To obtain condition for energy minimisation we differentiate partially equation (21) with respect to V_i , V_j and V_k separately. Thus partially differentiating equation (21) with respect to V_i and making use of equations (19) and (20).

We have $$\frac{\partial W_{\Delta e}}{\partial V_i} = \frac{1}{2} \in \Delta_e (2a_2 \frac{\partial a_2}{\partial V_i} + \frac{\partial a_3}{\partial V_i}) = \frac{1}{2} \in (a_2\beta_i + a_3\gamma_i)$$

$$= \frac{\varepsilon}{4\Delta_e} [({\beta_i}^2 + {\gamma_i}^2)V_i + (\beta_i\beta_j + \gamma_i\gamma_j)V_j + (\beta_i\beta_k + \gamma_i\gamma_k)V_k] \quad \text{...(22)}$$

Similarly, finding partial derivatives of equation (21) with respect to V_j and V_k and following the procedure outlined above for partial derivative with respect to V_i and arranging all the three equation in matrix from we have

$$\frac{\partial W_{\Delta e}}{\partial V_e} = \frac{\varepsilon}{4\Delta_e} \begin{bmatrix} ({\beta_i}^2 + {\gamma_i}^2) & (\beta_i\beta_j + \gamma_i\gamma_j) & (\beta_i\beta_k + \gamma_i\gamma_k) \\ (\beta_j\beta_i + \gamma_j\gamma_i) & ({\beta_j}^2 + {\gamma_j}^2) & (\beta_j\beta_k + \gamma_j\gamma_k) \\ (\beta_k\beta_i + \gamma_k\gamma_i) & (\beta_k\beta_j + \gamma_k\gamma_j) & ({\beta_k}^2 + {\gamma_k}^2) \end{bmatrix} \begin{bmatrix} V_i \\ V_j \\ V_k \end{bmatrix} \quad \text{...(22a)}$$

$$= \frac{\varepsilon}{4\Delta_e} \begin{bmatrix} (C_{ii}) & (C_{ij}) & C_{ik} \\ (C_{ji}) & C_{jj} & C_{jk} \\ C_{ki} & C_{kj} & C_{kk} \end{bmatrix}_e \begin{bmatrix} V_i \\ V_j \\ V_k \end{bmatrix}_e = [C]_e[V]_e \quad \text{...(23)}$$

After considering a typical element *e*, the next step is to take into account all such elements in the region under consideration and the energy associated with all the elements will then be

$$W = \sum_{e=1}^{N} W_e = \frac{1}{2} \in [V^T][C][V] \quad \text{...(24)}$$

where $$[V] = \begin{bmatrix} V_1 \\ V_2 \\ \vdots \\ V_n \end{bmatrix}$$

and *n* is the total number of nodes in the system and *N* is the no. of elements and [*C*] is called the global stiffness matrix which is the sum of the individual matrices.

In general $\frac{\partial W}{\partial V_h}$ leads to

$$\sum_{i=1}^{n} V_i C_{ik} = 0 \quad \text{...(25)}$$

The solution of the above equations gives voltage distribution in the region. Of course while seeking the final solution the boundary conditions must be satisfied and hence this would require some iterative method for the exact solution.

The second approach could be to formulate energy function in terms of the unknown nodal voltage. This energy function is subjected to certain constraints in terms of boundary conditions. The objective then is to min. [*W*] subject to certain constraints. For this various mathematical programming techniques like, Fletcher Powell technique, Fletcher technique, direct search techniques, self-scaling variable metric techniques can be used. A computer program can be developed and accuracy of the result can be obtained depending upon the convergence critsion fed into the computer. A suitable initial guess for the solution can always be made depending upon the system configuration and during every iteration the voltage can be updated till all the boundary conditions are satisfied and the energy function is minimised that is when the change in the energy function between two consecutive iterations is less than a prespecified value.

The finite element method is useful for estimating electric fields at highly curved and thin electrode surfaces with composite dielectric materials especially when the electric fields are uniform or weakly non-uniform and can be expressed in two dimensioned geometrics. The method is normally not recommended for three dimensional non-uniform fields.

III.4 CHARGE SIMULATION METHOD

As suggested by the name itself, in this method, the distributed charges on the surface of a conductor/ electrode or dielectric interfaces is simulated by replacing these charges by *n* discrete fictitious individual charges arranged suitably inside the conductor or outside the space in which the field is to be computed. These charges could be in the form of point, line or ring, depending upon the shape of the electrode under consideration. It could be a suitable combination of these fictitious charges. The position and type of simulation charges are to be determined first and then the field on the electrode surface is determined by the potential function of these individual charges. In order to determine the magnitude of these charges *n* no. of points are chosen on the surface of the conductor. These points are known as “contour points’’. The sum of the potentials due to fictitious

charge distribution at any contour points should correspond to the conductor potential V_C which is known a priori.

Suppose q_i, is one of the fictitious charges and V_i is the potential of any point P_i in space which is independent of the coordinate system chosen, the total potential V_i due to all the charges is given as

$$V_i = \sum_{j=1}^{n} p_{ij} q_j \qquad \text{...(26)}$$

where p_{ij} are known as ''potential Co-efficient'' which are to be determined for different types of charges by using Laplace's equation. We know that potential at a point *P* at a distance '*a*' from a point charge *q* is given as

$$V = \frac{q}{4\pi\epsilon a} \qquad \text{...(27)}$$

So here the potential co-efficient *p* is. $\frac{1}{4\pi\epsilon a}$

Similarly, these coefficients for linear and ring or circular charges can also be obtained. It is found these are also dependent upon various distance of these charges from the point under consideration where potential is to be obtained and the permittivity of the medium as in case of a point charge and hence potential coefficients are constant number and hence the potential due to various types of charges are a linear function of charges and this is how we get the potential at a point due to various charges as an algebraic sum of potential due to individual charges.

A few contour points must also be taken at the electrode boundaries also and the potential due to the simulated charge system should be obtained at these points and this should correspond to the equipotentials or else, the type and location of charges should be changed to acquire the desired shape and the given potential. Suppose we take '*n*' number of contour points and *n* no. of charges, the following set of equations can be written

$$\begin{bmatrix} p_{11} & p_{12} & \cdots & p_{1n} \\ p_{21} & p_{22} & \cdots & p_{2n} \\ \vdots & & & \\ p_{n1} & p_{n2} & \cdots & p_{nn} \end{bmatrix} \begin{bmatrix} q_1 \\ q_2 \\ \vdots \\ q_n \end{bmatrix} = \begin{bmatrix} V_1 \\ V_2 \\ \vdots \\ V_n \end{bmatrix} \qquad \text{…(28)}$$

The solution of these equations gives the magnitude of the individual charges and which corresponds to electrode potential ($V_{1\ldots\ldots}V_{\boldsymbol{n}}$) at the given discrete points. Next, it is necessary to check whether the type and location of charges as obtained from the

solution of equation (28) satisfies the actual boundary conditions every where on the electrode surfaces. It is just possible that at certain check points the charges may not satisfy the potential at those points. This check for individual point is carried out using equation (26). If simulation does not meet the accuracy criterion, the procedure is repeated by changing either the number or type or location or all, of the simulation charges till adequate charge system (simulation) is obtained. Once, this is achieved, potential or electric field intensity at any point can be obtained.

The field intensity at a point due to various charges is obtained by vector addition of intensity due to individual charges at that point. However, it is desirable to obtain the individual directional components of field intensity separately. In cartesion coordinate system, the component of electric field intensity along *x*-direction for *n* number of charges is given as

$$\bar{E}_x = \sum_{j=1}^{n} \frac{\partial p_{ij}}{\partial x} q_j = \sum_{j=1}^{n} (f_{ij})_x q_j \qquad ...(29)$$

where $(f_{ij})_x$ are known as field intensity coefficients in *x*-direction.

In this method it is very important to select a suitable type of simulation charges and their location for faster convergence of the solution *e.g.* for cylindrical electrodes finite line charges are suitable, spherical electrodes have point charges or ring charges as suitable charges. However, for fields with axial symmetry having projected circular structures, ring charges are found better. Experience of working on such problems certainly will play an important role for better and faster selection. The procedure for CSM is summarised as follows :

1. Choose a suitable type and location of simulation charges within the electride system.
2. Select some contour point on the surface of the electrodes. A relatively larger no. of contour points should be selected on the curved or corner points of the electrode.
3. Calculate the p_{ij} for different charges and locations (contour points) and assemble in the form of a matrix.
4. Obtain inverse of this matrix and calculate the magnitude of charges (simulation).
5. Test whether the solution so obtained is feasible or not by selecting some check points on the conductor surface. If the solution is feasible stop and calculate the electric field

intensity at requisite point. If not, repeat the procedure by either changing the type or location of the simulation charges.

CSM has proved quite useful for estimation of electric field intensity for two and three dimensional fields both with or without axial symmetry. It is a simple method and is found computationally efficient and provides accurate results.

The simplicity with which CSM takes care of curved and rounded surfaces of electrodes or interfaces of composite dielectric medium makes it a suitable method for field estimation. The computation time is much less as compared to FDM and FEM.

However, it is difficult to apply this methods for thin electrodes *e.g.* foils, plates or coatings as some minimum gap distance between the location of a charge and electrode contours is required. Also, it is found difficult to apply this method for electrodes with highly irregular and complicated boundaries with sharp edges etc.

However, as mentioned earlier a good experience of selecting type and location of simulation charge may solve some of these problem.

An improved version of CSM known as surface charge simulation method (SCSM) described below is used to overcome the problem faced in CSM.

III.5 SURFACE CHARGE SIMULATION METHOD

Here a suitably distributed surface charge is used to simulate the complete equipotential surface *i.e.* the electrode contour since the surface charge is located on the contour surface itself. In actual practice the existing surface charge on the electrode configuration is simulated by integration of ring charges placed on the electrode contour and dielectric boundaries. This results into a physically correct reproduction of the whole electrode configuration.

The electrode contours are segmented as shown in figure III.3 and to each segment '*S'* a surface charge density is assigned by a given function $S_k(x)$ which could be a first degree approximation or a polynomial as follows

$$\sigma(x) = \sum_{k=0}^{n} S_k(x).\sigma_k \qquad ...(29)$$

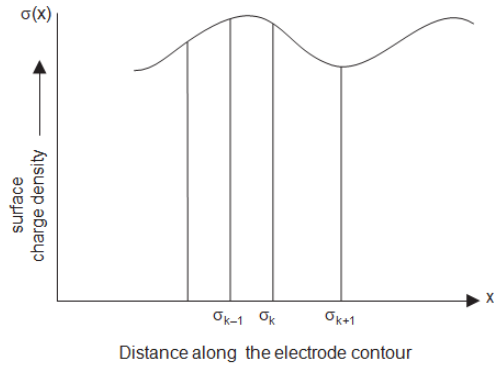

Figure III.3- Segmented Contour path with assigned

The individual segments along the contour path can be represented as shown in Figure III.4.

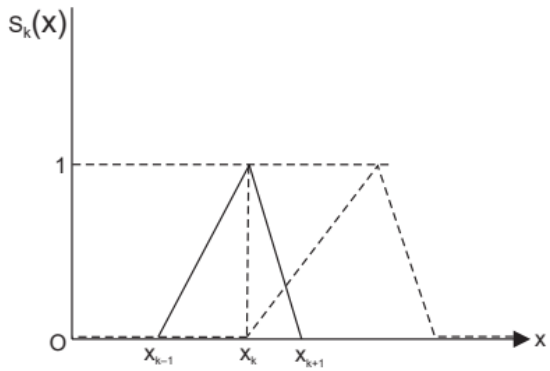

Figure III.4- Representation of a segment $S_k(x)$

The value of S_k (x) is zero for $x < x_{k-1}$ and is unity at $x = x_k$ and in between x_{k-1} and x_k is given as

$$\frac{x - x_{k-1}}{x_k - x_{k-1}}$$

With the representation the contour sarface is reproduced accurately and exactly and thus the continuity of charge between the segments is assumed. Surface charges can be simulated either by line or ring charges. Ring charge simulation is found to be more useful for fields with symmetry of rotation.

Each contour segment is assigned *m* no. of charges and the potential due to a charge q_j, is given by equation (26) and is rewritten here

$$V_i = \sum_{j=1}^{m} p_i q_j$$

The potential co-efficient p_{ik} for a contour point *i* due to *k*th contour segment is obtained as shown in Figure III.5.

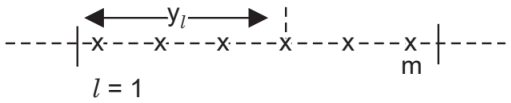

Figure III.5-Concentrated charges to simulate surface charges

and is give as

$$p\ \ \sigma\ =\ \ \sigma(x)\ .\ p_{ix}\ dx \qquad ...(30)$$

Now substituting equation (29) in equation (30) we have

$$p_{ik}\sigma_k = \int_x \sum_{k=0}^{n} S_k(x).\sigma_k p_{ix} dx \qquad ...(31)$$

Since each segment is divided into *m* intervals as shown in Figure III.5, equation (31) can be

rewritten as

$$p_{ik}\sigma_k = \int_{x_{k-1}}^{xk} s_k(x) p_{ix} dx = \sum_{l=1}^{m} s_k(y_l) p_{il} \sigma_k \qquad ...(32)$$

The potential coefficient p_{il} are similar to the coefficients derived from a single concentrated charge in CSM. This coefficient, therefore, can be obtained for a line charge or by solving elliptical integral for a ring charge. The electric field intensity at any contour point *i* due to *k*th contour segment

is given as

$$E_i = \sum_{x=1}^{m} \sigma_k f_{ik} \qquad ...(33)$$

where f_{ik} are the field intensity co-efficients.

As discussed this method requires a large number of elements, normally more than 2500, inde- pendent of the surface shape and thus require large computational efforts. Also, due to certain practical difficulties this method is not used as frequently as other numerical methods for estimation of electric fields.

III.6 COMPARISON OF VARIOUS TECHNIQUES

Out of the various techniques FDM is the simplest to compute and understand but the computation effort and computer memory requirements are the highest. Also, since all difference equations are approximation to the actual field conditions, the final solution may have considerable error.

Finite element method is a general method and has been used for almost all fields of engineer- ing. The method is suitable for estimating fields at highly curved and thin electrode surfaces with different dielectric materials. However, this method is more useful for uniform or weakly non-uniform fields and which can be represented by two dimensional geometries. This method is recommended for three dimensional complicated field configurations.

Charge Simulation Method (CSM) is considered to be one of the most superior and acceptable method for two and three dimensional configuration with more than one dielectric and with electrode systems of any desired shape since this method is based on minimization of the energy function which could be subjected to any operating constraints *e.g.* environmental condition, it has proved to be highly accurate method. Because of inherent features of the technique, this method also helps in optimising electrode configuration. In this electrode configuration optimisation problems the objective is to have field intensity as low as possible subject to the condition that a constant field intensity exists on the complete electrode surface. With this optimisation, a higher life expectancy of high voltage equipments can be achieved.

However, as mentioned earlier this method can not be used for thin electrodes *e.g.* foils, plates or coatings due to the requirement of a minimum gap distance between the location of a charge and electrode contour. Also, this method is not suitable for highly irregular electrode boundaries.

The surface charge simulation method even though takes into account the actual surface charge distribution on the electrode surface, this method is not normally recommended for solution of field problem due to some practical difficulties.

An important difference between the various method is that the FDM and FEM can

be used only for bounded field whereas CSM and SCMS can also be used for unbounded fields.

III.7 ELECTROLYTIC TANK

For assessing electric field distribution in complex three dimensional situations, analytical methods are unsuitable. Two other approaches in use are, experimental analog and numbrical techniques. The numerical techniques have already been discussed in the previous section. We now study analog techniques especially the use of electrolytic tank.

The potential distribution in conductive media in current equilibrium condition satisfies Laplace's equation the same as the electric fields in space-charge-free regions *i.e.* $\rho_V = 0$. This fact makes it possible to obtain solutions to many difficult electrostatic field problems by constructing an analyogous

potential distribution in a conductive medium where the potential and field distributions can be meas- ured directly. The conductors and insulation arrangements can be represented using an electrolytic tank. Due to its simplicity and accuracy this method has been used for decades.

A scale model of the electrode configuration is set up in a tank with insulating walls, filled with suitable electrolyte *e.g.* tap water. An alternating voltage is the appropriate choice of working voltage to avoid polarisation voltage arising in the case of direct voltages. The equipotential lines or equipotential areas in the case of the electric field are measured by means of a probe which can be fed with different voltages from a potential divider *via* a null indicator.

Guiding the probe along the lines corresponding to the potential selected on the divider as well as their graphical representation, can be undertaken manually or automatically in large systems. For the two-dimensional field model, various dielectric constants can be simulated by different heights of electrolyte as shown in Figure III.6 for a cylinder-plane configuration.

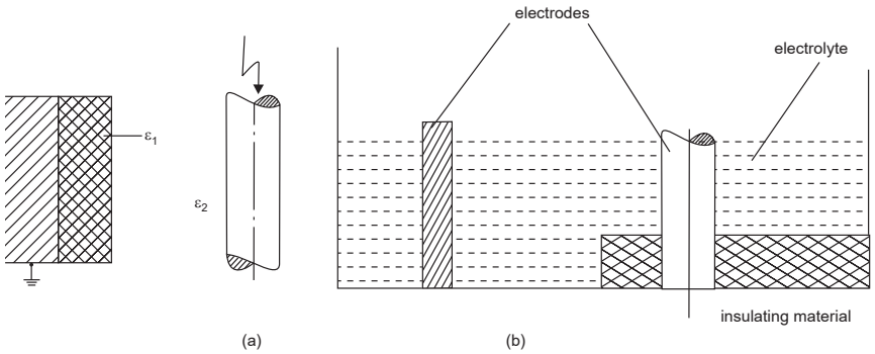

Figure III.6- Simulation of a cylinder-plane configuration in the electrolytic tank (a) Original (b) Simulation for the case $\varepsilon_1 = 2\varepsilon_2$

Three dimensional fields with rotational symmetry can be readily simulated in a wedge shaped tank where as for fields with no rotational symmetry one has to resort to much more complex forms of three dimensional simulation.

Equipotential boundaries are represented in the tank by specially formed sheets of metal. For example a single dielectric problem such as a three core cable may be represented using a flat tank as shown in Figure III.7. Different permittivities are represented by electrolytes of different conductivities separated by special partitions. Otherwise, the tank base can be specially shaped.

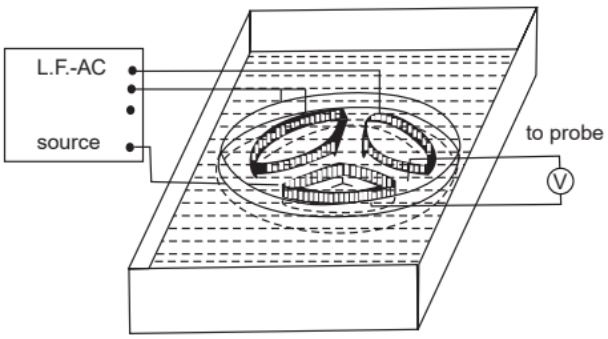

Figure III.7- Electrolytic tank model of a three-core cable represented at the instant when one core is at zero voltage, the same as the sheath.

III.8 CONTROL OF ELECTRIC FIELD INTENSITY

It is a common knowledge that if the field in a dielectric material is uniform, the material is properly utilised. If it is non-uniform the material is under-utilised. Under normal situation an electric field is not uniform due to imperfection in the dielectric

material during manufacture or it could be due to undesirable shapes and sizes of electrodes.

Sudden change in shape of electrodes in the form of corners or edges in high voltage equipments leads to concentration of electric fields at such locations resulting in higher electric stresses on the dielectric. The area around such location becomes highly vulnerable to breakdown of insulation. In order to avoid this breakdown, the electrodes should be suitably designed and shaped so that concentra- tion of the field is not allowed. The electrodes are extended and so shaped that a higher field intensity than the main field does not appear anywhere in the dielectric material. To achieve this objective Rogowaski suggested a shape by which electrodes should be extended known as Rogowaski profile as shown in Figure III.8 (*b*).

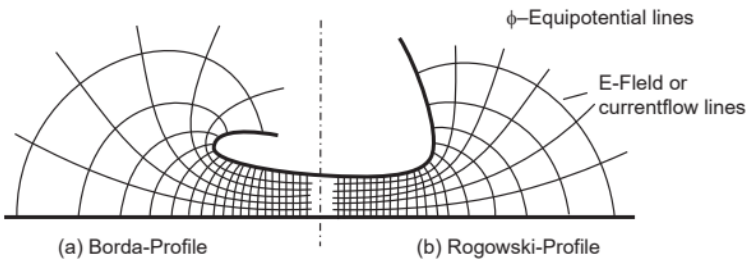

Figure III.8- equipotential and the field (current flow) lines between plane and brim field.

It is clear from the Figure III.7 that the electric field intensity continuously reduces beyond the edges of the electrodes. Another profile of electrodes suggested by Borda for reducing electric field stresses is shown in Figure III.8(*a*) . Comparing the two profiles, it is found that the Borda profile achieves a lower field intensity beyond the edges as compared to Rogowski profile.

Also, it is found that the space requirements for high voltage equipments is smaller with Borda profile electrodes as compared to Rogowski profile. In many situations for high voltage equipment

space requirements become a serious problem and hence electric field optimisation techniques have received a great importance.

A visit to a high voltage laboratory shows that electrodes at high potential are given large, smooth shaped dome like shapes to bring down the electric field stress surrounding

the area *i.e.* the atmospheric air. The modern trend is to design segmented electrodes in which a number of small, identical, smooth discs are given a desired continuous shapes as per requirement.

Electric stress control shields of various shapes and sizes are used for high voltage equipments Figure III.9. Sometimes sharp electrode ends are enclosed by a large diameter hemispherical electrode having a smooth aperture.

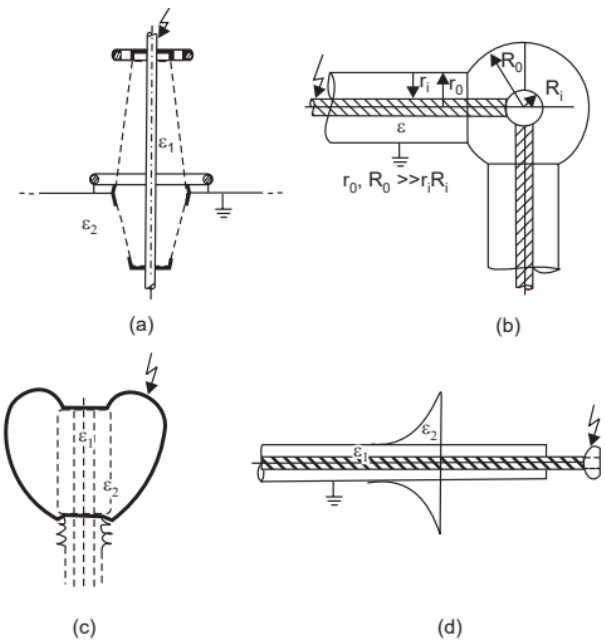

Figure III.9- Extended shapes of electrodes for stress control (a) A bushing with toroids (a) Right angle turn of a bus bar in gas insulated switchgear (*GIS*), (b) HV electrode on a condenser, (d) Stress cone on a screened cable end.

Circular and tubular electrodes are provided with spherical shields at bends. In high voltage laboratories tubular electrodes of large diameter are used for connection rather than insulated wire thereby electric field intensity is reduced considerably.

For transmission voltage 400 kV and above we make use of more than one conductor which is known as bundling of conductors or these conductors are known as bundled conductor. This is done to reduce electric field intensity in the atmospheric air thereby the corona loss on the line and radio interference with communication lines is reduced.

The design of high voltage bushing used for large capacity power transformers,

potential transformers or cable termination is based on capacitance grading thereby a uniform voltage distribution is achieved which results in a uniform electric field intensity within the dielectric. This is done by

interposing concentric sheets of metals of suitable lengths and position. This is known as "inter-sheath grading" to control electric field intensity. The inter-sheaths are held at suitable potential which enables economic utilisation of the insulating material by evenly distributing the equipotential surfaces.

A simple rule to control electric field intensity in high voltage equipments is to avoid sharp points and edges in the electrodes. These electrodes should be large symmetrical and should have smooth surface. The surface should not be rough as this would lead to higher stresses at high voltages. Micro protrusion on the surface of the electrode may penetrate deeper into the dielectric material which may result in high electric field intensity at those points and may lead to breakdown of the dielectric material.

III.9 OPTIMISATION OF ELECTRODE CONFIGURATION

Various numerical techniques have been used to optimise the electrode configuration so that the dielectric material is optimally utilised as a result a considerable improvement in dielectric behaviour is achieved and a higher life expectancy of high voltage equipments can be anticipated. When we talk of electrode configuration optimisation, we really mean the electric field intensity optimisation. Even though some work has been dedicated for electrode configurations optimisation by FDM and FEM methods, yet the inherent suitability of CSM for optimisation, lot of work has been reported in literature using this technique.

The objective of optimisation is to determine the configuration of electrodes which may result into a minimum and constant field intensity on the complete electrode surface. The optimisation technique is based on the partial discharge inception electric field intensity E_{pd} which depends upon the dielectric material, its pressure (if gas is the medium) and the electrode configuration. It is to be noted that if the electric field is uniform or weakly non-uniform, the partial discharge or normal breakdown takes place at the same electric field intensity. Therefore, it is only the electrode configuration which

can be optimised. If E_{pd} is more than the electric field intensity E applied, partial discharge can not take place which means the electrode can be said to be optimised, if at a given voltage the maximum value of $\frac{E}{E_{pd}}$ on its surface is as small as possible. Since the maximum value of E/E_{pd} depends upon three parametres the shape, size and position of electrodes, three different types of optimisation possibilities exist. The optimum shape of an electrode in characterised by

$$\text{Min. } (E/E_{pd})_{\max} = \text{constant} \qquad ...(34)$$

The optimisation methods are based on iterative process and when equation (34) is satisfied, the optimum electrode configuration is obtained. While using CSM, following strategies are used for optomisation of electrode configuration.

(i) Displacement of contour points perpendicular to the surface

(ii)Changing the position of the ‘‘optimisation charges’’ and contour points

(iii) Modification of contour elements

A brief view of these methods is given below.

III.8.1 Displacement of Contour Points

In this method a constant magnitude of electric field intensity is achieved using an iterative process by differential displacement of contour points perpendicular to the surface during every iteration. We start with a suitable contour of the electrode and on this we fix some contour points, and, electric field intensity is evaluated for this contour. If this field intensity is within the permissible value of desired field intensity we stop as the optimal configuration is obtained right at the first step. However, it is very unlikely to hit at the optimal configuration in the first step itself and hence the curvature of this contour is changed step by step depending upon the difference between the calculated electric field intensity and the desired field intensity. A good experience in field theory will be quite helpful in deciding the new contour points during different iterations. Figure III.10 shows the flows chart for the optimisation process.

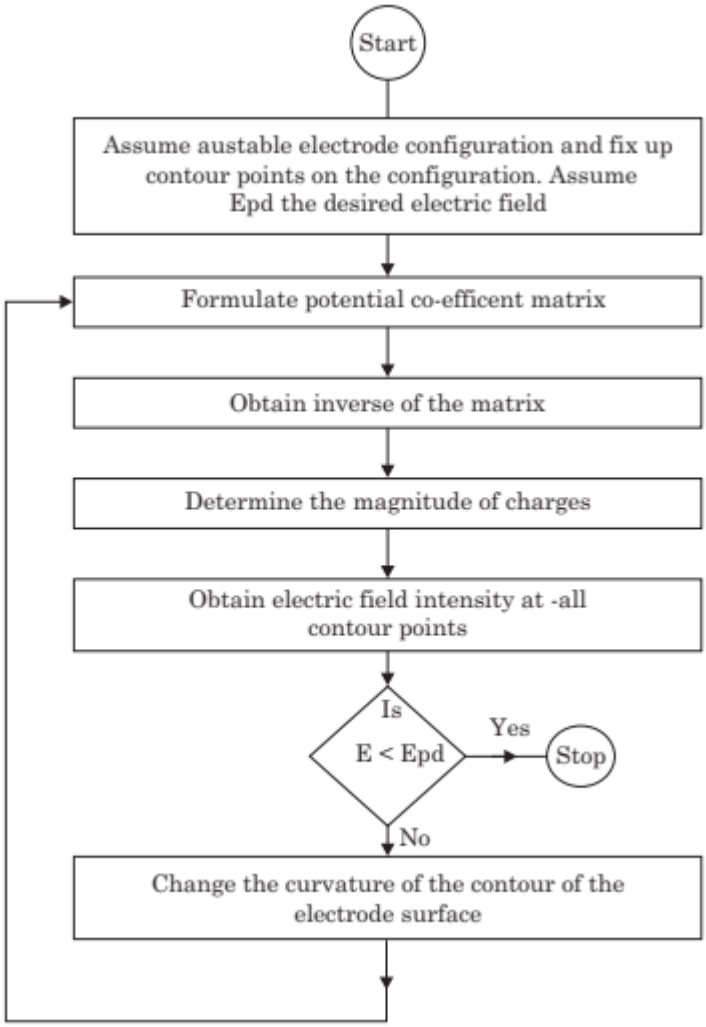

Figure III.10- Flow chart for optimisation by displacement of contour points method

It is to be noted that for electric field calculation on the electrode surface (assumed or updated) is caried out using CSM technique. Since during every iteration the complete CSM technique is to be used for calculation of electric field intensity, computer time requirement is high and this is its major disadvantage.

III.8.1 Changing the Position of the Optimisation Charges and Contour Points

In CSM we start with certain configuration of the electrode and we calculate electrode field intensity at various contour points of the electrode and from this we should be able to identity which part of the electrode surface needs optimisation (the contour points where $E > E_{pd}$). Normally in CSM, the identified region of electrode

configuration is reproduced by a set of contour points and a set of simulation charges at fixed locations but of unknown magnitudes. However, in optimisation method, the optimisation region is reproduced like in CSM by a suitable '*n*' number of contour optimisation points as shown in Figure III.11.

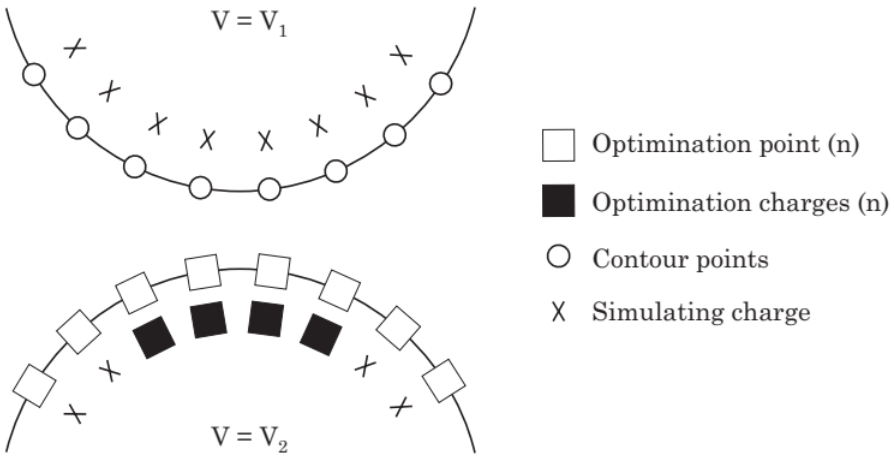

Figure III.11- Optimisation region in an electrode configuration

This optimisation region is then provided with '*n*' optimisation charges which have fixed position and known magnitudes. The optimisation charges are obtained corresponding to a partial solution of mathematical problem.

The optimisation procedure proceeds with iterative steps as follows :

(i) The optimisation charges which affect the field intensity in optimisation region more than the simulation charges are shifted in position such that the field intensity in the optimisation region is less than a prespecificd value.

(ii) When we shift the optimisation charges the potential at the contour points in the region is changed. In order to bring the known potential (new) at the contour points, the magnitude of the simulation charges should be changed to fulfil the new potential requirement at the contour points.

(iii) The new equipotential line having the known potential is calculated with the help of a complete new set of optimisation charges. This will be our new optimised contour of the electrode.

(iv) The field intensity in the optimisation region is calculated and compared it with a prespecified value of *E* and this may not satisfy equation (34) or even after changing the shape of the electrode and the charge magnitudes in the other region.

(v) The optimisation points are now located at the newly obtained contour of the electrode. The location of the respective optimisation charges should, therefore, be suitably corrected to start the next iteration.

The iteration procedure is continued with lower magnitude of electric field intensity till it con- verges to a prespecified value or instruct to stop the computation process if it goes to a very low value which is physically not feasible.

III.8.2 Modification of Contour Elements

This method is based on the qualitative correlation between the curvature of an electrode sur- face and its electric field intensity. The larger yer the curvature the larger is the value E/E_{pd} . Therefore, the radii of the contour element will have to be increased for the region where E/E_{pd} is large and decreased where E/E_{pd} is small. The optimisation method is explained here for a cylindrical rod and plane electrode configuration. It is required to optimise the contour of the rod end. Suppose r is the radius of the rod end and 'd' is its distance from the plane as shown as Figure III.12 (*a*). As an initial approximation, the rod end is assumed to be hemispherical. Since the rod end is symmetrical about the vertical axis, the corresponding semicircle is divided into segments Figure III.12 (*b*). Depending upon the accuracy requirements of the final result a suitable number of segments are selected. The circular arcs on the periphery are called the 'contour segment'. The procedure is explained as follows :

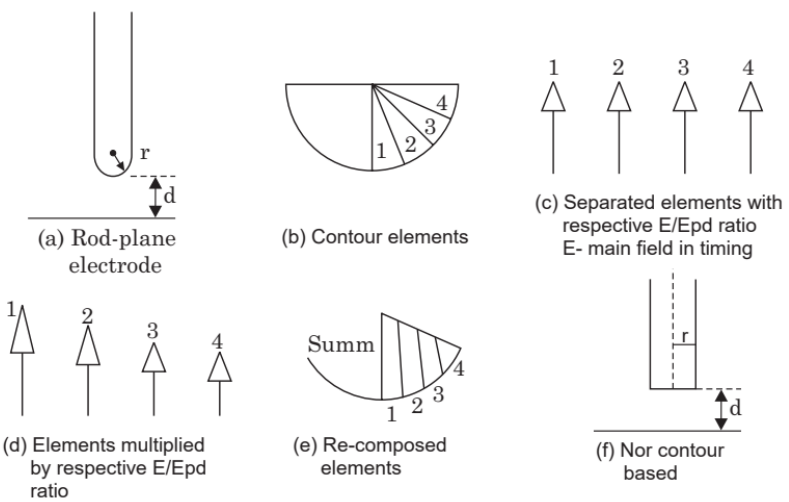

Figure III.12- Optimisation by contour elements

(i) At the outset, mean electric field intensity E on each contour element is calculated using any of the numerical techniques mentioned in article 0.8. Contour elements are shown separately with their corresponding magnitudes of E/E_{pd} ratio in Figure III.12 (*c*).

(ii) The radius of each element which is same in this case as all elements lie along the arc of a circle is multiplied by their respective $(E/E_{pd})^n$ whereas the angles of the elements and therefore, the shapes remain unchanged. The exponent which represents no. of iterations required to converge, is recommended to be four. As a result of multiplication a new set of elements of different sizes is obtained Figure III.12(*d*). The new set of elements are recomposed as shown in Figure III.12(*e*) thereby a new contour is obtained. The radius of the new contour is made equal to *r* by multiplying the radius of the new contour by a suitable scale factor.

(iii) The new contour is placed at the distance '*d'* from the plane as shown in Figure III.12(*f*). The steps (*i*) and (*ii*) are repeated until the remaining differences in E/E_{pd} ratio are sufficiently small. As seen in Figure III.12(*e*) during each iteration the surface region is flattened where E/E_{pd} exceeds its mean value whereas the remaining region becomes more curved which results into a more uniform distribution of E/E_{pd} It is to be noted that in step (*ii*) if the E_{pd} depends upon the curvature of the electrode surface, then instead of the element radii, the reciprocal of the curvature is multiplied by $(E/E_{pd})^n$. It is to be noted with caution that the boundary conditions in terms of operating constraints if any must be included during the process of optimisation of electrode configuration otherwise it may turn out to an infeasible solution.

Chapter IV:
IONIZATION PHENOMENA IN GASES

IV.1 Ionisation of Gases

Electrical Insulating Materials (or Dielectrics) are materials in which electrostatic fields can remain almost indefinitely. These materials thus offer a very high resistance to the passage of direct currents. However, they cannot withstand an infinitely high voltage. When the applied voltage across the dielectric exceeds a critical value the insulation will be damaged. The dielectrics may be gaseous, liquid or solid in form.

Gaseous dielectrics in practice are not free of electrically charged particles, including free electrons. The electrons, which may be caused by irradiation or field emission, can lead to a breakdown process to be initiated. These free electrons, however produced, on the application of an electric field are accelerated from the cathode to the anode by the electric stress applying a force on them. They acquire a kinetic energy (½ mu^2) as they move through the field. The energy is usually expressed as a voltage (in electron-volt, eV, where e is the charge on an electron) as the energies involved are extremely small. [The energy $E_i = e\ V_i$ is expressed in electron volt. $1\ e\ V = 1.6 \times 10^{-19}$ J]. These free electrons, moving towards the anode collide with the gas molecules present between the electrodes. In these collisions, part of the kinetic energy of the electrons is lost and part is transmitted to the neutral molecule. If this molecule gains sufficient energy (more than the energy E_i necessary for ionisation to occur), it may ionise by collision. The (mean) number of ionising collisions by one electron per unit drift across the gap is not a constant but subject to statistical fluctuations. The newly liberated electron and the impinging electron are then accelerated in the field and an electron avalanche is set up. Further increase in voltage results in additional ionising processes. Ionisation increases rapidly with voltage once these secondary processes take place, until ultimately breakdown occurs.

It is worth noting that in uniform fields, the ionisation present at voltages below breakdown is normally too small to affect engineering applications. In non-uniform fields, however, considerable ionisation may be present in the region of high stress, at voltages well below breakdown, constituting the well known corona discharge.

IV.1.1 Ionisation processes in gas discharges

The electrical breakdown of a gas is brought about by various processes of ionisation. These are gas processes involving the collision of electrons, ions and photons with gas molecules, and electrode processes which take place at or near the electrode surface [Electrons can be emitted from the cathode if the stress is around 100 - 1000 kV/cm due to field emission].

Ionisation is the process by which an electron is removed from an atom, leaving the atom with a nett positive charge (positive ion). Since an electron in the outermost orbit is subject to the least attractive force from the nucleus, it is the easiest removed by any of the collision processes. The energy required to remove an outer electron completely from its normal state in the atom to a distance well beyond the nucleus is called the first ionisation potential.

The reciprocal process of an electron falling from a great distance to the lowest unoccupied orbit is also possible. In this case, a photon will be emitted having the same energy as previously absorbed.

IV.1.2 Relevant gas ionisation processes

(i) Ionisation by simple collision

When the kinetic energy of an electron (½ mu²), in collision with a neutral gas molecule exceeds the ionisation energy ($E_i = e V_i$) of the molecule, then ionisation can occur.
(i.e. when ½ mu² > E_i)

$$M + e^- (½ mu^2) \rightarrow M^+ + 2 e^-$$

In general, a positive ion and 2 slow moving electrons will result. The probability of this process is zero for electron energies equal to the ionisation energy E_i, but increases almost linearly at first, and then gradually with electron energy up to a maximum.

When the gas molecules are bombarded with electrons, other electrons bound to atoms may be freed by the collision with the high energy electron. The ratio of the electrons given by collision to the primary electrons depend, mainly on the energy of the primaries. This is maximum at primary electron energies of about 200 - 500 eV. For lower energy values, the energy transferred may not be sufficient to cause electrons to escape from the surface of the molecules, and thus the probability of ionisation is small. For much higher values of primary energies, the energy of the impinging electron would be sufficient for this electron to penetrate the surface deeper into the molecule, so that again the chance of escape of other electrons decreases.

Thus the variation of the ionisation probability in air with increase of electron energy is as shown in figure IV.1.

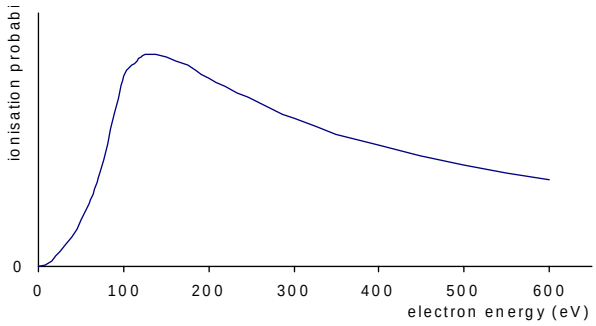

Figure **IV**.1 - Ionisation probability curve in air

(ii) Excitation

In the case of simple collision, the neutral gas molecule does not always gets ionised on electron impact. In such cases, the molecule will be left in an excited state M^*, with energy E_e.

$$M + e^- (½ mu^2) \rightarrow M^* + e^-$$

This excited molecule can subsequently give out a photon of frequency v with energy emitted h v. The energy is given out when the electron jumps from one orbit to the next.

$$M^* \rightarrow M + h v$$

where h = Planck's constant = 6.624×10^{-34} J s

(iii) Ionisation by Double electron impact

If a gas molecule is already raised to an excited state (with energy E_e) by a previous collision, then ionisation of this excited molecule can occur by a collision with a relatively slow electron. This electron would need less energy than the ionisation energy, but the energy must exceed the additional energy required to attain the ionisation energy.

(i.e. $\frac{1}{2} mu^2 > E_i - E_e$)

$$M^* + e^- (\tfrac{1}{2} mu^2) \rightarrow M^+ + 2\, e^-$$

(iv) Photo-ionisation

A molecule in the ground state can be ionised by a photon of frequency v provided that the quantum of energy emitted h v (by an electron jumping from one orbit to another), is greater than the ionisation energy of the molecule.

(i.e. $h\,v > E_i$, where h = Plank's constant = 6.624×10^{-34} joule)

$$M + h\,v \rightarrow M^+ + e^-$$

(v) Electron Attachment

If a gas molecule has unoccupied energy levels in its outermost group, then a colliding electron may take up one of these levels, converting the molecule into a negative ion M^-.

$$M + e^- \rightarrow M^-$$

The negative ion thus formed would be in an excited state, caused by the excess energy.

Note: Electron attachment decreases the number of free electrons, unlike ionisation which increases the free electrons.

(vi) Electron detachment

This occurs when a negative ion gives up its extra electron, and becomes a neutral molecule.

$$M^- \rightarrow M + e^-$$

(vii) Other Processes

The above processes are the most important in relation to the gas discharge phenomena. Other possible gas processes include ion-atom collisions, excited atom-molecule collisions, and atom-atom collisions. It should be noted that collisions between ions and atoms rarely result in ionisation, due to the relatively slow interaction time, which allows the internal motion of the atomic system to adjust itself gradually to the changing condition without any energy transition occurring.

In order to cause ionisation of a neutral unexcited atom of its own kind, a positive ion must possess energy of at least 2 eV. Normally ions and atoms having such energies are encountered only in high current arcs and thermonuclear discharges.

IV.2 Breakdown Characteristic in gases

Two mechanisms of breakdown in gasses is known. These are the **avalanche** and **streamer** mechanisms

IV.2.1 Electron Avalanche Mechanism (Townsend Breakdown Process)

One of the processes which are considered in breakdown is the Townsend breakdown mechanism. It is based on the generation of successive secondary avalanches to produce breakdown.

Suppose a free electron exists (caused by some external effect such as radio-activity or cosmic radiation) in a gas where an electric field exists. If the field strength is sufficiently high, then it is likely to ionize a gas molecule by simple collision resulting in 2 free electrons and a positive ion. These 2 electrons will be able to cause further ionization by collision leading in general to 4 electrons and 3 positive ions. The process is cumulative, and the number of free electrons will go on increasing as they continue to move under the action of the electric field. The swarm of electrons and positive ions produced in this way is called an electron avalanche. In the space of a few millimetres, it may grow until it contains many millions of electrons. This is shown in Figure IV.2.

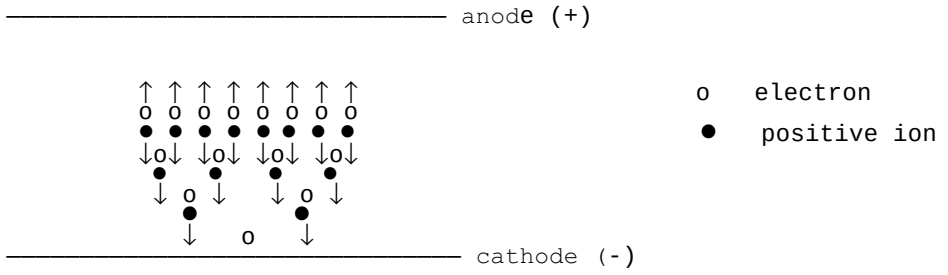

Figure IV.2 - Electron Avalanche

IV.2.1.1 Mathematical Analysis

When the voltage applied across a pair of electrodes is increased, the current throughout the gap increases slowly, as the electrons emitted from the cathode move through the gas with an average velocity determined by their mobility for the field strength existing for the particular value of voltage. Impact ionization by electrons is probably the most important process in the breakdown of gasses, but this process alone is not sufficient to produce breakdown.

Let n_0 = number of electrons/second emitted from the cathode,

n_x = number of electrons/second moving at a distance x from the cathode [$n_x > n_0$ due to ionising collisions in gap]

α = number of ionising collisions, on average, made by one electron per unit drift in the direction of the field. [Townsend's first ionisation coefficient]

then $1/\alpha$ = average distance traversed in the field direction between ionising collisions.

Consider a laminar of thickness dx at a distance x from the cathode. The n_x electrons entering the laminar will traverse it in the presence of the applied field E. The ionising collisions generated in the gas gap will be proportional to both dx and to n_x.

Thus

$$dn_x \propto n_x$$

$$\propto dx$$

Therefore $dn_x = \alpha \, . \, n_x \, . \, dx$ (from definition of α)

Rearranging and integrating gives

$$\int_{n_0}^{n_x} \frac{d\, n_x}{n_x} = \alpha \int_0^x dx$$

$$\log_e (n_x / n_0) = \alpha \,.\, x$$

$$n_x = n_0 \cdot e^{\alpha x}$$

If the anode is at a distance x = d from the cathode, then the number of electrons n_d striking the anode per second is given by

$$n_d = n_0 \,.\, e^{\alpha d}$$

Therefore, on the average, each electron leaving the cathode produces $(n_d - n_0)/n_0$ new electrons (and corresponding positive ions) in the gap.

In the **steady state**, the number of positive ions arriving at the cathode/second must be exactly equal to the number of newly formed electrons arriving at the anode. Thus the circuit current will be given by

$$I = I_0 \,.\, e^{\alpha d}$$

where I_0 is the initial photo-electric current at the cathode.

In the actual breakdown process, the electron impact ionization is attended by secondary processes on the cathode, which replenish the gas gap with free electrons, with every newly formed avalanche surpassing the preceding one in the number of electrons.

Consider now the current growth equations with the secondary mechanism also present.

Let γ = number of secondary electrons (on average) produced at the cathode per ionising collision in the gap. [Townsend's second ionisation coefficient]

n_0 = number of primary photo-electrons/second emitted from the cathode

n_0' = number of secondary electrons/second produced at the cathode

n_0'' = total number of electrons/second leaving the cathode

Then $n_0' = n_0 + n_0''$

On the average, each electron leaving the cathode produces $[e^{\alpha d} - 1]$ collisions in the gap, giving the number of ionising collisions/second in the gap as $n_0'' (e^{\alpha d} - 1)$. Thus by definition

$$\gamma = \frac{n_0'}{n_0''(e^{\alpha d} - 1)}$$

giving $n_{0'} = \gamma\, n_0''(e^{\alpha d} - 1)$

but $n_0'' = n_0 + n_{0'}$

so that $n_0'' = n_0 + n_0''(e^{\alpha d} - 1).\gamma$

This gives the result

$$n_0'' = \frac{n_0}{1 - \gamma (e^{\alpha d} - 1)}$$

Similar to the case of the primary process (with α only), we have

$$n_d = n_0'' \, e^{\alpha d} = \frac{n_0 \, e^{\alpha d}}{1 - \gamma \, (e^{\alpha d} - 1)}$$

Thus, in steady state, the circuit current I will be given by

$$I = \frac{I_0 \, e^{\alpha d}}{1 - \gamma \, (e^{\alpha d} - 1)}$$

This equation describes the growth of average current in the gap before spark breakdown occurs.

As the applied voltage increases, $e^{\alpha d}$ and $\gamma \, e^{\alpha d}$ increase until $\gamma \, e^{\alpha d} \rightarrow 1$, when the denominator of the circuit current expression becomes zero and the current $\mathbf{I \rightarrow \infty}$. In this case, the current will, in practice, be limited only by the resistance of the power supply and the conducting gas.

This condition may thus be defined as the breakdown and can be written as

$$\gamma \, (e^{\alpha d} - 1) \; = \; 1$$

This condition is known as the **Townsend criteria for spark breakdown**.

The avalanche breakdown develops over relatively long periods of time, typically over 1 μs and does not generally occur with impulse voltages.

IV.2.1.2 Determination of Townsend's Coefficients α and γ

Townsend's coefficients are determined in an ionisation chamber which is first evacuated to a very high vacuum of the order of 10^{-4} and 10^{-6} torr before filling with the desired gas at a pressure of a few torr. The applied direct voltage is about 2 to 10 kV, and the electrode system consists of a plane high voltage electrode and a low voltage electrode surrounded by a guard electrode to maintain a uniform field. The low voltage electrode is earthed through an electrometer amplifier capable of measuring currents in the range 0.01 pA to 10 nA. The cathode is irradiated using an ultra-violet lamp from the outside to produce the initiation electron. The voltage current characteristics are then obtained for different gap settings. At low voltage the current growth is not steady. Afterwards the steady Townsend process develops as shown in figure IV.3.

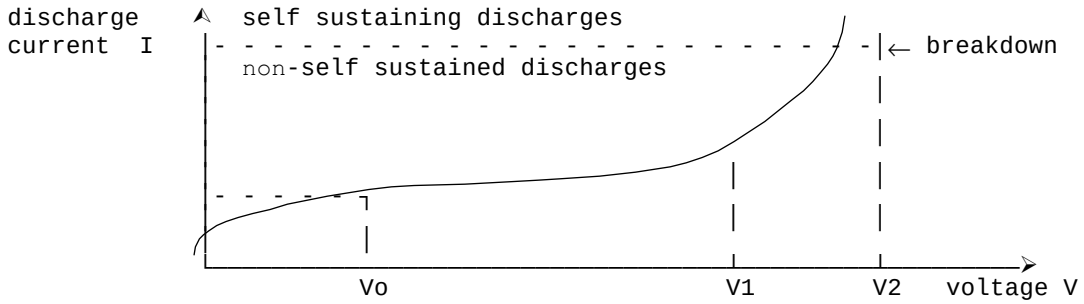

Figure IV.3 - Typical Current growth

From the Townsend mechanism, the discharge current is given by

$$I = \frac{I_0 \, e^{\alpha d}}{1 - \gamma \, (e^{\alpha d} - 1)} \approx I_0 \, e^{\alpha d} \quad \text{when } \alpha \, \text{d} \gg 1$$

This can be written in logarithmic form as

$$\ln I = \alpha d + \ln I_0$$

$$y = m x + c$$

From a graph of ln I vs d, the constants α and I_0 can be determined from the gradient and the intercept respectively, as in figure IV.4.

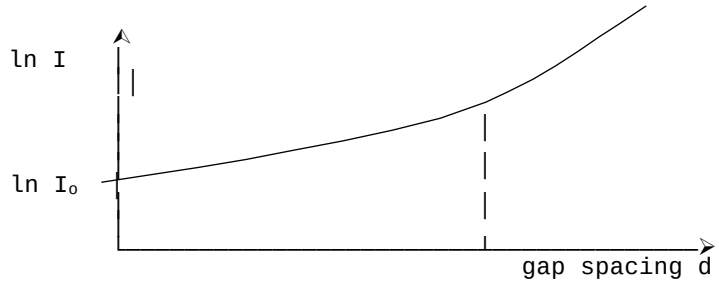

Figure IV.4 - Variation of ln I vs d

Once I_0 and α are known, γcan be determined from points on the upward region of the curve. The experiment can be repeated at different pressures if required.

IV.2.1.3 Breakdown in electronegative gases

In the above analysis, electron attachment to neutral molecules was not considered. Electron attachment removes free electrons and thus gives gases very high dielectric strengths. The gases in which electron attachment occurs are electro-negative gases.

An attachment coefficient η can be defined, analogous with α, as the number of attachments per electron per unit drift in the direction of the field. Under these conditions, the equation for the average current growth in a uniform field can be shown to be as follows.

$$I = I_0 \frac{\left[\frac{\alpha}{\alpha-\eta} e^{(\alpha-\eta)d} - \frac{\eta}{\alpha-\eta}\right]}{1-\gamma\frac{\alpha}{\alpha-\eta}\left[e^{(\alpha-\eta)d}-1\right]}$$

The corresponding criteria for spark breakdown is

$$\gamma\frac{\alpha}{\alpha-\eta}\left[e^{(\alpha-\eta)d}-1\right]=1$$

IV.2.2 Paschen's Law

When electrons and ions move through a gas in a uniform field E and gas pressure p, their mean energies attain equilibrium values dependant on the ratio E/p; or more precisely

$\alpha/p = f_1(E/p)$ and $\gamma = f_2(E/p)$

For a uniform field gap, the electric field E = V/d. Thus applying Townsend's criterion for spark breakdown of gases gives

$$\gamma (e^{\alpha d} - 1) = 1$$

which may be written in terms of the functions as

$$f_2\left(\frac{V}{p\,d}\right)\left[e^{p\,d\,f_1\left(\frac{V}{p\,d}\right)} - 1\right] = 1$$

This equation shows that the breakdown voltage V is an implicit function of the product of gas pressure p and the electrode separation d.

That is V = f (p.d)

In the above derivation the effect of temperature on the breakdown voltage is not taken into account. Using the gas equation **pressure . volume = mass . R . absolute Temperature**, we see that **pressure = density . R . absolute Temperature**. Thus the correct statement of the above expression is **V = f(ρ.d)**, where ρ is the gas density. This is the statement of **Paschen's Law**.

Under constant atmospheric conditions, it is experimentally found that the breakdown voltage of a uniform field gap may be expressed in the form

$$V = A \,.\, d + B \,.\, \sqrt{d}$$ where **d** is the gap spacing

For air, under normal conditions, A = 24.4 kV/cm and B = 6.29 kV/cm$^{1/2.}$

[The breakdown voltage gradient is about 30 kV/cm in uniform fields for small gaps of the order of 1 cm, but reduces to about 6 kV/cm for large gaps of several meters]

Figure IV.5 shows a typical breakdown vs spacing characteristic.

Figure IV.5 - Breakdown characteristic

This variation with spacing can be modified using Paschen's Law to include the variation with gas density as follows.

$$V = \frac{A}{\rho_0} \,.\, \rho\, d + \frac{B}{\rho_0^{1/2}} \,.\, (\rho\, d)^{1/2}$$

$$= A(\delta\, d) + B(\delta\, d)^{1/2}$$

where δ = relative density (or gas density correction factor).

This equation is true for gap spacings of more than 0.1 mm at N.T.P. However, with very low products of **pressure x spacing**, a minimum breakdown voltage occurs, known as the **Paschen's minimum**. This can be explained in the following manner.

Consider a gap of fixed spacing, and let the pressure decrease from a point to the right of the minimum (Figure IV.6).

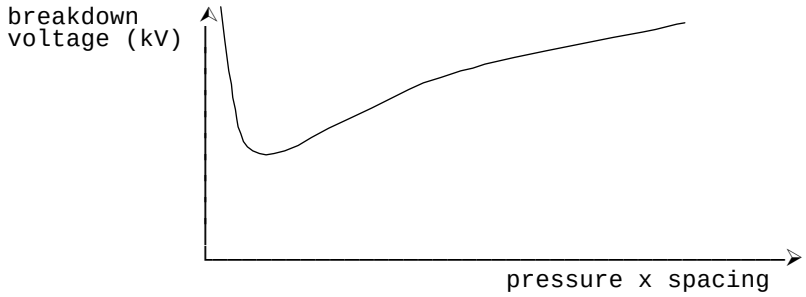

Figure IV.6 - Breakdown characteristic

The density therefore, decreases and an electron moving in the field consequently makes fewer collisions with gas molecules as it travels towards the anode. Since each collision results in a loss of energy, it follows that a lower electric stress suffices to impart to electrons the kinetic energy (½ m u^2) required to ionize by collision.

Gas	V_{min} (V)	p.d at V_{min} (torr-cm)
Air	327	0.567
Argon	137	0.9
Hydrogen	273	1.15
Helium	156	4.0
Carbon dioxide	420	0.51
Nitrogen	251	0.67
Nitrous oxide	418	0.5
Oxygen	450	0.7
Sulphur dioxide	457	0.33
Hydrogen Sulphide	414	0.6

Table IV.1 - Minimum sparking voltages

Near the minimum of the characteristic, the density is low and there are relatively few collisions. It is necessary now to take into account the fact that an electron does not necessarily ionize a molecule on collision with it, even if the energy of the electron exceeds the ionisation energy. The electrons have a finite chance of ionizing, which depends upon its energy. If the density and hence the number of collisions is decreased, breakdown can occur only if the chance of ionising is increased, and this accounts for the increase in voltage to the left of the minimum.

It is worth noting that if the density is fixed, breakdown to the left of the minimum occurs more readily (i.e. at lower voltage) at longer distances. Typically the voltage minimum is 300 V and occurs at a product or **p.d** of **5 torr mm**, or at a gap of about 0.06 mm at N.T.P.

At very low pressures, and at very high pressures (compared with atmospheric), Paschen's Law fails. Also, Paschen's Law is valid for temperatures below about 1100^0C. A further increase in temperature ultimately results in the failure of Paschen's Law because of thermal ionisation.

It can be seen from the breakdown characteristic, that for a constant gap spacing, the breakdown voltage, and hence the breakdown stress required, is very much higher than at atmospheric conditions, under very high pressure and under very low pressures (high vacuum) conditions. Thus both high vacuum as well as high gas pressure can be used as insulating media. [The vacuum breakdown region is that in which the breakdown voltage becomes independent of the gas pressure] Under normal conditions, operation is well to the right of Paschen's minimum.

The table 1.1 gives the minimum sparking potential for various gases.

IV.2.3 Streamer Mechanism

This type of breakdown mainly arises due to the added effect of the space-charge field of an avalanche and photo-electric ionization in the gas volume. While the Townsend mechanism predicts a very diffused form of discharge, in actual practice many discharges are found to be filamentary and irregular. The Streamer theory predicts the development of a spark discharge directly from a single avalanche. The space charge produced in the avalanche causes sufficient distortion of the electric field that those free electrons move towards the avalanche head, and in so doing generate further avalanches in a process that rapidly becomes cumulative. As the electrons advance rapidly, the positive ions are left behind in a relatively slow-moving tail.The field will be enhanced in front of the head. Just behind the head the field between the electrons and the positive ions is in the opposite direction to the applied field and hence the resultant field strength is less. Again between the tail and the cathode the field is enhanced. (Figure IV.7)

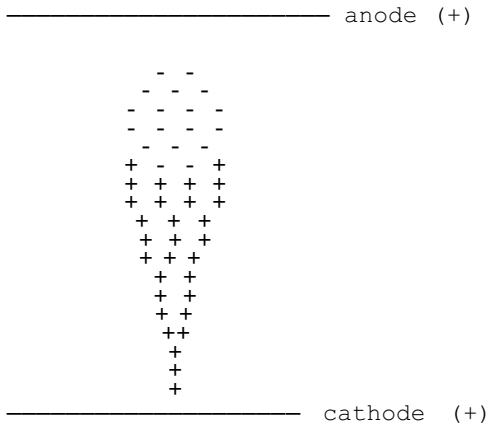

Figure IV.7 - Streamer Mechanism

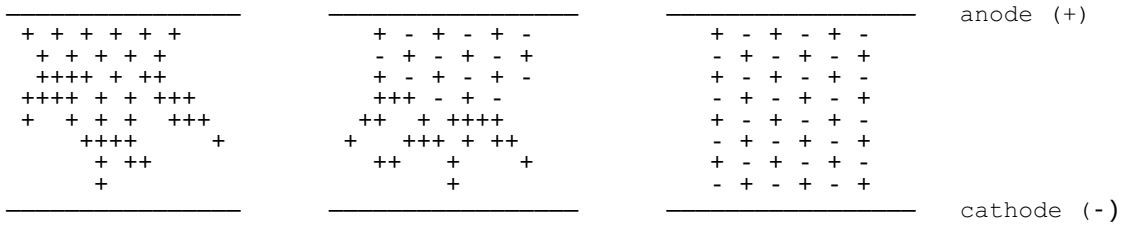

Figure IV.8 - Streamer breakdown

Due to the enhanced field between the head and the anode, the space charge increases, causing a further enhancement of the field around the anode. The process is very fast and the positive space charge extends to the cathode very rapidly resulting in the formation of a streamer . Figure IV.8 shows the breakdown process.

IV.2.4 Factors affecting the breakdown voltage a Vacuum gap

Vacuum is ideally the best insulator, with breakdown strengths of the order of 10^4 kV/c. The breakdown voltage of a high vacuum is the voltage which when increased by a small amount will cause the breakdown of the gap that was held at that voltage for an infinite time. However, this definition is not always practicable as the breakdown is affected by many factors.

(i) Electrode Separation

For vacuum gaps less than about 1 mm, the breakdown voltage is approximately proportional to the length, all other parameters remaining constant. This gives a constant breakdown strength. For these small gaps, the breakdown stress is relatively high, being of the order of 1 MV/cm. Field emission of electrons probably plays an important part in the breakdown process.

$$V = k \, . \, d \qquad \text{for } d < 1 \text{ mm}$$

For gaps greater than about 1 mm, the breakdown voltage does not increase at an equal rate and the apparent breakdown stress for longer gaps is much reduced, being about 10 kV/cm at a spacing of 10 cm. [Apparent stress is defined as the voltage required to cause breakdown divided by the distance between the electrodes]. Figure IV.9.

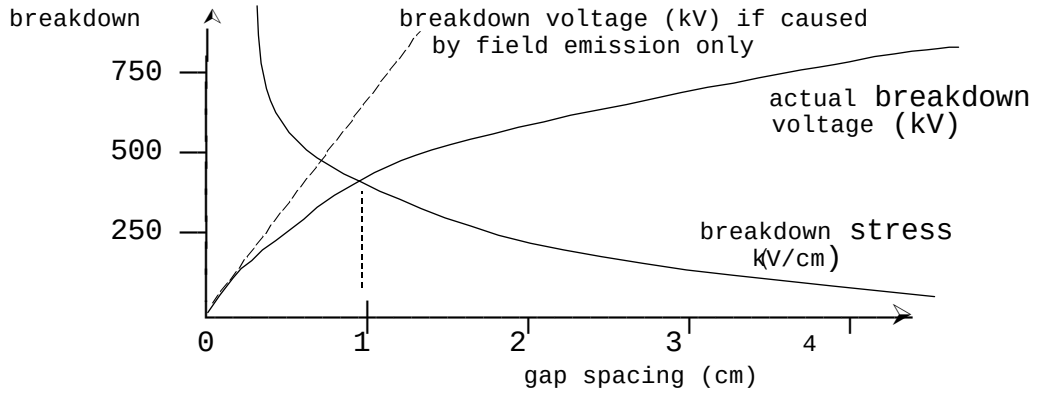

Figure VI.9 - Breakdown characteristic

Cranberg has shown theoretically that for longer gaps, it is the product of breakdown voltage and breakdown stress that remains constant.

$$V \, . \, E = k_1 \qquad \text{for } d > 1 \text{ mm.}$$

where the constant k_1 depends on the material and surface conditions of the electrodes.

For an **Uniform field gap**, E = V/d, so that

$$V = k_2 \, d^{1/2}$$

Or in a more general form, both regions can be expressed by the equation

$$V = k \, d^{x} \qquad \text{where } x = 0.5 \text{ for long gaps} > 1 \text{ mm}$$
$$= 1 \quad \text{for gaps} < 1\text{mm}$$

(ii) Electrode Effects

Conditioning

The breakdown voltage of a gap increases on successive flashovers, until a constant value is reached. The electrodes are then said to be conditioned. This increase in voltage is ascribed to the burning off by sparking of microscopic irregularities or impurities which may exist on the electrodes. When investigating the effect of various factors on breakdown, the electrodes must first be conditioned in such a way that reproducible results are obtained.

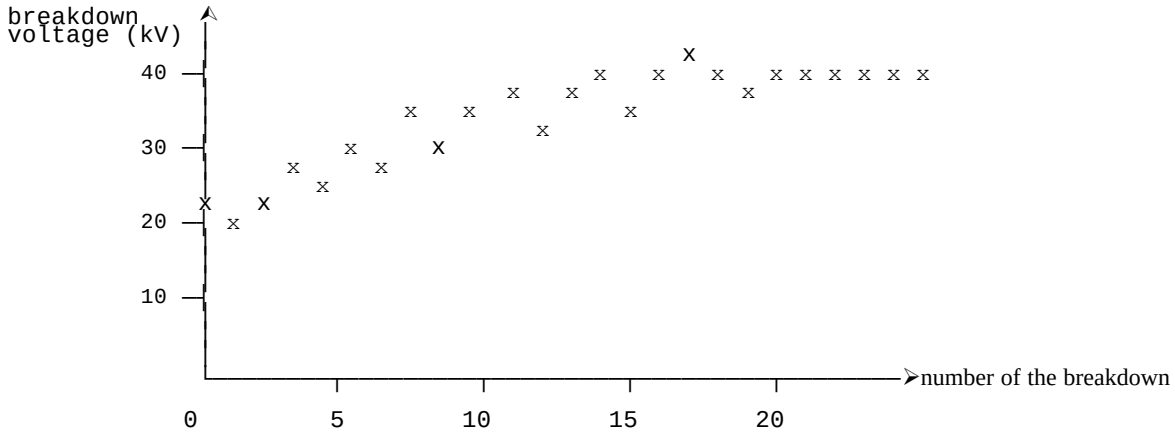

Figure IV.10 - Breakdown characteristics

The effect of conditioning is shown in figure IV.10. The breakdown voltage of conditioned electrodes or gaps is very much reproducible than otherwise , and hence breakdown values that are normally obtained experimentally are those of conditioned electrodes. Unconditioned electrodes may have breakdown values a low as 50% of the breakdown voltage with conditioned electrodes.

(iii) Material and Surface Finish

Electrode Material	Voltage across 1 mm gap (kV)
Steel	122
Stainless Steel	120
Nickel	96
Monel metal	60
Aluminium	41
Copper	37

Table IV.2 - Effect of electrode material on breakdown

The electrode surfaces form the physical boundaries between which the breakdown finally takes place. Thus it is not surprising to find that the breakdown strength of a given size of gap is strongly dependant on the material of the electrodes. In general, the smoother the surface finish, the greater the breakdown voltage.

(iv) Surface contamination

Presence of contamination in the test cell reduces the breakdown voltage sometimes by as much as 50% of the clean electrode value.

(v) Area and configuration of electrodes

Increasing the area of the electrodes makes it more difficult to maintain a given breakdown voltage. Thus breakdown voltage decreases slightly with increase in surface area. For example, electrodes of 20 cm^2 area gives the breakdown voltage across a 1 mm gap of 40 kV, whereas electrodes of the same material of area 1000 cm^2 gives a breakdown voltage across the same 1 mm gap as 25 kV.

Up to 1 mm gap, the more convex electrodes have higher breakdown voltage than the more nearly plane electrodes even though at the same voltage they carried a higher electric field at the surface.

(vi) Temperature

The variation of the breakdown voltage with temperature is very small, and for nickel and iron electrodes, the strength remains unchanged for temperatures as high as 500^0C. Cooling the electrodes to liquid Nitrogen temperature increases the breakdown voltage.

(vii) Frequency of applied voltage

It is known that a given gap stands a higher impulse voltage than an alternating voltage, and a higher alternating voltage than a direct voltage. However, it has been shown that for a small gap (2 mm) there is no dependence of the breakdown voltage on the frequency in the range 50 Hz to 50 kHz.

(viii) Vacuum Pressure

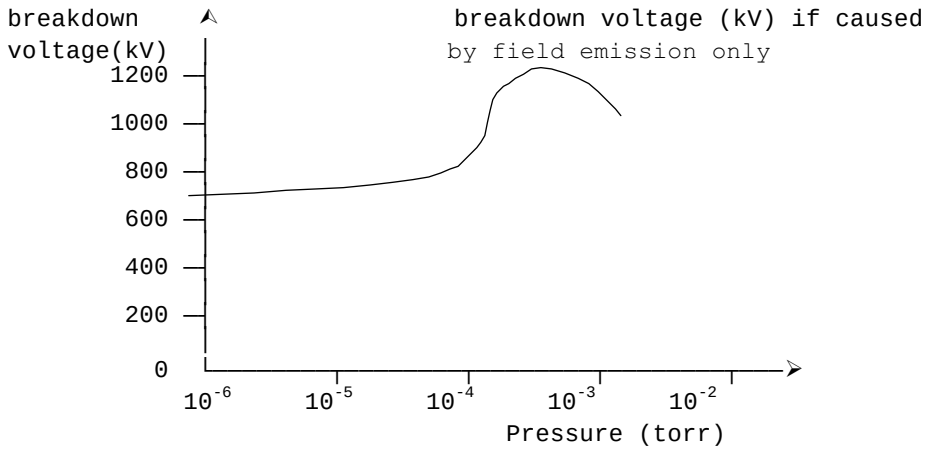

Figure IV.11 - Breakdown characteristic

For small gaps, increasing the degree of vacuum increases the breakdown voltage until below a certain pressure there is no change. The vacuum breakdown region is the region in which the breakdown voltage becomes independent of the nature of the pressure of the gap between the electrodes.

However, for large gaps (about 200 mm spacing) it is found that below a certain pressure the breakdown voltage starts decreasing again, so that the breakdown stress at this stage could in fact be improved by actually worsening the vacuum.

For example, using a 1.6 mm diameter sphere opposite a plane cathode and a gap of 200 mm, the characteristics shown in figure 1.11 was obtained. The breakdown voltage was constant for pressure less than 5×10^{-4} torr, but rose with increasing pressure to a maximum at 5×10^{-4} torr, with further increase in pressure the voltage fell sharply.

IV.2.5 Time lags of Spark breakdown

In practice, particularly in high voltage engineering, breakdown under impulse fields is of great importance. On the application of a voltage, a certain time elapses before actual breakdown occurs even though the applied voltage may be much more than sufficient to cause breakdown.

In considering the time lag observed between the application of a voltage sufficient to cause breakdown and the actual breakdown the two basic processes of concern are the appearance of avalanche initiating electrons and the temporal growth of current after the criterion for static breakdown is satisfied.

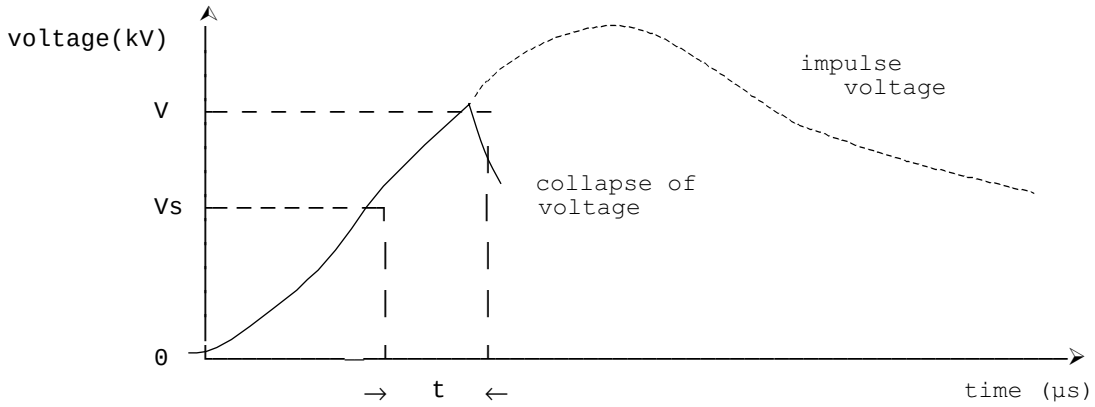

Figure IV.12 - Time lag of impulse breakdown

In the case of slowly varying fields, there is usually no difficulty in finding an initiatory electron from natural sources (ex. cosmic rays, detachment of gaseous ions etc). However, for impulses of short duration (around 1 μs), depending on the gap volume, natural sources may not be sufficient to provide an initiating electron while the voltage is applied, and in the absence of any other source, breakdown will not occur. Figure IV.12 shows the time lag for an impulse voltage waveform.

The time t_s which elapses between the application of a voltage greater than or equal to the static breakdown voltage (V_s) to the spark gap and the appearance of a suitably placed initiatory electron is called the statistical time lag of the gap, the appearance being usually statistically distributed.

After such an electron appears, the time t_f required by the ionisation processes to generate a current of a magnitude which may be used to specify breakdown of the gap is known as the formative time lag. The sum $t_f + t_s = t$ is the total time lag, and is shown in the diagram. The ratio V/V_s, which is greater than unity, is called the impulse ratio, and clearly depends on $t_s + t_f$ and the rate of growth of the applied voltage.

The breakdown can also occur after the peak of the voltage pulse, (i.e. on the wavetail). Depending on the time lag, the breakdown may occur in the wavefront or the wavetail of the impulse waveform.

(i) Statistical Time lag t_s

The statistical time lag is the average time required for an electron to appear in the gap in order that breakdown may be initiated.

If β = rate at which electrons are produced in the gap by external irradiation
P_1 = probability of an electron appearing in a region of the gap where it can lead to a spark
P_2 = probability that such an electron appearing in the gap will lead to a spark

then, the average time lag $$t_s = \frac{1}{\beta P_1 P_2}$$

If the level of irradiation is increased, β increases and therefore t_s decreases. Also, with clean cathodes of higher work function β will be smaller for a given level of illumination producing longer time lags.

The type of irradiation used will be an important factor controlling P_1, the probability of an electron appearing in a favourable position to produce breakdown. The most favourable position is, of course near the cathode.

If the gap is overvolted, then the probability of producing a current sufficient to cause breakdown rapidly increases. P_2 therefore increases with overvoltage and may tend to unity when the overvoltage is about 10%. As $P_2 \rightarrow 1$ with increasing overvoltage, $t_s \rightarrow 1/\beta P_1$.

(ii) Formative time lag

After the statistical time lag, it can be assumed that the initiatory electron is available which will eventually lead to breakdown. The additional time lag required for the breakdown process to form is the formative time lag. An uninterrupted series of avalanches is necessary to produce the requisite gap current (μA) which leads to breakdown, and the time rate of development of ionisation will depend on the particular secondary process operative. The value of the formative time lag will depend on the various secondary ionisation processes. Here again, an increase of the voltage above the static breakdown voltage will cause a decrease of the formative time lag tf.

(iii) Time lag characteristic

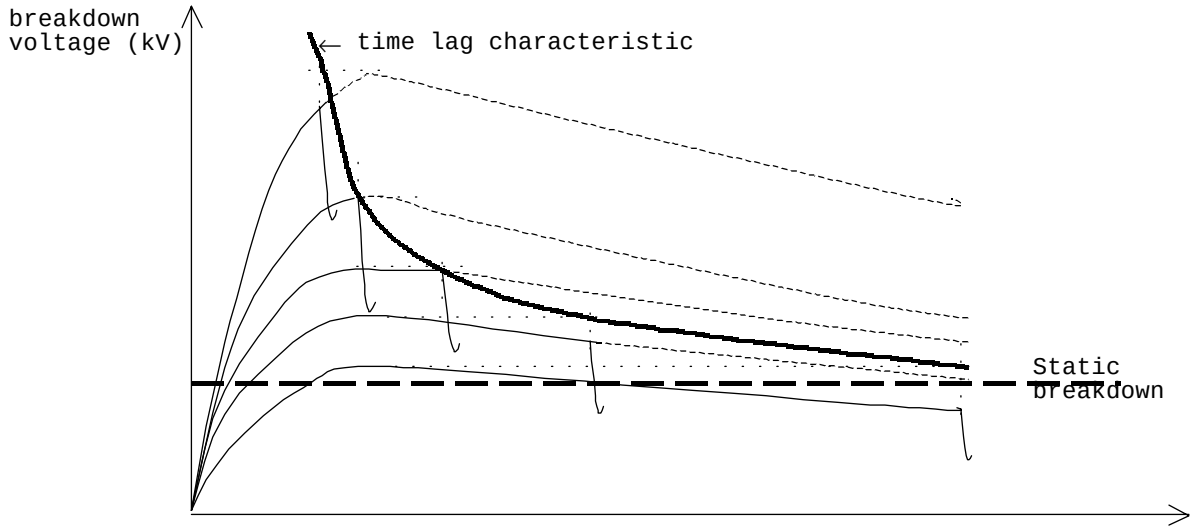

Figure IV.13 - Time-lag characteristics

The time lag characteristic is the variation of the breakdown voltage with time of breakdown, and can be defined for a particular waveshape. The time lag characteristic based on the impulse waveform is shown in figure IV.13.

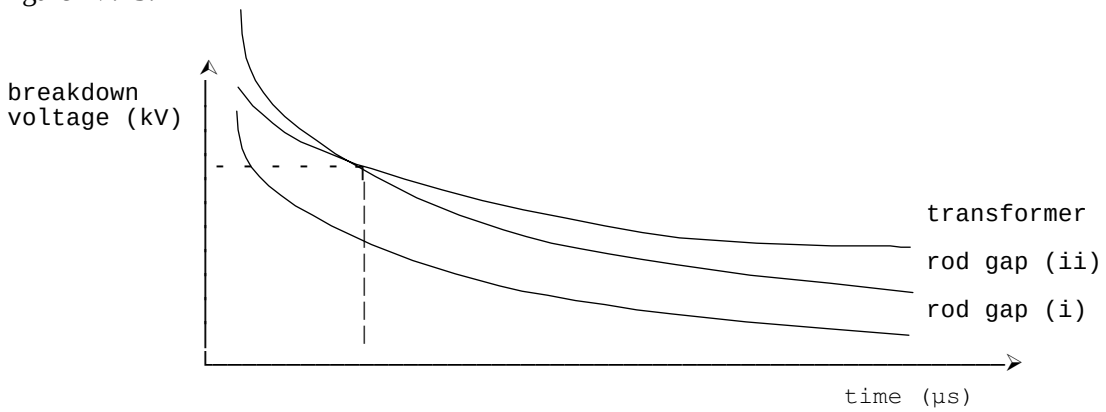

Figure IV.14 - Typical Time lag characteristics

The time lag characteristic is important in designing insulation. If a rod gap is to provide secondary protection to a transformer, then the breakdown voltage characteristic of the rod gap must be less than that of the transformer at all times (gap i) to protect it from dangerous surge voltages. This will ensure that the gap will always flashover before the protected apparatus. This is shown in figure IV.14.

However, with such a rod gap, the gap setting will be low, as the sharpness of the two characteristics are different. Thus it is likely that there would be frequent interruptions, even due to the smallest overvoltages which would in fact cause no harm to the system. Thus it is usual to have the rod gap characteristic slightly higher (gap ii) resulting in the intersection of the characteristics as shown. In such a case, protection will be offered only in the region where the rod gap characteristic is lower than that of the transformer. This crossing point is found from experience for a value of voltage which is highly unlikely to occur. The other alternative is of course to increase the transformer characteristic which would increase the cost of the transformer a great deal. [This decision is something like saying, it is better and cheaper to replace 1 transformer a year due to this decision than have to double the cost of each of 100 such transformers in the system.]

IV.2.6 Corona Discharges

In a uniform electric field, a gradual increase in voltage across a gap produces a breakdown of the gap in the form of a spark without any preliminary discharges. On the other hand, if the field is non-uniform, an increase in voltage will first cause a localised discharge in the gas to appear at points with the highest electric field intensity, namely at sharp points or where the electrodes are curved or on transmission line conductors. This form of discharge is called a corona discharge and can be observed as a bluish luminance. This phenomena is always accompanied by a hissing noise, and the air surrounding the corona region becomes converted to ozone. Corona is responsible for considerable power loss in transmission lines and also gives rise to radio interference.

IV.2.6.1 Mechanism of Corona formation on a 2 conductor line

When a gradually increasing voltage is applied across two conductors, initially nothing will be seen or heard. As the voltage is increased, the air surrounding the conductors get ionised, and at a certain voltage a hissing noise is heard caused by the formation of corona. This voltage is known as the disruptive critical voltage (**dcv**). A further increase in the voltage would cause a visible violet glow around the conductors. This voltage is the visual corona inception voltage.

If the applied voltage is direct, the glow observed will be uniform on the positive conductor, while the negative conductor will be more patchy and often accompanied by streamers at rough points. In the case of alternating voltages, both conductors appear to have a uniform glow, but when observed stroboscopically the effect is seen to be similar to the direct voltage case.

If the voltage is further increased, the corona increases and finally spark over would occur between the two conductors. If the conductors are placed quite close together, corona formation may not occur before the spark over occurs. The condition for this will be considered later.

The formation of corona causes the current waveform in the line, and hence the voltage drop to be non-sinusoidal. It also causes a loss of power.

There is always some electrons present in the atmosphere due to cosmic radiation etc. When the line voltage is increased, the velocity of the electrons in the vicinity of the line increases, and the electrons acquire sufficient velocity to cause ionisation.

To prevent the formation of corona, the working voltage under fair weather conditions should be kept at least 10% less than the disruptive critical voltage.

Corona formation may be reduced by increasing the effective radius. Thus steel cored aluminium has the advantage over hard drawn copper conductors on account of the larger diameter, other conditions remaining the same. The effective conductor diameter can also be increased by the use of bundle conductors.

Corona acts as a safety valve for lightning surges, by causing a short circuit. The advantage of corona in this instance is that it reduces transients by reducing the effective magnitude of the surge by partially dissipating its energy due to corona.

The effect of corona on radio reception is a matter of some importance. The current flowing into a corona discharge contains high-frequency components. These cause interference in the immediate vicinity of the line. As the voltage is gradually increased, the disturbing field makes its appearance long before corona loss becomes appreciable. The field has its maximum value under the line and attenuates rapidly with distance. The interference fails to about a tenth at 50 m from the axis of the line.

IV.2.6.2 Waveform of Corona Current

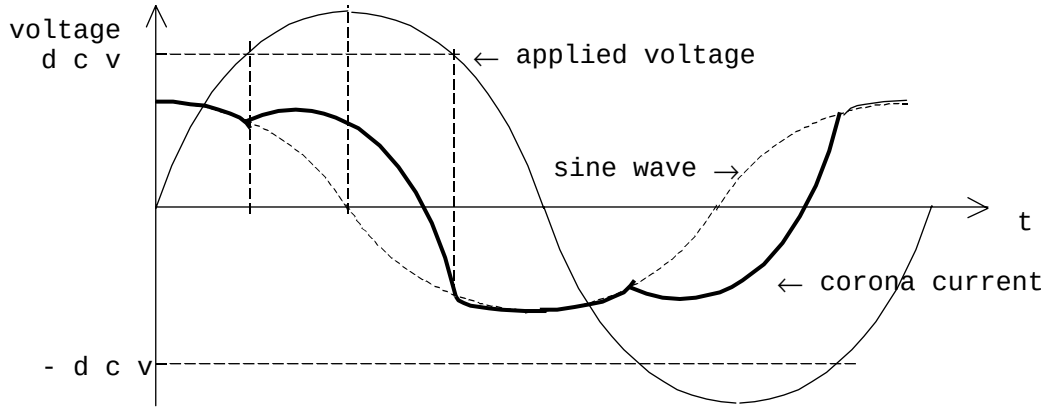

Figure IV.15 Waveform of corona current

The shunt current in a line is almost purely capacitive under normal conditions, and leads the applied voltage by 90^0, and there is no power loss in the line under no-load conditions. When the applied voltage is increased and corona is formed, the air is rendered conducting, and power loss occurs. The shunt current would no longer be leading the voltage by 90^0. Thus the current waveform would consist of two components. The lossy component would be non-sinusoidal and would occur only when the disruptive critical voltage is exceeded in either polarity. This resultant waveform is shown in figure IV.15. The corona current can be analysed and shown to possess a strong third harmonic component.

IV.2.6.3 Mechanism of corona formation

The stress surrounding the conductor is a maximum at the conductor surface itself, and decreases rapidly as the distance from the conductor increases. Thus when the stress has been raised to critical value immediately surrounding the conductor, ionisation would commence only in this region and the air in this region would become conducting. The effect is to increase the effective conductor diameter while the voltage remains constant. This results in two effects. Firstly, an increase in the effective sharpness of the conductor would reduce the stress outside this region, and secondly, this would cause a reduction of the effective spacing between the conductors leading to an increase in stress. Depending on which effect is stronger, the stress at increasing distance can either increase or decrease. If the stress is made to increase, further ionisation would occur and flashover is inevitable.

Under ordinary conditions, the breakdown strength of air can be taken as 30 kV/cm. Corona will of course be affected by the physical state of the atmosphere. In stormy weather, the number of ions present is generally much more than normal, and corona will then be formed at a much lower voltage than in fair weather. This reduced voltage is generally about 80% of the fair weather voltage.

The condition for stable corona can be analysed as follows.

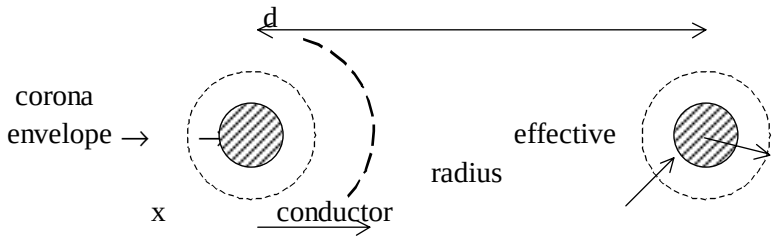

Figure IV.16 - Electric Stress in two conductor system

The electric stress ξ at a distance x from a conductor of radius x, and separated from the return conductor by a distance d is given by

$$\xi = \frac{1}{\varepsilon_0} . \frac{q}{2\pi x l}$$

where q is the charge on each conductor in length *l*.

Thus the potential V can be determined from $V = \int \xi \, dx$

$$V = \int_{r}^{d-r} \frac{q}{2\pi x \varepsilon_0} . dx$$

Since both charges (+q and -q) produce equal potential differences, the total potential difference between the two conductors is double this value. Thus the conductor to neutral voltage, which is half the difference would be equal to this value. Thus the conductor to neutral voltage is

$$V = \frac{q}{2\pi \varepsilon_0} . \log_e \left(\frac{d - r}{r} \right)$$

Therefore the electric stress at distance x is given by

$$\xi_x = \frac{V}{x \log_e \frac{d - r}{r}}$$

$$\xi_x = \frac{V}{x \log_e \frac{d}{r}} \quad \text{if } d \ll r$$

[Note; ξ_x and V can both be peak values or both rms values]

For three phase lines, with equilateral spacing, it can be shown that the stress is still given by the same expression when V is the voltage to neutral and d is the equilateral spacing.

For air, ξ_{max} = 30 kV/cm, so that ξ_{rms} = 30/√2 = 21.2 kV/cm.

Since there is no electric stress within the conductor, the maximum stress will occur when x is a minimum, that is at x = r.

Thus if $E_{0,rms}$ is the rms value of the disruptive critical voltage to neutral,

$$\xi_{rms} = 21.2 = \frac{E_{0,rms}}{r \log_e \frac{d}{r}}$$

When the surface of the conductor is irregular, it is more liable to corona. Thus an irregularity factor m_0 is introduced to account for this reduction. Typical values of this factor are

m_0 =	1.0	for smooth polished conductors,
=	0.98 to 0.93	for roughened conductors,
≈	0.90	for cables of more than 7 strands, and
=	0.87 to 0.83	for 7 strand cables.

Since the corona formation is affected by the mean free path, and hence by the air density, a correction factor δ is introduced. This air density correction factor is given by the usual expression, with **p** being the pressure expressed in **torr** and **t** being the temperature expressed in ^{0}C.

$$\delta = \frac{p}{760} \cdot \frac{273 + 20}{273 + t} = \frac{0.386\ p}{273 + t}$$

The disruptive critical voltage can then be written as in the following equation.

$$E_{0,rms} = 21.2\ \delta\ m_0\ r \log_e (d/r) \qquad \text{kV to neutral}$$

IV.2.6.4 Visual Corona

Visual corona occurs at a higher voltage than the disruptive critical voltage. For the formation of visual corona, a certain amount of ionization, and the raising of an electron to an excited state are necessary. The production of light by discharge is not due to ionisation, but due to excitation, and subsequent giving out of excess energy in the form of light and other electromagnetic waves. To obtain the critical voltage for visual corona formation, the disruptive critical voltage has to be multiplied by a factor dependant on the air density and the conductor radius. Further the value of the irregularity factor is found to be different.

The empirical formula for the formation of visual corona is

$$E_{v,rms} = 21.2\ m_v\ \delta\ r \left[1 + \frac{0.3}{\sqrt{\delta\ r}}\right] . \log_e \frac{d}{r}$$

The values of the irregularity factor m_v for visual corona is given by

m_v =	1.0	for smooth conductors,
=	0.72	for local corona on stranded wires (patches)
=	0.82	for decided corona on stranded wires (all over the wire)

IV.2.6.5 Stable Corona formation

Consider two conductors, just on the limit of corona formation. Assume that there is a thin layer Δr of ionised air around each conductor, so that the effective radius becomes (r + Δr). The change in electric stress Δξ due to this layer can be determined using differentiation.
Thus

$$\Delta\xi = \Delta\left(\frac{E}{r\log_e\frac{d}{r}}\right)$$

$$\Delta\xi = \left[\frac{-E}{(r\log_e\frac{d}{r})^2}.\left(\log_e\frac{d}{r} + r.\frac{r}{d}.\frac{-d}{r^2}\right)\right].\Delta r$$

$$\Delta\xi = \frac{E(1-\log_e\frac{d}{r}).\Delta r}{(r\log_e\frac{d}{r})^2}$$

When $\log_e > 1$, the above expression is negative. i.e. d/r > e (=2.718)

Under this condition, the effective increase in diameter lowers the electric stress and no further stress increase is formed, and corona is stable. If on the other hand, d/r < e, then the effective increase in the diameter raises the electric stress, and this causes a further ionisation and a further increase in radius, and finally leads to flash-over.

In practice, the effective limiting value of d/r is about 15 and not **e** (=2.718). For normal transmission lines, the ratio d/r is very much greater than 15 and hence stable corona always occurs before flashover.

For example, in a 132 kV line with a spacing of 4 m and a radius of conductor of 16 mm, the ratio has a value $d/r = 4/16\text{x}10^{-3} = 250 >> 15$.

IV.2.6.6 Power Loss due to Corona

The formation of corona is associated with a loss of power. This loss will have a small effect on the efficiency of the line, but will not be of sufficient importance to have any appreciable effect on the voltage regulation. The more important effect is the radio interference.

The power loss due to corona is proportional to the square of the difference between the line-to-neutral voltage of the line and the disruptive critical voltage of the line. It is given by the empirical formula

$$P_c = \frac{243}{\delta}.(f+25).\sqrt{\frac{r}{d}}.(E - E_{0,rms})^2.10^{-5} \text{ kW/km/phase}$$

where $E_{0,rms}$ = disruptive critical voltage (kV)
f = frequency of supply (Hz)
E = Phase Voltage (line to neutral) (kV)

For storm weather conditions, the disruptive critical voltage is to be taken as 80% of disruptive critical voltage under fair weather conditions.

Example

Determine the Disruptive Critical Voltage,the Visual Corona inception voltage, and the power loss in the line due to corona, both under fair weather conditions as well as stormy weather conditions for a 100 km long 3 phase, 132 kV line consisting of conductors of diameter 1.04 cm, arranged in an equilateral triangle configuration with 3 m spacing. The temperature of the surroundings is 40^0 C and the pressure is 750 torr. The operating frequency is 50 Hz. [The irregularity factors may be taken as $m_o = 0.85$, $m_v = 0.72$]

The Air density correction factor δ is given by

$$\delta = \frac{p}{760}.\frac{273+20}{273+t} = \frac{0.386\ p}{273+t}$$

$$\delta = \frac{750}{760}.\frac{293}{313} = 0.925$$

$\therefore$ Disruptive critical voltage = 21.2 δ m_0 r $\log_e$ (d/r) kV to neutral
= 21.2 x 0.925 x 0.85 x 0.52 x $\log_e$ (3/0.0052)
= 55.1 kV

Similarly,
Visual corona voltage = 21.2 x 0.925 x 0.72 x 0.52 x $\log_e$ (3/0.0052) x [1 + 0.3/(0.895 x 0.52)^{½}]
= 67.2 kV

Power loss under fair weather condition is given by

$$P_c = \frac{243}{0.925}.(50+25).\sqrt{\frac{0.0052}{3}}.\left(\frac{132}{\sqrt{3}} - 55.1\right)^2.10^{-5}.100 \quad \text{kW/phase}$$

$$= 365 \ \text{kW/phase}$$

Similarly, power loss under stormy weather condition is given by

$$P_c = \frac{243}{0.925}.(50+25).\sqrt{\frac{0.0052}{3}}.\left(\frac{132}{\sqrt{3}} - 55.1*0.8\right)^2.10^{-5}.100 \quad \text{kW/phase}$$

$$= 847 \ \text{kW/phase}$$

Chapter V:

HIGH VOLTAGE GENERATORS

Chapter V: HIGH VOLTAGE GENERATORS

In the fields of electrical engineering and applied physics, high voltages (dc, ac, and impulse) are required for several applications. For example, electron microscopes and X-ray units require high dc voltages of the order of 100 kV or more. Electrostatic precipitators, particle accelerators in nuclear physics, etc. require high voltages (dc) of several kilovolts and even megavolts. High ac voltages of one million volts or even more are required for testing power apparatus rated for extra high transmission voltages (400 kV system and above). High impulse voltages are required for testing purposes to simulate overvoltages that occur in power systems due to lightning or switching action. For electrical engineers, the main concern of high voltages is for the insulation testing of various components in power systems for different types of voltages, namely, power frequency ac, high frequency, ac switching or lightning impulses. Hence, generation of high voltages in laboratories for testing purposes is essential and is discussed in this chapter.

Different forms of high voltages mentioned above are classified as

(i) high dc voltages,
(ii) high ac voltages of power frequency,
(iii) high ac voltages of high frequency,
(iv) high transient or impulse voltages of very short duration such as lightning overvoltages, and
(v) transient voltages of longer duration such as switching surges.

Normally, in high-voltage testing, the current under conditions of failure is limited to a small value (less than an ampere in the case of dc or ac voltages and few amperes in the case of impulse or transient voltages). But in certain cases, like the testing of surge diverters or the short-circuit testing of switchgear, high-current testing with several hundreds of amperes is of importance. Tests on surge diverters require high-surge currents of the order of several kiloamperes. Therefore, test facilities require high-voltage and high-current generators. High impulse current generation is also required along with voltage generation for testing purposes.

Chapter V: HIGH VOLTAGE GENERATORS

V.1 GENERATION OF HIGH DIRECT-CURRENT VOLTAGES

Generation of high dc voltages is mainly requited in research work in the areas of pure and applied physics. Sometimes, high direct voltages are needed in insulation tests on cables and capacitors. Impulse generator charging units also require high dc voltages of about 100 to 200 kV. Normally, for the generation of dc voltages of up to 100 kV, electronic valve rectifiers are used and the output currents are about 100 mA. The rectifier valves require special construction for cathode and filaments since a high electrostatic field of several kV/cm exists between the anode and the cathode in the non-conduction period. The ac supply to the rectifier tubes may be of power frequency or may be of audio frequency from an oscillator. The latter is used when a ripple of very small magnitude is required without the use of costly filters to smoothen the ripple.

V.1.1 Half- and Full-Wave Rectifier Circuits

Rectifier circuits for producing high dc voltages from ac sources may be (a) half wave, (b) full wave, or (c) voltage doubler-type rectifiers. The rectifier may be an electron tube or a solid-state device. Nowadays single electron tubes are avai lable for peak inverse voltages up to 250 kV, and semiconductor or solid state diodes up to 20 kV. For higher voltages, several units are to be used in series. When a number of units are used in series, transient voltage distribution along each unit becomes non-uniform and special care should be taken to make the distribution uniform. Commonly used half-wave and full-wave rectifiers are shown in Figure V.1. In the half wave rectifier (Figure V.1a) the capacitor is charged to V_{max}, the maximum ac voltage of the secondary of the high-voltage transformer in the conducting half cycle. In the other half cycle, the capacitor is discharged into the load. The value of the capacitor C is chosen such that the time constant CR_L is at least 10 times that of the period of the ac supply. The rectifier valve must have a peak inverse rating of at least $2V_{max}$. To limit the charging current, an additional resistance R is provided in series with the secondary of the transformer (not shown in the figure).

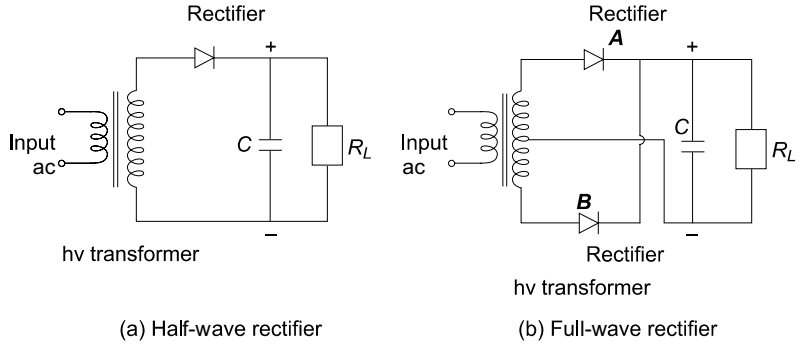

Figure. V.1 *Full- and half-wave rectifiers*

A full-wave rectifier circuit is shown in Fig. V.1b. In the positive half-cycle, the rectifier *A* conducts and charges the capacitor *C*, while in the negative half-cycle, the rectifier *B* conducts and charges the capacitor. The source transformer requires a centre-tapped secondary with a rating of 2 V.

For applications at high voltages of 50 kV and above, the rectifier valves used are of special construction. Apart from the filament, the cathode and the anode, they contain a protective shield or grid around the filament and the cathode. The anode will usually be a circular plate. Since the electrostatic field gradients are quite large, the heater and the cathode experience large electrostatic forces during the non-conduction periods. To protect the various elements from these forces, the anode is firmly fixed to the valve cover on one side. On the other side, where the cathode and filament are located, a steel mesh structure or a protective grid kept at the cathode potential surrounds them so that the mechanical forces between the anode and the cathode are reflected on the grid structure only.

In modern high-voltage laboratories and testing installations, semiconductor rectifier stacks are commonly used for producing dc voltages. Semiconductor diodes are not true valves since they have finite but very small conduction in the backward direction. The more commonly preferred diodes for high-voltage rectifiers are silicon diodes with *Peak Inverse Voltage (PIV)* of 1 kV to 2 kV. However, for laboratory applications, the current requirement is small (a few milliamperes, and less than one ampere) and as such, a selenium element stack with PIV of up to 500 kV may be employed without the use of any voltage grading capacitors.

Both full wave and half-wave rectifiers produce dc voltages less than the ac maximum voltage. Also, ripple or the voltage fluctuation will be present, and this has to be kept within a reasonable limit by means of filters.

Ripple Voltage with Half-Wave and Full-Wave Rectifiers

When a full-wave or a half-wave rectifier is used along with the smoothing capacitor *C*, the voltage on no load will be the maximum ac voltage. But when on load, the capacitor gets charged from the supply voltage and discharges into load resistance R_L whenever the supply voltage waveform varies from peak value to zero value. These waveforms are shown in Figure.V.2. When loaded, a fluctuation in the output dc voltage δV appears, and is called a ripple. The ripple voltage δV is larger for a half-wave rectifier than that for a full-wave rectifier, since the discharge period in the case of half-wave rectifier is larger as shown in Figure V.3. The ripple δV depends on (a) the supply voltage frequency f, (b) the time constant CR_L, and (c) the reactance of the supply transformer X_L. For half-wave rectifiers, the ripple frequency is equal to the supply frequency and for full-wave rectifiers, it is twice that value. The ripple voltage is to be kept as low as possible with the proper choice of the filter capacitor and the transformer reactance for a given load R_L.

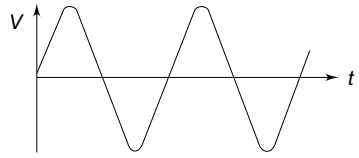

(a) Input sine wave

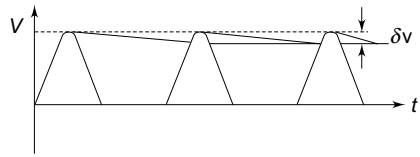

(b) Output with half-wave rectifier and capacitor filter

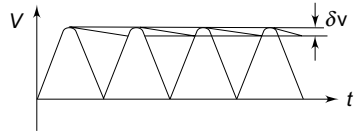

(c) Output with full-wave rectifier and capacitor filter

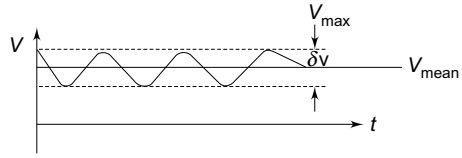

(d) V_{max} V_{mean} , and ripple voltage and δV with capacitor filter of a full wave rectifier.

Figure. V.2 *Input and output waveforms of half- and full-wave recti fiers*

V.1.2 Voltage Doubler Circuits

Both full-wave and half-wave rectifier circuits produce a dc voltage less than the ac maximum voltage. When higher dc voltages are needed, a voltage doubler or cascaded rectifier doubler circuits are used. The schematic diagram of voltage doublers are given in Figure V.3a and b.

In the voltage doubler circuit shown in Figure .V.3a, the capacitor C_1 is charged through rectifier R_1 to a voltage of $+V_{max}$ with polari ty as shown in the figure during the negative half cycle. As the voltage of the transformer rises to positive $+V_{max}$ during the next half cycle, the potential of the other terminal of C_1 rises to a voltage of $+2V_{max}$

Thus, the capacitor C_2 in turn is charged through $\mathbf{R}_2$ to $2V_{max}$. Normally, the dc output voltage on load will be less than $2V_{max}$, depending on the time constant C_2R_L and the forward charging time constants. The ripple voltage of these circuits will be about 2% for $R_L/r \leq 10$ and $X/r \leq 0.25$, where X and r are the reactance and resistance of the input transformer . The rectifiers are rated to a peak inverse voltage of $2V_{max}$, and the capacitors C_1 and C_2 must also have the same rating. If the load current is large, the ripple also is more.

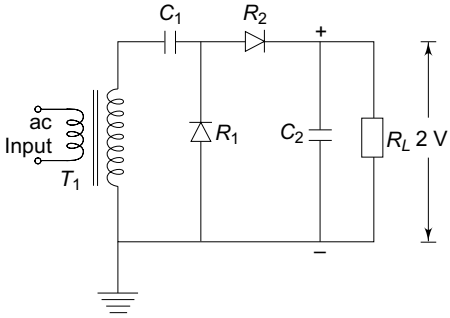

Figure. V.3a *Simple voltage doubler*

Cascaded voltage doublers are used when larger output voltages are needed wit hout changing the input transformer voltage level. A typical voltage doubler is shown in Figure . V.3b and its input and output waveforms are shown in Figure. V.3c. The rectifiers R_1 and R_2 with transformer T_1 and capacitors C_1 and C_2 produce an output voltage of 2 V in the same way as described above . This circuit is duplicated and connected in series or cascade to obtain a further voltage doubling to 4 V. T is an isolating transformer to give an insulation for $2V_{max}$ since the transformer T_2 is at a potential of $2V_{max}$ above the ground. The voltage distribution along the recti fier string R_1, R_2, R_3, and R_4 is made uniform by having capacitors C_1, C_2, C_3,and C_4 of equal values. The arrangement may be extend ed to give 6 V, 8V, and so on, by repeating further stages with suitable isolating transformers. In all the voltage doubler cir cuits, if valves are used, the filament transformers have to be suitably designed and insulated , as all the cathodes will not be at the same potential from ground. The arrangement becomes cum bersome if more than 4 V is needed with cascaded steps.

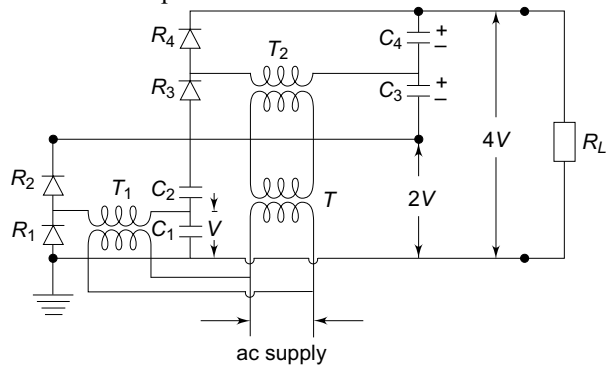

T_1, T_2 — $h\nu$ transformers
C_1, C_2, C_3, C_4 — capacitors
T — isolating transformer
R_1, R_2, R_3, R_4 — rectifiers
R_L — Load resistance

Figure. V.3b *Cascaded voltage doubler*

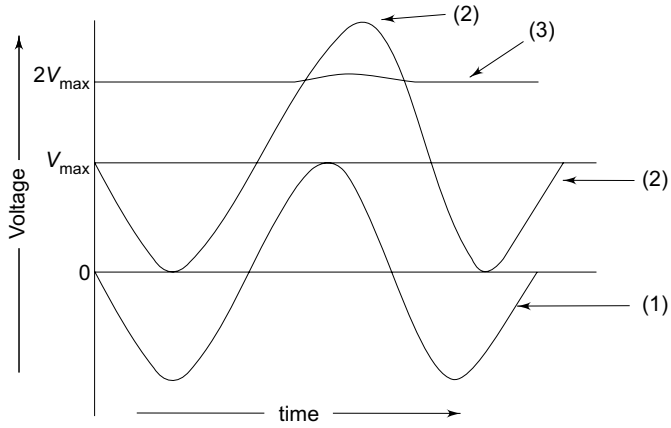

(1) ac input voltage waveform
(2) ac output voltage waveform with capacitor filter
(3) dc output voltage waveform with capacitor filter.

Figure. V.3c *Waveforms of ac voltage and the dc output voltage on no-load of the voltage doubler shown in Figure. V.3b*

Figure. V.3 *Voltage doubler circuits*

V.1.3 Voltage Multiplier Circuits

Cascaded voltage multiplier circuits for higher voltages are cumbersome and require too many supply and isolating transformers. It is possible to generate very high dc voltages from single supply transformers by extending the voltage doubler circuits. This is simple and compact when the load current requirement is less than one milliampere, such as for cathode ray tubes, etc. Valve-type pulse generators may be used instead of conventional ac supply and the circuit becomes compact. A typical circuit of this form is shown in Figure.V.4a.

The pulses generated in the anode circuit of the valve P are rectified and the voltage is cascaded to give an output of $2nV_{\max}$ across the load R_L. A trigger voltage pulse of triangular waveform (ramp) is given to make the valve switched on and off. Thus a voltage across the coil L is produced and is equal to $V_{\max} = I\sqrt{L/C_P}$, where C_P is the stray capacitance across the coil of inductance L. A dc power supply of about 500 V applied to the pulse generator, is sufficient to generate a high voltage dc of 50 to 100 kV with suitable number of stages. The pulse frequency is high (about 500 to 1000 Hz) and the ripple is quite low (< 1%). The voltage drop on the load is about 5% for load currents of about 150 μA. The voltage drops rapidly at high load currents.

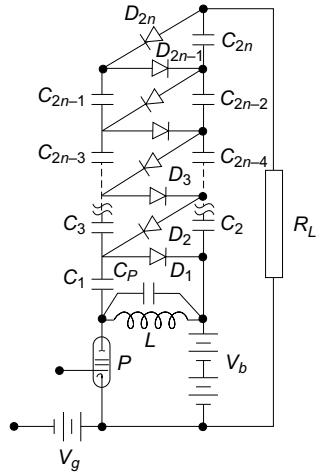

Figure. V.4a *Cascaded rectifier unit with pulse generator*

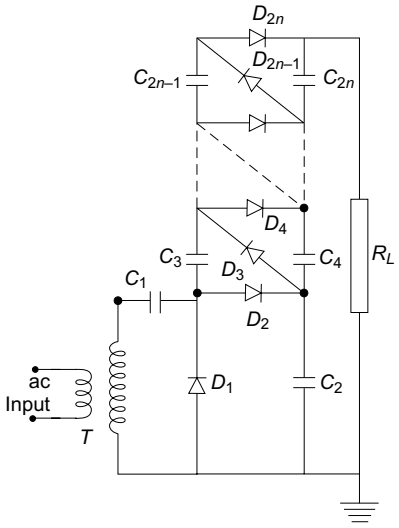

Figure. V.4b *Cockcroft–Walton voltage multiplier circuit*

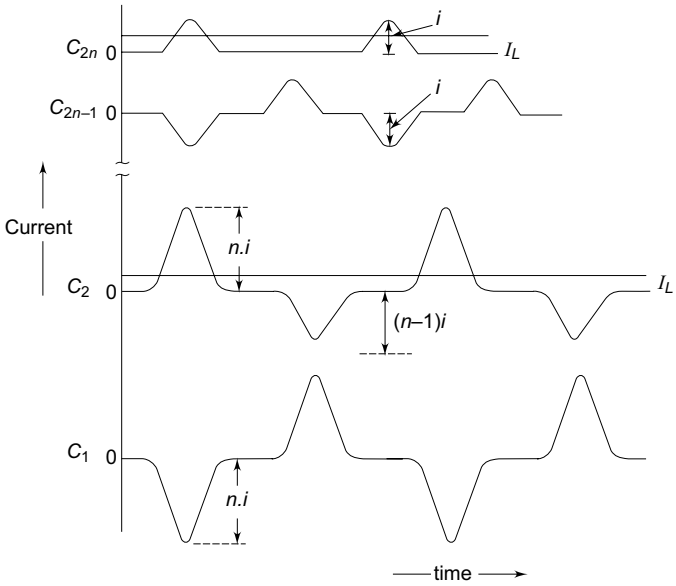

Figure. V.4c *Schematic current waveforms across the first and the last capacitors of the cascaded voltage multiplier circuit shown in Figure. V.4b*

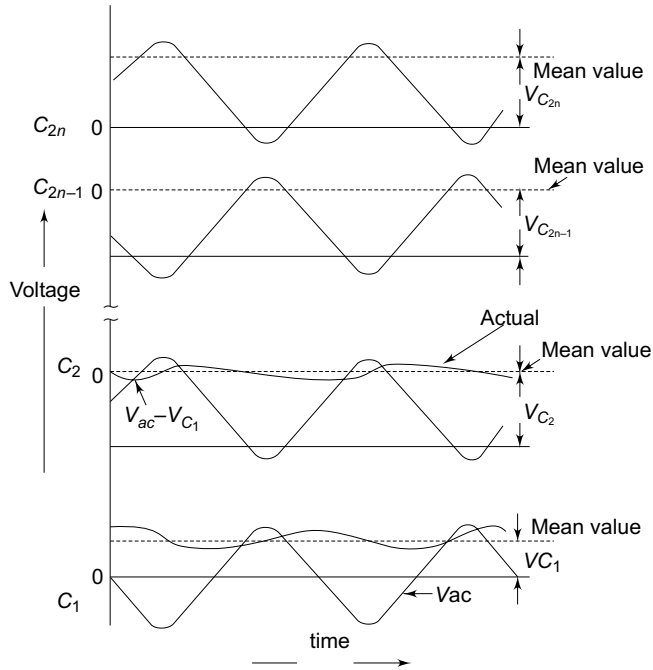

Figure. V.4d *Voltage waveforms across the first and the last capaci tors of the cascaded voltage multiplier circuit shown in Figure. V.4b*

Voltage multiplier circuit using the Cockcroft–Walton principle is shown in Fig. V.4b. The first stage, i.e., D_1, D_2, C_1, C_2, and the transformer T are identical as in the voltage doubler shown in Figure.V.3. For higher output voltage of 4, 6, ... $2n$ of the input voltage V, the circuit is repeated with cascade or series connection. Thus, the capacitor C_1 is charged to $4V_{max}$ and C_{2n} to $2nV_{max}$ above the earth potential. But the voltage across any individual capacitor or rectifier is only $2V_{max}$.

The rectifiers D_1, D_3, D_{2n-1} shown in Figure V.4b operate and conduct during the positive half cycles while the rectifiers D_2, D_4 ... D_{2n} conduct during the negative half cycles. Typical current and voltage waveforms of such a circuit are shown in Figure V.4c and V.4d respectively. The voltage on C_2 is the sum of the input ac voltage, V_{ac} and the voltage across condenser C_1, V_{C1}) as shown in Fig. V.4. The mean voltage on C_2 is less than the positive peak charging voltage (V_{ac} + V_{C1}). The voltage across other capacitors C_2 to C_{2n} can be derived in the same manner (i.e.) from the difference between voltage across the previous capacitor and the charging voltage. Finally, the voltage after $2n$ stages will be V_{ac} ($n_1 + n_2 + \ldots$), where n_1, n_2, … are factors when ripple and regulation are considered in the next rectifier. The ripple voltage δV and the voltage drop ΔV in a cascaded voltage multiplier unit are shown in Figure V.4e.

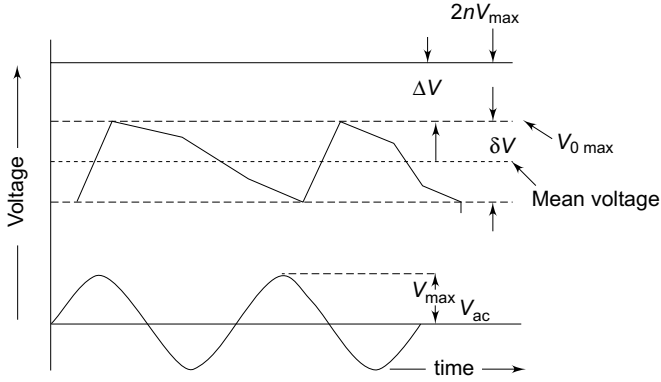

Figure. V.4e *Ripple voltage δV and the voltage drop ΔV in a cascaded voltage multiplier circuit shown in Figure. V.4b*

(a) Ripple in Cascaded Voltage Multiplier Circuits With load, the output voltage of the cascaded rectifiers is less than $2nV_{max}$, where n is the number of stages. The ripple and the voltage regulation of the rectifier circuit may be estimated as follows.

Let f = supply frequency,
q = charge transferred in each cycle,
I_1 = load current from the rectifier,
t_1 = conduction period of the rectifiers,
t_2 = non-conduction period of rectifiers, and
δV = ripple voltage (peak to peak)

Referring to Figure. V.3a, when load current I is supplied from capacitor C to load R during the non-conducting period, the charge transferred per cycle from the capacitor C_2 to the load during the non-conduction period t_2 is q, and is related as follows.

$$I_1 = \frac{dq}{dt} \approx \frac{q}{t_2}$$

Since $t_1 \ll t_2$ and $t_1 + t_2 = \frac{1}{f}$ (i.e., the period of the ac supply voltage),

$$t_2 = \frac{1}{f}$$

Also, $$q = C_2\, \delta V$$

Hence, $$\delta V = \text{the ripple} = \frac{I_1}{fC_2}$$

At the same time a charge q is transferred from C_1 to C_2 during each cycle equal to I_1/fC_2. Thus the total voltage drop that occurs will be $I_1/fC_1 + 2I_1/fC_2$.

Hence, regulation = mean voltage drop from $2V_{max}$

$$= \frac{I_1}{f}\left[\frac{1}{C_1} + \frac{2}{C_2}\right] \qquad \text{(V.1)}$$

Therefore, the mean output voltage $= 2V_{max} - \frac{I_1}{f}\left(\frac{1}{C_1} + \frac{2}{C_2}\right)$.

For the cascade circuit, on no load, the voltages between stages are raised by $2V_{max}$ giving an output voltage of $2nV_{max}$ for n stages.

Referring to Figure. V.4b, to find and expression for the total ripple voltage, let assumed that all capacitances it be C_1, C_2, ... C_{2n} be equal to C. Let q be the charge transferred from C_{2n} to the load per cycle.

Then the ripple at the capacitor C_{2n} will be $\frac{I_1}{fC}$.

Simultaneously, C_{2n-2} transfers as charge q to the load and to C_{2n-1}.

Hence, the ripple at the capacitor C_{2n-2} is $\frac{2I_1}{fC}$.

Similarly, C_{2n-4} transfers a charge q to the load, to C_{2n-3}, and to C_{2n-2}.

Therefore, the ripple at capacitor C_{2n-4} is $\frac{3I_1}{fC}$.

Proceeding in the same way, the ripple at C_2 will be $\frac{nI_1}{fC}$.

Hence, for n stages the total ripple (peak to peak) will be

$$d\,V_{total} = \frac{I_1}{fC}\,[1 + 2 + 3 \ldots + n] = \frac{I_1}{fC}\,\frac{(n)(n+1)}{2} \qquad \text{(V.2)}$$

and the average ripple $= \frac{\delta V_{total}}{2} = \frac{I_1}{4fC}\,(n)\,(n+1)$ (V.2a)

The major contribution to the ripple is from the lowest or ground end capacitors, C_1, C_2, C_3, C_4, etc. Ripple can be reduced if the capacitance of these capacitors is increased proportionately, i.e., C_1, C_2 are made nC, C_3, C_4 are made $(n-1)\,C$ and so on so that the total ripple will be equal to

$$\frac{nI_1}{fC}$$

Note: '*n*' capacitors here mean *n*/2 stages only since two capacitors from each stage or a doubler unit.

(b) Voltage Drop on Load and Regulation The change of average voltage across the load from the no load theoretical value expressed as a percentage of no load voltage is called the regulation. The change in voltage (i.e.) the voltage drop 'ΔV' is caused due to the ripple δV, and the capacitors not getting charged to the full voltage V_m when they are supplying the load current I_1.

The voltage drop under load condition ΔV is found by assuming that all the capacitors are of equal value 'C'. It is seen from the analysis of ripple that all the capacitors are not charged to $2V_{max}$. The capacitor C_{2n} is charged to $(2V_{max} - n\, I_1/fC)$ only instead of $2V_{max}$ because the charge given through C_{2n-1} in one cycle is equal to a voltage drop of $n\, I_1/fC$. This is because, in each stage the loss of charge equal to a voltage drop of I_1/fC to the load. In a similar manner the capacitor C_{2n-2} is charged to only $[2V_{max} - nI_1/fC - nI_1/fC - (n-1)\, I_1/fC]$ since the reduction in voltage at this stage is further equal to nI_1/fC at the capacitor C_{2n-1} and $(n-1)\, I_1/fC$ at capacitor C_{2n-2}. Thus, if the voltage drops at each of the capacitor C_{2n}, C_{2n-2}, etc., to C_2 are designated as ΔV_{2n}, ΔV_{2n-2}, … ΔV_2, the total voltage drop will be

$$\Delta V_{2n} = \frac{nI_1}{fC} = \frac{I_1}{fC}\ [2n - n]$$

$$\Delta V_{2n-2} = \frac{nI_1}{fC} + \frac{nI_1}{fC} + \frac{(n-1)\, I_1}{fC} = \frac{I_1}{fC}\,[2n + n - 1]$$

$$= \frac{I_1}{fC}\,[2n + 2\,(n-1) - (n-1)]$$

$$\cdots$$

$$\cdots$$

$$\cdots$$

$$\cdots$$

$$\Delta V_4 = \frac{I_1}{fC}\,[2n + 2\,(n-1) + \ldots + 2]$$

$$= \frac{I_1}{fC}\,[2n + 2\,(n-1) + \ldots + 2.2 - 2]$$

$$\Delta V_2 = \frac{I_1}{fC}\,[2n + 2\,(n-1) + \ldots + 2.1 - 1]$$

Summing up all the voltage drops,

$$\Delta V = \frac{I_1}{fC}\sum_{n=1}^{n} \Delta V_{2n} = \frac{I_1}{fC}\left\{\sum_{n=1}^{n} n \cdot 2n - \sum_{n=1}^{n} n\right\}$$

$$= \frac{I_1}{fC}\left[\sum_{1}^{n} 2n^2 - \sum_{1}^{n} n\right]$$

$$= \frac{I_1}{fC}\left[2 \cdot \frac{(n)(n+1)(2n+1)}{6} - \frac{n(n+1)}{2}\right]$$

$$= \frac{I_1}{fC}\left[n(n+1)\left(\frac{2n+1}{3} - \frac{1}{2}\right)\right]$$

$$= \frac{I_1}{fC}\left[\frac{n(n+1)(4n-1)}{6}\right]$$

$$= \frac{I_1}{fC}\left[\frac{2n^3}{3} + \frac{n^2}{2} - \frac{n}{6}\right] \qquad \text{(V.3)}$$

It is seen from Eq. (V.3) that most of the voltage drop is at the lowest stage capacitors C_1, C_2, C_3, C_4, etc. Hence it is advantageous to increase their values to be proportional to the stage number counted from the top. In other words C_1 C_2 may be chosen as nC, C_3 C_4 as $(n-1)C$, etc.

For large values of n (≥ 5), $\frac{n^2}{2}$ and $\frac{n}{6}$ terms in Eq. (V.3) will become small compared to $\frac{2}{3}n^3$ and may be neglected; then the optimum number of stages for the minimum voltage drop may be expressed as

$$n_{\text{optimum}} = \sqrt{\frac{V_{\max} fC}{I}} \qquad \text{(V.4)}$$

where I is the load current.

Thus, for a multiplier or a cascaded circuit with f = 50 Hz, C = 0.1 μF, $V_{\max}$ = 100 kV and I = 5 mA, the number of stages $n \approx 10$.

The regulation can be improved by increasing f, but an upper limit is set by the high voltage appearing across the inductances and high capacitor currents which are considerable. At present, the Cockcroft–Walton type voltage multipliers are available using selenium rectifiers and a.c. supply frequencies of 500 to 1000 Hz for output voltages of more than one million volts and load currents of 30 mA.

The voltage multiplier described in Sec.V .1.3 is a single pulse voltage multiplier since it has only one rectified

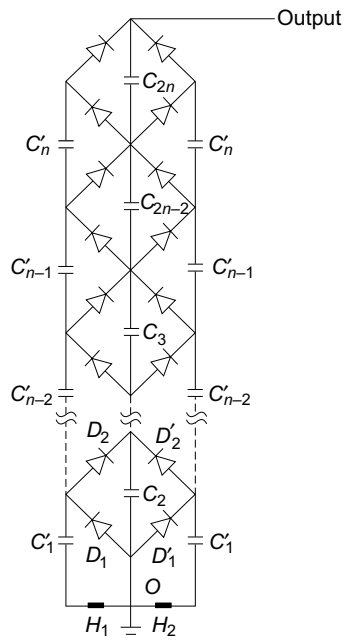

Figure. V.**5a** *One-phase, two-pulse, voltage multiplier circuit*

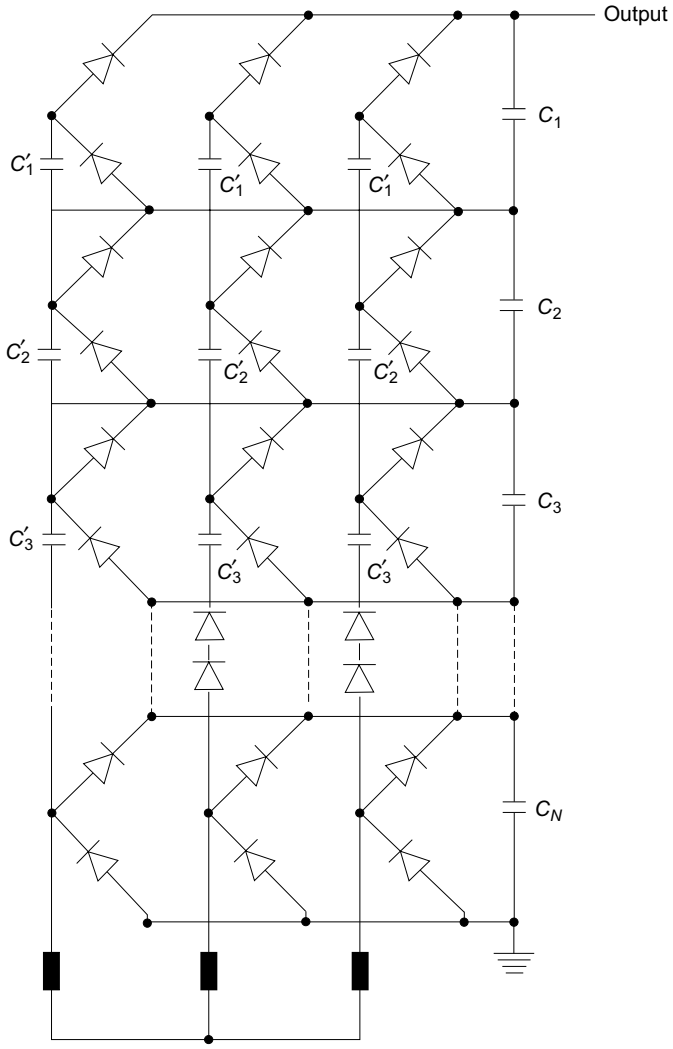

Figure. V.5b *Three-phase, six-pulse, voltage multiplier circuit*

wave or pulse per cycle. Hence its ripple content is high. In order to reduce the ripple as well as regulation and to improve the efficiency and power output, two or more pulse units per cycle are preferred. Single or three phase bridge is used as the basic rectifier or stage and the multiplier circuit is built in the same manner as that of the Cockcroft–Walton multiplier.

The arrangement for single phase two pulse and three phase six pulse circuits are shown in Figures V.5(a) and V.5(b) respectively.

(c) Single-phase Two-pulse Cascade Multiplier The basic voltage doubler unit consisting of D_1, D_2, C_1, C_2 is replaced by the bridge circuit D_1, D_2, D'_1, D'_2 with an extra capacitor C'_1. The centre tap of the supply transformer is connected to the junction of rectifiers D_1, D_2. The arrangement is simply an addition of another voltage doubler circuit D'_1, D'_2, C'_1, C'_2 along with the transformer H_1H_2 for the negative cycle rectification.

The multiplier circuit is built for both positive and negative cycle rectification and the arrangement is called *Symmetrical Cascade Unit*. The ripple for this arrangement is $nI/2fC$ as against $n(n + 1)I/2fC$ with all capacitors of value equal to C and the regulation is $\frac{nI}{3fC}\left(\frac{n^2}{2}+1\right)$.

(d) Three-phase Six-pulse Arrangement The three-phase six-pulse arrangement is a 3-phase bridge or Gratz circuit cascaded into a multiplier unit as shown in Fig. V.5b. Two more multiplier units for the other two phases of the three phase supply are connected in parallel to build this circuit. The ripple in this case is reduced to $\frac{nI}{6fC}$ and regulation to $\frac{nI}{3fC}\left(\frac{n^2}{6}-\frac{n}{4}+\frac{1}{3}\right)$

The two-pulse circuit requires double the number of diodes and one and a half times the capacitors required for single-pulse circuits. The six-pulse circuit requires twice the number of diodes and capacitors used in a single-pulse circuit and as such, the cost increases. But the regulation and ripple are very much reduced and requirements needed in the specifications of dc test sources are easily met with much smaller ratings for the capacitors. Further, large currents required for pollution testing can be obtained only with three-phase six-pulse arrangement.

V.1.4 Electrostatic Machines: Basic Principle

In electromagnetic machines, current-carrying conductors are moved in a magnetic field, so that the mechanical energy is converted into electrical energy. In electrostatic machines, charged bodies are moved in an electric field against the electrostatic field in order that mechanical energy is converted into electrical energy. Thus, if an insulated belt with a charge density δ moves in an electric field '$E(x)$' between two electrodes with separation 's' then

(i) the charge on the strip of belt at a distance dx is $dq = \delta b.dx$ where b is the width of the belt, and

(ii) the force on the belt, F is

$$F = \int_o^s E(x)\cdot dq = \int_o^s \delta\cdot b\cdot E(x)dx$$

If the belt moves with a velocity, v, then the mechanical power P, required to move the belt is $P = F\cdot v = \delta\cdot b\cdot v\int_o^s E(x)\,dx$

The current, I, in the system is given as

$$I = dq/dt = \delta b \cdot dx/dt = \delta \cdot b \cdot v$$

and the potential difference, V, between the electrodes is

$$V = \int_{o}^{s} E(x)\,dx$$

Thus, in an electrostatic machine, the mechanical power required to move the belt at a velocity v, i.e., $P = F \cdot v$ is converted into the electrical power, $P = V.I$, assuming that there are no losses in the system. The Van de Graaff generator is one such electrostatic machine which generates very high voltages, with small output current (Plate 1).

(a) Van de Graaff Generators The schematic diagram of a Van de Graaff generator is shown in Figure. V.V. The generator is usually enclosed in an earthed metallic cylindrical vessel and is operated under pressure or in vacuum. Charge is sprayed onto an insulating moving belt from corona points at a potential of 10 to 100 kV above earth and is removed and collected from the belt connected to the inside of an insulated metal electrode through which the belt moves. The belt is driven by an electric motor at a speed of 1000 to 2000 metres per minute. The potential of the high voltage electrode above the earth at any instant is $V = Q/C$, where Q is the charge stored and C is the capacitance of the high-voltage electrode to earth. The potential of the high-voltage electrode rises at a rate

$$\frac{dV}{dt} = \frac{1}{C}\frac{dQ}{dt} = \frac{I}{C}$$ where I is the net charging current.

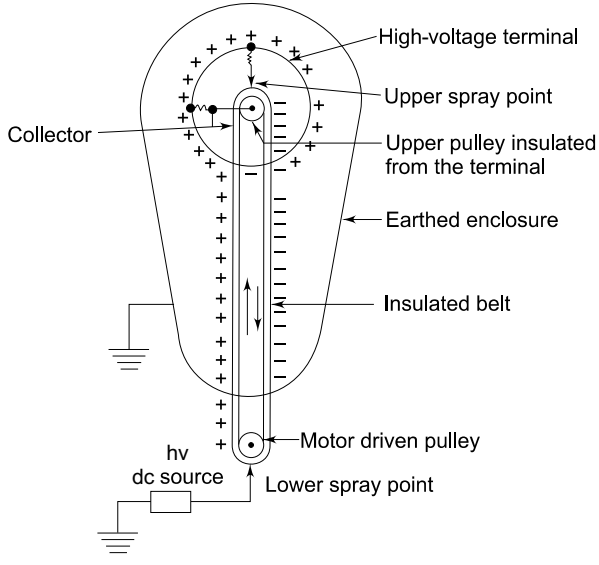

Figure. V.6 *Van de Graaff generator*

A steady potential will be attained by the high-voltage electrode when the leakage currents and the load current are equal to the charging current. The shape of the high-voltage electrode is so made with re-entrant edges as to avoid high surface field gradients, corona and other local discharges. The shape of the electrode is nearly spherical.

The charging of the belt is done by the lower spray points which are sharp needles and connected to a dc source of about 10 to 100 kV, so that the corona is maintained between the moving belt and the needles. The charge from the corona points is collected by the collecting needles from the belt and is transferred on to the high-voltage electrode as the belt enters into the high-voltage electrode. The belt returns with the charge dropped, and fresh charge is sprayed onto it as it passes through the lower corona point. Usually, in order to make the charging more effective and to utilize the return path of the belt for charging purposes, a self-inducing arrangement or a second corona-point system excited by a rectifier inside the high-voltage terminal is employed. To obtain a self-charging system, the upper pulley is connected to the collector needle and is therefore maintained at a potential higher than that of the high-voltage terminal. Thus, a second row of corona points connected to the inside of the high-voltage terminal and directed towards the pulley above its point of entry into the terminal gives a corona discharge to the belt. This neutralizes any charge on the belt and leaves an excess of opposite polarity to the terminal to travel down with the belt to the bottom charging point. Thus, for a given belt speed the rate of charging is doubled.

The charging current for unit surface area of the belt is given by $I = bv\delta$, where b is the breadth of the belt in metres, v is the velocity of the belt in m/sec, and δ is the surface charge density in coulombs/m^2. It is found that δ is $\leq 1.4 \times 10^{-5}$ C/m^2 to have a safe electric field intensity normal to the surface. With $b = 3$ m and $v = 3$ m/s, the charging current will be approximately 125 μA. The generator is normally worked in a high-pressure gaseous medium, the pressure ranging from 5 to 15 atm. The gas may be nitrogen, air, air-freon (CCl_2F_2) mixture, or sulphur hexafluoride (SF_6).

Van de Graaff generators are useful for very high-voltage and low-current applications. The output voltage is easily controlled by controlling the corona source voltage and the rate of charging. The voltage can be stabilized to 0.01%. These are extremely flexible and precise machines for voltage control.

(b) Electrostatic Generators Van de Graaff generators are essentially high-voltage but low-power devices, and their power rating seldom exceeds few tens of kilowatts. As such, electrostatic machines which effectively convert machanical energy into electrical energy using variable capacitor principle were developed. These are essentially duals of electromagnetic machines and are constant voltage variable capacitance machines. An electrostatic generator consists of a stator with interleaved rotor vanes forming a variable capacitor and operates in vaccum.

The current through a variable capacitor is given by $I = \frac{dV}{dt} + V\frac{dC}{dt}$ where C is a capacitor charged to a potential V.

The power input into the circuit at any instant is

$$P = VI = CV\frac{dV}{dt} + V^2\frac{dC}{dt} \qquad \text{(V.5)}$$

If $\frac{dC}{dt}$ is negative, mechanical energy is converted into electrical energy.

With the capacitor charged with a dc voltage V, $C\frac{dV}{dt} = 0$ and the power output will be $P = V^2\frac{dC}{dt}$.

A schematic diagram of a synchronous electrostatic generator with interleaved stator and rotor plates is shown in Figure. V.7. The rotor is insulated from the ground, and is maintained at a potential of $+V$. The rotor to stator capacitance varies from C_m to C_0 and the stator is connected to a common point between two rectifiers across the dc output which is $-E$ volts. When the capacitance of the rotor is maximum (C_m), the rectifier **B** does not conduct and the stator is at ground potential. The potential E is applied across the rectifier A and V is applied across C_m. As the rotor rotates, the capacitance C decrease and the voltage across C increases.

Thus, the stator becomes more negative with respect to ground. When the stator reaches the line potential $-E$ the rectifier **A** conducts, and further movement of the rotor causes the current to flow from the generator. Rectifier **B** will now have E across it and the charge left in the generator will be $Q_0 = C_0 (V + E) + E (C_s + C_r)$, where C_s is the stator capacitance to earth, C_r is the capacitance of rectifier **B** to earth, and C_0 is the minimum capacitance value of C (stator to rotor capacitance).

A generator of this type with an output voltage of one MV and a field gradient of 1 MV/cm in high vacuum and having 16 rotor poles, 50 rotor plates of 4 feet maximum and 2 feet minimum diameter, and at a speed of 4000 rpm would develop 7 MW of power.

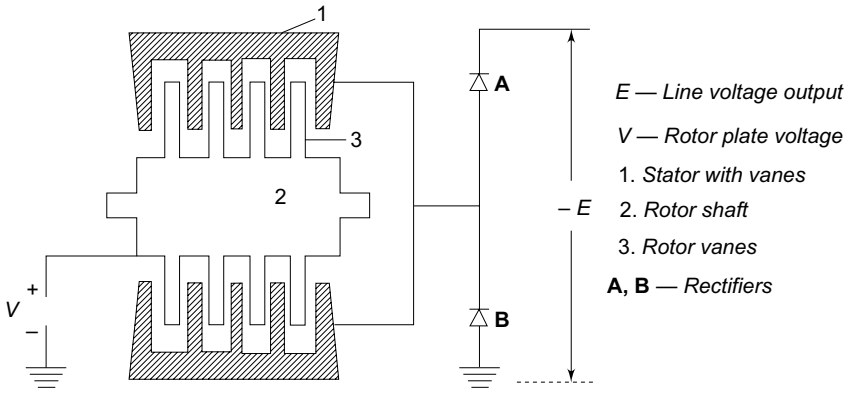

Figure. V.**7** *Electrostatic generator*

V.1.5 Regulation of dc Voltages

The output voltage of a dc source, whether it is a rectifier or any other machine, changes with the load current as well as with the input voltage variations. In order to maintain a constant voltage at the load terminals, it is essential to have a regulator circuit which corrects the variation in voltage. It is essential to keep the change in voltage between ± 0.1% to ± 0.001% depending on the applications.

A dc voltage regulator consists of detecting elements which sense the change in voltage from the desired value and controlling elements actuated by the detector in such a manner as to correct the changes. The regulators are generally of two types (a) series type, and (b) shunt or parallel type. Schematic diagrams of these regulators are given in Figure. V.8.

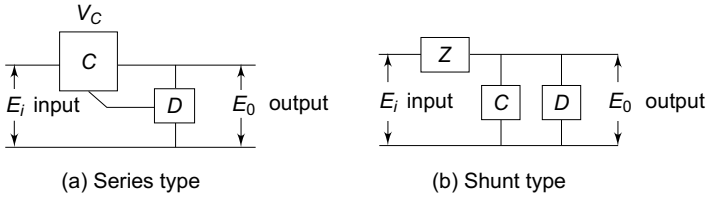

Figure. V.8 *Schematic diagram of voltage stabilizers*

If ΔE_0 is the change in E_0 as a result of a change of ΔE_i in E_i, then the stabilization ratio S is defined as

$$S = [\Delta E_i/E_i]/[\Delta E_0/E_0]$$
$$= \frac{\Delta E_i}{\Delta E_0}\frac{E_0}{E_i}. \qquad \text{(V.6)}$$

A second parameter R_0 is introduced to define completely the functional performance of a regulator. R_0 is the effective internal resistance of the regulator as seen from the output terminals.

$$R_0 = \frac{\Delta E_0}{\Delta I_0}$$

where ΔE_0 is the change in the output voltage caused due to a change in load current of ΔI_0, with the input voltage remaining constant.

The regulation R is defined as,

$$R = [\Delta E_0/E_0]/[\Delta I_0/I_0] = \frac{R_0}{R_L} \qquad \text{(V.7)}$$

where R_L is the load resistance.

Typical series type regulator and degenerative feedback system of voltage regulation are shown in Figures V.9a and b respectively.

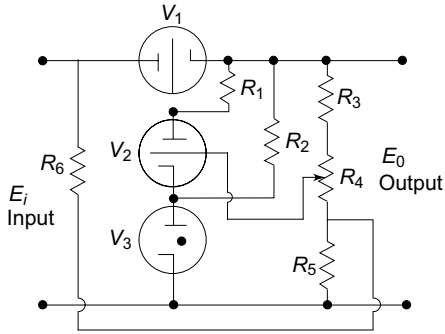

V_1 — Series regulating tube
V_2 — Sensing and amplifying tube
V_3 — Reference tube
R_1 — Grid control resistance for tube 1
R_3, R_4, R_5 — Output potential divider
R_6 — Input fluctuation correction resistance

Figure V.9a *Series dc voltage regulator*

Figure V.9a shows the simplified diagram of a series type of voltage regulator Here the gas tube V_3 provides the reference voltage which keeps the potential of the cathode of the tube V_2 constant. When the output voltage E_0 changes, the current through the divider R_2, R_4 and R_5 changes, and hence the bias voltage of the tube V_2 with respect to its cathode changes in the opposite manner (reduces when the output voltage increases and vice versa). Thus, the grid potential of V_1 is altered in such a manner as to oppose the variation in output voltage E_0; that is, the voltage drop across the tube V_1 reduces, if the output voltage decreases and vice versa. Resistance R_6 together with R_5 provides a voltage input to the dc amplifier (the detector) in proportion to fluctuations in the input voltage in such a way as to reduce the effect of these variations in the output voltage.

A convenient method of regulating high dc voltages is the degenerative feedback system, shown in Figure.V.9b. The fluctuations in the output voltage are measured by a detecting device, amplified by a dc amplifier and fed back into the high-voltage set so as to correct for the original fluctuations. The detecting device in the above circuit is the potential divider of ratio $\beta = R_1/(R_1 + R_2)$. The amplifier is directly coupled and the difference in potential between the tapping on the divider and the amplifier grid voltage is made up by the battery voltage V.

The output voltage E_0 is given as follows:

$$E_0 = NE_i - I_l R_i - Ae \qquad \text{(V.7a)}$$

where N = ratio between the output voltage of the hv set and the main supply voltage, E_i,
I_l = load current,
R_i = internal resistance of the hv set,
A = gain of the feedback amplifier,
e = amplifier input voltage.

Since $e = \beta E_0 - V$, the output voltage becomes

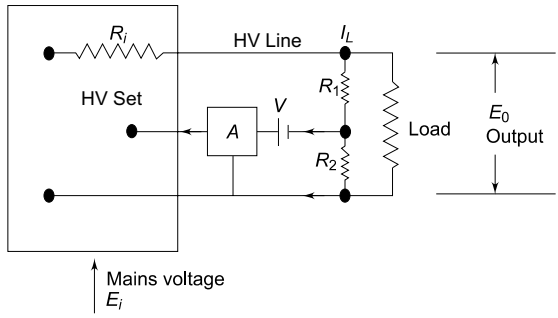

R_1, R_2 — Potential divider
A — dc amplifier
R_i — Internal resistance of control source, the hv set

Figure.V.**9b** *Degenerative feedback system of voltage regulation*

$$E_0 = NE_i - I_l R_i - (\beta E_v - V)\, A = NE_i - I_l R_i - A\beta E_0 + AV$$

or, $$E_0(1 + A\beta) = NE_i + AV - I_l R_i$$

or, $$E_0 = \frac{NE_i}{(1 + A\beta)} + \frac{AV}{(1 + A\beta)} - \frac{I_l R_i}{(1 + A\beta)}$$

For large values of A

$$E_0 = \frac{AV}{(1 + A\beta)} \approx \frac{V}{\beta}.$$

The stabilization ratio = $[\Delta E_i/E_i]/[\Delta E_0/E_0] = 1 + A\beta$.

In practice, values of $A\beta$ of the order of 1000 are common. It can be seen that for given value of A, stabilization ratio can be increased by making β as large as possible.

Stabilities to about 2 parts in 10^4 in high voltage are easily obtained by this method if load changes are kept small.

V.2 GENERATION OF HIGH ALTERNATING VOLTAGES

When test voltage requirements are less than about 300 kV, a single transformer can be used for test purposes. The impedance of the transformer should be generally less than 5% and must be capable of giving the short-circuit current for one minute or more depending on the design. In addition to the normal windings, namely, the low- and high-voltage windings, a third winding known as meter winding is provided to measure the output voltage. For higher voltage requirements, a single-unit construction becomes difficult and costly due to insulation problems. Moreover, transportation and erection of large transformers become difficult. These drawbacks are overcome by series connection or cascading of the several identical units of transformers, wherein the high voltage windings of all the units effectively come in series.

Schematic diagrams of the cascade transformer units are shown in Figs V.10 and V.11.

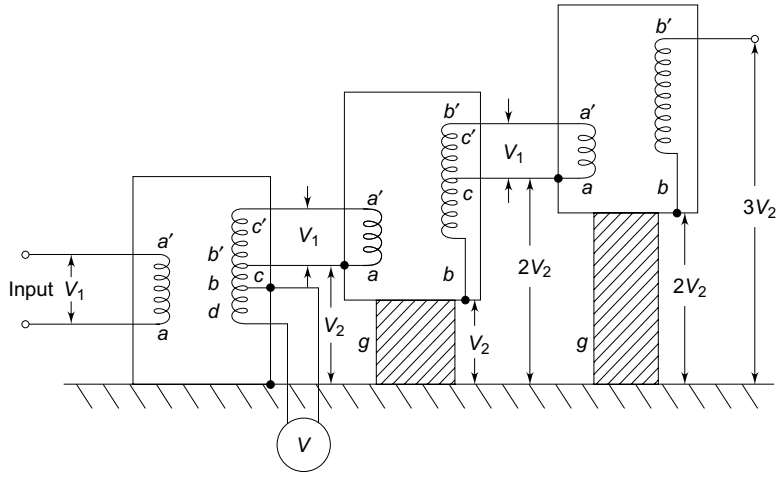

V_1 — Input voltage
V_2 — Output voltage
g — Insulation support
aa' — LV primary winding
bb' — HV secondary winding
cc' — Excitation winding
bd — Meter winding (200 to 500 V)

Figure. V.10 *Cascade transformer connection (schematic)*

V.2.1 Cascade Transformers

Figure V.10 shows the cascade transformer units in which the first transformer is at the ground potential along with its tank. The second transformer is kept on insulators and maintained at a potential of V_2, the output voltage of the first unit above the ground. The high-voltage winding of the first unit is connected to the tank of the second unit. The low-voltage winding of this unit is supplied from the excitation winding of the first transformer, which is in series with the high-voltage winding of the first transformer at its high-voltage end. The rating of the excitation winding is almost identical to that of the primary or the low-voltage wind ing. The high-voltage connection from the first transformer wind ing and the excitation winding terminal are taken through a bushing to the second transformer. In a similar manner, the third transformer is kept on insulators above the ground at a potential of $2V_2$ and is supplied likewise from the second transformer. The number of stages in this type of arrangement are usually two to four, but very often, three stages are adopted to facilitate a three-phase operation so that $\sqrt{3}V_2$, V_2 can be obtained between the lines.

Supply to the units can be obtained from a motor-generator set or through an induction regulator for variation of the output voltage. The rating of the primary or the low-voltage winding is usually 230 or 400 V for small units up to 100 kVA. For larger outputs, the rating of the low-voltage winding may be 3.3 kV, V.6 kV or 11 kV.

In Figure. V.11, a second scheme for providing the excitation to the second and the third stages is shown. Isolating transformers Is_1, Is_2, and Is_3 are 1 : 1 ratio transformers insulated to their respective tank potentials and are meant for supplying the exci-tation for the second and the third stages at their tank poten tials. Power supply to the isolating transformers is also fed from the same ac input. This scheme is expensive and requires more space. The advantage of this scheme is that the natural cooling is sufficient and the transformers are light and compact. Transportation and assembly is easy. Also, the construction is identical for isolating transformers and the high-voltage cascade units. Three phase connection in delta or star is possible for three units. Testing transformers of ratings up to 10 MVA in cascade connection to give high voltages up to 2.25 MV are avai lable for both indoor and outdoor applications (Plate 2).

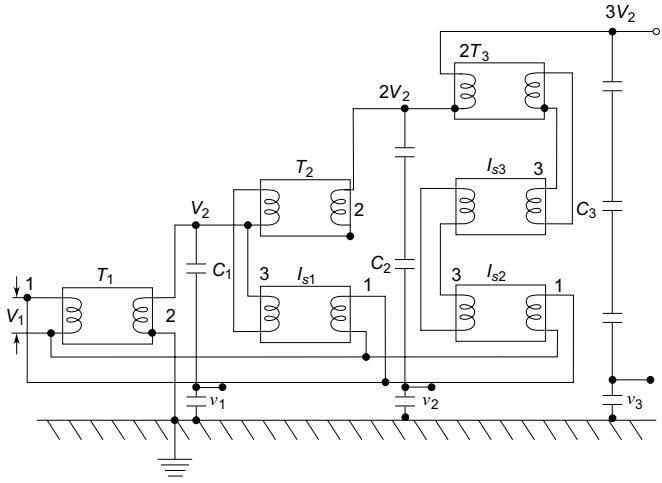

T_1, T_2, T_3 — Cascade transformer units
I_{s1}, I_{s2}, I_{s3} — Isolation transformer units
C_1, C_2, C_3 — Capacitance voltage dividers for hv measurement after 1st, 2nd, and 3rd stages
V_1, V_2, V_3 — For metering after 1st, 2nd, and 3rd stages
1. Primary (lv winding), 2. hv winding, 3. Excitation winding

Figure. V.11 *Cascade transformer unit with isolating transformers for excitation*

Testing of an hv apparatus or insulation always involves sup plying of capacitive loads with very low power dissipation. Thus if C is the capacitance of the test object, V is the rms value of the nominal output voltage of the transformer at an angular frequency ω, then the nominal rating of the transformer in kVA will be $P = K \cdot V^2 \omega C$, where K (> 1.0) is a factor to account for any extra capacitance in the test circuit like that of the meas uring capacitance divider, etc. K may have values of the order of 2 or more for very high voltages (> 1 MV). Typical capacitance values for high capacitance test objects like power transformers, cables, etc. are as follows:

Power transformers (rating < 1 MVA)	1000 pF
Power transformers (rating > 1 MVA)	1000–10,000 pF
High-voltage power cables (with solid insulation)	250–300 pF/m
High-voltage power cables (with gas insulation)	50–80 pF/m
Metal-clad sub-station with gas insulation (GIS)	100–10,000 pF

The charging currents for the test apparatus may range from 10 mA at 100 kV to a few milliamperes in the megavolt range. As such the transformers should have only a short time rating (10 to 15 min) for high power ratings, as compared to those with nominal power ratings.

Large testing transformers rated for more than 1 MVA at 1 MV are nowadays designed for outdoor use only. The design is of the type mentioned in the second scheme and ensures that the units are enclosed by large-size metal rings to prevent corona, and are terminated with near spherical polycone electrodes. Modern test transformers are built to withstand transients during the flashover of the test object. However, particular care need to be taken to see that steady state voltage distribution within the cascade units is uniform. Sometimes reactor compensation may have to be provided for excessive load currents of capacitive nature. Cascade transformers are very expensive apparatus and are diffi cult to repair. Therefore it is necessary to limit the high short-circuit currents by using limiting reactors in the input stage.

Power Supply for ac Test Circuits Large cascade transformers units are supplied power through a separate motor-generator set or by means of voltage regulators. Supply through a voltage regulator will be cheaper, and will be more flexible in the sense that the units in the cascade set can be operated in cascade, or in parallel, or as three-phase units. It is also necessary that the impedance of the voltage regulating transformer is low in all voltage positions, from the minimum to the rated value.

V.2.2 Resonant Transformers

The equivalent circuit of a high-voltage testing transformer consists of the leakage reactance of the windings, the winding resistances, the magnetizing reactance, and the shunt capacitance across the output terminal due to the bushing of the high-voltage terminal and also that of the test object. This is shown in Figure.V.12a with its equivalent circuit in Figure.V.12b. It may be seen that it is possible to have series resonance at power frequency ω, if $(L_1 + L_2) = 1/\omega C$. With this condition, the current in the test object is very large and is limited only by the resistance of the circuit. The waveform of the voltage across the test object will be purely sinusoidal. The magnitude of the voltage across the capacitance C of the test object will be

$$V_C = \left| \frac{-jVX_C}{R + j(X_L - X_C)} \right| = \frac{V}{R} X_C = \frac{V}{\omega CR} \qquad \text{(V.8)}$$

where R is the total series resistance of the circuit.

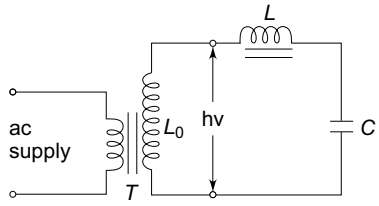

T — Testing transformer
L — Choke
C — Capacitance of hv terminal and test object
L_0 — Magnetizing inductance

Figure. V.12a *Transformer*

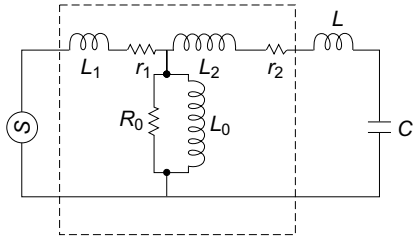

L_1, L_2 — Leakage inductances of the transformer
r_1, r_2 — Resistances of the windings
R_0 — Resistance due to core loss

Figure. V.12b *Equivalent circuit*

The factor $X_C/R = 1/\omega CR$ is the Q factor of the circuit and gives the magnitude of the voltage multiplication across the test object under resonance conditions. Therefore, the input voltage required for excitation is reduced by a factor $1/Q$, and the output kVA required is also reduced by a factor $1/Q$. The secondary power factor of the circuit is unity.

This principle is utilized in testing at very high voltages and on occasions requiring large current outputs such as cable testing, dielectric loss measurements, partial discharge measurements, etc. A transformer with 50 to 100 kV voltage rating and a relatively large current rating is connected together with an additional choke, if necessary. The test condition is set such that $\omega(L_e + L) = 1/\omega C$ where L_e is the total equivalent leakage inductance of the transformer including its regulating transformer. The chief advantages of this principle are

(a) it gives an output of pure sine wave,
(b) power requirements are less (5 to 10% of total kVA required),
(c) no high-power arcing and heavy current surges occur if the test object fails, as resonance ceases at the failure of the test object,
(d) cascading is also possible for very high voltages,
(e) simple and compact test arrangement, and
(f) no repeated flashovers occur in case of partial failures of the test object and insulation recovery. It can be shown that the supply source takes Q number of cycles at least to charge the test specimen to the full voltage.

The disadvantages are the requirements of additional variable chokes capable of withstanding the full test voltage and the full current rating.

A simplified diagram of the series resonance test system is given in Figure V.12c and that of the parallel resonant test system in V.12d. A voltage regulator of either the auto-transformer type or the induction regulator type is connected to the supply mains and the secondary winding of the exciter transformer is connected across the hv reactor, L, and the capacitive load C. The induc tance of the reactor L is varied by varying its air gap and operating range is set in the ratio 10 : 1.

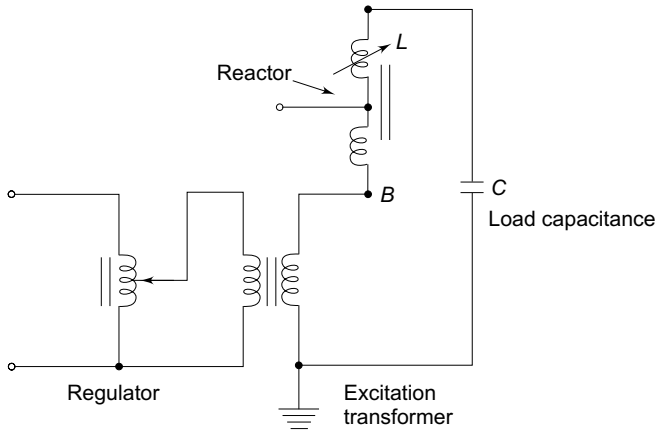

Figure.V.**12c** *Series resonant ac test system*

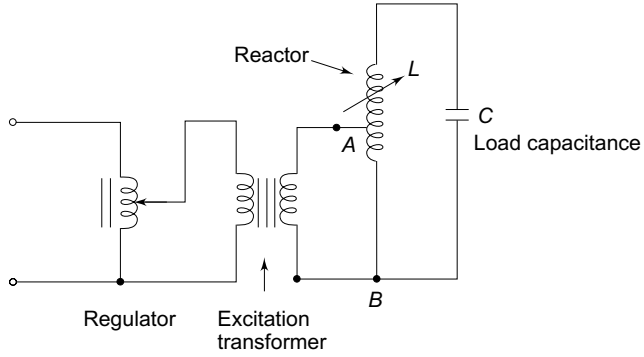

Figure. V.**12d** *Parallel resonant ac test system*

Ratings: *Regulator: 10 – 100 kVA*
Excitation transformer: 10 – 100 kVA with an output voltage of about 10 kV
Reactor voltage — each unit up to 300 kV

Figure.**V.12** *Resonant transformer and equivalent circuit*

Capacitance C com prises of the capacitance of the test object, capacitance of the measuring voltage divider, capacitance of the high-voltage bus hing, etc. The Q-factor obtained in these circuits will be typi cally of the order of 50. In the parallel resonant mode the high voltage reactor is connected as an auto-transformer and the circuit is connected as a parallel resonant circuit. The advan tage of the parallel resonant circuit is that more stable output voltage can be obtained along with a high rate of rise of test voltage, independent of the degree of tuning and the Q-factor. Single unit resonant test systems are built for output voltages up to 500 kV, while cascaded units for outputs up to 3000 kV, 50/60 Hz are available.

V.2.3 Generation of High-Frequency ac High Voltages

High-frequency high voltages are required for rectifier dc power supplies as discussed in Sec. V.1. Also, for testing electrical apparatus for switching surges, high frequency high voltage damped oscillations are needed which need high-voltage high-frequency transformers. The advantages of these high-frequency transformers are:

(i) the absence of iron core in transformers and hence saving in cost and size,
(ii) pure sine-wave output,
(iii) slow build-up of voltage over a few cycles and hence no damage due to switching surges, and
(iv) uniform distribution of voltage across the winding coils due to subdivision of coil stack into a number of units.

The commonly used high-frequency resonant transformer is the Tesla coil, which is a doubly tuned resonant circuit shown schematically in Fig. V.13a. The primary voltage rating is 10 kV and the secondary may be rated to as high as 500 to 1000 kV. The primary is fed from a dc or ac supply through the capacitor C. A spark gap G connected across the primary is triggered at the desired voltage V_1 which induces a high self-excitation in the secondary. The primary and the secondary windings (L_1 and L_2) are wound on an insulated former with no core (air-cored) and are immersed in oil. The windings are tuned to a frequency of 10 to 100 kHz by means of the capacitors C_1 and C_2.

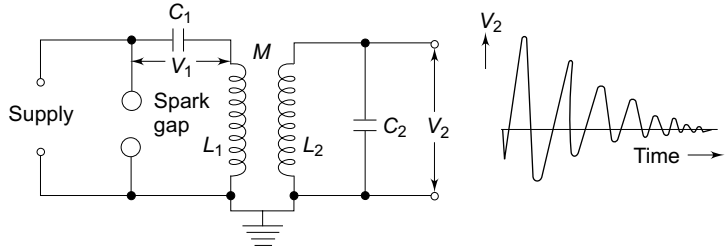

Figure. V.13 *Tesla coil equivalent circuit and its output waveform* The

primary coil is wound on an insulator fibre tube of about 1 m length to represent a cylindrical or helical winding and consists of a few tens of turns (usually copper strip or tubings). The secondary winding is spaced quite away from the primary winding on another concentric fibre or pyrex tube with a few thousand turns. The whole assembly will be immersed in an oil tank under pressure. With separate bushings taken out for the primary and the secondary windings, the primary winding is supplied through a high-voltage capacitor rectifier unit rated for 10 kV to 50 kV or more and the power rating of the transformer may be 10 kVA or more.

The output voltage V_2 is a function of the parameters L_1, L_2, C_1, C_2, and the mutual inductance M. Usually, the winding resistances will be small and contribute only for damping of the oscillations.

The analysis of the output waveform can be done in a simple manner neglecting the winding resistances. Let the capacitor C_1 be charged to a voltage V_1 when the spark gap is triggered. Let a current i_1 flow through the primary winding L_1 and produce a current i_2 through L_2 and C_2.

Then,
$$V_1 = \frac{1}{C_1}\int_0^t i_1 dt + L_1\frac{di_1}{dt} + M\frac{di_2}{dt} \tag{V.9}$$

and,
$$0 = \frac{1}{C_1}\int_0^t i_2 dt + L_2\frac{di_2}{dt} + M\frac{di_1}{dt}$$

The Laplace transformed equations for the above are

$$\frac{V_1}{s} = \left[L_1 s + \frac{1}{C_1 s}\right] I_1 + MsI_2 \tag{V.10}$$

and,
$$0 = [Ms]I_1 + \left[L_2 s + \frac{1}{[C_2 s]}\right] I_2$$

where I_1 and I_2 are the Laplace transformed values of i_1 and i_2.

The output voltage V_2 across the capacitor C_2 is

$$V_2 = \frac{1}{C_2}\int_0^t i_2 dt; \text{ or its transformed equation is}$$

$$V_2(s) = \frac{I_2}{C_2 s} \tag{V.11}$$

where $V_2(s)$ is the Laplace transform of V_2.

The solution for V_2 from the above equations will be

$$V_2 = \frac{-MV_1}{\sigma L_1 L_2 C_2}\frac{1}{\gamma_2^2 - \gamma_1^2}\left[\cos \gamma_1 t - \cos \gamma_2 t\right] \tag{V.12}$$

where,
$$\sigma^2 = 1 - \frac{M^2}{L_1 L_2} = 1 - K^2$$

K = coefficient of coupling between the windings L_1 and L_2

$$\gamma_1^2 = \frac{\omega_1^2 + \omega_2^2}{2} + \sqrt{\left(\frac{\omega_1^2 + \omega_2^2}{2}\right)^2 - \sigma^2\omega_1^2\omega_2^2}$$

$$\gamma_2^2 = \frac{\omega_1^2 + \omega_2^2}{2} - \left[\left\{\left(\frac{\omega_1^2 + \omega_2^2}{2}\right)\right\}^2 - \sigma^2\omega_1^2\omega_2^2\right]^{1/2}$$

$$\omega_1 = \frac{1}{\sqrt{L_1 C_1}} \text{ and } \omega_2 = \frac{1}{\sqrt{L_2 C_2}}$$

The output waveform is shown in Figure. V.13b The peak amplitude of the secondary voltage . V_2 can be expressed as,

$$V_{2\max} = V_1 e \sqrt{\frac{L_2}{L_1}} \tag{V.13}$$

where,

$$e = \frac{2\sqrt{1-\sigma^2}}{\sqrt{(1+a)^2 - 4\sigma a}}$$

$$a = \frac{L_2 C_2}{L_1 C_1} = \frac{\omega_1^2}{\omega_2^2}$$

A more simplified analysis for the Tesla coil may be presented by considering that the energy stored in the primary circuit in the capacitance C_1 is transferred to C_2 via the magnetic coupling. If W_1 is the energy stored in C_1 and W_2 is the energy transferred to C_2 and if the efficiency of the transformer is η, then

$$W = \frac{1}{2}\eta C_1 V_1^2 = \left(\frac{1}{2} C_2 V_2^2\right) \tag{V.14}$$

from which

$$V_2 = V_1 \sqrt{\eta \frac{C_1}{C_2}} \tag{V.14a}$$

It can be shown that if the coefficient of coupling K is large the oscillation frequency is less, and for large values of the winding resistances and K, the waveform may become a unidirectional impulse. This is shown in the next sections while dealing with the generation of switching surges.

V.3 GENERATION OF IMPULSE VOLTAGES

V.3.1 Standard Impulse Waveshapes

Transient overvoltages due to lighting and switching surges cause steep build-up of voltage on transmission lines and other electrical apparatus. Experimental investigations showed that these waves have a rise time of 0.5 to 10 μs and decay time to 50% of the peak value of the order of 30 to 200 μs. The waveshapes are arbitrary, but mostly unidirectional. It is shown that lightning overvoltage wave can be represented as double exponential waves defined by the equation

$$V = V_0 [\exp(-\alpha t) - \exp(-\beta t)] \tag{V.15}$$

where α and β are constants of microsecond values.

The above equation represents a unidirectional wave which usually has a rapid rise to the peak value and slowly falls to zero value. The general waveshapes is given in Figure. V.14. Impulse waves are specified by defining their rise of front time, fall or tail time to 50% peak value, and the value of the peak voltage. Thus 1.2/50 μs, 1000 kV wave represents an impulse voltage wave with a front time of 1.2 μs, fall time to 50 % peak value of 50 μs, and a peak value of 1000 kV. When impulse waveshapes are recorded, the initial portion of the wave may not be clearly defined or sometimes may be missing. Moreover, due to disturbanc es it may contain superimposed oscilla-tions in the rising por tion. Hence, the front and tail times have to be redefined.

Referring to the waveshape in Figure. V.14, the peak value A is fixed and referred to as 100% value. The points corresponding to 10% and 90% of the peak values are located in the front portion (points C and D). The line joining these points is extended to cut the time axis at O_1. O_1 is taken as the virtual origin. 1.25 times the interval between times

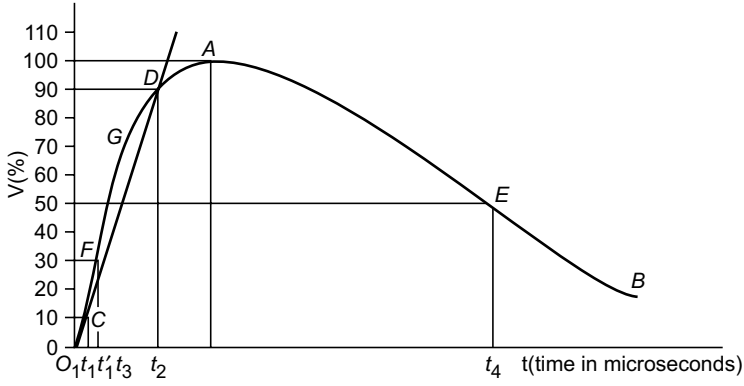

Figure. V.**14** *Impulse wave and its definitions*

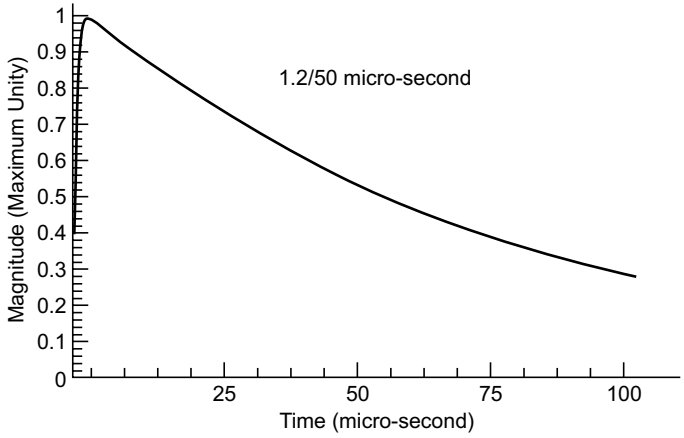

Figure. V.**14a** *Typical 1.2/50 μs waveform*

t_1 and t_2 corresponding to points C and D (projections on the time axis) is defined as the front time, i.e., 1.25 ($O_1t_2 - O_1t_1$). The point E is located on the wave tail corresponding to 50% of the peak value, and its projection on the time axis is t_4. O_1t_4 is defined as the fall or tail time. In case the point C is not clear or missing from the waveshape record, the point corresponding to 30% peak value F is taken and its projection t_1' is located on time axis. The wavefront time in that case will be defined as 1.67 ($O_1t_3 - O_1t_1'$). The tolerances that can be allowed in the front and tail times are respectively ±30% and ±20%. Indian standard specifications define 1.2/50 μs wave to be the standard lightning impulse. The tolerance allowed in the peak value is ±3%.

V.3.2 Theoretical Representation of Impulse Waves

The impulse waves are generally represented by Eq. (V.15) given earlier. V_0 in the equation represents a factor that de pends on the peak value. For impulse wave of 1.2/50 μs, $\alpha = -0.0146$, $\beta = -2.467$, and $V_0 = 1.04$ when time t is expressed in micro-seconds, α and β control the front and tail times of the wave respectively. Values of α and β for different waveforms are given in Table V.1.

Table V.1 *Values of α and β for different waveforms (Double exponential type) (t in μ seconds)*

Wave form	α	β	V_o
0.5/5	0.1793	3.714	1.225
1/5	0.2650	1.294	1.892
1/50	0.01477	1.933	1.039
1.2/50	0.01460	2.467	1.046
1.5/40	0.01907	1.482	1.072
4/10	0.1866	0.3978	3.677
8/20	0.0535	0.113	2.010

V.3.3 Circuits for Producing Impulse Waves

A double exponential waveform of the type mentioned in Eq. (V.15) may be produced in the laboratory with a combination of a series *R-L-C* circuit under over damped conditions or by the combination of two *R-C* circuits. Different equivalent circuits that produce impulse waves are given in Figures V.15a to d. Out of these circuits, those shown in Figures V.15a to V.15d are commonly used. Circuit shown in Figure. V.15a is limited to model generators only, and commercial generators employ circuits shown in Figures V.15b to V.15d.

A capacitor (C_1 or C) previously charged to a particular dc voltage is suddenly discharged into the waveshaping network ($L - R$ or R_1 R_2 C_2 or other combination) by closing the switch S. The discharge voltage $V_0(t)$ shown in Figure. V.15 gives the desired double exponential waveshape.

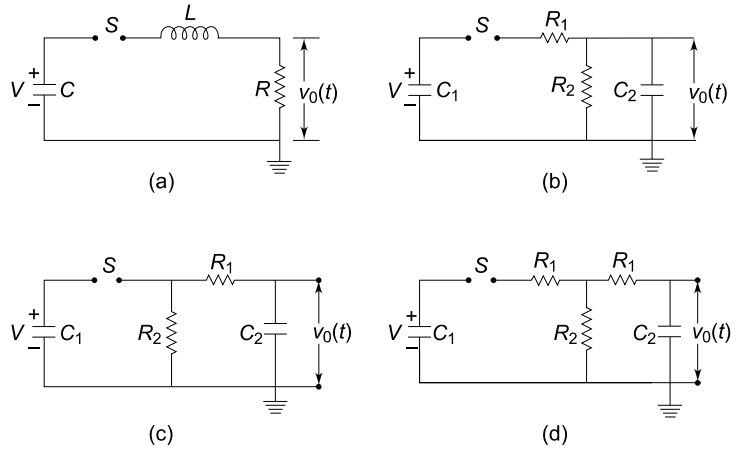

Figure. V.15 *Circuits for producing impulse waves*

(a) Analysis of Impulse Generator Circuit of Series R-L-C Type

Referring to Figure. V.15a the current through the load resistance R is given by

$$V = \frac{1}{C}\int_0^t i\,dt + Ri + L\frac{di}{dt} \tag{V.16}$$

with initial condition at $t = 0$ being $i(0) = 0$ and the net charge in the circuit $q = 0$. Writing the above equation as a Laplace transform equation,

$$V/s = \left(\frac{1}{Cs} + R + Ls\right) I(s)$$

or,

$$I(s) = \frac{V}{L}\left[\frac{1}{s^2 + \frac{Rs}{L} + \frac{1}{LC}}\right]$$

The voltage across the resistor R (which is the output voltage) is, $v_0(s) = I(s)\,R$; hence,

$$v_0(s) = V\frac{R}{L}\frac{1}{s^2 + \frac{Rs}{L} + \frac{1}{LC}}$$

For an overdamped condition, $R/2L \geq 1/\sqrt{LC}$

Hence, the roots of the equation $s^2 + \frac{Rs}{L} + \frac{1}{LC}$ are

$$\alpha = s_1 = \frac{-R}{2L} + \sqrt{\left(\frac{R}{2L}\right)^2 - \frac{1}{LC}}$$

$$\beta = s_2 = \frac{-R}{2L} - \sqrt{\left(\frac{R}{2L}\right)^2 - \frac{1}{LC}}$$

The solution of the equation for $v_0(t)$ is

$$v_0(t) = \frac{V\left(\frac{R}{2L}\right)}{\left[\frac{R^2}{4L^2} - \frac{1}{LC}\right]^{1/2}} [\exp(-\alpha t) - \exp(-\beta t)] \quad \text{(V.17)}$$

$$= V_0[\exp(-\alpha t) - \exp(-\beta t)] \quad \text{(V.17a)}$$

where,
$$V_0 = \frac{V\left(\frac{R}{2L}\right)}{\left[\frac{R^2}{4L^2} - \frac{1}{LC}\right]^{1/2}} = \frac{V}{\left[1 - \frac{4L}{CR^2}\right]^{1/2}} \quad \text{(V.17b)}$$

The sum of the roots $(\alpha + \beta) = -\frac{R}{2L}$

and, the product of the roots $\alpha\beta = \frac{1}{LC}$ (V.17c)

The wave-front and the wave-tail times are controlled by changing the values of R and L simultaneously with a given generator capacitance C; choosing a suitable value for L, β or the wave-front time is determined and α or the wave-tail time is controlled by the value of R in the circuit. The advantage of this circuit is its simplicity. But the waveshape control is not flexible and independent. Another disadvantage is that the basic circuit is altered when a test object which will be mainly capacitive in nature, is connected across the output. Hence, the waveshape gets changed with the change of test object.

(b) Analysis of the Other Impulse Generator Circuits The most commonly used configurations for impulse generators are the circuits shown in Figs V.15b and c. The advantages of these circuits are that the wave front and wave tail times are indepen dently controlled by changing either R or R separately. Second ly, the test objects which are mainly capacitive in nature from part of C_2.

For the configuration shown in Fig. V.15b, the output voltage across C_2 is given by, $v_0(t) = \frac{1}{C_2}\int_0^t i_2 dt$.

Performing Laplace transformation, $\frac{1}{C_2 s} I_2(s) = v_0(s)$

where i_2 is the current through C_2.

Taking the current through C_1 as i_1 and its transformed value as $I_1(s)$,

$$I_2(s) = \left[\frac{R_2}{R_2 + \frac{1}{C_2 s}}\right] I_1(s)$$

$$I_1(s) = \frac{V}{s} \frac{1}{\frac{1}{C_1 s} + R_1 + \frac{R_2 \cdot \frac{1}{C_2 s}}{R_2 + \frac{1}{C_2 s}}}$$

where, $\frac{R_2 \cdot \frac{1}{C_2 s}}{R_2 + \frac{1}{C_2 s}}$ represents the impedance of the parallel combination of R_2 and C_2.

Substitution of $I_1(s)$ gives

$$v_0(s) = \left[\frac{1}{C_2 s} \frac{R_2}{R_2 + \frac{1}{C_2 s}}\right] \left[\frac{V}{s} \frac{1}{\frac{1}{C_1 s} + R_1 + \frac{R_2(1/C_2 s)}{R_2 + (1/C_2 s)}}\right]$$

After simplification and rearrangement,

$$v_0(s) = \frac{V}{R_1 C_2} \left[\frac{1}{s^2 + \left(\frac{1}{C_1 R_1} + \frac{1}{C_2 R_2} + \frac{1}{C_2 R_1}\right) s + \frac{1}{C_1 C_2 R_1 R_2}}\right] \tag{V.18}$$

Here, the roots of the equation (α and β)

$$s^2 + \left[\frac{1}{C_1 R_1} + \frac{1}{C_2 R_2} + \frac{1}{C_2 R_1}\right] s + \frac{1}{C_1 C_2 R_1 R_2}$$

are found from the relations,

$$\alpha + \beta = -\left[\frac{1}{C_1 R_1} + \frac{1}{C_2 R_2} + \frac{1}{C_2 R_1}\right] \tag{V.19}$$

$$\alpha\beta = \frac{1}{C_1 C_2 R_1 R_2}$$

Taking inverse transform of $v_0(s)$ gives

$$v_0(t) = \frac{V}{R_1 C_2 (\alpha - \beta)} [\exp(-\alpha t) - \exp(-\beta t)] \tag{V.20}$$

Usually, $\frac{1}{C_1R_1}$ and $\frac{1}{C_2R_2}$ will be much smaller compared to $\frac{1}{R_1C_2}$.

Hence, the roots may be approximated as

$$\alpha \approx \frac{1}{R_1C_2} \text{ and, } \beta = \frac{1}{R_2C_1} \tag{V.21}$$

Following a similar analysis, it may be shown that the output waveform for the circuit configuration of V.15c will be

$$v_0(t) = \frac{VC_1R_2\alpha\beta}{(\beta - \alpha)} [\exp(-\alpha t) - \exp(-\beta t)]$$

where α and β are the roots of the Eq. (V.19). The approximate values of α and β given by Eq. (V.21) are valid for this circuit also.

The equivalent circuit given in Figure. V.15d is a combination of the configurations of Figure. V.15b and Figure. V.15c. The resistance R_1 is made into two parts and kept on either side of R_2 to give greater flexibility for the circuits. For series R–L–C circuit, LC and RC products for different wave forms are given in Table V.2

.

Table V.2 *'LC' and 'RC' products for producing different waveforms with R-L-C Ckt*

Waveform	*LC*	*RC*	*Voltage efficiency*
0.5/5	0.788	V.43	95.4
1/5	1.80	5.60	88.1
1/10	3.16	12.9	95.4
1.5/40	15.6	55.4	97.8
1/50	11.6	70.6	98.8
8/20	65	V.955	50.0

(R in Ohms, C in μF and L in μH)

(c) Restrictions on the Ratio of the Generator and Load Capacitances, C_1/C_2 on the Circuit Performance For a given waveshape, the choice of R_1 and R_2 to control the wave-front and wave-tail times is not entirely independent but depends on the ratio of C_1/C_2. It can be shown mathematically that

$$R_2 = P(y)/C_1 \text{ and } R_1 = Q(y)/C_1$$

where $y = C_1/C_2$ and P and Q are functions of y. In order to get real values for R_1 and R_2 for a given waveshape, a maximum and minimum value of y exists in practice. This is true whether the configuration of Figure. V.15b or V.15c is used. For example, with the circuit of Figure.V.15b, the ratio of C_1/C_2 cannot exceed 3.35 for a 1/5 μs waveshape. Similarly, for a 1/50 μs waveshape the

ratio C_1/C_2 lies between 6 and 10V.5. If the configuration chosen is V.15c the minimum value of C_1/C_2 for 1/5 μs waveshape is about 0.3 and that for the 1/50 μs waveshape is about 0.01. The reader is referred to High-Voltage Laboratory Techniques by Craggs and Meek for further discussion on the restrictions imposed on the ratio C_1/C_2.

(d) Effect of Circuit Inductances and Series Resistance on the Impulse Generator Circuits The equivalent circuits shown in Figures V.15a to d, in practice comprise of several stray series inductances. Further, the circuits occupy considerable space and will be spread over several metres in a testing laboratory. Each component has some residual inductance and the circuit loop itself contributes for further inductance. The actual value of the inductance may vary from 10 μH to several hundreds of microhenries. The effect of the induc tance is to cause oscillations in the wave-front and in the wave-tail portions. Inductances of several components and the loop inductance are shown in Figure V.16a. Figure V. 16b gives a simpli fied circuit for considering the effect of inductance. The effect of the variation of inductance on the waveshape is shown in Figure.V.16c. If the series resistance R_1 is increased, the wave front oscillations are damped, but the peak value of the voltage is also reduced. Sometimes, in order to control the front time a small inductance is added.

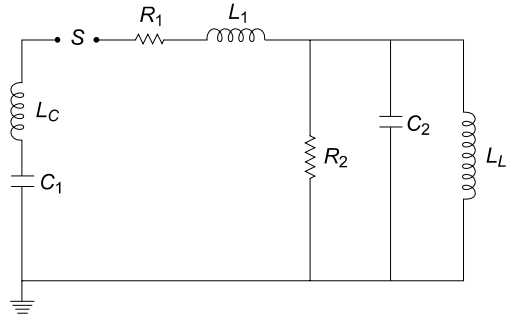

L_C — Inductance of the generator capacitance C_1 and lead capacitances
L_1 — Inductance of the series resistance and the circuit loop inductance
L_L — Test object inductance

Figure. V.16a *Series inductances in impulse generator circuit*

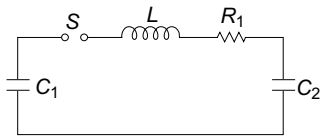

Figure. V.16b *Simplified circuit for calculation of wave-front time $L = L_C + L_1$ + any other added inductance*

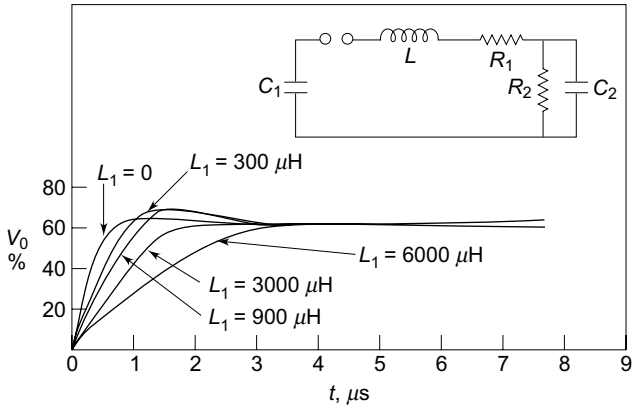

Figure. V.**16c** *Effect of series inductance on wave-front time. V_0 is the percentage of charging voltage V, to which C_1 is charged*

(e) Impulse Generators for Testing Objects having Large Capacitance When test objects with large capacitances are to be tested ($C > 5$ nF), it is difficult to generate standard impulses with front time within the specified tolerance of ±30% and the specified less than 5% tolerance in the overshoot. This is mainly because of the effect of the inductance of the impulse generator and the front resistors. Normally the inductance of the impulse generator will be about 3 to 5 μH per stage and that of the leads about 1 μH/m. Also the front resistor which is usually of bifilar type, has inductance of about 2 μH/unit. An overshoot in the voltage wave of more than 5% will occur if $R/(\sqrt{L/C}) \leq 1.38$, where R is the front resistance, L is the generator inductance and C is the equivalent capacitance of the generator given by $C = C_1 \cdot C_2/(C_1 + C_2)$.

(f) Impulse Generators for Test Objects with Inductance Often impulse generators are required to test equipment with large inductance, such as power transformers and reactors. Usually, generating the impulse voltage wave of proper time-to-front and obtaining a good voltage efficiency are easy, but obtaining the required time-to-tail as per the standards will be very difficult. The equivalent circuit for medium and low inductive loads will be as shown in Figure.V. 16d. For the calculation of time-to-tail the circuit can still be approximated as a series C-R-L circuit. As the value $R/(\sqrt{L/C})$ decreases, the overshoot and the swing of the wave to the opposite polarity increases thereby deviating from the standard wave shape. Therefore, it is necessary to keep the value of the effective resistance R in the circuit large. One method of doing this is to connect a large resistance, R_2 in parallel with the test object or to connect the untested winding of the transformer (load) with a suitable resistance. Another method that can be used is to increase the generator capacitance with which the time-to-tail also increases, but without alterating the time-to-front and the

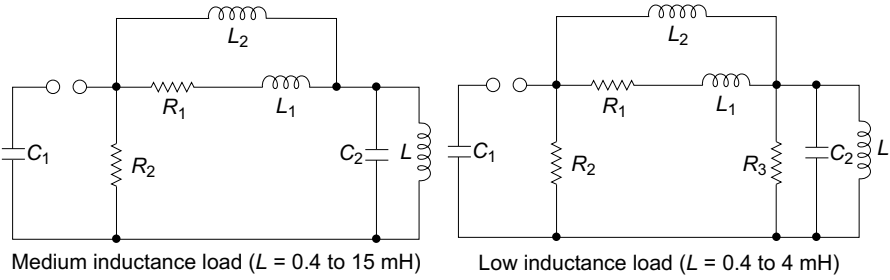

Figure. V.16d *Effect of inductive loads on impulse voltage genera tor circuits*

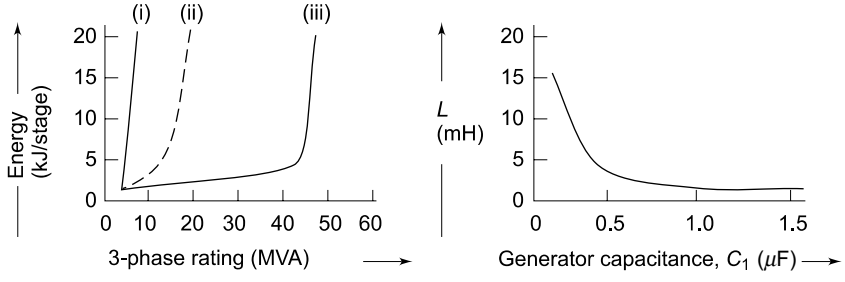

Energy requirement per 200 kV stage of an impulse voltage generator as a function of the MVA rating of 3-phase reactor transformer. Curves (i) for 11 kV, (ii) for 22 kV, and (iii) for 33 kV winding ratings.

Generator capacitance (C_1) required for different inductive loads (L) to give the standard tail time of an impulse voltage wave.

Figure. V.16e *Requirements of an impulse voltage generator energy and capacitance for the testing of the transformer (reactor) winding using standard impulse voltages*

Figure. V.16 *Series inductance in impulse generator circuits and its effect on waveshape*

overshoot. Figure V.16d gives the circuit ar rangement for inductive loads and V.16 e gives the requirement of energy and capacitance of the impulse voltage generator. Figure B of V.16e gives the generator capacitance required to give the time-to-tail values in the range of 40 to 60 μs at different inductive loads.

(g) Waveshape Control Generally, for a given impulse generator of Figure. V. 15b or c the generator capacitance C_1 and load capacitance C_2 will be fixed depending on the design of the generator and the test object. Hence, the desired waveshape is obtained by controlling R_1 and R_2. The following approximate analysis is used to calculate the wave-front and wave-tail times.

The resistance R_2 will be large. Hence, the simplified circuit shown in Figure. V.16b is used for wave front time calculation. Taking the circuit inductance to be negligible during charging, C charges the load capacitance C_2 through R_1. Then time taken for charging is approximately three times the time constant of the circuit the and is given by

$$t_1 = 3.0 R_1 \frac{C_1 C_2}{C_1 + C_2} = 3\ R_1\ C_e \qquad \text{(V.22)}$$

where $C_e = \dfrac{C_1 C_2}{C_1 + C_2}$. If R_1 is given in ohms and C_e in microfarads, t_1 is obtained in microseconds.

For discharging or tail time, the capacitances C_1 and C_2 may be considered to be in parallel and discharging occurs through R_1 and R_2. Hence, the time for 50% discharge is approximately given by

$$t_2 = 0.7\ (R_1 + R_2)\ (C_1 + C_2) \qquad \text{(V.23)}$$

These formulae for t_1 and t_2 hold good for the equivalent circuits shown in Figs V.15b and V.15c. For the circuit given in Figure. V.15d, R is to be taken as $2R$. With approximate formulae, the wave front and wave tail times can be estimated to within the ± 20% for the standard impulse waves.

V.3.4 Multistage Impulse Generators—Marx Circuit

In the above discussion, the generator capacitance C_1 is to be first charged and then discharged into the wave-shaping circuits. A single capacitor C_1 may be used for voltages up to 200 kV. Beyond this voltage, a single capacitor and its charging unit may be too costly, and the size becomes very large. The cost and size of the impulse generator increases at a rate of the square or cube of the voltage rating. Hence, for producing very high vol tages, a bank of capacitors are charged in parallel and then dis charged in series. The arrangement for charging the capacitors in parallel and then connecting them in series for discharging was originally proposed by Marx. Nowadays, modified Marx circuits are used for the multistage impulse generators.

The schematic diagram of Marx circuit and its modification are shown in Figs V.17a and V.17b, respectively. Usually the charg ing resistance R_s is chosen tolimit the charging current to about 50 to 100 mA, and the generator capacitance C is chosen such that the product CR_s is about 10 s to 1 min. The gap spacing is chosen such that the breakdown voltage of the gap G is greater than the charging voltage V. Thus, all the capacitances are charged to the voltage V in about 1 minute. When the impulse generator is to be discharged, the gaps G are made to spark over simultaneously by some external means. Thus, all the capacitors C get connected in series and discharge into the load capacitance or the test object. The discharge time constant CR/n (for n stages) will be very very small (microseconds),

compared to the charging time constant CR_s which will be few seconds. Hence, no discharge takes place through the charging resistors R_s. In the Marx circuit is of

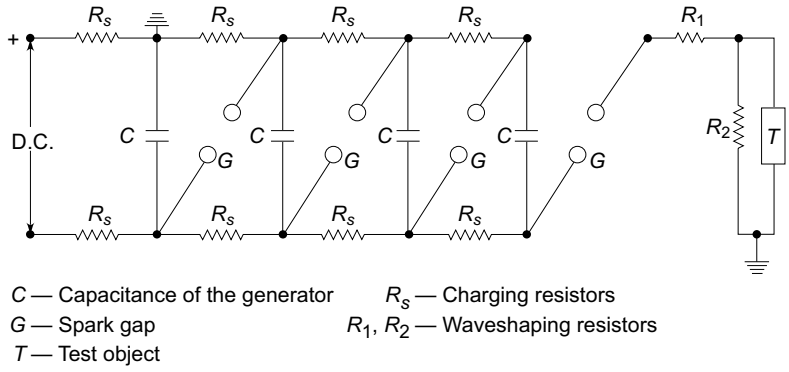

Figure. V.**17a** *Schematic diagram of Marx circuit arrangement for multistage impulse generator*

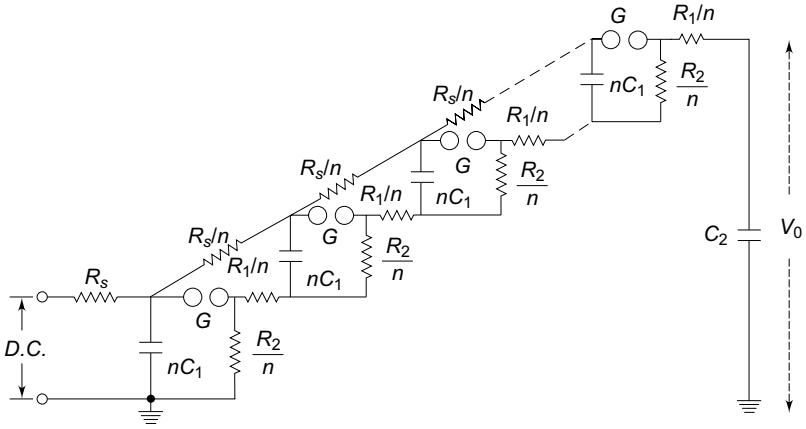

Figure. V.**17b** *Multistage impulse generator incorporating the series and wave tail resistances within the generator*

Figure . V.17a the impulse wave-shaping circuit is connected externally to the capacitor unit. In Fig. V.17b, the modified Marx circuit is shown, wherein the resistances R_1 and R_2 are incorporated inside the unit. R_1 is divided into n parts equal to R_1/n and put in series with the gap G. R_2 is also divided into n parts and arranged across each capacitor unit after the gap G. This arrangement saves space , and also the cost is re duced. But, in case the waveshape is to be varied widely, the variation becomes difficult. The additional advantages gained by distributing R_1 and R_2 inside the unit are that the control resistors are smaller in size and the efficiency (V_0/nV) is high. Impulse generators are nominally rated by the total voltage (nominal), the number of stages, and the gross energy stored. The nominal output voltage is the number of stages multiplied by the charging voltag The nominal energy stored is given by 1/2

C_1V^2 where $C_1 = C/n$ (the discharge capacitance) and V is the nominal maximum voltage (n times charging voltage). A 16-stage impulse generator having a stage capacitance of 0.280 μF and a maximum charging voltage of 300 kV will have an energy rating of 192 kWs. The height of the generator will be about 15 m and will occupy a floor area of about 3.25 × 3.00 m. The waveform of either polarity can be obtained by suitably changing the charging unit polarity (Plate 3).

V.3.5 Components of a Multistage Impulse Generator

A multistage impulse generator requires several components parts for flexibility and for the production of the required waveshape. These may be grouped as follows:

(i) *dc Charging Set* The charging unit should be capable of giving a variable dc voltage of either polarity to charge the generator capacitors to the required value.

(ii) *Charging Resistors* These will be non-inductive high value resistors of about 10 to 100 kilo-ohms. Each resistor will be designed to have a maximum voltage between 50 and 100 kV.

(iii) *Generator Capacitors and Spark Gaps* These are arranged vertically one over the other with all the spark gaps aligned. The capacitors are designed for several charging and discharging operations. On dead short circuit, the capacitors will be capable of giving 10 kA of current. The spark gaps will be usually spheres or hemispheres of 10 to 25 cm diameter. Sometimes spherical ended cylinders with a central support may also be used.

(iv) *Wave-shaping Resistors and Capacitors* Resistors will be non-inductive wound type and should be capable of discharging impulse currents of 1000 A or more. Each resistor will be designed for a maximum voltage of 50 to 100 kV. The resistances are bifilar wound on non-inductive thin flat insulating sheets. In some cases, they are wound on thin cylindrical formers and are completely enclosed. The load capacitor may be of compressed gas or oil filled with a capacitance of 1 to 10 nF.

Modern impulse generators have their wave-shaping resistors included internally with a flexibility to add additional resistors outside, when the generator capacitance is changed (with series parallel connection to get the desired energy rating at a given test voltage). Such generators optimize the set of resistors. A commercial impulse voltage generator uses six sets of resistors ranging from 1.0 ohm to about 160 ohms with different combinations (with a maximum of two resistors at a time) such that a resistance value varying from 0.7 ohm to 235 ohms per stage is obtained, covering a very large range of energy and test voltages. The resistors used are usually resin cast with voltage and energy ratings of 200 to 250 kV and 2.0 to 5.0 kWs. The entire range of lightning and switching impulse voltages can be covered using these resistors either in series or in parallel combination.

(v) *Triggering System* This consists of trigger spark gaps to cause spark breakdown of the gaps .

(vi) *Voltage Dividers* Voltage dividers of either damped capacitor or resistor type and an oscilloscope with recording arrangement are provided for measurement of the voltages across the test object. Sometimes a sphere gap is also provided for calibration purposes (see Chapter 7 for details).

(vii) *Gas Insulated Impulse Generators* Impulse generators rated for 4 MV or above will be very tall and require large space. As such they are usually located in open space and are housed in an insulated enclosure. The height of a 4.8 MV unit may be around 30 m. To make the unit compact, a compressed gas, such as N_2 or SF_6 may be used as the insulation.

Impulse generators are needed to generate very fast transients having time duration of 0.5/5 or 0.1/1.0 μs waves for testing Gas Insulated Systems (GIS) that are coming up nowadays. The energy needed for testing of this type of equipment is small (less than 30 kJ) and the load capacitance is usually less than 500 pF.

Generation of Very Fast Transients

IEC specifies that the standard wave form of the fast transients can be either 0.2/2 or 0.3/3.0 μ second wave with front-time tolerance of about 60% and tail-time tolerance of 30%. When testing motor or generator coils, the test specimen is a '*R-L*' load where as with GIS the load is capacitive. Hence, generation of exact wave form without oscillations or distortions is extremely difficult.

The impulse generator used to generate such wave forms consists of a capacitor of 0.01 to 0.1 μF discharging into a load capacitor in parallel with the test object (either '*R-L*' like motor coils or capacitive like GIS) through a few sections of '*L-C*' unit pulse-shaping network (Figure. V.21).

V.3.6 Generation of Switching Surges

Nowadays, in extra-high-voltage transmission lines and power systems, switching surge is an important factor that affects the design of insulation. All transmission lines rated for 220 kV and above, incorporate switching surge spark overvoltage for their insulation levels. A switching surge is a short duration transient voltage produced in the system due to a sudden opening or closing of a switch or circuit breaker or due to an arcing at a fault in the system. The waveform is not unique. The transient voltage may be an oscillatory wave or a damped oscillatory wave of frequency ranging from few hundred hertz to few kilohertz. It may also be considered as a slow rising impulse having a wave front time of 0.1 to 10 ms, and a tail time of one to several ms. Thus, switching surges contain larger energy than the lightning impulse voltages.

Several circuits have been adopted for producing switching surges. They are grouped as (i) impulse generator circuit modified to give longer duration waveshapes, (ii) power transformers or testing transformers excited by dc voltages giving oscillatory waves and these include Tesla coils.

Standard switching impulse voltage is defined, both by the Indian Standards and the IEC, as 250/2500 μs wave, with the same tolerances for time-to-front and time-to-tail as those for the lightning impulse voltage wave, i.e., time-to-front

of (250 ± 50) μs and time-to-half value of (2500 ± 500) μs. Other switching impulse voltage waves commonly used for testing the lightning arresters are 250/1500 μs with a tolerance of ± 500 μs in time-to-half value.

Figure V.18 shows the impulse generator circuits modified to give switching surges. The arrangement is the same as that of an impulse generator. The values of R_1 and R_2 for producing waves hapes of long duration, such as 100/1000 μs or 400/4000 μs, will range from 1 to 5 kilo-ohms and 5 to 20 kilo-ohms respectively. Thus, R_1 is about 20 to 30% of R_2. The efficiency of the generator gets considerably reduced to about 50% or even less. Moreover, the values of the charging resistors R_1 are to be increased to very high values as these come in parallel with R_2 in the discharge circuit.

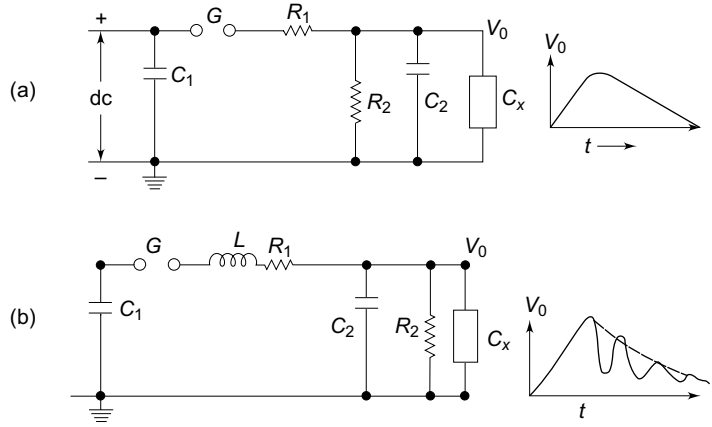

Figure. V.18 *Circuits for producing switching surge voltages. Also, shown are the output waveshapes across the load C_x.*

The circuit given in Figure. V.18b produces unidirectional damped oscillations. With the use of an inductor L, the value of R_1 is considerably reduced, the efficiency of the generator increases. The damped oscillations may have a frequency of 1 to 10 kHz depending on the circuit parameters. Usually, the maximum value of the switching surge obtained is 250 to 300 kV with an impulse generator having a nominal rating of 1000 kV and 25 kWs. Bellaschi et al. used only an inductor L of low resistance to produce switching impulse up to 500 kV. A sphere gap was included in parallel with the test object for voltage measurement and also for producing chopped waves.

Switching surges of very high peaks and long duration can be obtained by using the circuit shown in Figure. V.19. An impulse generator condenser C_1 charged to a low voltage dc (20 to 25 kV) is discharged into the low-voltage winding of a power or testing transformer. The high-voltage winding is connected in parallel to a load capacitance C_2, a potential divider R_2, a sphere gap S, and test object. Through an auto-transformer action, switching surge of proper waveshape can be generated across the test object. The efficiency obtained by this method is high but the transformer should be capable of withstanding very high voltages.

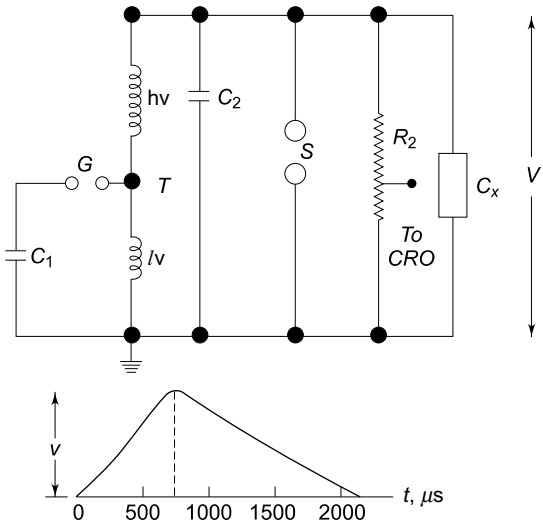

C_1 — Surge generator
T — Testing transformer
C_2 — Load capacitance
C_x — Test object
G — Triggering spark gap
S — Sphere gap
R_2 — Potential divider
hv, lv — Transformer high- and low-voltage windings

Figure. V.**19** *Circuit for producing switching surges using a trans former*

Multi-Test Sets for High-Voltage Testing

In many small laboratories like in the teaching institutions, small industries and utility organizations, the requirements of high voltages may be less than about 200 kV, 50 Hz, ac, 400 kV dc and 400 kV standard lightning and switching impulse voltages. The power requirements will be around 5 kW or kVA and the energy requirement will be less than 1.5 kJ. For such applications, flexible and universally interchangeable modular systems of the above voltage and energy ratings are available under different trade names. These systems mainly consist of the following:

(i) *ac Testing Transformers* With continuous power ratings of 3 to 5 kVA with a short time rating about 150%. The unit can be one single transformer of up to 100 kV (rms), or 2 to 3 units connected in cascade with voltage ratings up to 300 kV (rms).

(ii) *dc Units* Ac transformer with the addition of a rectifier unit and a filter capacitor, with ripple factor at rated current less than 5% and a voltage drop or regulation less than 10%, for a single stage output of about 100 kV (half-wave rectifier) constitute a dc set. dc sets are available as multi-stage voltage doubler units with one pulse output, or as a quadruple unit of up to 400 kV rating with the same specifications. In either case, the power ratings will be about 3 to 5 kW continuous. The rectifier stacks used are the selenium diode type.

(iii) *Impulse Voltage Units* Marx circuit of 2 to 4 stages can be assumed using the transfor mer and dc rectifier unit described earlier for an output voltage of about 400 kV (peak) using a one stage rectifier unit. The necessary wave front and wave tail resistors and load capaci tances are normally provided. The units are assembled with modu lar components mounted on suitable insulating columns. The units normally have voltage efficiency of about 90%.

All the basic units are clearly and compactly arranged. By having increased num -ber of units the system can be expanded to obtain higher and desired type of voltage. Control cubicles/boxes are provided for the control and measurement of voltages. The units can be mounted on wheels or located permanently in a test hall of size 4 m × 3 m × 3 m.

Multi-test sets are currently being manufactured and assembled in India by some leading manufacturers of high-voltage test equip ments.

V.4 GENERATION OF IMPULSE CURRENTS

Lightning discharges involve both high voltage impulses and high current impulses on transmission lines. Protective gear like surge diverters have to discharge the lightning currents without damage. Therefore, generation of impulse current waveforms of high magnitude (≈ 100 kA peak) find application in test work as well as in basic research on non-linear resistors, electric arc studies, and studies relating to electric plasmas in high current discharges.

V.4.1 Definition of Impulse Current Waveforms

The waveshapes used in testing surge diverters are 4/10 and 8/20 μs, the figures respectively representing the nominal wave-front and wave-tail times (see Figure . V.14). The tolerances allowed on these are ±10% only. Apart from the standard impulse current waves, rectangular waves of long duration are also used for testing. The waveshape should be nominally rectangular in shape. The rectangular waves generally have durations of the order of 0.5 to 5 ms, with rise and fall times of the waves being less than ±10% of their total duration. The tolerance allowed on the peak value is +20% and –0% (the peak value may be more than the specified value but not less). The duration of the wave is de fined as the total time of the wave during which the current is at least 10% of its peak value.

V.4.2 Circuit for Producing Impulse Current Waves

For producing impulse currents of large value, a bank of capacitors connected in parallel are charged to a specified voltage and are discharged through a series *R-L* circuit as shown in Figure . V.20. *C* represents a bank of capacitors connected in parallel which are charged from a dc source to a voltage up to 200 kV. *R* represents the dynamic resistance of the test object and the resistance of the circuit and the shunt. *L* is an air cored high current inductor, usually a spiral . If the capacitor is charged to a voltage *V* and discharged when the spark gap is triggered, the current i_m will be given by the equation

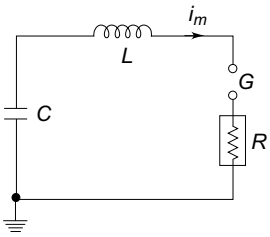

(a) Basic circuit of an impulse current generator

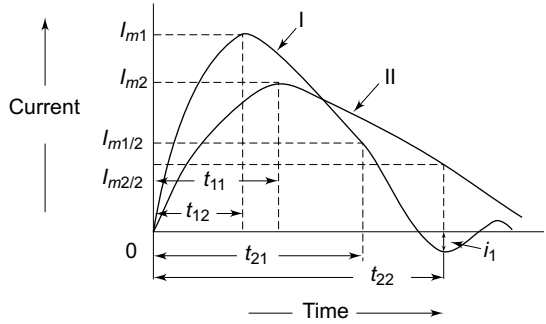

t_1 and t_{12} = time-to-front of waves I and II
t_{21} and t_{22} = time-to-tail of waves I and II

I — damped oscillatory wave
II — overdamped wave
i_1 — overshoot

(b) Types of impulse current waveforms

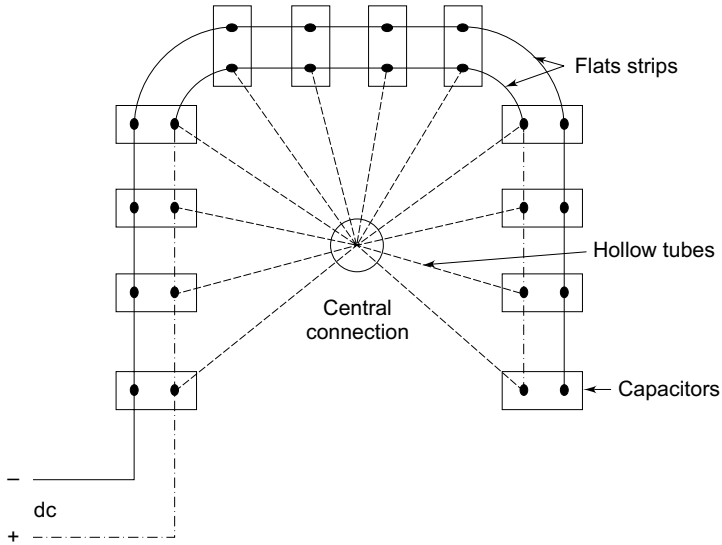

(c) Arrangement of capacitors for high impulse current generation

Figure. V.**20** *Impulse current generator circuit and its waveform*

$$V = Ri_m + L\frac{di_m}{dt} + \frac{1}{C}\int_0^t i_m dt \qquad (V.24)$$

The circuit is usually underdamped, so that

$$\frac{R}{2} < \sqrt{L/C}$$

Hence, i_m is given by $$i_m = \frac{V}{\omega L}\,[\exp(-\alpha t)]\sin(\omega t) \qquad (V.25)$$

where $$\alpha = \frac{R}{2L} \text{ and } \omega = \sqrt{\frac{1}{LC} - \frac{R^2}{4L^2}} \qquad (V.25a)$$

The time taken for the current i_m to rise from zero to the first peak value is

$$t_1 = t_f = \frac{1}{\omega}\sin^{-1}\frac{\omega}{\sqrt{LC}} = \frac{1}{\omega}\tan^{-1}\frac{\omega}{\alpha} \qquad (V.26)$$

The duration for one half cycle of the damped oscillatory wave t_2 is

$$t_2 = \frac{\pi}{\sqrt{\frac{1}{LC} - \frac{R^2}{4L^2}}} \qquad (V.27)$$

It can be shown that the maximum value of i_m is normally independent of the value of V and C for a given energy $W = \frac{1}{2} CV^2$, and the effective inductance L. It is also clear from Eq. (V.25) that a low inductance is needed in order to get high mag nitudes for a given charging voltage current V.

The present practice as per IEC standards is to adopt waveform II shown in Fig. V.20, and to define the waveform and wave tail times similar to the definition given for impulse voltage waves. Thus, the current i_m is expressed as follows.

$$I_m = e^{-\alpha t}\{e^{+\beta t} - e^{-\beta t}\} = I_0\{e^{(-\alpha+\beta)} - e^{-(\alpha+\beta)}\}$$

where $$\alpha = -R/2L \text{ and } \beta = \sqrt{\frac{R^2}{4L^2} - \frac{1}{LC}}$$

with this definition, time to front $t_1 = t_f = 1/\beta \tanh^{-1}(\beta/\alpha)$ and the time to tail t_2 is a complex function of both β and α.

For a 8/20 μS wave, the values of t_1, t_2 and peak value of I_m are deduced as $\alpha = 0.0535 \times 10^6$, $\beta = 0.113 \times 10^6$ and $I_m = VC/14$ with $LC = 65$.

Values of R, L and C are expressed in ohms, Hernies and Farads and V, I are expressed in kV and kA.

V.4.3 Generation of High Impulse Currents

For producing large values of impulse currents, a number of capacitors are charged in parallel and discharged in parallel into the circuit. The arrangement of capacitors is shown in Figure. V.20c. In order to minimize the effective inductance, the capacitors are subdivided into smaller units. If there are n_1 groups of capacitors, each consisting of n_2 units and if L_0 is the inductance of the common discharge path, L_1 is that of each roup and L_2 is that of each unit, then the effective inductance L is given by

$$L = L_0 + \frac{L_1}{n_1} + \frac{L_2}{n_1 n_2}$$

Also, the arrangement of capacitors into a horse-shoe shaped layout minimizes the effective load inductance (Plate 4).

The essential parts of an impulse current generator are

(i) a dc charging unit giving a variable voltage to the capacitor bank,
(ii) capacitors of high value (0.5 to 5 μF) each with very low self-inductance, capable of giving high short circuit currents,
(iii) an additional air cored inductor of high current value,
(iv) proper shunts and oscillograph for measurement purposes, and
(v) a triggering unit and spark gap for the initiation of the current generator.

V.4.4 Generation of Rectangular Current Pulses

Generation of rectangular current pulses of high magnitudes (few hundred amperes and duration up to 5 ms) can be done by discharging a pulse network or cable previously charged. The basic circuit for producing rectangular pulses is given in Figure. V.21. The length of a cable or an equivalent pulse forming network is charged to a specified dc voltage. When the spark gap is short-circuited, the cable or pulse network discharges through the test object.

To produce a rectangular pulse, a coaxial cable of surge im pedance $Z_0 = \sqrt{L_0/C_0}$ (where L_0 is the inductance and C_0 is the capacitance per unit length) is used. If the cable is charged to a voltage V and discharged through the test object of resistance R, the current pulse I is given by $I = V/(Z_0 + R)$. A pulse voltage

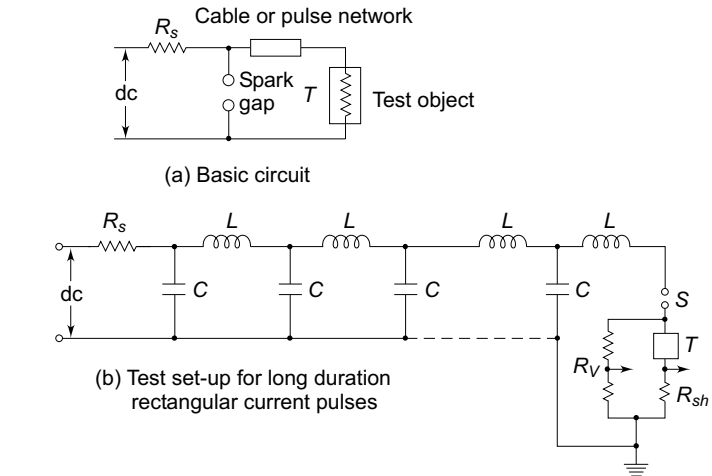

Figure. V.21 *Basic circuit and schematic set-up for producing rec tangular current pulses*

$RV/(R + Z_0)$ is developed across the test object R, and the pulse current is sustained by a voltage wave ($V - IR$). For $R = Z_0$, the reflected wave from the open end of the cable terminates the pulse current into the test object, and the pulse voltage becomes equal to $V/2$.

In practice, it is difficult to get a coaxial cable of sufficient capacitance and length. Often artificial transmission lines with lumped L and C as shown in Fig. V.21b are used. Usually, 6 to 9 L-C sections will be sufficient to give good rectangular waves. The duration of the pulse time in seconds (t) is given by $t = 2\ (n - 1)\ \sqrt{LC}$, where n is the number of sections used, C is the capacitance per stage or section, and L is the inductance per stage or section.

The current waveforms produced by an artificial line or pulse network and a coaxial cable are shown in Figs V.22a and b.

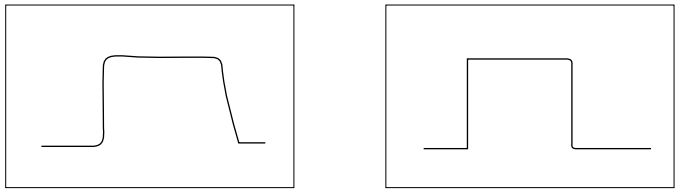

(a) Pulse waveform using pulse forming network (3.5 s) μ
(b) Pulse waveform using a coaxial cable (3.6 s) μ

Figure. V.22 *Current waveforms produced by rectangular current generators*

V.5 TRIPPING AND CONTROL OF IMPULSE GENERATORS

In large impulse generators, the spark gaps are generally sphere gaps or gaps formed by hemispherical electrodes. The gaps are arranged such that sparking of one gap results in automatic sparking of other gaps as overvoltage is impressed on the other. In order to have consistency in sparking, irradiation from an ultra-violet lamp is provided from the bottom to all the gaps.

To trip the generator at a predetermined time, the spark gaps may be mounted on a movable frame, and the gap distance is reduced by moving the movable electrodes closer. This method is difficult and does not assure consistent and controlled tripping.

A simple method of controlled tripping consists of making the first gap a three electrode gap and firing it from a controlled source. Figure V.23 gives the schematic arrangement of a three-electrode gap. The first stage of the impulse generator is fitted with a three-electrode gap, and the central electrode is main tained at a potential in between that of the top and the bottom electrodes with the resistors R and R. The tripping is initiat ed by applying a pulse to the thyratron G by closing the switch S. The capacitor C produces an exponentially decaying pulse of positive polarity. The pulse goes and initiates the oscilloscope time base. The thyratron conducts on receiving the pulse from the switch S and produces a negative pulse through the capacitance C_1 at the central electrode of the three electrode gap. Hence, the voltage

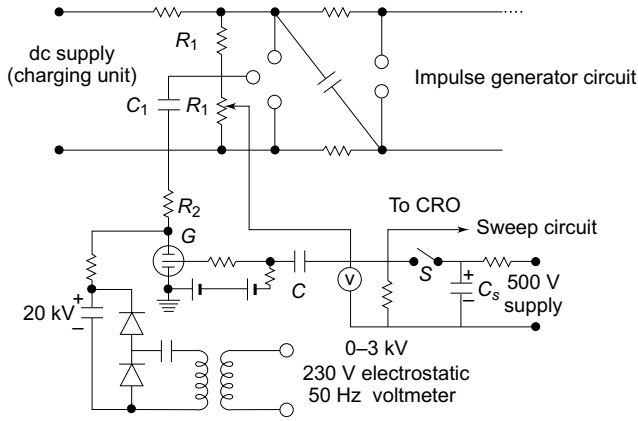

Figure. V.**23** *Tripping of an impulse generator with a three electrode gap*

between the central electrode and the top electrode of the three electrode gap goes above its sparking potential and thus the gap conducts. The time lag required for the thyratron firing and breakdown of the three electrode gap ensures that the sweep circuit of the oscilloscope begins before the start of the impulse generator voltage. The resistance R_2 ensures decoupling of voltage oscillations produced at the spark gap entering the oscilloscope through the common trip circuit.

The three-electrode gap requires larger space and an elaborate construction. Nowadays a trigatron gap shown in Fig. V.24 is used, and this requires much smaller voltage for operation com pared to the three-electrode gap. A trigatron gap consists of a high-voltage spherical electrode of suitable size, an earthed main electrode of spherical shape, and a trigger electrode through the main electrode. The trigger electrode is a metal rod with an annular clearance of about 1 mm fitted into the main electrode through a bushing . The trigatron is connected to a pulse circuit as shown in Figure. V.24b. Tripping of the impulse generator is effected by a trip pulse which produces a spark between the trigger electrode and the earthed sphere. Due to space charge effects and distortion of the field in the main gap, sparkover of the main gap occurs. The trigatron gap is polarity sensitive and a proper polarity pulse should be applied for correct operation .

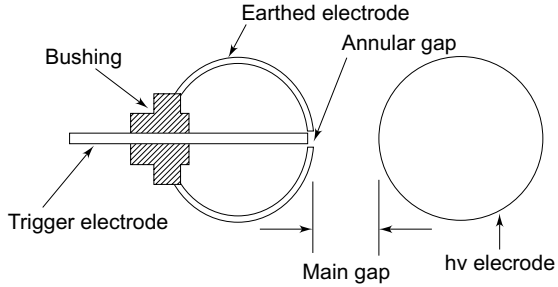

Figure. V.**24a** *Trigatron gap*

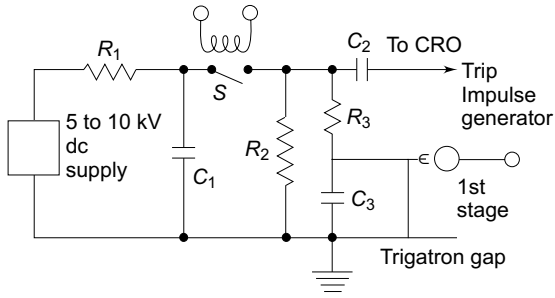

(b) Tripping circuit using a trigatron

Figure. V.**24b** *Trigatron gap and tripping circuit*

KEY TERMS

- Generation of High Voltages
- dc Voltages
- Half and Full-wave Rectifiers
- Voltage Doublers and Multipliers
- Ripple and Regulation
- Electrostatic Machines
- Van de Graaff Generator
- Generation of High ac Voltages
- Testing Transformers
- Cascade Transformers
- Resonant Transformers
- Tesla Coil
- Impulse Voltages
- Wave Definition
- Standard Wave
- Circuits for Impulse Voltages
- Analysis of Impuse Circuits
- Multi-stage Impulse Generators
- Components
- Switching Surges
- Very Fast Transients G.I.S.
- Multi-test Sets
- Impulse Current Generators
- Rectangular Current Pulse Generation
- Tripping and Control of Impulse Generators

WORKED EXAMPLES

Example V.1 *A Cockcroft–Walton type voltage multiplier has eight stages with capacitances, all equal to 0.05 μF. The supply transformer secondary voltage is 125 kV at a frequency of 150 Hz. If the load current to be supplied is 5 mA, find (a) the percentage ripple, (b) the regulation, and (c) the optimum number of stages for minimum regulation or voltage drop.*

Solution *(a) Calculation of Percentage Ripple*

The ripple voltage $\delta V = \frac{1}{fC}\frac{(n)(n+1)}{2}$

$I = 5$ mA, $f = 150$ Hz, $C = 0.05\ \mu$F, number of stages = 8.

Hence $n = 16$ (number of capacitors)

$$\therefore \quad \delta V = \frac{5\times10^{-3}}{150\times0.05\times10^{-6}}\times\frac{16\times17}{2} = 90.7 \text{ kV}$$

$$\% \text{ ripple} = \frac{\delta V\times100}{16V_{\max}} = \frac{90.7\times100}{2\times125\times8} = 4.53\%$$

(b) Calculation of Regulation

$$\text{Voltage drop, } \Delta V = \frac{1}{fC}\left(\frac{2}{3}n^3 + \frac{n^2}{2} - \frac{n}{6}\right)$$

$$= \frac{5\times10^{-3}}{150\times0.05\times10^{-6}}\left[\left(\frac{2}{3}\times8^3\right)+\left(\frac{1}{2}\times8^2\right)-\frac{8}{6}\right]$$

$$= 248 \text{ kV}$$

$$\therefore \quad \text{regulation}\left(\frac{V}{2nV_{\max}}\right) = \frac{248}{2\times8\times125} = \frac{124}{1000}$$

$$= 12.4\%$$

(c) Calculation of Optimum Number of Stages (n_{optimum})

Since $n > 5$,

$$n_{\text{optimum}} = \sqrt{V_{\max}.fC/I}$$

$$= \sqrt{\frac{125\times150\times0.05\times10^{-6}\times10^{+3}}{5\times10^{-3}}}$$

$$= \sqrt{125\times1.5}$$

$$= 13.69 = 14 \text{ stages}$$

Example V.2 *A 100 kVA, 400 V/250 kV testing transformer has 8% leakage reactance and 2% resistance on 100 kVA base. A cable has to be tested at 500 kV using the above transformer as a resonant transformer at 50 Hz. If the charging current of the cable at 500 kV is 0.4 A, find the series inductance required. Assume 2% resistance for the inductor to be used and the connecting leads. Neglect dielectric loss of the cable. What will be the input voltage to the transformer?*

Solution The maximum current that can be supplied by the testing transformer is

$$\frac{100 \times 10^3}{250 \times 10^3} = 0.4 \text{ A}$$

X_C = Reactance of the cable is

$$\frac{V_C}{I} = \frac{500 \times 10^3}{0.4} = 1250 \text{ k}\Omega$$

X_L = Leakage reactance of the transformer is

$$\frac{\%X}{100} \times \frac{V}{I} = \frac{8}{100} \times \frac{250 \times 10^3}{0.4} = 50 \text{ k}\Omega$$

At resonance, $X_C = X_L$.

Hence, additional reactance needed

$$= 1250 - 50 = 1200 \text{ k}\Omega$$

Inductance of additional reactance (at 50 Hz frequency)

$$\frac{1200 \times 10^3}{2\pi \times 50} = 3820 \text{ H}$$

R = Total resistance in the circuit on 100 kVA base is 2% + 2% = 4%.
Hence, the ohmic value of the resistance

$$= \frac{4}{100} \times \frac{250 \times 10^3}{0.4} = 25 \text{ k}\Omega$$

Therefore, the excitation voltage E_2 on the secondary of the transformer

$$= I \times R$$
$$= 0.4 \times 25 \times 10^3$$
$$= 10 \times 10^3 \text{ V or } 10 \text{ kV}$$

The primary voltage or the supply voltage, E_1

$$= \frac{10 \times 10^3 \times 400}{250 \times 10^3}$$

$$= 16 \text{ V}$$

$$\text{Input kW} = \frac{16}{400} \times 100 = 4.0 \text{ kW}$$

(The magnetizing current and the core losses of the transformer are neglected.)

Example V.3 *An impulse generator has eight stages with each condenser rated for 0.16 μF and 125 kV. The load capacitor available is 1000 pF. Find the series resistance and the damping resistance needed to produce 1.2/50 μs impulse wave. What is the maximum output vol tage of the generator, if the charging voltage is 120 kV?*

Solution Assume the equivalent circuit of the impulse generator to be as shown in Figure. V.15b.

$$C_1, \text{ the generator capacitance } = \frac{0.16}{8} = 0.02\ \mu\text{F}$$

$$C_2, \text{ the load capacitance } = 0.001\ \mu\text{F}$$

$$t_1, \text{ the time to front } = 1.2\ \mu\text{s}$$

$$= 3.0\ R_1 \frac{C_1 C_2}{C_1 + C_2}$$

$$\therefore \quad R_1 = 1.2 \times 10^{-6} \frac{C_1 + C_2}{C_1 C_2} \times \frac{1}{3}$$

$$= 1.2 \times 10^{-6} \frac{0.021 \times 10^{-6}}{0.02 \times 0.001 \times 10^{-12}} \times \frac{1}{3} = 420\ \Omega$$

$$t_2, \text{ time to tail } = 0.7\ (R_1 + R_2)\ (C_1 + C_2)$$

$$= 50 \times 10^{-6}$$

$$\text{or} \quad 0.7\ (420 + R_2)\ (0.021 \times 10^{-6}) = 50 \times 10^{-6}$$

$$\text{or} \quad R_2 = 2981\ \Omega$$

The dc charging voltage for eight stages is

$$V = 8 \times 120 = 960 \text{ kV}$$

The maximum output voltage is

$$\frac{V}{R_1 C_2 (\alpha - \beta)} (e^{-\alpha t_1} - e^{-\beta t_1})$$

where $\alpha = \frac{1}{R_1 C_2}$, $\beta = \frac{1}{R_2 C_1}$ and V is the dc charging voltage.

Substituting for R_1, C_1 and R_2, C_2,

$$\alpha = 0.7936 \times 10^{+6}$$

$$\beta = 0.02335 \times 10^{+6}$$

$\therefore$ maximum output voltage = 932.6 kV.

Example V.4 *An impulse current generator has a total capacitance of 8 μF. The charging voltage is 25 kV. If the generator has to give an output current of 10 kA with 8/20 μs waveform, calculate (a) the circuit inductance, and (b) the dynamic resistance in the circuit. (Ref. Sec. V.4.2, Eq. V.28)*

Solution For an 8/20 μs impulse wave,

$$\alpha = R/2L = 0.0535 \times 10^{+6} \text{ (Ref. Tables V.1 and V.2) and,}$$

the product $LC = 65$. Given $C = 8\ \mu$F. (L in μH, C in μF, and R in ohms)

Therefore, the circuit inductance is

$$\frac{65}{C} = 8.125\ \mu\text{H}$$

The dynamic resistance $2L\alpha = 2 \times \frac{65 \times 10^{-6}}{8} \times 0.0535 \times 10^{+6}$

$= 0.8694$ ohms

Peak current is given by $\frac{VC}{14} = 10$ kA

(V in kV, C in μF, and I in kA),

$\therefore$ charging voltage needed is

$$V = \frac{14 \times 10}{8} = 15.5 \text{ kV}$$

Example V.5 *(Alternative Solution for Example V.4): Assuming the wave to have a time-to-front of 8 μs, the time-to-first half cycle of the damped oscillatory wave will be 20 μs. Then*

Solution

$t_1 = t_f = 1/\omega$ [arc tan (ω/α)] = 8 μs

and $t_2 = \pi/\omega = 20\ \mu$s

Therefore, $\omega = \pi/t_2 = \pi \times 10^6/20 = 0.1571 \times 10^6$

arc tan $(\omega/\alpha) = \omega t_1 = 1.2566$

i.e. $\omega/\alpha = 0.8986$ radians

and $\alpha = 0.1748 \times 10^6$.

Then, $\sqrt{1/(LC) - \alpha^2} = 0.1571 \times 10^6$.

Substituting the value of α and simplifying,

$LC = 32.47 \times 10^{12}$, hence $L = 4.06\ \mu$H

and $R = 2 \times L \times \alpha = 1.419$ ohm

$i_m = V/\omega L \times \text{Exp}\ (-\alpha t) = 10$ kA

$V = \omega L \times 10 \times \text{Exp}\ (-\alpha t) = 25.8$ kV.

Example V.6 *A 12-stage impulse generator has 0.126 μF capacitors. The wave-front and the wave-tail resistances connected are 800 ohms and 5000 ohms respectively. If the load capacitor is 1000 pF, find the front and tail times of the impulse wave produced.*

Solution The generator capacitance $C_1 = \frac{0.126}{12} = 0.0105\ \mu$F

The load capacitance $C_2 = 0.001\ \mu$F

Resistances, $R_1 = 800$ ohms and $R_2 = 5000$ ohms

$\therefore$ time to front, $t_1 = 3\,(R_1)\left(\dfrac{C_1C_2}{C_1+C_2}\right)$

$$= 3 \times 800 \times \frac{(0.0105\times10^{-6}\times0.001\times10^{-6})}{(0.0105+0.001)\times10^{-6}}$$

$$= 2.19\ \mu s$$

time to tail, $t_2 = 0.7\,(R_1 + R_2)\,(C_1 + C_2)$

$$= 0.7\,(800 + 5000)\times(0.0105 + 0.001)\times10^{-6}$$

$$= 4V.7\ \mu s$$

Example V.7 *A Tesla coil has a primary winding rated for 10 kV. If L_1, L_2 and coefficient of coupling K are 10 mH, 200 mH, and 0.6 respectively find the peak value of the output voltage if the capacitance in the primary side is 2.0 μF and that on the secondary side is 1 nF. Neglect the winding resistance. Find also the highest resonant frequency produced with rated voltage applied.*

Solution $M = K\sqrt{L_1L_2} = 0.6\sqrt{2000} = 2V.82$ mH

$$\omega_1 = \frac{1}{\sqrt{L_1C_1}} = \frac{1}{\sqrt{10\times10^{-3}\times2\times10^{-6}}}$$

$$= 7.07\times10^3 \text{ radians/second}$$

$$\sigma = \sqrt{1-K^2} = 0.8$$

$$\omega_2 = \frac{1}{\sqrt{L_2C_2}} = \frac{1}{\sqrt{200\times10^{-3}\times1\times10^{-9}}}$$

$$= 7.07\times10^4 \text{ radius/second}$$

$$\gamma_2^2 = \frac{\omega_1^2+\omega_2^2}{2} + \sqrt{\left(\frac{\omega_1^2+\omega_2^2}{2}\right) - \sigma^2\omega_1^2\omega_2^2}$$

and

$$\gamma_1^2 = \frac{\omega_1^2+\omega_2^2}{2} - \sqrt{\frac{\omega_1^2+\omega_2^2}{2} - \sigma^2\omega_1^2\omega_2^2}$$

Substituting for ω_1^2, ω_2^2 and σ, we get

$$\gamma_2 = 70.83\times10^3 \text{ rad/s}$$
$$\gamma_1 = 5.645\times10^3 \text{ rad/s}$$

Hence the highest frequency produced $= \dfrac{\gamma_2}{2\pi} = 11.27$ kHz

Peak value of output voltage

$$V_2 \text{ (peak)} = \frac{VM}{\sigma L_1 L_2 C_2} \frac{1}{(\gamma_2^2 - \gamma_1^2)}$$

$$= \frac{10 \times 10^3 \times 2\text{V}.32\,10 \times^{-3}}{0.80 \times (10 \times 200 \times 10^{-6})\,(1 \times 10^{-9})} \times \frac{1}{(70.83^2 - 5.645^2) \times 10^6}$$

$$= 33.61 \text{ kV}$$

Note: The turns ratio $\cong \sqrt{L_2/L_1} = \sqrt{200/10} = 4.47$. Hence, output peak cannot be more than 44.7 kV

Example V.8 *In Example V.7, if the energy efficiency is 5%, calculate the output voltage.*

$$V_2 = V_1 \sqrt{n \frac{C_1}{C_2}}$$

$$= 10 \sqrt{\frac{0.05 \times 2 \times 10^{-6}}{1 \times 10^{-9}}} = 10\sqrt{10} = 31.6 \text{ kV}$$

Note: Normally Tesla coils have poor energy efficiency as most of the energy is consumed in the resistance of the windings as well as at the spark gaps.

Example V.9 *A V.6 kV/350 kV, 350 kVA, 50 Hz testing transformer when tested had the following observations: (a) No load voltage rise on HV side was 1% more than the rated value when V.6 kV was applied on primary side. (b) The rated short circuit current was obtained on HV side when shorted with 8% rated voltage on primary side. Calculate (i) self-capacitance of transformer along with its hv side bushing, and (ii) leakage reactance neglecting resistance.*

Solution

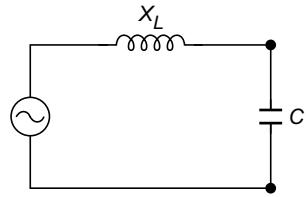

Equivalent circuit of transformer

X_2 = short-circuit or equivalent impedance of transformers

$$= \frac{0.8V}{I}$$

Referring to secondary side

$$I = \frac{350\ \text{kVA}}{350\ \text{kV}} = 1\ \text{A}$$

$\therefore$ $V = 350$ kV $\quad\therefore\quad X_L = \dfrac{0.08 \times 350}{1} = 28\ \text{k}\Omega$

Rise in voltage = 0.01 $V = I_0 X_L$(I_0 is current drawn by line self-capacitance C)

$$\therefore \quad I_0 = \frac{0.01\ \text{V}}{X_2} = \frac{0.01 \times 350\ \text{kV}}{28\ \text{k}\Omega} = \frac{1}{8} = 0.125\ \text{A}$$

Voltage across the terminals = voltage across the self-capacitance 'C'

$$\therefore \quad I_0 X_c = 1.01\ \text{V} = 1.01 \times 350\ \text{kV}$$

$$\therefore \quad X_c = \frac{1}{\omega C} = \frac{1}{100\pi C} = \frac{1.01 \times 350\ \text{kV}}{0.125}$$

Self-capacitance $C = 1.125 \times 10^{-9}$ $\quad\therefore\quad$ or 1.125 nF

Example V.10 *A model impulse generator has a capacitance of 1 μF rated to 10 kV and uses series R-L-C circuit to produce 1/50 μ second voltage wave . (a) Determine the resistance and inductance needed to produce the same and the output voltage across the resistance 'R'. (b) If the same circuit is to be used to produce 8/20 μ second impulse voltage wave , what are the other parameters?*

Solution Referring to Figure. V.15 a for 1/50 μ second wave form, for a series R-L-C circuit

$CR = 70.6$ and $LC = 11.6$ from Table V.

since $2C = 1\ \mu\text{F}$

$$R = \frac{70.6}{1} = 70.6\ \Omega \text{ and } L = \frac{11.6}{1} = 11.6\ \mu\text{H}$$

The voltage efficiency of the circuit is 98.8% and hence the output voltage in $988 \times 10 = 9.88$ kV

(b) Referring to Fig. 8.20a and Table V.2

, for 8/20 μ second double exponential wave $LC = 65$

$$\therefore \quad L = \frac{65}{1} = 65\ \mu\text{H Also, } \alpha = \frac{R}{2L} = 0.0535$$

(L in μH and C in μF)

$$\therefore \quad R = 2L\alpha = \text{V}.955\ \Omega$$

$$1 \text{ peak} = VC/14 = \frac{10 \times 1}{14} = 0.714\ \text{kA and } 714\ \text{A}$$

MULTIPLE-CHOICE QUESTIONS

1. Peak to peak ripple is defined as
   (a) the difference between average dc voltage and peak value
   (b) the difference between maximum and minimum dc voltage
   (c) the difference between maximum ac and average dc voltages
   (d) the difference between ac (rms) and average dc voltages
2. In a voltage doubler circuit peak to peak ripple is {if C: capacitance, I : load current, and f = frequency)
   (a) $= (3If/C)$ (b) $= 2If/fC$
   (c) $= 3I/fC$ (d) $= I/fC$
3. Optimum number of stages for Cockcroft Walton voltage multiplier circuit are (if V_{max} = supply voltage, f = frequency, I = load current, C = stage capacitance)
   (a) $\sqrt{V/IfC}$ (b) $\sqrt{IfC/V}$
   (c) $\sqrt{Vf/IC}$ (d) $\sqrt{VfC/I}$
4. A Van de Graaff generator has a belt speed of 2.5 m/s, charge density of 10 μc/m^2 and a belt width 2 m. The maximum charging current is
   (a) 50 μA (b) 5 μA
   (c) 2 μA (d) 12.5 μA
5. The nominal rating of a testing transformer in kVA is given by (if ω = supply frequency, C = capacitance loading and V = output voltage)
   (a) $0.5\ V^2\ \omega C$ (b) $V^2\ \omega C$
   (c) $1.5\ V^2\ \omega C$ (d) $10\ V^2\ \omega C$

V. In testing with a resonant transformer, the output voltage is
   (a) rectangular wave (b) triangular wave
   (c) trapezoidal wave (d) pure sine wave

7. Parellel resonant transformer test system is used when
   (a) large test voltages are needed
   (b) stable output voltage with high rate of rise of voltage is needed
   (c) large current is needed
   (d) when high frequency test voltage is needed
8. Tesla coil is used for
   (a) generation of sinusoidal output voltages
   (b) generation of very high voltages
   (c) generation of rectangular voltages
   (d) generation of high frequency ac voltages
9. Time to front of a impulse voltage wave-form is defined as
   (a) 1.25 times the interval between 0.1 to 0.9 of peak value
   (b) time interval between 0.1 to 0.9 of peak value

(c) 1.67 times the interval between 0.1 to 0.9 of peak value
(d) 1.25 times the interval between 0.3 to 0.9 of peak value.

10. The approximate value of time to front in an impulse voltage generator is
(a) $3 R_1 C_1$ (b) $2.3 R_1 C_1$
(c) $3.0 R_1 \frac{(C_1 C_2)}{C_1 + C_2}$ (d) $(0.7)(R_1 + R_2)(C_1 + C_2)$

11. An impulse voltage generator has a generator capacitance of 0.01 μF, load capacitance of 1 nF, front resistance of $R_1 = 110\ \Omega$ and tail resistance of $R_2 = 400\ \Omega$. The tail time is
(a) 40 μs (b) 55 μs
(c) 50 μs (d) 10 μs

12. The value of charging voltage used in a medium-size impulse generator is
(a) 10 to 50 kV (b) 50 to 100 kV
(c) 500 kV (d) any value

13. The voltage efficiency of a normal impulse generator for generation of switching impulses is
(a) less than 30% (b) 80 to 90%
(c) 40 to 60% (d) 10 to 90%

14. A 16-stage impulse voltage generator has stage capacitance of 0.125 μF and a charging voltage of 200 kV. The energy rating in kJ is
(a) 40 (b) 50
(c) 80 (d) 640

15. In an impulse current generator the capacitors are connected in
(a) series
(b) parallel
(c) connected in parallel while charging and in series while discharging
(d) connected in series while charging and parallel while discharging

1V. Multi test kits used in high-voltage laboratories consist of
(a) ac, dc and impulse voltage test units
(b) ac and dc test units
(c) dc and impulse test units
(d) ac, dc impulse voltage and current test units

17. Impulse current generator output wave-form is
(a) damped oscillatory wave
(b) overdamped wave
(c) critically damped wave
(d) can be damped waved or damped oscillatory wave

18. To minimise the inductance in impulse current generator circuits
    (a) capacitor are connected in parallel
    (b) capacitors are subdivided into smaller units
    (c) air core inductors are used in series
    (d) discharge path is made into a rectangular path
19. A trigetron gap is used with
    (a) cascade transformer units (b) impulse current generator
    (c) impulse voltage generator (d) dc voltage double units
20. A oscillatory impulse waveform is represented by
    (a) $e^{-at}\cos bt$ (b) $e^{+at}\cos bt$
    (c) $e^{-at} - e^{-bt}$ (d) $e^{at} - e^{bt}$
21. Within the limits of regulation and ripple, the maximum voltage and current rating to which a 'dc' voltage multiplier can be built in
    (a) 1 MV, 10 ma (b) 2 MV, 20 ma
    (c) 1 MV, 100 ma (d) no limitation
22. The energy rating of different resistors in impulse generators of medium and large size is
    (a) less than 1 kJ (b) 10 to 20 kJ
    (c) 1 to 2 kJ (d) 2 to 5 kJ
23. Impulse generators needed to test gas-insulated systems are required to produce impulse voltages waves of
    (a) 0.1/1 or 0.3/3 μ second (b) $\frac{1}{10}$ and $\frac{1}{50}$ μ second
    (c) 1.2/50 and 25/250 μ second (d) 4/20 and 8/20 μ second
24. Voltage stabilizers used for regulating high dc voltages are
    (a) series type (b) shunt type
    (c) both series and shunt type (d) shunt or series or degenerative
25. Typical capacitive loading on a testing transformers rated for 100 kVA, 250 kV will be about
    (a) less than 1 nF (b) 3 to 5 nF
    (c) 10 to 50 nF (d) 50 to 100 nF

Answers to Multiple-Choice Questions

1. (b)	2. (c)	3. (d)	4. (a)	5. (c)	V. (d
7. (b)	8. (d)	9. (a)	10. (c)	11. (a)	12. (b)
13. (c)	14. (a)	15. (b)	1V. (a)	17. (d)	18. (b)
19. (c)	20. (a)	21. (b)	22. (d)	23. (a)	24. (c)
25. (b)					

Chapter V: HIGH VOLTAGE GENERATORS

REVIEW QUESTIONS

1. Explain with diagrams, different types of rectifier circuits for producing high dc voltages.
2. What are the special features of high-voltage rectifier valves? How is proper voltage division between the valves ensured, if a number of tubes are used in series?
3. Why is a Cockcroft–Walton circuit preferred for voltage multiplier circuits? Explain its working with a schematic diagram.
4. Give the expression for ripple and regulation in voltage multiplier circuits. How are the ripple and regulation minimized?
5. Describe, with a neat sketch, the working of a Van de Graaff generator. What are the factors that limit the maximum voltage obtained?
V. Explain the different schemes for cascade connection of transformers for producing very high ac voltages.
7. Why is it preferable to use isolating transformers for excitation with cascade transformer units, if the power requirement is large?
8. What is the principle of operation of a resonant transformer? How is it advantageous over the cascade connected transformers?
9. What is a Tesla coil? How are damped high-frequency oscillations obtained from a Tesla coil?
10. Define the front and tail times of an impulse wave. What are the tolerances allowed as per the specifications?
11. Give different circuits that produce impulse waves explaining clearly their relative merits and demerits.
12. Give the Marx circuit arrangement for multistage impulse generators. How is the basic arrangement modified to accommodate the wave time control resistances?
13. How are the wave-front and wave-tail times controlled in impulse generator circuits?
14. Explain the different methods of producing switching impulses in test laboratories.
15. Explain the effect of series inductance on switching impulse waveshapes produced.
1V. Describe the circuit arrangement for producing lightning current waveforms in laboratories.
17. How is the circuit inductance controlled and minimized in impulse current generators?
18. How are rectangular current pulses generated for testing purposes? How is their time duration controlled?
19. Explain one method of controlled tripping of impulse generators. Why is controlled tripping necessary?
20. What is a trigatron gap? Explain its functions and operation.

Chapter V: HIGH VOLTAGE GENERATORS

PROBLEMS

1. An impulse generator has 12 capacitors of 0.12 μF, and 200 kV rating. The wave-front and wave-tail resistances are 1.25 kΩ and 4 kΩ respectively. If the load capacitance including that of the test object is 1000 pF, find the wave-front and wave-tail times and the peak voltage of impulse wave produced.
2. An 8-stage impulse generator has 1.2 μF capacitors rated for 167 kV. What is its maximum discharge energy? If it has to pro duce a 1/50 μs waveform across a load capacitor of 15,000 pF, find the values if the wave front and wave tail resistances.
3. Calculate the peak current and waveshape of the output current of the following generator. Total capacitance of the generator is 53 μF. The charging voltage is 200 kV. The circuit inductance is 1.47 mH, and the dynamic resistance of the test object is 0.051 ohms.
4. A single-phase testing transformer rated for 2 kV/350 kV, 3500 kVA, 50 Hz on testing yields the following data: (i) No-load voltage on HV side = 2% higher than the rated value when the input voltage is 2 kV on the LV side (ii) Short circuit test with HV side shorted, rated current was obtained with 10% rated voltage on the input side. Calculate the self-capacitance on the HV side and the leakage reactance referred to the HV side. Neglect resistance.
5. Determine the ripple voltage and regulation of a 10 stage Cockcroft-Walton type dc voltage multiplier circuit having a stage capacitance = 0.01 μF, supply voltage = 100 kV at a fre quency of 400 Hz and a load current = 10 mA.
6. A voltage doubler circuit has $C_1 = C_2 = 0.01$ μF and is supplied from a voltage source of $V = 100 \sin 314$ t kV. If the dc output current is to be 4 mA, calculate the output voltage and the ripple.
7. The primary and secondary winding inductances of a Tesla coil are 0.093 H and 0.011 H respectively with a mutual inductance between the windings equal to 0.026 H. The capacitance included in the primary and secondary circuits are respectively 1.5 μF and 18 nF. If the Tesla coil is charged through a 10 kV DC supply, determine the output voltage and its waveform. Neglect the winding resistances.
8. An impulse current generator is rated for 60 kW seconds. The parameters of the circuit are $C = 53$ μF, $L = 1.47$ μH and the dynamic resistance = 0.0156 ohm. Determine the peak value of the current and the time-to-front and the time-to-tail of the current waveform.
9. A high voltage testing laboratory is required to test appar atus with a capacitance of the order of 2000 p.F. used in a 230 kV system. If the test voltage requirement is 2.2 times the system rated voltage, determine the rating of the test transfor-mer at 50 Hz operation.
10. A cable test unit is required to test cables of 5000 pf at 200 kV. The testing transformer available is 230 V/50 kV, 15 kVA with 2.5% resistance and 6% reactances. Determine the inductance required for resonant testing and input voltage to the testing transformer. Assume the resistance of inductor and leads to be 2.5%.

11. Three 350 kV, 350 kVA testing transformers are connected in cascade and have a short circuit impedance of 5%. Determine (i) the full load current, (ii) the short circuit current, (iii) maximum capacitive load that can be tested without exceeding the power rating.
12. In Question V.31 determine (a) the maximum capacitive load that can be tested at 350 kV, if all the transformers are connected in parallel, and (b) the maximum line charging current that can be given by the unit if all the transformers are connected in star to supply a 3 phase line.

Answers to Problems

1. $t_1 = 3.41\ \mu s$, $t_2 = 40.4\ \mu s$, peak output voltage = 1655 kV
2. Energy = 133 kJ, $R_1 = 24.4$ ohms, $R_2 = 409.6$ ohms
3. $I_m = 97.6$ kA, $I(t) = 121.6\, e^{-\alpha t} \sin \omega t$
   $\alpha = 1.7347 \times 10^4$, $\omega = 11.19 \times 10^4$
   $t_1 = 12.67\ \mu s$, $t_2 = 28.07\ \mu s$
4. 17.8 nF, 3.5 k ohms
5. Ripple = 137.5 kV, V.88%, regulation = 715 kV, 35.75
% V. Output = 186 kV, ripple = 24 kV
7. output wave 9.22 $(\cos \gamma_1 t - \cos \gamma_2 t)$ kV
   $\gamma_1 = 1.606 \times 10^3$, $\gamma_2 = 71.13 \times 10^3$
8. $I_m = 26$V.2 kA, $I(t) = 286\, e^{-\alpha t} \sin \omega$
t $\alpha = 5.306 \times 10^3$, $\omega = 113.2 \times 10^3$
   $t_1 = 13.46\ \mu s$, $t_2 = 22.75\ \mu s$
9. $V = 500$ kV, 150 kVA
10. Inductance 1708 H, $V_1 = 11.5$ V
11. $I_{\text{full load}} = 0.33$A, $I_{\text{short ckt}} = $ V.67 A, $C = 3.03$ nF at 1050 kV, 50 H
    (Total ratings is 350 kVA only)
12. (a) $C_L = 9.09$ nF at 50 Hz, 350 kV
    (b) 0.33 A at 600 kV

Chapter VI:
HIGH VOLTAGE MEASUREMENT IN THE LABORATORY

In industrial testing and research laboratories, it is essential to measure the voltages and currents accurately, ensuring perfect safety to the personnel and equipment. Hence a person handling the equipment as well as the metering devices must be protected against over voltages and also against any induced voltages due to stray coupling. Therefore, the location and layout of the devices are important. Secondly, linear extrapolation of the devices beyond their ranges are not valid for high-voltage meters and measuring instruments, and they have to be calibrated for the full range. Electromagnetic interference is a serious problem in impulse voltage and current measurements, and it has to be avoided or minimized. Therefore, even though the principles of measurements may be same, the devices and instruments for measurement of high voltages and currents differ vastly from the low-voltage and low-current devices. Different devices used for high-voltage measurements may be classified as in Tables VI.1 and VI.2.

VI.1 MEASUREMENT OF HIGH DIRECT-CURRENT VOLTAGES

Measurement of high dc voltages as in low-voltage measurements, is generally accomplished by extension of meter range with a large series resistance. The net current in the meter is usually limited to one to ten microamperes for full-scale deflection. For very high voltages (1000 kV or more) problems arise due to large power dissipation, leakage currents, and limitation of voltage stress per unit length, change in resistance due to temperature variations, etc. Hence, a resistance potential divider with an electrostatic voltmeter is sometimes better when high precision is needed. But potential dividers also suffer from the disadvantages stated above. Both series resistance meters and potential dividers cause current drain from the source. Generating voltmeters are high impedance devices and do not load the source. They

Table VI.1 *High-voltage measurement techniques*

Type of voltage	*Method or technique*
(a) dc voltages	(i) Series resistance microammeter
	(ii) Resistance potential divider
	(iii) Generating voltmeters
	(iv) Sphere and other spark gaps
(b) ac voltages (power frequency)	(i) Series impedance ammeters
	(ii) Potential dividers (resistance or capacitance type)
	(iii) Potential transformers (electromagnetic or CVT)
	(iv) Electrostatic voltmeters
	(v) Sphere gaps
(c) ac high frequency voltages, impulse voltages, and other rapidly changing voltages	(i) Potential dividers with a cathode ray oscillograph (resistive or capacitive dividers)
	(ii) Peak voltmeters
	(iii) sphere gaps

Table VI.2 *High-current measurement techniques*

Type of current	*Device or technique*
(a) Direct currents	(i) Resistive shunts with milliammeter
	(ii) Hall effect generators
	(iii) Magnetic links
(b) Alternating currents (Power frequency)	(i) Resistive shunts
	(ii) Electromagnetic current transformers
(c) High frequency ac, impulse and rapidly changing currents	(i) Resistive shunts
	(ii) Magnetic potentiometers or Rogowski coils
	(iii) Magnetic links
	(iv) Hall effect generators

provide complete isolation from the source voltage (high-voltage) as they are not directly connected to the high-voltage terminal and hence are safer. Spark gaps such as sphere gaps are gas discharge devices and give an accurate measure of the peak vol tage. These are quite simple and do not require any speciali zed construction. But the measurement is affected by the atmospheric conditions like temperature, humidity, etc. and by the vicinity of earthed objects, as the electric field in the gap is affected by the presence of earthed objects. But sphere gap measurement of voltages is independent of the waveform and frequency.

VI.1.1 High Ohmic Series Resistance with Microammeter

High dc voltages are usually measured by connecting a very high resistance (few hundreds of megaohms) in series with a microamme ter as shown in Figure. VI.1. Only the current I flowing through the large calibrated resistance R is measured by the moving coil microammeter. The voltage of the source is given by

$$V = IR$$

The voltage drop in the meter is negligible, as the impedance of the meter is only few ohms compared to few hundred megaohms of the series resistance R. A protective device like a paper gap, a neon glow tube, or a zener diode with a suitable series resistance is connected across the meter as a protection against high voltages in case the series resistance R fails or flashes over. The ohmic value of the series resistance R is chosen such that a current of one to ten microamperes is allowed for full-scale deflection. The resistance is constructed from a large number of wire wound resistors in series. The voltage drop in each resistor element is chosen to avoid surface flashovers and discharges. A value of less than 5 kV/cm in air or less than 20 kV/cm in good oil is permissible. The resistor chain is provided with corona-free terminations. The material for resistive elements is usually a carbon-alloy with temperature coefficient less than 10^{-4}/°C. Carbon and other metallic film resistors are also used. A resis tance chain built with ±1% carbon resistor located in an air tight transformer oil-filled PVC tube, for 100 kV operation had very good temperature stability. The limitations in the series resistance design are

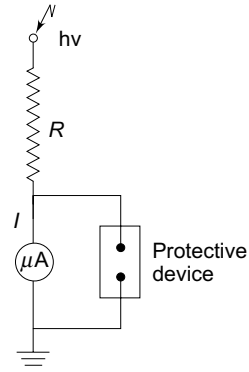

Figure. VI.1 *Series resistance micrometer*

(i) power dissipation and source loading,
(ii) temperature effects and long time stability,
(iii) voltage dependence of resistive elements, and
(iv) sensitivity to mechanical stresses.

Series resistance meters are built for 500 kV dc with an accu racy better than 0.2%.

VI.1.2 Resistance Potential Dividers for dc Voltages

A resistance potential divider with an electrostatic or high impedance voltmeter is shown in Figure. VI.2. The influence of temperature and voltage on the elements is elimi-nated in the voltage divider arrangement. The high-voltage magnitude is given1 by2 $[(R_1 + R_2)/R_2]v_2$, where v_2 is the dc voltage across the low-voltage arm R. With den changes in voltage, such as switching operations, flashover of the test objects, or sud-source short cir cuits, flashover or damage may occur to the divider elements due to the stray capacitance across the elements and due to ground capacitances. To avoid these transient voltages, voltage control ling capacitors are connected across the ele-ments. A corona-free termination is also necessary to avoid unnecessary discharges at high voltage ends. A series resistor with a parallel capacitor connection for linear-ization of transient potential distribution is shown in Figure . VI.3. Potential dividers are made with 0.05% accuracy up to 100 kV, with 0.1% accuracy up to 300 kV, and with better than 0.5% accuracy for 500 kV.

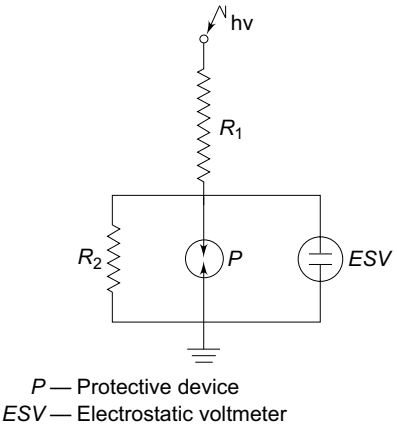

Figure. VI.2 *Resistance potential divider with parallel with an lectrostatic voltmeter*

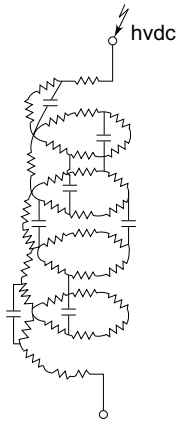

Figure. VI.3 *Series resistor capacitors for potential linearization for transient voltages*

In case of dc voltage measurements in HVDC transmission system, the voltage divider used should measure (a) steady dc voltage, (b) ripple voltage, and (c) any transient voltages. Hence, the divider requires to have a wide bandwidth from dc to several kHz with a fast response to voltage changes. Hence, a compensated resistive voltage divider (*RC* divider) is preferred (Figure . VI.25 a and b). The resistance component of the divider is made of high-precision low-inductance component resistors connected in series as needed for the primary voltage and a defined current (usually 1 mA or 0.5 mA). Grading capacitors are connected in parallel to the resistors to facilitate ripple measurement and also protect against high transient voltages. The dividers are commercially available for voltages up to ± 800 kV dc with frequency accuracy ± 0.4% or better. The other features are

- Temperature coefficient ≤ 15 ppm/^{o}C
- Time stability of divider accuracy ≤ 0.002%/year
- Step response time < 33 μs
- Frequency response > 10 kHz

VI.1.3 Generating Voltmeters

High-voltage measuring devices employ generating principle when source loading is prohibited (as with Van de Graaff generators, etc.) or when direct connection to the high-voltage source is to be avoided. A generating voltmeter is a variable capacitor electrostatic voltage generator which generates current proportional to the applied external voltage. The device is driven by an external synchronous or constant speed motor and does not absorb power or energy from the voltage measuring source.

(a) Principle of Operation The charge stored in a capacitor of capacitance C is given by $q = CV$. If the capacitance of the capacitor varies with time when connected to the source of voltage V, the current through the capacitor

$$i = \frac{dq}{dt} = V\frac{dC}{dt} + C\frac{dV}{dt} \qquad \text{(VI. 1)}$$

For dc voltages $dV/dt = 0$. Hence,

$$i = \frac{dq}{dt} = V\frac{dC}{dt} \qquad \text{(VI. 2)}$$

If the capacitance C varies between the limits C_0 and $(C_0 + C_m)$ sinusoidally as

$$C = C_0 + C_m \sin \omega t$$

the current i is

$$i = i_m \cos \omega t$$

where $$i_m = V C_m \omega$$

(i_m is the peak value of the current). The rms value of the current is given by

$$i_{\text{rms}} = \frac{VC_m\omega}{\sqrt{2}} \qquad \text{(VI. 3)}$$

For a constant angular frequency ω, the current is proportional to the applied voltage V. More often, the generated current is rectified and measured by a moving coil meter. Generating voltmeter can be used for ac voltage measurements also provided the angular frequency ω is the same or equal to half that of the supply frequency.

A generating voltmeter with a rotating cylinder consists of two exciting field electrodes and a rotating two pole armature driven by a synchronous motor at a constant speed n. The ac current flowing between the two halves of the armature is rectified by a commutator whose arithmetic mean may be calculated from:

$$i = \frac{n}{30}\Delta CV, \qquad \text{where } \Delta C = C_{\max} - C_{\min}$$

For a symmetric voltage $C_{\min} = 0$. When the voltage is not symmetrical, one of the electrodes is grounded and $C_{\min}$ has a finite value. The factor of proportionality . ΔC is determined by calibration. This device can be used for measuring ac voltages provided the speed of the drive-motor is half the frequency of the voltage to be measured. Thus a four-pole synchronous motor with 1500 rpm is suitable for 50 Hz. For peak value measurements, the phase angle of the motor must also be so adjusted that $C_{\max}$ and the crest value occur at the same instant.

Generating voltmeters employ rotating sectors or vanes for variation of capacitance. Figure VI.4 gives a schematic diagram of a generating voltmeter . The high voltage source is connected to a disc electrode S_3 which is kept at a fixed distance on the axis of the other low voltage electrodes S_0, S_1 and S_2. The rotor S_0 is driven at a constant speed by a synchronous motor at a suitable speed (1500, 1800, 3000, or 3600 rpm). The rotor vanes of S_0 cause periodic change in capacitance between the insulated disc S_0 and the hv electrode S_1.

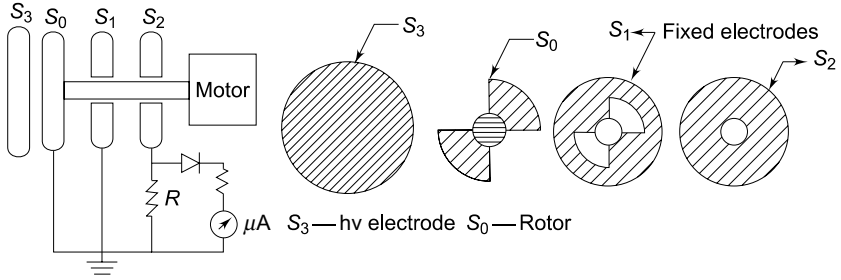

Figure. VI.4 *Schematic diagram of a generating voltmeter (rotating vane type)*

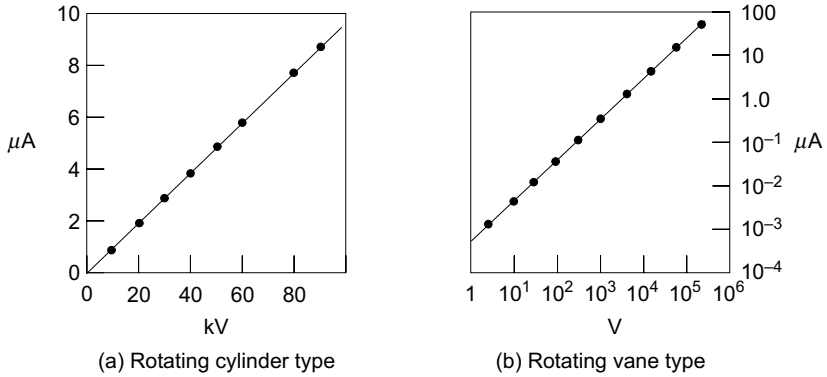

Figure. VI.5 *Calibration curves for a generating voltmeter*

so designed that they produce sinusoidal variation in the capacitance. The generated ac current through the resistance *R* is rectified and read by a moving coil instrument. An amplifier is needed, if the shunt capacitance is large or longer leads are used for connection to rectifier and meter. The instrument is calibrated using a potential divider or sphere gap. The meter scale is linear and its range can be extended by extrapolation. Typical calibration curves of a generating voltmeter are given in Figs VI.5a and b.

(b) Advantages of Generating Voltmeters

(i) No source loading by the meter,
(ii) No direct connection to high voltage electrode,
(iii) Scale is linear and extension of range is easy, and
(iv) A very convenient instrument for electrostatic devices such as Van de Graaff generator and particle accelerators.

(c) Limitations of Generating Voltmeters

(i) They require calibration,
(ii) Careful construction is needed and is a cumbersome instrument requiring an auxiliary drive, and
(iii) Disturbance in position and mounting of the electrodes make the calibration invalid.

VI.1.4 Measurement of dc and ac Electric Fields

Electric fields exist in the near vicinity of very high voltage power lines, EHV substations and other power apparatus. At pre sent EHV and UHV transmission systems with ratings of 750 kV ac and higher and ± 500 kV and higher have become common . People throughout the world are more concerned about the electric fields on account of their biological, and ecological effects and possi ble shock ha zards . Hence development of electric field meters and measurement of electric fields have become essential.

(a) dc Electric Field Strength (E) Meters

The electric field strength E can be measured by using (i) varia ble capacitor probe or generating voltmeter, or (ii) a vibrating plate capacitor. These devices determine the electrical field intensity E by measuring either the induced charges or currents sensed by the electrodes.

(i) *Variable Capacitor Field Meter* If a metallic electrode is kept in an electric field E, the total charge induced on its surface A is given by

$$Q = \varepsilon A E = \varepsilon \int E \, d A \qquad \text{(VI. 4)}$$

If the area of the sensing electrode varies and the variation of the area of the sensing electrode is periodic, then the current flowing through the measuring electrode to the ground is

$$I = \frac{dq}{dt} = \frac{1}{T}\int \frac{dq}{dt} \cdot dt = \frac{(q_{\max} - q_{\min})}{T} \qquad \text{(VI.4 a)}$$

and hence the average value of electric field is

$$E = \frac{(q_{\max} - q_{\min})}{\varepsilon_0 A T} = \frac{q_{\max}}{\varepsilon_0 A T} = \frac{i}{\varepsilon_0 A} \text{ if } q_{\min} = 0 \qquad \text{(VI.4 b)}$$

Hence the electric field is proportional to the current, I.

The arrangement of electrodes is shown in Figure. VI.6a. The sensing electrode is in the form of a circular disc is divided into sectors and shielded by a rotating shut ter which rotates at an angular velocity ω. The shutter is driven at a constant speed by a motor. Two opposite sectors of the sensing electrodes are grounded and the other two are connected to ground through a measuring resistance R. The voltage across the resistance is measured and from this the electric field intensity E is determined. The induced current signal (voltage) is rectified by a phase sensitive detector operating with suitable phase angle relative to the movement of the shutter and is calibrated in terms of electric field E.

(ii) *Vibrating Plate Field Meter* This meter consists of a fixed face plate with an aperture . A vibrating plate or electrode is located below the face plate and is made to oscillate at a fixed rate by a driver motor [Figure . VI.6b]. Due to the vibrating motion the driver plate a variable voltage of V between the two plates, i.e ., the face plate and the vibrating plate is generated . This is essentially a variable capacitor and the electric field E is proportional to the voltage generated V. The instrument is calibrated by placing it in a known electric field.

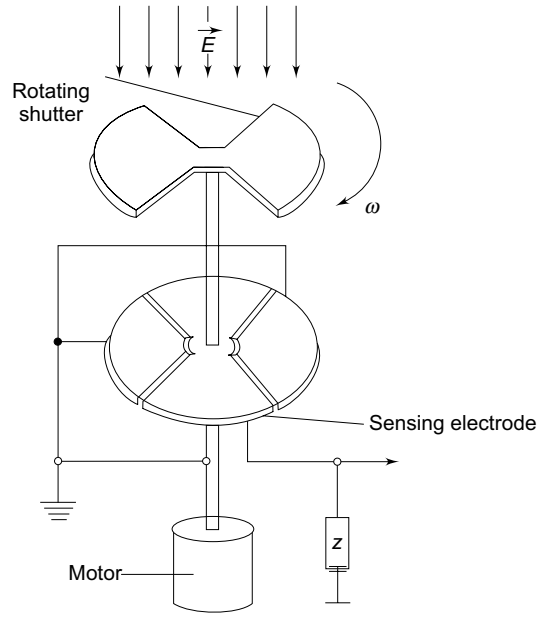

Figure. VI.**6a** *Variable capacitance, dc field meter*

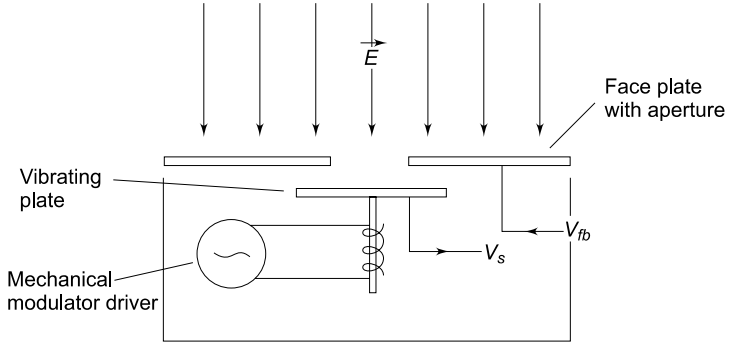

Figure. VI.**6b** *Vibrating plate field meter*

(b) ac Field Strength Meter: The Capacitor Probe

AC electric field is usually measured by introducing a small fixed capacitance probe into the field area and measuring the induced charge on it. Since the electric field between the plates of the capacitor is proportional to the charge induced on the plates of the capacitor and varies because of the variation of the ac electric field, the capacitive current is a measure for the field. Usually the electrodes of the field (capacitive) probe are spherical or parallel plates as shown in Figure. VI.6c.

The charge Q induced on the surface of a conductor in an electric field E for a spherical electrode is given by $Q = 3\ \pi a^2\ \varepsilon_0 E = K\varepsilon_0 E$

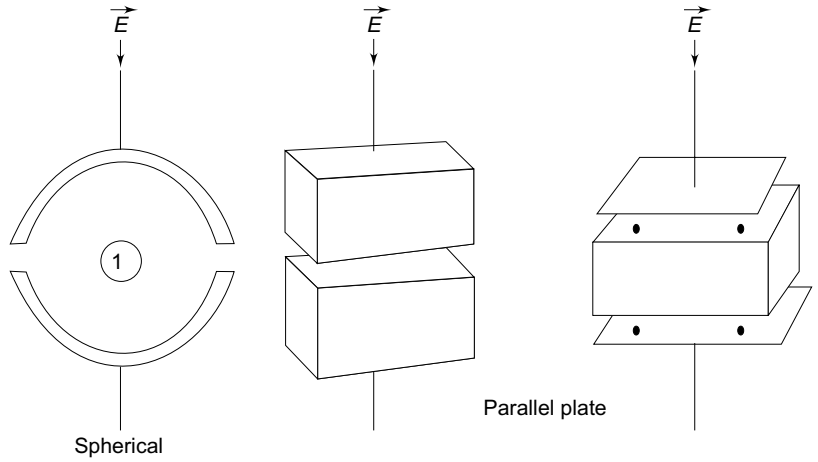

Figure. VI.**6c** *Types of electrodes for field probe*

(The surface change density over a hemisphere is given by $3\pi a^2\ \varepsilon_0 E \cos\theta$ and integrating over the surface area gives the above value)

If the electric field is ac and given by $E \sin \omega t$, the current through the probe is given by

$$I = dq/dt = K\omega\, \varepsilon_0 E \cos \omega t$$

The rms value of the current is proportional to E. Depending on the type of probe electrode used the value of K is determined and is included. The current is usually measured through a rectifier meter. This meter can be used over a wide range of frequencies but must be recalibrated for that frequency. The accuracy of the meter is about 0.5% and depends on the harmonic content, atmospheric conditions like temperature, humidity, etc., and the position or location of the meter in the electric field.

VI.**1.5 Measurement of Ripple Voltage in dc Systems**

It has been discussed in the previous chapter that dc rectifier circuits contain ripple, which should be kept low (<< 3%). Ripple voltages are ac voltages of non-sinusoidal nature, and as such oscillographic measurement of these voltages is desirable. However, if a resistance potential divider is used along with an oscilloscope, the measurement of small values of the ripple δV will be inaccurate.

A simple method of measuring the ripple voltage is to use a capacitance-resistance (C-R) circuit and measure the varying component of the ac voltage by blocking the dc component. If V_1 is the dc source voltage with ripple (Figure . VI.7a) and V_2 is the voltage across the measuring resistance R, with C acting as the blocking capacitor, then

$$V_2(t) = V_1(t) - V_{dc} = \text{ripple voltage}$$

The condition to be satisfied here is $\omega CR >> 1$.

Measurement of Ripple with CRO

The detailed circuit arrangement used of this purpose is shown in Figure. VI.7b. Here, the capacitance '*C*' is rated for the peak voltage. It is important that the switch '*S*' be closed when the *CRO* is connected to the source so that the *CRO* input terminal does not receive any high-voltage signal while '*C*' is being charged. Further , *C* should be larger than the capacitance of the cable and the input capacitance of the *CRO*, taken together.

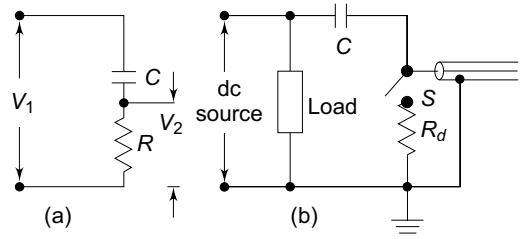

Figure. VI.7 *Circuit arrangement for the measurement of ripple voltage*

VI.2 MEASUREMENT OF HIGH AC AND IMPULSE VOLTAGES

Measurement of high ac voltages employ conventional methods like series impedance voltmeters, potential dividers, potential transformers, or electrostatic voltmeters. But their designs are different from those of low-voltage meters, as the insulation design and source loading are the important criteria. When only peak value measurement is needed, peak voltmeters and sphere gaps can be used. Often, sphere gaps are used for calibration purpos es. Impulse and high frequency ac measurements invariably use potential dividers with a cathode ray oscillograph for recording voltage waveforms. Sphere gaps are used when peak values of the voltage are only needed and also for calibration purposes.

VI.2.1 Series Impedance Voltmeters

For power frequency ac measurements the series impedance may be a pure resistance or a reactance. Since resistances involve power losses, often a capacitor is preferred as a series reactance. Moreover, for high resistances, the variation of resistance with temperature is a problem, and the residual inductance of the resistance gives rise to an impedance different from its ohmic resistance. High resistance units for high voltages have stray capacitances and hence a unit resistance will have an equivalent circuit as shown in Figure . VI.8. At any frequency ω of the ac voltage, the impedance of the resistance *R* is

$$Z = \frac{R + j\omega L}{(1 - \omega^2 LC) + j\omega CR} \qquad \text{(VI. 5)}$$

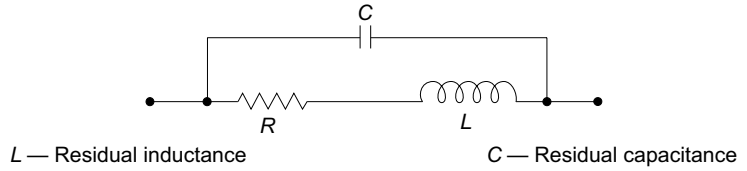

Figure. VI.**8** *Simplified lumped parameter equivalent circuit of a high ohmic resistance R*

If ωL and ωC are small compared to R,

$$Z \approx R\left[1 + j\left(\frac{\omega L}{R} - \omega CR\right)\right] \qquad \text{(VI. 6)}$$

and the total phase angle is

$$\tan \phi \approx \left(\frac{\omega L}{R} - \omega CR\right) \qquad \text{(VI. 7)}$$

This can be made zero and independent of frequency, if

$$L/C = R^2 \qquad \text{(VI. 8)}$$

For extended and large dimensioned resistors, this equivalent circuit is not valid and each elemental resistor has to be approximated with this equivalent circuit.

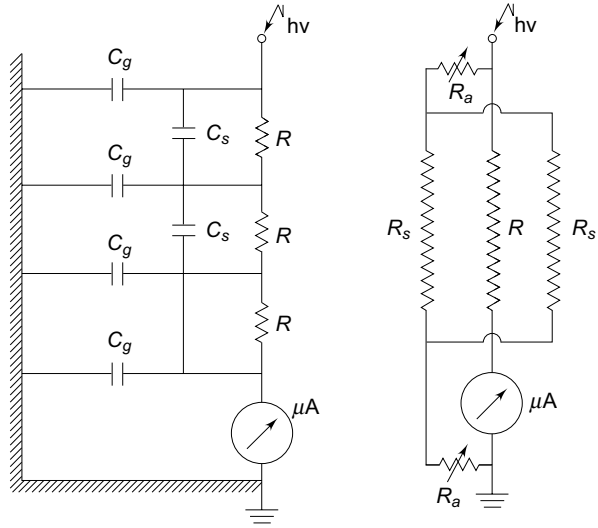

(a) Extended series resistance with inductance neglected

C_g — Stray capcitance to ground
C_s — Winding capacitance

(b) Series resistance with guard and tuning resistances

R — Series resistor
R_s — Guard resistor
R_a — Tuning resistor

Figure. VI.**9** *Extended series resistance for high ac voltage measur ements*

The entire resistor unit then has to be taken as a transmission line equivalent, for calculating the effective resistance. Also, the ground or stray capacitance of each element influences the current flowing in the unit, and the indication of the meter results in an error. The equivalent circuit of a high voltage resistor neglecting inductance and the circuit of compensated series resistor using guard and tuning resistors is shown in Figs VI.9 a and b respectively. Stray ground capacitance effects (refer Figure. VI.9b) can be removed by shielding the resistor R by a second surrounding spiral R, which shunts the actual resistor but does not contribute to the current through the instrument. By tuning the resistors R_a, the shielding resistor and potentials may be adjusted with respect to the actual measuring resistor so that the resulting compensation currents between the shield and the measuring resistors provide a minimum phase angle.

Series Capacitance Voltmeter

To avoid the drawbacks pointed out earlier, a series capacitor is used instead of a resistor for ac high voltage measurements. The schematic diagram is shown in Figure. VI.10. The current I_c through the meter is

$$I_c = j\,\omega CV \qquad \text{(VI. 9)}$$

where, C = capacitance of the series capacitor,
ω = angular frequency, and
V = applied ac voltage.

If the ac voltage contains harmonics, error due to changes in series impedance occurs. The rms value of the voltage V with harmonics is given by

$$V = \sqrt{V_1^2 + V_2^2 + \cdots + V_n^2} \qquad \text{(VI. 10)}$$

where V_1, V_2, ... V_n represent the rms value of the fundamental, second ... and nth harmonics.
The currents due to these harmonics are

$$I_1 = \omega CV_1$$
$$I_2 = 2\,\omega CV_2, \ldots, \qquad \text{(VI. 11)}$$
and $$I_n = n\,\omega CV_n$$

Hence, the resultant rms currents is:

$$I = \omega C\,(V_1^2 + 4V_2^2 + \cdots + n^2V_n^2)^{1/2} \qquad \text{(VI. 12)}$$

With a 10% fifth harmonic only, the current is 11.2% higher, and hence the error is 11.2% in the voltage measurement.

This method is not recommended when ac voltages are not pure sinusoidal waves but contain considerable harmonics.

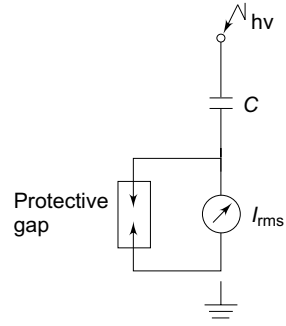

Figure . VI . 10 *Series capacitance with a milliammeter for measurement of high ac voltages*

Series capacitance voltmeters were used with cascade transformers for measuring rms values up to 1000 kV. The series capacitance was formed as a parallel plate capacitor between the high voltage terminal of the transformer and a ground plate

suspended above it. A rectifier ammeter was used as an indicating instrument and was directly calibrated in high voltage rms value. The meter was usually a 0–100 μA moving coil meter and the overall error was about 2%.

VI.2.2 Capacitance Potential Dividers and Capacitance Voltage Transformers

The errors due to harmonic voltages can be eliminated by the use of capacitive voltage dividers with an electrostatic voltmeter or a high impedance meter such as a TVM. If the meter is connected through a long cable, its capacitance has to be taken into account in calibration. Usually, a standard compressed air or gas capacitor is used as C_1 (Figure. VI. 11), and C_2 may be any large capacitor (mica, paper, or any low loss capacitor. C_1 is a three terminal capacitor and is connected to C_2 through a shielded cable, and C_2 is completely shielded in a box to avoid stray capacitances. The applied voltage V_1 is given by

$$V_1 = V_2 \begin{pmatrix} C_1 + C_2 + C_m \\ C_1 \end{pmatrix} \qquad \text{(VI. 13)}$$

where C_m is the capacitance of the meter and the connecting cable and the leads and V_2 is the *potential divider* meter reading.

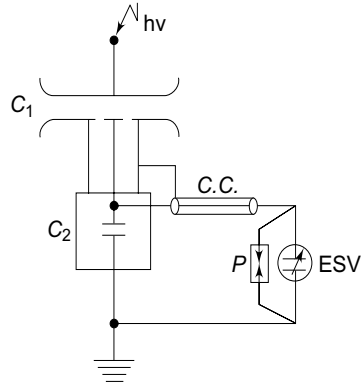

C_1 — Standard compressed gas hv capacitor
C_2 — Standard low voltage capacitor
ESV — Electrostatic voltmeter
P — Protective gap
C.C. — Connecting cable

Figure. VI.11 *Capacitance*

(a) Capacitance Voltage Transformer—CVT Capacitance divider with a suitable matching or isolating potential transformer tuned for resonance condition is often used in power systems for voltage measurements. This is often referred to as CVT. In contrast to simple capacitance divider which requires a high impedance meter like a TVM or an electrostatic voltmeter, a CVT can be connected to a low impedance device like a wattmeter pressure coil or a relay coil. CVT can supply a load of a few VA. The schematic diagram of a CVT with its equivalent circuit is given in Figure. VI.12. C_1 is made of a few units of high-voltage capacitors, and the capacitance will be around a few thousand picofarads as against a gas filled standard total capaci tor of about 100 pF. A matching transformer is connected between the load or meter M and C_2. The transformer ratio is chosen on economic grounds, and the hv winding rating may be 10 to 30 kV with the l.v. winding rated from 100 to 500 V.

The value of the tuning choke L is chosen to make the equivalent circuit of the CVT purely resistive or to bring resonance condition. This condition is satisfied when

$$\omega (L + L_T) = \frac{1}{\omega (C_1 + C_2)} \qquad \text{(VI.14)}$$

where, L = inductance of the choke, and
L_T = equivalent inductance of the transformer referred to hv side.

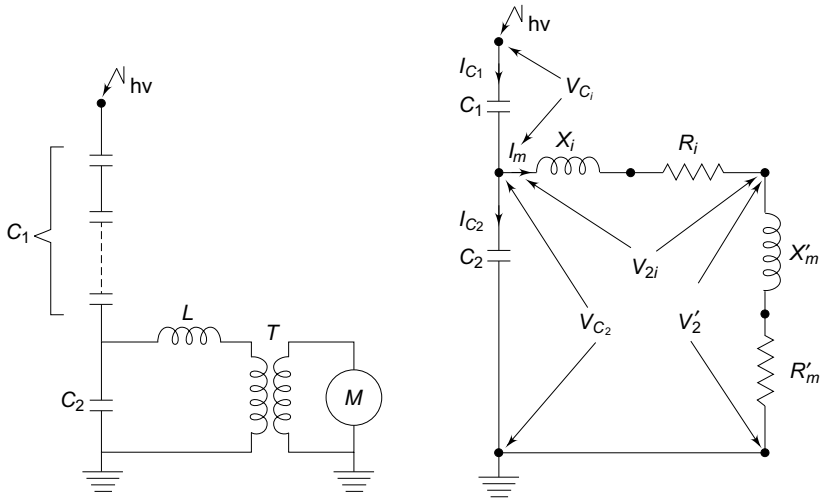

Figure. VI.**12** *Capacitive voltage transformer (CVT)*

The phasor diagram of the CVT under resonant conditions is shown in Figure . VI.13. The meter reactance , X_m is neglected and is taken as a resistance load R_m when the load is connected to the voltage divider side. The error across the potential transformer $V_2 = I_m R_m$ and the voltage across the capacitor $V_2 = V_2 + I_m(R_e + j X_e)$. The phasor diagram is written taking V_1 as the reference phasor. $V_1 = V_{C_1} + V_{C_2}$ and total current = $I_m + I_{C_2}$. It can be seen that with proper tuning V_2 will be in phase with V_1. The potential transformer resistance and reactance are not shown separately and are included in R_i and X_i, the resistance and reactance of tuning inductor L.

The voltage ratio,
$$a = \frac{V_1}{V_2} = \frac{V_{C_1} + V_{Ri} + V_2}{V_2} \qquad \text{(VI. 15)}$$

Neglecting the reactance drop $I_m X_e$, V_{Ri} is the voltage drop across the tuning inductor and the transformer resistance. The voltage V_2 (meter voltage) will be in phase with the input voltage V_1.

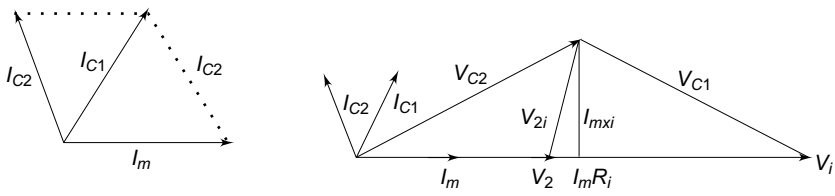

Figure. VI.**13** *Phasor diagram of a CVT under resonance conditions*

The advantages of a CVT are

(i) simple design and easy installation,
(ii) can be used both as a voltage measuring device for meter and relaying purposes and also as a coupling condenser for power line carrier communication and relaying.
(iii) frequency independent voltage distribution along elements as against conventional magnetic potential transformers which require additional insulation design against surges, and
(iv) provides isolation between the high-voltage terminal and low-voltage metering.

The disadvantages of a CVT are the

(i) voltage ratio is susceptible to temperature variations, and
(ii) problem of inducing ferro-resonance in power systems.

(b) Resistance Potential Dividers Resistance potential dividers suffer from the same disadvantages as series resistance voltmeters for ac applications. Moreover, stray capacitances and inductances (Figs VI.7 and VI.8) associated with the resistances make them inaccurate, and compensation has to be provided. Hence, they are not generally used.

VI.2.3 Potential Transformers (Magnetic Type)

Magnetic potential transformers are the oldest devices for ac measurements. They are simple in construction and can be designed for any voltage. For very high voltages, cascading of the transformers is possible. The voltage ratio is:

$$\frac{V_1}{V_2} = a = \frac{N_1}{N_2} \qquad \text{(VI.16)}$$

where V_1 and V_2 are the primary and secondary voltages, and N_1 and N_2 are the respective turns in the windings.

These devices suffer from the ratio and phase angle errors caused by the magnetizing and leakage impedance of the transformer windings. The errors are compensated by adjusting the turns ratio with the tappings on the high-voltage side under load conditions. Potential transformers (PT) do not permit fast rising transient or high frequency voltages along with the normal supply frequency, but harmonic voltages are usually measured with sufficient accuracy. With high-voltage testing transformers, no separate potential transformer is used, but a PT winding is incorporated with the high voltage windings of the testing transformer.

With test objects like insulators, cables, etc. which are capacitive in nature, a voltage rise occurs on load with the testing transformer, and the potential transformer winding gives voltage values less than the actual voltages applied to the test object. If the percentage impedance of the testing transformer is known, the following correction can be applied to the voltage measured by the PT winding of the transformer.

$$V_2 = V_{20}\,(1 + 0.01\, v_x C/C_N) \qquad \text{(VI.17)}$$

where, V_{20} = open circuit voltage of the PT winding,
C_N = load capacitance used for testing,
C = test object capacitance ($C << C_N$), and
v_x = % reactance drop in the transformer.

VI.2.4 Electrostatic Voltmeters

(a) Principle In electrostatic fields, the attractive force between the electrodes of a parallel plate capacitor is given by

$$F = \left|\frac{-\delta W_s}{ds}\right| = \left|\frac{\delta}{\delta s}\left(\frac{1}{2}CV^2\right)\right| = \left|\frac{1}{2}V^2\frac{\delta C}{\delta s}\right|$$

$$= \frac{1}{2}\varepsilon_0 V^2\frac{A}{s^2} = \frac{1}{2}\varepsilon_0 A\left(\frac{V}{s}\right)^2 = \frac{d^2}{2825}\left(\frac{V}{s}\right)^2 \text{ gm.wt} \qquad \text{(VI. 18)}$$

where, V = applied voltage between plates,
C = capacitance between the plates,
A = area of cross-section of the plates,
d = diameter of plates,
s = separation between the plates,
ε_0 = permittivity of the medium (air or free space), and
W_s = work done in displacing a plate

When one of the electrodes is free to move, the force on the plate can be measured by controlling it by a spring or balancing it with a counter weight. For high-voltage measurements, a small displacement of one of the electrodes by a fraction of a millimetre to a few millimetres is usually sufficient for voltage measurements. As the force is proportional to the square of the applied voltage, the measurement can be made for ac or dc voltages.

(b) Construction Electrostatic voltmeters are made with parallel plate configuration using guard rings to avoid corona and field fringing at the edges. An absolute voltmeter is made by balancing the plate with a counter weight and is calibrated in terms of a small weight. Usually the electrostatic voltmeters have a small capacitance (5 to 50 pF) and high insulation resistance ($R \geq 10^{13}\Omega$). Hence, they are considered devices with high input impedance. The upper frequency limit for ac applications is determined from the following considerations:

(i) natural frequency of the moving system,
(ii) resonant frequency of the lead and stray inductances with meter capacitance, and
(iii) the *R-C* behaviour of the retaining or control spring (due to the frictional resistance and elastance).

An upper frequency limit of about one MHz is achieved in careful designs. The accuracy for ac voltage measurements is better than ±0.25%, and for dc voltage measurements it may be ±0.1% or less.

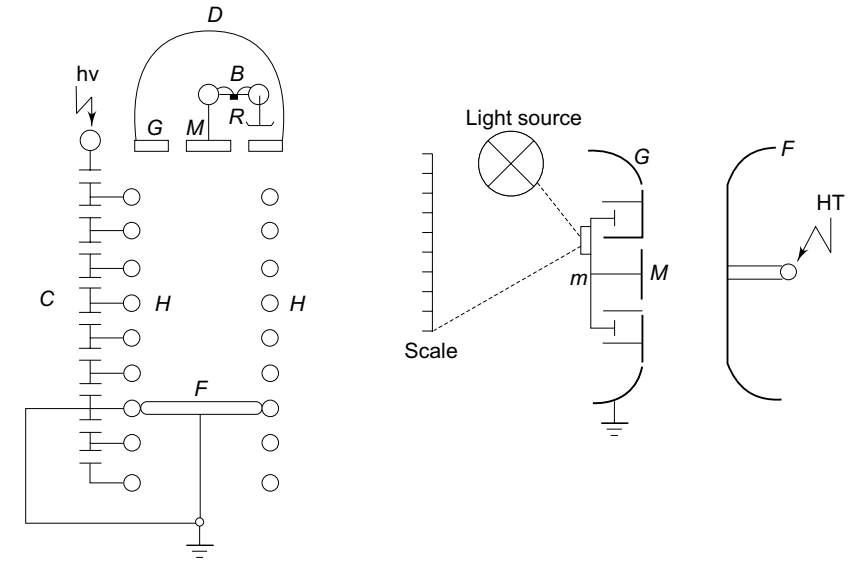

(a) Absolute electrostatic voltmeter

(b) Light beam arrangement

M — Mounting plate
G — Guard plate
F — Fixed plate
H — guard hoops or rings

m — Mirror
B — Balance
C — Capacitance divider
D — Dome
R — Balancing weight

Figure. VI.**14** *Electrostatic voltmeter*

The schematic diagram of an absolute electrostatic voltmeter is given in Figure. VI.14. It consists of parallel-plane disc-type electrodes separated by a small distance. The moving electrode is surrounded by a fixed guard ring to make the field uniform in the central region. In order to measure the given voltage with precision, the disc diameter is to be increased, and the gap distance is to be made less. The limitation on the gap distance is the safe working stress (*V*/*s*) allowed in air which is normally 5 kV/cm or less. The main difference between several forms of voltmeters lies in the manner in which the restoring force is obtained. For conventional versions of meters, a simple spring control is used, which actuates a pointer to move on the scale of the instruments. In more versatile instruments, only small move ments of the moving electrodes is allowed, and the movement is amplified through optical means (lamp and scale arrangement as used with moving coil galvanometers). Two air vane dampers are used to reduce vibrational tendencies in the moving system, and the elongation of the spring is kept minimum to avoid field disturbances. The range of the instrument is easily changed by changing the gap separation so that *V*/*s* or electric stress is the same for the maximum value in any range. Multi-range instruments are constructed for 600 kV rms and above.

The constructional details of an absolute electrostatic voltmeter is given in Figure. VI.14a. The control torque is provided by a balancing weight. The moving disc *M* forms the central core of the guard ring *G* which is of the same diameter as the

fixed plate *F*. The cap *D* encloses a sensitive balance *B*, one arm of which car ries the suspension of the moving disc. The balance beam carries a mirror which reflects a beam of light. The movement of the disc is thereby magnified. As the spacing between the two electrodes is large, the uniformity of the electric field is maintained by the guard rings *H* which surround the space between the discs *F* and *M*. The guard rings *H* are maintained at a constant potential in space by a capacitance divider ensuring a uniform special potential distribution.

Some instruments are constructed in an enclosed structure con taining compressed air, carbon dioxide, or nitrogen. The gas pressure may be of the order of 15 atm. Working stresses as high as 100 kV/cm may be used in an electrostatic meter in vacuum. With compressed gas or vacuum as medium, the meter is compact and much smaller in size.

VI.2.5 Peak Reading ac Voltmeters

In some occasions, the peak value of an ac waveform is more important. This is necessary to obtain the maximum dielectric strength of insulating solids, etc. When the waveform is not sinusoidal, rms value of the voltage multiplied by 2 is not correct. Hence a separate peak value instrument is desirable in high voltage applications.

(a) Series Capacitor Peak Voltmeter When a capacitor is connected to a sinusoidal voltage source, the charging current $i_0 = \int vdt = j\,\omega\, CV$ where V is the rms value of the voltage and ω is the angular frequency. If a half-wave recti fier is used, the arithmetic mean of the rectifier current is proportional to the peak value of the ac voltage. The schematic diagram of the circuit arrangement is shown in Figure. VI .15. The dc meter reading is proportional to the peak value of the value V_m or

$$V_m = \frac{1}{2\pi fC}$$

where I is the dc current read by the meter and C is the capacitance of the capacitor. This method is known as the Chubb–Frotscue method for peak voltage measurement.

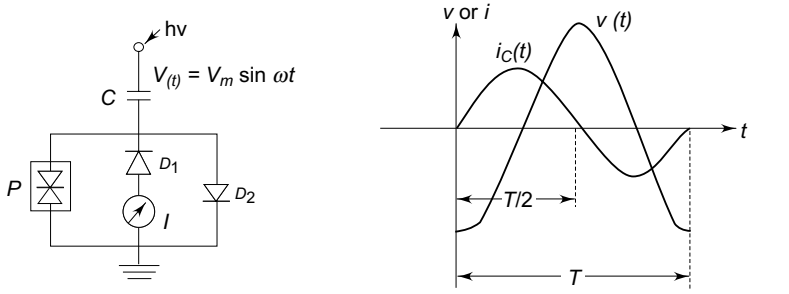

C — Capacitor
*D*1, *D*2 — Diodes
P — Protective device
I — Indicating meter (rectified current indicated)
v (*t*) — Voltage waveform
*I*c (*t*) — Capacitor current waveform
T — Period

Figure. VI.15 *Peak voltmeter with a series capacitor*

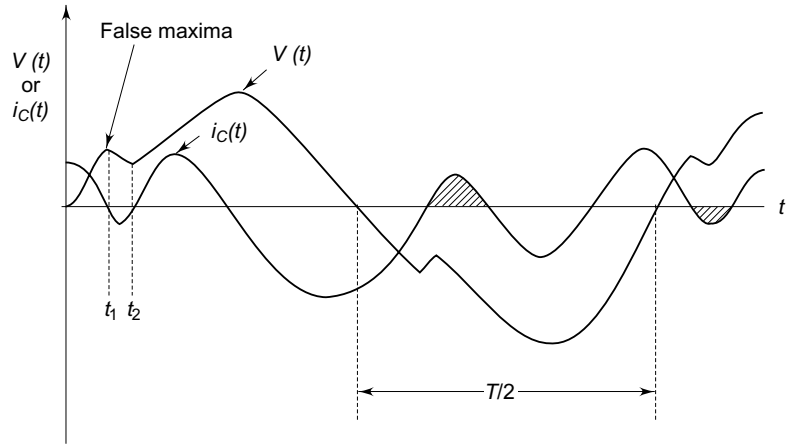

Figure. VI.16 *Voltage waveform with harmonic content showing false*

maxima The 1diode *D* is used to rectify the ac current in one half cycle 2by-passes in the other half cycle. This arrange ment is suitable only of positive or negative half cycles and hence is valid only when both half cycles are while *D* symmetrical and equal . This method is not suitable when the voltage waveform is not sinusoidal but contains more than one peak or maximum as shown in Figure . VI.16. The charging current through the capacitor changes its polarity within one half cycle itself. The shaded areas in Figure . VI.16 give the reverse current in any one of the half cycles and the current within that period subracts from the net current. Hence the reading of the meter will be less and is not proportional to *V* as the current flowing during the inter vals $(t_1 - t_2)$ etc. will notin the mean value . The 'second' or the false maxima is easily spotted out by be included observing the waveform of the charging current on an oscilloscope. Under normal conditions with ac testing, such waveforms do not occur and as such do not give rise to errors. But pre-discharge cur rents within the test circuits cause very short duration voltage drops which may introduce errors. This problem can also be over come by using a resistance *R* in series with capacitor *C* such that $CR << 1/\omega$ for 50 Hz application.

The error due to the resistance is

$$\frac{\Delta V}{V} = \frac{V - V_m}{V} = \left(1 - \frac{1}{1+\omega^2 C^2 R^2}\right) \qquad \text{(VI.19)}$$

where, V = actual value, and
V_m = measured value

In determining the error, the actual value of the angular frequency ω has to be determined.

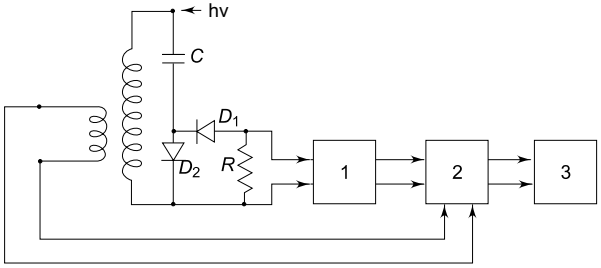

C — Series capacitor
D1,D2 — Diodes
R — Input resistor
1 — Voltage to frequency converter
2 — Gate circuit
3 — Read out counter (indicator)

Figure. VI.17 *Digital peak voltmeter*

The different sources that contribute to the error are

(i) the effective value of the capacitance being different from the measured value of *C*.
(ii) imperfect reftifiers which allows small reverse currents.
(iii) non-sinusoidal voltage waveforms with more than one peak or maxima per half cycle.
(iv) deviation of the frequency from that of the value used for calibration. As such, this method in its basic form is not suitable for wave forms with more than one peak in each half cycle.

A digital peak reading meter for voltage measurements is shown in Figure. VI. 1VI. Instead of directly measuring the rectified charging current, a analog voltage signal is derived which is then converted into a proportional mean proportional frequency, f_m. The frequency ratio f/f_m is measured with a gate circuit controlled by the ac power frequency (f) and a counter that opens for an adjustable number of periods $\Delta t = p/f$. During this interval, the number of impulses counted, n, is

$$n = f_m \cdot \Delta t = p \cdot \frac{f_m}{f} = 2pCV_m AR \qquad \text{(VI. 20)}$$

where p is a constant of the instrument and A represents the conversion factor of the ac to dc converter. $A = f/(Ri)$; i is the rectified current through resistance R. An immediate reading of the voltage in kV can be obtained by suitable choice of the parameter R and the number of periods p. The total esti mated error in this instrument was less than 0.35%. Conventional instruments of this type are available with less than 2% error.

(b) Peak Voltmeters with Potential Dividers Peak voltmeters using capacitance dividers, designed by Bowlder *et al*., are shown in Figure. VI. 18a. The voltage across C is made use of in charging the storage capacitor C_s. R_d is adischarge resistor employed to permit variation of V_m whenever V_2 is reduced. C_s is charged to a voltage proportional to the peak value to be measured. The indicating meter is either an electrostatic voltmeter or a high impedance VTVM. This discharge time constant Cs R_d is designed to be about 1 to 10 s. This gives rise to a discharge error which depends on the frequency of the supply voltage. To compensate for the charging and discharging errors due to the resistances, the circuit is modified as shown in Figure . VI.18b. Measurement of the average peak is done by a microammeter . Rabus' modification to compensate the charging errors is given in Figure. VI.18c.

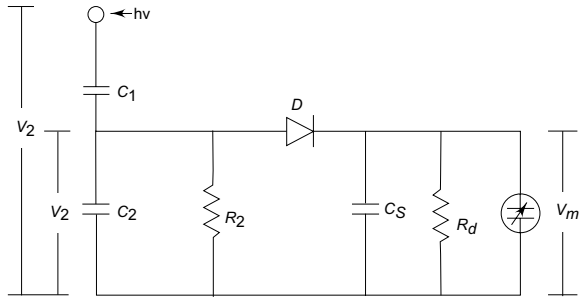

Figure. VI.**18a** *Peak voltmeter with a capacitor potential divider and electrostatic voltmeter*

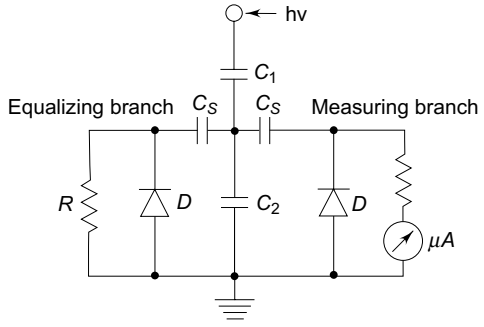

Figure. VI.**18b** *Peak voltmeter as modified by Haefely (Ref. 8)*

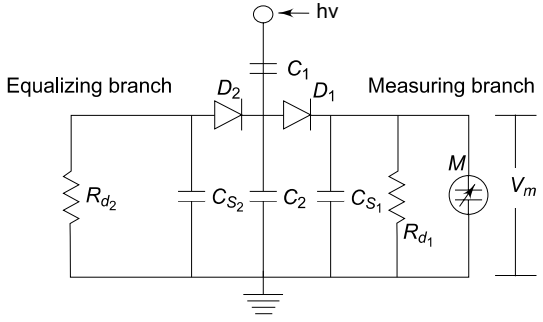

M — Electrostatic voltmeter or T.V.M. of high impedance

C_{s_2} — C_{s_1} + C meter

Rd_2 — Rd_1

Figure. VI.**18c** *Peak voltmeter with equalizing branch as designed by Rabus*

VI.**2.6 Spark Gaps for Measurement of High dc, ac, and Impulse Voltages (Peak Values)**

A uniform field spark gap will always have a sparkover voltage within a known tolerance under constant atmospheric conditions. Hence a spark gap can be used for

measurement of the peak value of the voltage, if the gap distance is known. A spark-over voltage of 30 kV (peak) at 1 cm spacing in air at 20°C and 760 torr pressure occurs for a sphere gap or any uniform field gap. But experience has shown that these measurements are reliable only for certain gap configurations. Normally, only sphere gaps are used for voltage measurements. In certain cases uniform field gaps and rod gaps are also used, but their accuracy is less. The spark gap breakdown, especially the sphere gap breakdown, is independent of the voltage waveform and hence is highly suitable for all types of waveforms from dc to impulse voltages of short rise times (rise time ≥ 0.5 μs). As such, sphere gaps can be used for radio frequency ac voltage peak measurements also (up to 1 MHz).

(a) Sphere Gap Measurements

Sphere gaps can be arranged either (i) vertically with lower sphere grounded, or (ii) horizontally with both spheres connected to the source voltage or one sphere grounded. In horizontal configurations, it is generally arranged such that both spheres are symmetrically at high voltage above the ground. The two spheres used are identical in size and shape. The schematic arrangement is shown in Figs VI.19a and VI.19b. The voltage to be measured is applied between the two spheres and the distance or spacing *S* between them gives a measure of the spar-kover voltage. A series resistance is usually connected between the source and the sphere gap to (i) limit the breakdown current, and (ii) to suppress unwanted oscillations in the source voltage when break down occurs (in case of impulse voltages). The value of the series resistance may vary from 100 to 1000 kilo ohms for ac or dc voltages and not more than 500 Ω in the case of impulse voltages.

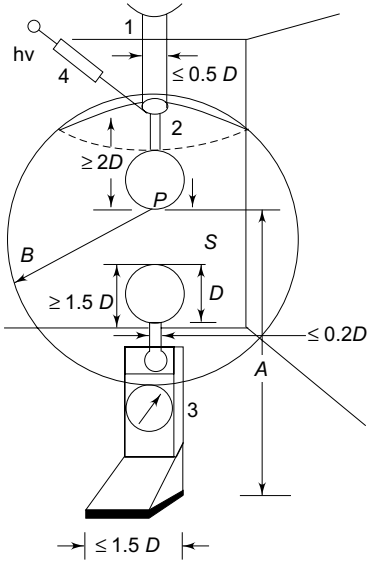

1 — Insulator support
2 — Sphere shank
3 — Operating gear and motor for changing gap distance
4 — HV connection
P — Sparking point
D — Diameter of the sphere
S — Spacing
A — Height of *P* above earth
B — Radius of the clearance from external structures
X — High voltage lead should not pass through this plane within a distance *B* from *P*

(a) Vertical arrangement of sphere gap

Figure. VI.**19a** *Sphere gap for voltage measurement*

Table VI.3 *Peak value of sparkover voltage in kV for ac., dc. voltages of either polarity, and for full negative standard impulse voltages (one sphere earthed) (A) positive polarity impulse voltages and impulse voltages with long tails (B) at temperature: 20^{0}C and pressure: 760 torr*

Gap spacing (cm)	*Sphere diameter (cm)*															
	5		*10*		*15*		*25*		*50*		*100*		*150*		*200*	
	A	*B*	*A*	*B*	*A*	*B*	*A*	*B*	*A*	*B*	*A*	*B*	*A*	*B*	*A*	*B*
0.5	1VI.4	1VI.4	16.9	16.8	16.9											
1.0	32.0	32.0	31.7	31.7	31.7	31.4	31.2	31.4								
1.5	44.7	45.5	44.7	45.1	44.7	45.1	44.7	44.7								
2.0	5VI.5	58.0	58.0	58.0	58.0	58.0	58.0	58.								
2.5			71.5	71.5	71.5	71.5	71.5	71.5	71.5	71.5						
3.0			85.0	85.0	85.0	85.0	85.0	85.0	85.0	85.0						
3.5			95.5	96.0	9VI.0	9VI.0	9VI.0	9VI.0	9VI.0	9VI.0						
4.0			96.0	108.0	108.0	110.0	110.0	110.0	110.0	110.0						
5.0			(123.0)	(12VI.0)	12VI.0	132.0	135.0	136.0	136.0							
VI.			136.0		(181.0)	(18VI.0)	195.0	196.0	199.0	199.						
10.0					0		257	268	259	259	262	262	262	262	262	262
12.5							277	294	315	317						
15.0							(309)	(331)	367	374	383	384	384	384	384	384
1VI.							(336)	(362)	413	425						
20.0									452	472	500	500	500	500	500	500
25.0									520	545	605	610				
30.0									(575)	(610)	700	715	730	735	735	740
35.0									(725)	(755)	785	800				
40.0											862	885	940	950	960	965
45.0											925	965				
50.0											1000	1020	1110	1130	1160	1170
75.0											(1210)	(1260)	1420	1460	1510	1590
100.0															1870	1900

Table VI.4 *Sphere gap sparkover voltages in kV (peak) in air for ac, dc, and impulse voltage of either polarity for symmetrical sphere gaps at temperature: 20°C and pressure: 760 torr*

Gap spacing (cm)	Sphere diameter (cm)								
	5	10	15	25	50	100	150	200	Remarks
0.5	1VI.5	16.9	16.5						For spacings less than 0.5 D, the accuracy is ± 3% and for spacing ≥ 0.5 D, the accuracy is ±5%.
1.0	32.2	31.6	31.3	31.0					
1.5	46.1	45.8	45.5	45.0					
2.0	58.3	59.3	59.2	59.0					
2.5	69.4	72.4	72.9	73.0					
3.0	(79.3)	84.9	85.8	86.0					
4.0		10VI.0	111.0	113.0	112.				
5.0		128.0	134.0	138.0	138.0	13VI.0	13VI.0		
8.0		(177)	194.0	20VI.0	214.	13VI.0			
10.0			0	248.0	263.0	266.0	26VI.0	26	
12.0				286.0	309.0	VI.0			
14.0				320.0	353.0				
16.0				352.0	394.0				
18.0					452.0				
20.0					495.0	504.0	511.0	511.0	
25.0					558.0	613.0	628.0	632.0	
30.0						744.0	741.0	746.0	
35.0						812.0	848.0	860.0	
40.0						902.0	950.0	972.0	
50.0						1070.0	1140.0	1180.0	
60.0						(1210)	1320.0	1380.0	
70.0							1490.0	1560.0	
80.0							(1640)	1730.0	
90.0								1900.0	
100.0								2050.0	

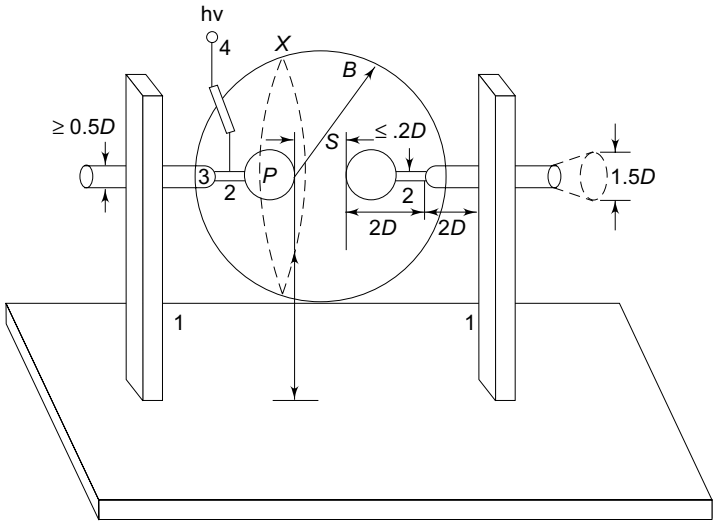

Figure. VI.**19b** *Horizontal arrangement of sphere gap (Legend as in* Figure. VI.*19a)*

In the case of ac peak value and dc voltage measurements, the applied voltage is uniformly increased until sparkover occurs in the gap. Generally, a mean of about five breakdown values is taken when they agree to within ±3%.

In the case of impulse voltages, to obtain 50% flashover voltage, two voltage limits, differing by not more than 2% are set such that on application of lower limit value either 2 or 4 flashovers take place and on application of upper limit value 8 or 6 flashovers take place respectively. The mean of these two limits is taken as 50% flashover voltage. In any case, a preliminary sparkover voltage measurement is to be made before actual measurements are made.

The flashover voltage for various gap distances and standard diameters of the spheres used are given in Tables VI.3 and VI.4 respectively . The values of sparkover voltages are specified in BS : 358, IEC Publication 52 of 1 960 and IS: 1876 of 1962. The clearances necessary are shown in Figs VI.19a and VI.19b for measurements to be within ±3%. The value of *A* and *B* indicated in the above figures are given in Table VI.5.

(b) Sphere Gap Construction and Assembly

Sphere gaps are made with two metal spheres of identical diameters *D* with their shanks , operating gear , and insulator supports (Figure . VI.19a or b). Spheres are generally made of copper, brass, or aluminium; the latter is used due to low cost. The standard diameters for the spheres are 2, 5, 6.25, 10, 12.5, 15, 25, 50 , 75, 100, 150, and 200 cm. The spacing is so designed and chosen such that flashover occurs near the spark-ing point *P*. The spheres are carefully designed and fabricated so that their surfaces are smooth and the curvature is uniform . The radius of curvature measured with a spherometer at various points over an area en closed by a circle of 0.3 *D* around the sparking point should not differ by more than ±2% or the nominal value. The surface

Table VI.5 *Clearances for sphere gaps*

D (cm)	*Value of A*		*Value of B (min)*
	Min	*Max*	
up to 6.25	7 *D*	9 *D*	14*S*
10 to 15	6 *D*	8 *D*	12*S*
25	5 *D*	7 *D*	10*S*
50	4 *D*	6 *D*	8*S*
100	3.5 *D*	5 *D*	7*S*
150	3 *D*	4 *D*	6*S*
200	3 *D*	4 *D*	6*S*

A and *B* are clearances as shown in Figs VI.19a and VI.19b.
D = diameter of the sphere; *S* = spacing of the gap; and S/D ≤ 0.5.

of the sphere should be free from dust, grease, or any other coating. The surface should be maintained clean but need not be polished. If excessive pitting occurs due to repeated sparkovers, they should be smoothened. The dimensions of the shanks used, the grading ring used (if necessary) with spheres, the ground clearances, etc. should follow the values indicated in Figs VI.19a and VI.19b and Table VI .5. The high voltage conductor should be ar ranged such that it does not affect the field configura-tion. Series resistance connected should be outside the shanks at a distance 2*D* away from the high voltage sphere or the sparking point *P*.

Irradiation of sphere gap is needed when measurements of voltages less than 50 kV are made with sphere gaps of 10 cm diameter or less. The irradiation may be obtained from a quartz tube mercury vapour lamp of 40 W rating. The lamp should be at a distance *B* or more as indicated in Table VI.5.

(c) Factors Influencing the Sparkover Voltage of Sphere Gaps

Various factors that affect the sparkover voltage of a sphere gap are

(i) nearby earthed objects,
(ii) atmospheric conditions and humidity,
(iii) irradiation, and
(iv) polarity and rise time of voltage waveforms.

Detailed investigations of the above factors have been made and analysed by Craggs and Meek[1], Kuffel and Abdullah[2], Kuffel, Davis and Bowlder, and several other investigators. Only a few important factors are presented here.

(i) *Effect of nearby Earthed Objects* The effect of nearby earthed objects was investigated by Kuffel by enclosing the earthed sphere inside an earthed cylinder. It was observed that the sparkover voltage is reduced. The reduction was observed to be

$$\Delta V = m \log (B/D) + C \qquad \text{(VI. 21)}$$

where, ΔV = percentage reduction,
B = diameter of earthed enclosing cylinder,
D = diameter of the spheres,
S = spacing, and m and C are constants.

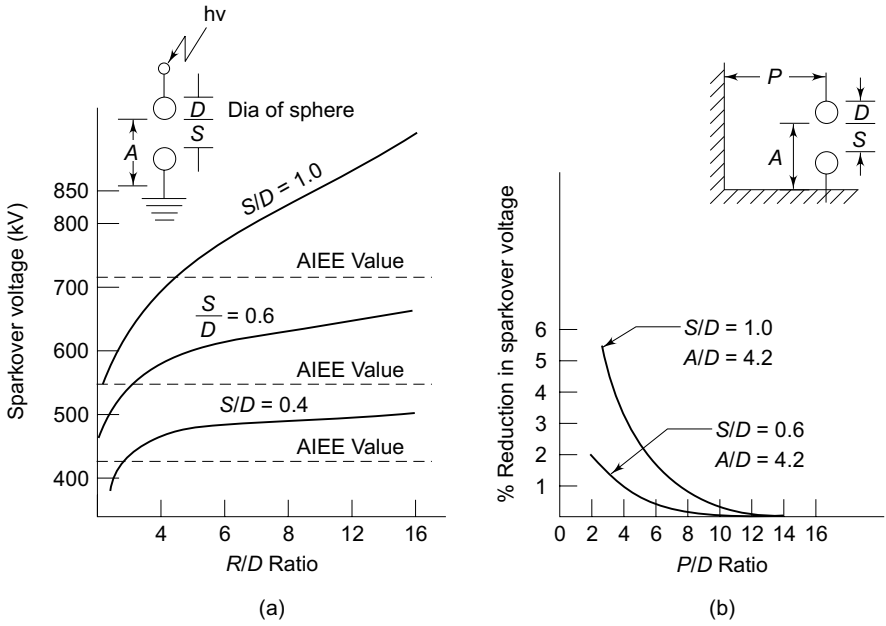

Figure. VI.**20** *Influence of ground planes on sparkover voltage*

The reduction was less than 2% for $S/D \leq 0.5$ and $B/D \geq 0.8$. Even for $S/D \approx 1.0$ and $B/D \geq 1.0$ the reduction was only 3%. Hence, if the specifications regarding the clearances are closely observed the error is within the tolerances and accuracy specified. The variation of breakdown voltage with A/D ratio is given in Figs VI.20a and b for a 50 cm sphere gap. The reduction in voltage is within the accuracy limits, if S/D is kept less than 0.6 A in the above ratio, A is the distance from sparking point to hori-zontal ground plane (also shown in Figure. VI.20).

(ii) Effect of Atmospheric Conditions The sparkover voltages of a spark gap depends on the air density which varies with the changes in both temperature and pressure. If the sparkover voltage is V under test conditions of temperature T and pressure p torr and if the sparkover voltage is V_0 under standard conditions of temperature $T = 20°C$ and pressure $p = 760$ torr, then

$$V = kV_0$$

where k is a function of the air density factor d, given by

$$d = \frac{p}{760}\left(\frac{293}{273+T}\right) \qquad \text{(VI. 22)}$$

The relationship between d and k is given in Table VI.
6.

Table VI.6 *Relation between correction factor k and air density factor d*

d	0.70	0.75	0.80	0.85	0.90	0.95	1.0	1.05	1.10	1.15
k	0.72	0.77	0.82	0.86	0.91	0.95	1.0	1.05	1.09	1.12

The sparkover voltage increases with humidity. The increase is about 2 to 3% over normal humidity range of 8 g/m^3 to 15 g/m^3. The influence of humidity on sparkover voltage of a 25 cm sphere gap for 1 cm spacing is presented in Figure. VI.21. It can be seen that the increase in sparkover voltage is less than 3% and the variation between ac and dc breakdown voltages is negligible (< 0.5%).

Hence, it may be concluded that (i) the humidity effect increases with the size of spheres and is maximum for uniform field gaps, and (ii) the sparkover voltage increases with the partial pressure of water vapour in air, and for a given humidity condition, the change in sparkover voltage increases with the gap length. As the change in sparkover voltage with humidity is within 3%, no correction is normally given for humidity.

(iii) *Effect of Irradiation* Illumination of sphere gaps with ultra-violet or X-rays aids easy ionization in gaps. The effect of irradiation is pronounced for small gap spacings. A reduction of about 20% in sparkover voltage was observed for spacings of 0.1 *D* to 0.3 *D* for a 1.3 cm sphere gap with dc voltages. The reduction in sparkover voltage is less than 5% for gap spacings more than 1 cm, and for gap spacings of 2 cm or more it is about 1.5%. Hence, irradiation is necessary for smaller sphere gaps of gap spacing less than 1 cm for obtaining consistent values.

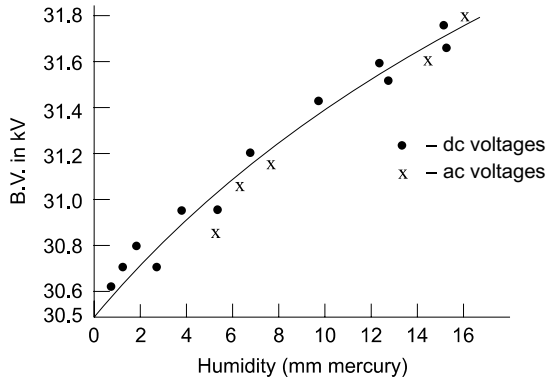

Figure. VI.21 *Influence of humidity on dc and ac breakdown vol tages (25 cm dia sphere gap, 1 cm spacing)*

(iv) *Effect of Polarity and Waveform* It has been observed that the sparkover voltages for positive and negative polarity impulses are different. Experimental investigation showed that for sphere gaps of 6.25 to 25 cm diameter, the difference between positive and negative dc voltages is not more than 1%. For smaller sphere gaps (2 cm diameter and less) the difference was about 8% between negative and positive impulses of 1/50 μs waveform. Similarly, the wave-front and wave-tail durations also influence the breakdown voltage. For wave fronts of less than 0.5 μs and wave tails less than 5 μs the breakdown voltages are not consistent and hence the use of sphere gap is not recommended for voltage measurement in such cases.

(d) Uniform Field Electrode Gaps

Sphere gaps, although widely used for voltage measurements, have only limited range with uniform electric field. Hence, it is not possible to ensure that the sparking always takes place along the uniform field region. Rogowski [see Craggs and Meek[1]] presented a design for uniform field electrodes for sparkover voltages up to 600 kV. The sparkover voltage in a uniform field gap is given by

$$V = AS + B\sqrt{S}$$

where A and B are constant, S is the gap spacing in cm, and V is the sparkove voltage. Typical uniform field electrodes are shown in Figure. VI.22. The were found to be 24.4 and VI.50 respectively at a temperatureconstants $T = 25$ A ° Cand and B pressure = 760 torr. Since the sparking potential is a function of air density, the sparkover volt-age for any given air density factor d (see Eq. VI.22) is modified as

$$V = 24.4\, dS + \text{VI.}\ \sqrt{dS} \qquad \text{(VI. 23)}$$

50

Bruce [see Craggs *et al.*[1] and Kuffel *et al.*[2]]. made uniform field electrodes with a sine curve in the end region. According to Bruce, the electrodes with diameters of 4.5, 9.0, and 15.0 in can be used for maximum voltages of 140, 280, and 420 kV respectively. For the Bruce profile, the constants A and B are respectively 24.22 and 6.08. Later, it was found that with humidity the sparkover voltage increases, and the relationship for sparkover voltage was modified as

$$V = 6.66\sqrt{dS} + [24.55 + 0.41\ (0.1e - 1.0)]dS \qquad \text{(VI. 24)}$$

where, V = sparkover voltage, kV_{peak} (in kV_{dc}),
e = vapour pressure of water in air (mmHg).

The constants A and B differ for ac, dc, and impulse voltages. A comparison between the sparkover voltages (in air at a temperature of 20°C and a pressure of 760 torr) of a uniform field electrode gap and a sphere gap is given in Table VI.7. From this table it may be concluded that within the specified limita tions and error limits, there is no significant difference among the sparkover voltages of sphere gaps and uniform field gaps.

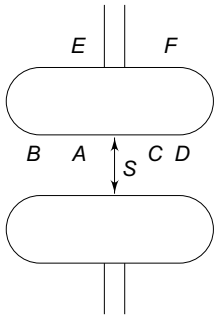

(a) Electrodes for 300 kV (rms) spark gap

AC, *EF* — Flat portion (≥ *S*)
Curvature *A* to *B* and *C* to *D* ≥ 108

Curvature *B* to *E* and *D* to *F* continuously increasing

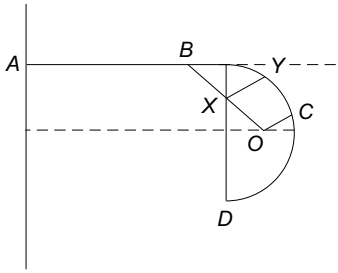

(b) Bruce profile (half contour)

AB — Flat portion
BC — Sine curve
CD — Arc of a circle with centre at *O*
XY — $OC \sin\left(\frac{p}{2} \cdot \frac{BX}{BO}\right)$
P — any point in the curve *BC*

Figure. VI.**22** *Uniform field electrode spark gap*

Table VI.**7** *Sparkover voltage of uniform field gaps and sphere gaps at T = 20° C and pr = 760 torr*

Gap spacing (cm)	*Sparkover voltage with uniform field electrodes as measured by*			*Sphere gap sparkover voltage (kV)*
	Ritz (kV)	*Bruce (kV)*	*Schumann (kV)*	
0.1	4.54	–	4.50	4.6
0.2	7.90	7.56	8.00	8.0
0.5	17.00	16.41	17.40	17.0
1.0	31.35	30.30	31.70	31.0
2.0	58.70	57.04	59.60	58.0
4.0	112.00	109.00	114.00	112.0
6.0	163.80	160.20	166.20	164.0
8.0	215.00	211.00	216.80	215.0
10.0	265.00	261.1	266.00	265.0
12.0	315.00	311.6	—	312.0

The sparkover voltage of uniform field electrode gaps can also be found from calculations. However, no such calculation is available for sphere gaps. In spite of

the superior performance and accuracy, the uniform field spark gap is not usually used for measurement purposes, as very accurate finish of the electrode surfaces and careful alignment are difficult to obtain in practice.

(e) Rod Gaps

A rod gap is also sometimes used for approximate measurement of peak values of power frequency voltages and impulse voltages. IEEE recognise that this method gives an accuracy within ±8%. The rods will be either square edged or circular in cross-section. The length of the rods may be 15 to 75 cm and the spacing varies from 2 to 200 cm. The sparkover voltage, as in other gaps, is affected by humidity and air density. The power frequency breakdown voltage for 1.27 cm square rods in air at 27°C and at a pressure of 760 torr with the vapour pressure of water of 15.5 torr is given in Table VI.8. The humidity correction is given in Table VI.9. The air density correction factor can be taken from Table VI.6.

Table VI.8 *Sparkover voltage for rod gaps*

Gap spacing (cm)	*Sparkover voltage (kV)*	*Gap spacing (cm)*	*Sparkover voltage (kV)*
2	26	30	172
4	47	40	225
6	62	50	278
8	72	60	332
10	81	70	382
15	102	80	435
20	124	90	488
25	147	100	537

The rods are 1.27 cm square edged at t = 27°C, p = 760 torr, and vapour pressure of water = 15.5 torr.

Table VI.9 *Humidity correction for rod gap sparkover voltages*

Vapour pressure of water (torr)	2.54	5	10	15	20	25	30
Correction factor %	–16.5	–13.1	–6.5	–0.5	4.4	VI. 9	10.1

In case of impulse voltage measurements, the IEC and IEEE recommend horizontal mounting of rod gaps on insulators at a height of 1.5 to 2.0 times the gap spacing above the ground. One of the rods is usually earthed. For 50% flashover voltages, the procedure followed is the same as that for sphere gaps. Corrections for humidity for 1/5 μs impulse and 1/5 μs impulse waves of either polarity are given in Figure . VI.23. The sparkover voltages for impulse waves are given in Table VI.10.

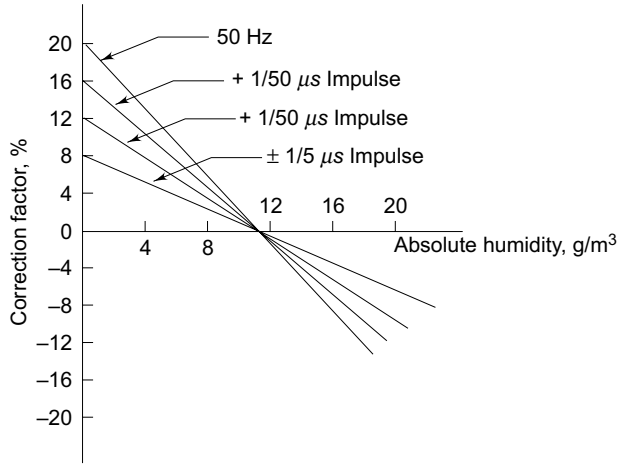

Figure. VI.**23** *Correction factor for rod gaps*

Table VI.**10** *Sparkover voltages of rod gaps for impulse voltages at temperature = 20°C, pressure = 760 torr and humidity =11 g/m³*

Gap length (cm)	*1/5 μ s wave (kV)*		*1/50 μ s wave (kV)*	
	Positive	*Negative*	*Positive*	*Negative*
5	60	66	56	61
10	101	111	90	97
20	179	208	160	178
30	256	301	226	262
40	348	392	279	339
50	431	475	334	407
60	513	557	397	470
80	657	701	511	585
100	820	855	629	703

VI.**2.7 Potential Dividers for Impulse Voltage Measurements**

Potential or voltage dividers for high-voltage impulse measure ments, high frequency ac measurements, or for fast rising transient voltage measurements are usually either resistive or capacitive or mixed element type. The low-voltage arm of the divider is usually connected to a fast recording oscillograph or a peak reading instrument through a delay cable. A schematic diagram of a potential divider with its terminat- ing equipment is given in Figure. VI.24. Z_1 is usually a resistor or a series of resistors in case of a resistance potential divider, or a single or a number of capacitors in case of a capacitance divider. It can also be a combination of both resistors and capacitors. Z_2 will be a resistor or a capacitor or an *R-C* impedance depending upon the type of the divider. Each element in the divider, in case of high-voltage dividers, has a self-resistance or ca pacitance. In addition, the resistive elements have residual induc- tances, a terminal stray capacitance to ground, and terminal to terminal capacitances.

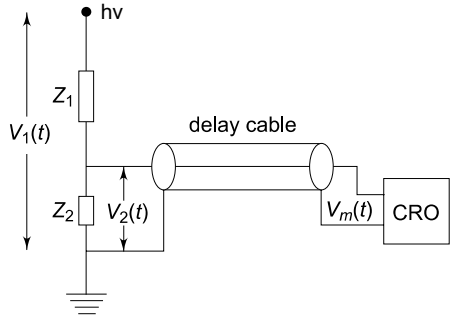

Figure. VI.24 *Schematic diagram of a potential divider with a delay cable and oscilloscope*

The lumped-circuit equivalent of a resistive element is already shown in Figure. VI.8 the equivalent circuit of the divider with inductance neglected is of the form shown in Figure . VI.9a. A capacitance potential divider also has the same equivalent cir-cuit as in Figure. VI.8a, where C will be the capacitance of each elemental capacitor, C_g will be the terminal capacitance to ground, and R will beresistance and resis tance due to dielectric loss in the element. When a step or fast the equivalent leakage rising voltage is applied at the high voltage terminal , the voltage developed across the element Z_2 will not have the true waveform as that of the applied voltage. The cable can also introduce distortion in the waveshape. The following elements mainly constitute the different errors in the measurements:

(i) residual inductance in the elements;
(ii) stray capacitance occurring
  (a) between the elements,
  (b) from sections and terminals of the elements to ground, and
  (c) from the high voltage lead to the elements or sections;
(iii) The impedance errors due to
  (a) connecting leads between the divider and the test objects, and
  (b) ground return leads and extraneous current in ground leads; and
(iv) parasitic oscillations due to lead and cable inductances and capacitance of high-voltage terminal to ground.

The effect to residual and lead inductances becomes pronounced when fast rising impulses of less than one microsecond are to be measured . The residual inductances damp and slow down the fast rising pulses. Secondly, the layout of the test objects , the impulse generator , and the ground leads also require special attention to minimize recording errors. These are discussed in Sec. VI.4.

(a) Resistance Potential Divider for Very Low Impulse Voltages and Fast Rising Pulses A simple resistance potential divider consists of two resistances R_1 and R_2 in series ($_1R > > _2R$) (see Figure . VI.25). The attenuation the divider or the voltage ratio is given by factor of

$$a = \frac{V_1(t)}{V_2(t)} = 1 + \frac{R_1}{R_2} \qquad \text{(VI. 25)}$$

The divider element R_2, in practice, is connected through the coaxial cable to the oscilloscope. The cable will generally have a surge impedance Z_0 and this will come in parallel with the oscilloscope input impedance (R_m, C_m). R_m will generally be greater than one megaohm and C_m may be 10 to 50 picofarads. For high frequency and impulse voltages (since they also contain high frequency fundamental and harmonics), the ratio in the frequency domain will be given by

$$a = \frac{V_1}{V_2} = 1 + \frac{R_1}{(R_2/1 + j\omega R_2 C_m)} \qquad \text{(VI. 26)}$$

Hence, the ratio is a function of the frequency. To avoid the frequency dependence of the voltage ratio a, the divider is compensated by adding an additional capacitance C_1 across R_1. The value of C_1, to make the divider independent of the frequency, may be obtained from the relation,

$$\frac{R_1}{R_2} = \frac{C_m}{C_1} \qquad \text{(VI.27)}$$

or,
$$R_1 C_1 = R_2 C_m$$

meaning that the time constant of both the arms should be the same. This compensation is used for the construction of high-voltage dividers and probes used with oscilloscopes. Usually, probes are made with adjustable values of C_m so that the value of C_m can include any stray capacitance including that of a cable, etc. A typical high-voltage probe with a four nanosecond rise time rated for 40 kV (peak) has an input impedance of 100 MΩ in parallel with 2.7 pF. The output waveforms of a compensated divider are shown in Figure VI.25c with over and under compensation for a square wave input. In Figure VI.25c (i) is shown the wavform of an R-C divider whem C_1 is too large or overcompensated, while in Figure VI.25c (iii) is shown the waveform when C_1 is small or undercompensated. For the exponential slope or for the rising portion of the wave, the time constant $\tau = [R_1 R_2/(R_1 + R_2)](C_1 + C_m)$. This will be too large when the value of C_1 is greater than that required for correct compensation, i.e., $R_1 C_1 = R_2 C_m$ and hence an overshoot with an exponential decay occurs as shown in Figure VI.25c (i). For undercompensation, the charging time is too high and as such an exponential rise occurs as shown in Figure VI.25c (iii). The schematic circuit of a compensated oscilloscope probe is shown in Figure VI.26.

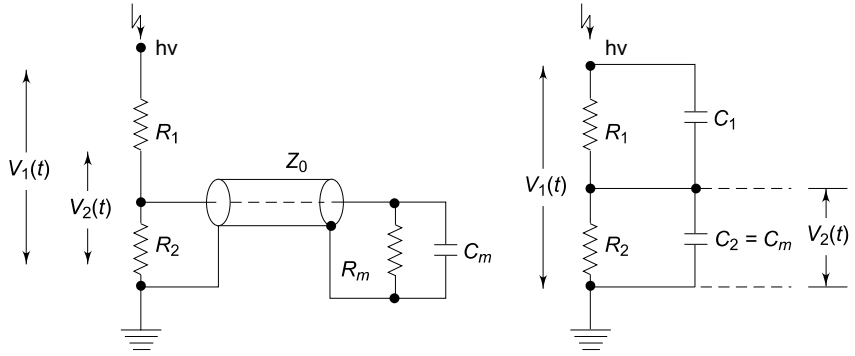

(a) Resistance potential divider with surge cable and oscilloscope terminations

(b) Compensated resistance potential divider

Figure. VI.**25a and b** *Resistance potential dividers*

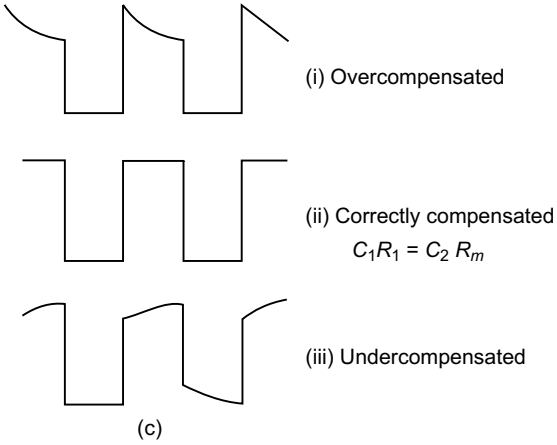

Figure. VI.**25c** *Output of compensated resistance voltage divider for different degrees of compensation*

(*b*) Potential Dividers Used for High-Voltage Impulse Measurements

In a resistance potential divider, R_1 and R_2 are considered as resistors of small dimensions in the previous section. For voltages above 100 kV, R is no longer small in dimension and is usually made of a number of sections. Hence the divider is no longer a small resistor of lumped parameters, but has to be considered as an equivalent distributed network with its terminal to ground capacitances and intersectional series capacitances as shown in Figure.V.27.The total series resistance R_1 is made of n resistors of value R_1' and $R = nR_1'.C_g$ is the terminal to ground capacitance of each of the resistor elements R_1', and C_s is the capacitance between the terminals of each section. The inductance of each element $(\hat{L}_1')$ is not shown in the figure as

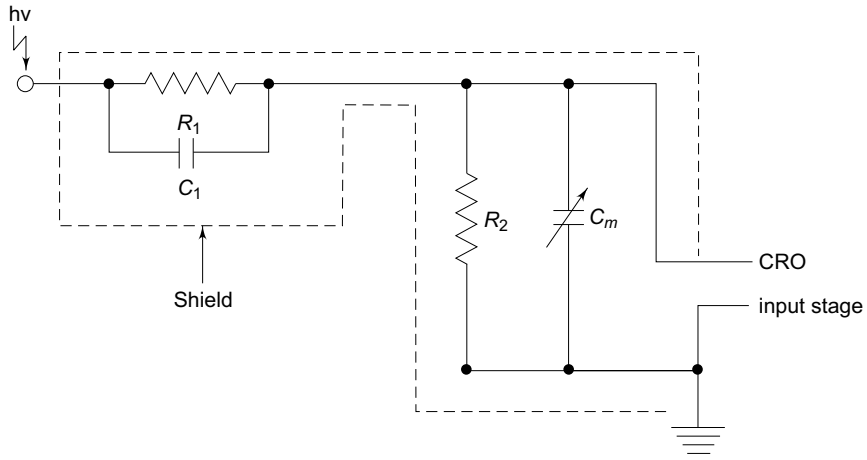

Figure. VI.**26** *Schematic circuit arrangement of a cathode ray oscillo scope voltage divider probe*

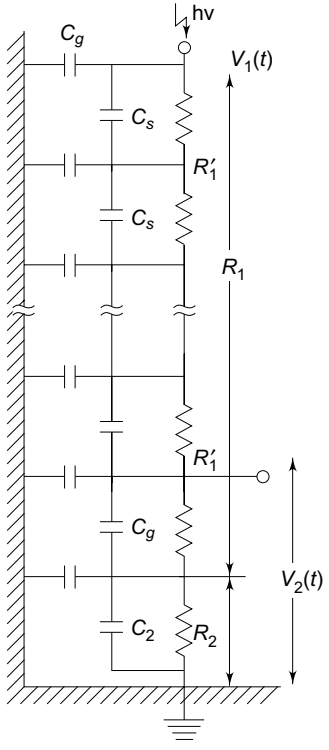

Figure. VI.**27** *Resistance potential divider the divider with inter-sectional and ground capacitances*

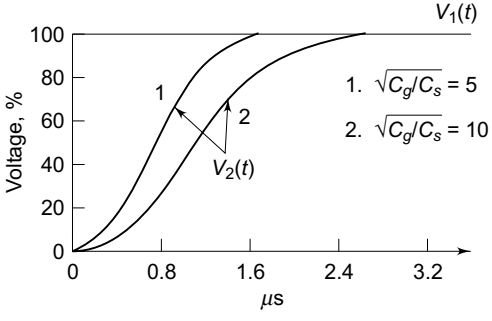

Figure. VI.**28** *Output of shown in* Figure. VI.*27 for a step input*

it is usually small compared to the other elements (i.e., R_1', C_s and C_g). This type of divider produces a non-linear voltage distribution along its length and also acts like an *R-C* filter for applied voltages. The output of such divider for various values of C_g/C_s ratio is shown in Figure. VI.28 for a step input. By arranging guard rings at various elemental points, the equivalent circuit can be modified as shown Figure. VI.29, where C_h represents the stray capacitance introduced between the high voltage lead and the guard elements. This reduces the distortion introduced by the original divider (Plate 5).

(c) Capacitance Voltage Dividers Capacitance voltage dividers are ideal for measurement of fast rising voltages and pulses. The capacitance ratio is independent of the frequency, if their leakage resistance is high enough to be neglected. But usually the dividers are connected to the source voltage through long leads which introduce lead inductanc es and residual resistances. Also, the capacitance used for very high-voltage work is not small in dimension and hence cannot be considered as a lumped element. Therefore, the output of the divider for high frequencies and impulses is distorted as in the case of resistance dividers.

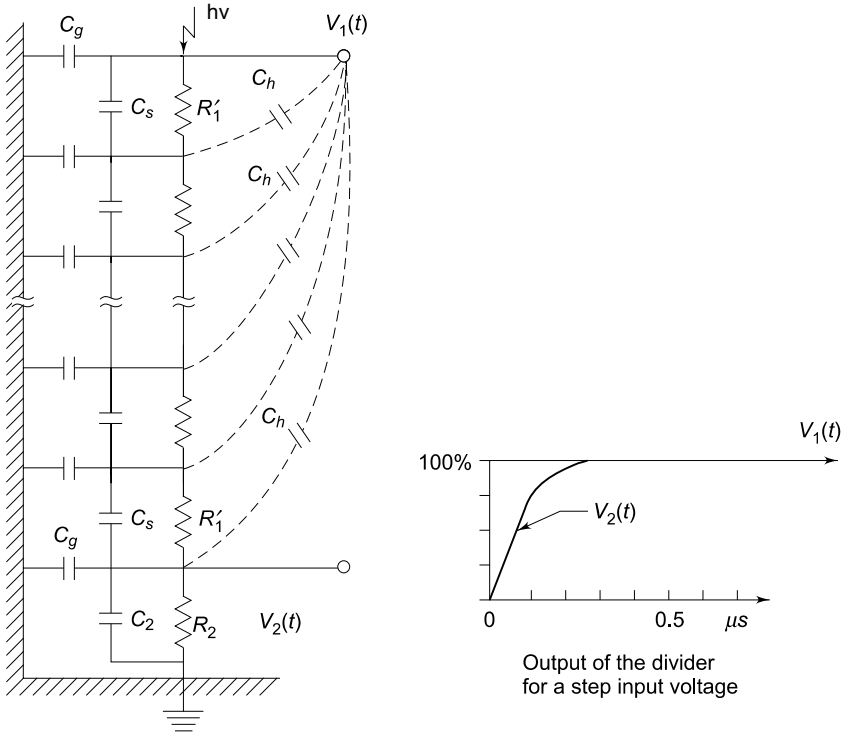

Figure. VI.**29** *Equivalent circuit of a resistance potential divider with shield and guard rings*

(d) Pure Capacitance Dividers A pure capacitance divider for high voltage measurements and its electrical equivalent network without stray elements is shown in Figure. VI.30. The ratio of the divider

$$a = \frac{V_1(t)}{V_2(t)} = 1 + \frac{C_2}{C_1} \qquad \text{(VI. 28)}$$

Capacitance C_1 is formed between the hv terminal of the source (impulse generator) and that of the test object or any other point of measurement. The CRO is located within the shielded screen surrounding capacitance C_2. C_2 includes the capacitance used, the lead capacitance, input capacitance of the CRO, and other ground capacitances. The advantage of this connection is that the loading on the source is negligible; but a small disturbance in the location of C_2 or hv electrode or the presence of any stray object nearby changes the capacitance C_1, and hence the divider ratio is affected.

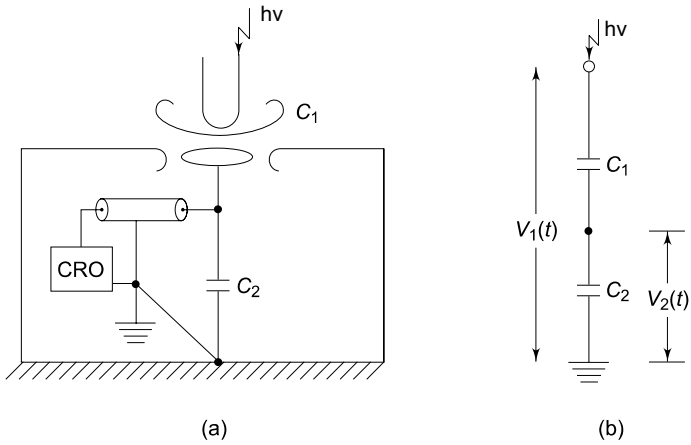

Figure. VI.**30** *Capacitance voltage divider for very high voltages and electrical equivalent circuit*

In many cases, a standard air or compressed gas capacitor is used which has coaxial cylindrical construction. Accurate ratios that could be calculated up to 1000 : 1 have been achieved for a maximum impulse voltage of 350 kV, and the upper frequency limit is about 10 MHz. For smaller or moderately high voltages (up to 100 kV) capacitance dividers are built with an upper frequency limit of 200 MHz.

Another type of design frequently used is to make C_1 to consist of a number of capacitors C'_1 in series for the given voltage V_1. In such cases the equivalent circuit is similar to that of a string insulator unit used in transmission lines (Figure. VI.31). The voltage distribution along the capacitor chain is non-linear and hence causes distribution of the output wave. But the ratio error is constant and is independent of frequency as compared to resis tance dividers. A simpli-fied equivalent circuit is shown in Figure. VI.31b, which can be used if $C_2 < C_g$ and $<< C_1$.

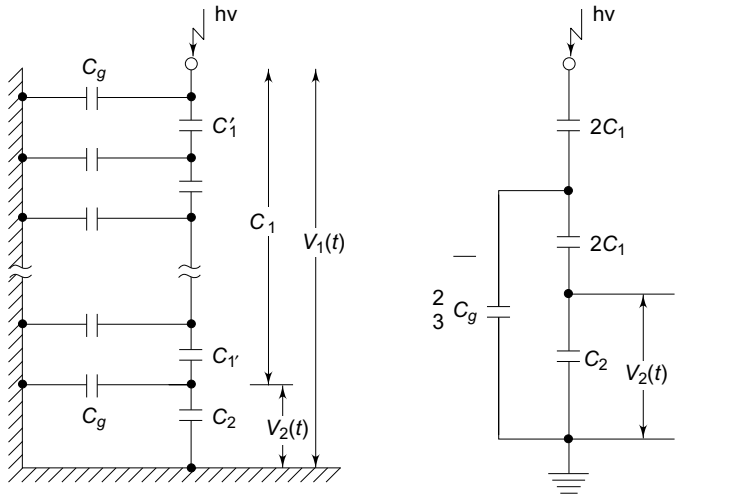

Figure. VI.31 *Capacitance voltage divider with distributed network and its equivalent circuit*

The voltage ratio is

$$a = \frac{V_1(t)}{V_2(t)} \approx \left[1+\frac{C_2}{C_1}\right]\left[1+\frac{C_g}{6C_1}\right] \qquad \text{(VI.29)}$$

This ratio is constant and gives an error of less than 5% when $C_1 \geq 3C$. This equivalent circuit is quite satisfactory up to 1 MHz.

(e) Field Controlled Voltage Dividers The electrostatic or capacitive field distribution of a shield or guard ring placed over a resistive divider to enforce a uniform field in the neighbourhood and along the divider may be adopted for high voltage measurements. The schematic diagram is shown in Figure. VI.32 and its circuit is same as that given in Figure. VI.29. The shield is of the form of a cone. R_1 is a non-linear resistance in the sense the resistance per unit the same but is variable. The main advantage is that the capacitance per unit length length is not is small and hence loading effect is reduced. Sometimes the parallel resistance R_2 together with the lead inductance and shunt capacitances cause oscillations as shown in Figure. VI.33a. The oscillations can be reduced by adding a damping resistance R_d as shown in Figure. VI.32 response times less than 30 ns. The resistance column, R_1 is made of woven Such dividers are constructed for very high voltages (up to 2 MV) with resistance of 20 kilo-ohms. The step response of such a divider is shown in Figure. VI.33, with and without a damping resistor. With a proper damping resis tor (the response time is much less and the overshoot is reduced. R_4)

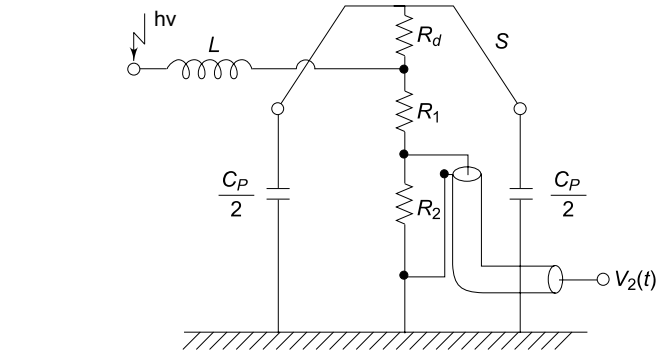

R_d — Damping resistor
C_p — Capacitance of the shield to ground
L — Lead inductance
S — Shield

Figure. VI.32 *Field-controlled resistance divider with a damping resistor*

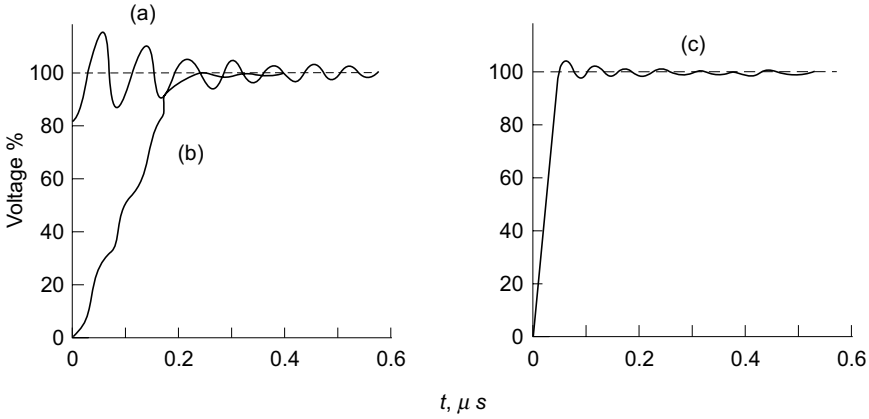

(a) R_d = 0 and long lead
(b) R_d = 0 and short lead of 14' long with low inductance
(c) R_d = 500 Ω and long lead

Figure. VI.33 *Step response of field controlled voltage divider of* Figure. VI.*32*

(f) Mixed R-C Potential Dividers Mixed potential dividers use *R-C* elements in series or in parallel. One method is to connect capacitance in parallel with each *R′* element. This is successfully employed for voltage dividers of rating 2 MV and above. A better construction is to make an *R-C* series element connection. The equivalent circuit of such a construction is shown in Figure . VI. 34. Such dividers are made up to 5 MV with response times less than 30 ns. The low voltage arm R_2 is given "*L* peaking" by connecting a variable inductance *L* in response of the divider and the schematic connection of low voltage arm are shown series with R_2. The step in Figure . VI.35. However , for a correctly designed voltage divider *L* peaking will not be necessary.

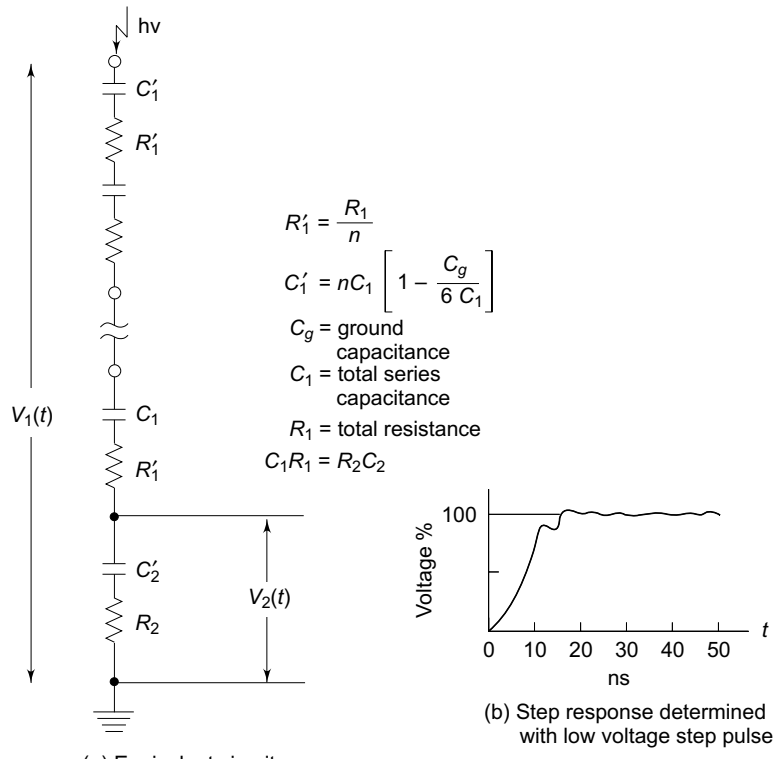

Figure. VI.**34** *Equivalent circuit of a series R-C voltage divider and its step response*

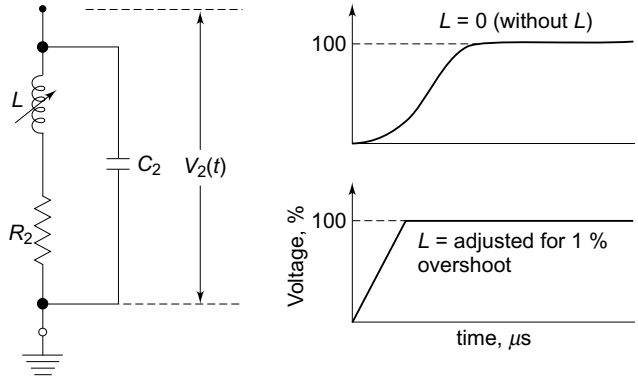

Figure. VI.**35** *L peaking in low-voltage arm and step response of the divider with L peaking*

(g) R-C Potential Dividers for 2 MV Rating and above

Voltage dividers used for measuring more than one million volts attenuate the measuring signal to a value in the range of 100 V to few hundreds of volts.

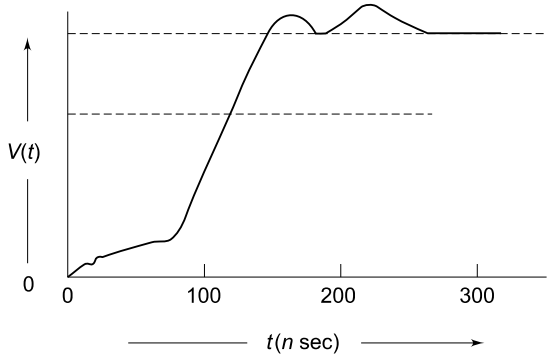

(i) Optimally damped

Response time	:	50 *n* sec
Front time	:	50 *n* sec
Oveshoot	:	$\simeq$ 3%
Parameters	:	R_1 = 1000 Ω C_1 = 360 pF
Damping resistance	:	500 Ω $(R_d + R_1)\, C_1 = R_2\, C_2$

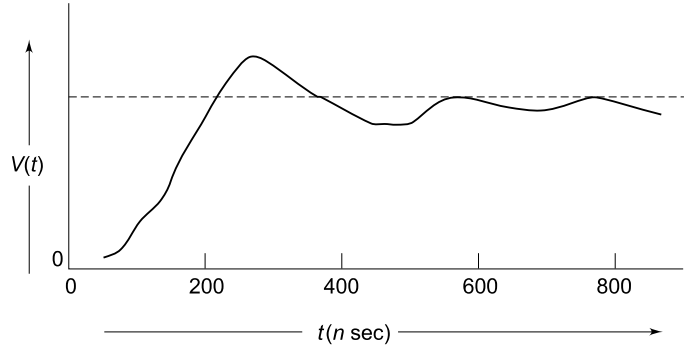

(ii) Underdamped

Response time	:	4 *n* sec
Front time	:	110 *n* sec
Overshoot	:	$\simeq$ 30%
Parameters	:	R_1 = 256 Ω C_1 = 400 pF
Damping resistance	:	0 Ω $R_1\, C_1 = R_2\, C_2$

Figure. VI.**36** *Step response of a 4 MV R-C divider*

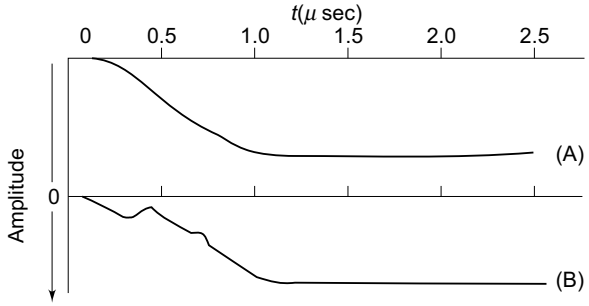

Figure. VI.**37** *Record of the front portion of a lightning impulse wave with underdamped (curve A) and optimally damped (curve B) divi ders for a negative polarity wave when both dividers are connect ed in parallel*

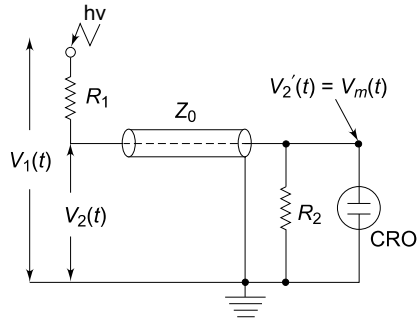

(a) Resistance potential divider with surge cable and CRO

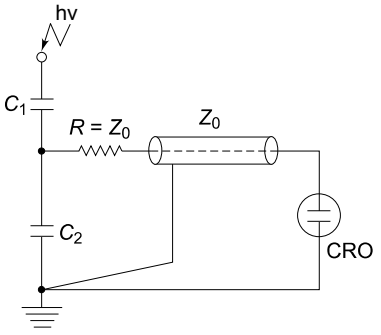

(b) Capacitance divider with surge cable and CRO

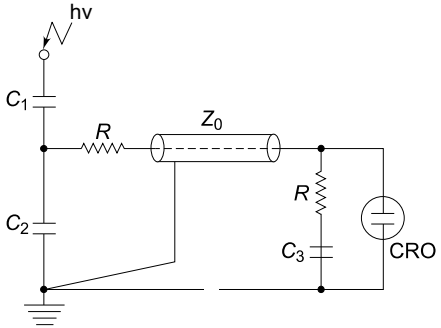

(c) Split capacitor arrangement $R = Z_0$

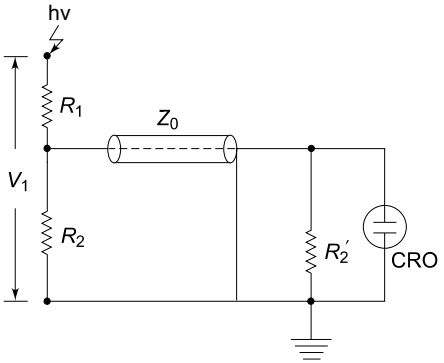

(d) Resistance potential divider with surge cable and CRO. Voltage ratio, $V_1/V_2 = 1 + (R_1/R_2) + (R_1/R_2')$ where $R_2' = Z_0$

Figure. VI.**38** *Potential divider arrangements*

The criteria required to assess the dividers are (i) the shape of the voltage in the test arrange ment should be transferred without any distortion to the LV side , (ii) simple determination of transfer behaviour should be ensured, and (iii) they should be suitable for multipurpose use, i.e., for use with ac power frequency voltages , switching im pulse voltages as well as with lightning impulse voltages . This condition necessitates that the dividers should have broad band widths. The above requirements are generally met by (a) optimally damped *R-C* dividers, (b) underdamped or low-damped *R-C* dividers. The high -voltage arm of such dividers consists of series *R-C* units while the secondary arm is usually an

R-C series or parallel circuit. In case of optimally damped dividers, $R_1 = 4\sqrt{L_1/C_g}$ where L_1 is the inductance of the high-voltage lead and the HV portion of the divider, and C_g is the equivalent capacitance to ground. Usually this resistance will be 400 to 1000 ohms. On the other hand, for low or underdamped dividers, R_1 will be equal to 0.25 to 1.5 times $\sqrt{L/C_1}$ where L is the inductance for the complete measuring loop and C_1 is the capacitance of the HV part of the divider. In this case the normal value of R_1 lies between 50 and 300 ohms. The step response of the two types of dividers mentioned above is shown in Figure. VI.36. In actual prac tice, because of the large time constant $_{d1}$ $(R_1 + R)\ C$, the opti mal damped divider affects the voltage the test object. Standard lightning impulses sometimes cannot be generated to the shape at correct standard specifications . As such, *R-C* potential divi ders are not suitable for measurements with test objects of very low capacitance . The low or underdamped *R-C* divider acts as a load capacitance and is suitable for applications over a broad bandwidth , i.e., ac, switching impuls es, lightning impulses, chopped waves, etc. Underdamped *R-C* dividers are also suitable for measurement of steep fronted impulse waves . A typical record of lightning impulse wave (1.2/50 μs wave) obtained using both the above types of divi ders is shown in Figure. VI

. It may be noted that even though the step response is poor in the case of underdamped dividers, they can be used to measure the standard impulse wave to a better accuracy.

(h) Different Connections Employed with Potential Dividers Different arrangements and connections of voltage or potential dividers with a cathode ray oscilloscope are shown in Figs VI.38 and VI.39.

A simple arrangement of a resistance divider is shown in Figure . VI.38a. The possible errors$_2$ are (0i) $R \neq Z$ (surge impedance of the cable), (ii) capacitance of the cable CRO shunting and R and hence introducing distortion , (iii) attenuation or voltage drop in surge cable Z_0, and (iv) ground capacitance effect. These errors are already discussed in Sec . VI.2.VI. To avoid reflections at the junction of the cable and$_2$ R_2, R is varied and adjusted to give the best possible step response . When a unit step vol tage is applied to the circuit shown in Figure. VI.38b, the effect of the cable is to take a fraction of the voltage $_{11}$ $[C/_2(C + C)]$ into it and cause reflections at the input end . In the cable acts like a resistance of value = Z the surge im pedance, but later behaves like a

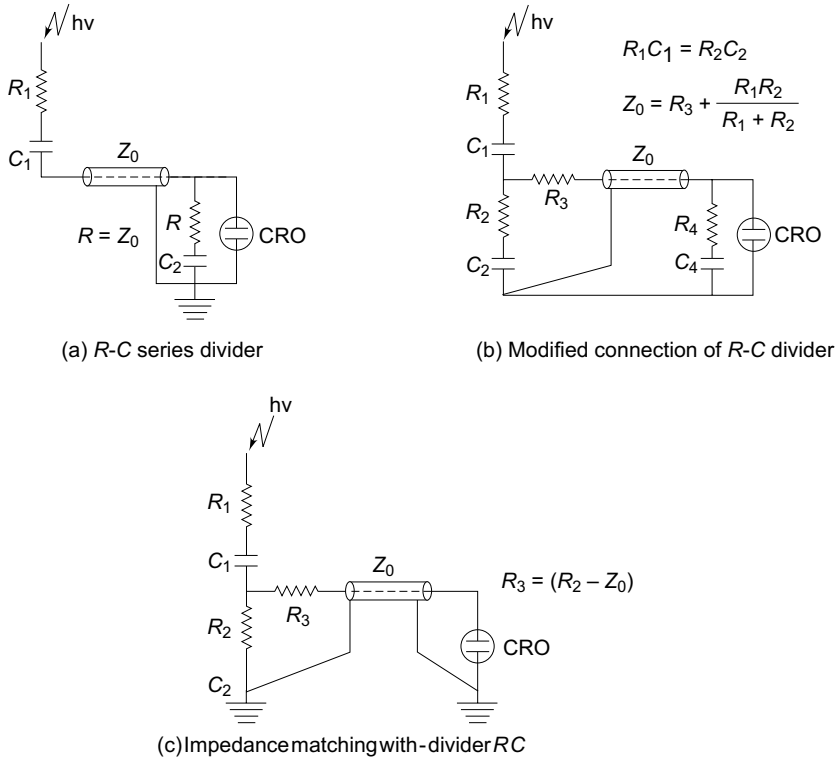

Figure. VI.39 *Mixed potential divider arrangements* distor tion and is compensated by using a split capacitor connection as shown in Figure. VI.38c with $(C_2 + C)_3 = (C_k + C_k)$ [C = capacitance of the cable]. On the other $C/(C + C + C) = 0.1$, the error will be less than 1.5%.

hand if

k 1 2 k

The arrangements for mixed potential dividers are shown in Figure. VI. 39. The arrangement shown in Figure. VI.39a is modified and im proved in the arrangement of Figure. VI.39b.

$$R_1C_1 = \frac{C_2Z_0(C_1 + C_2 + C_k)}{(C_1 + C_2)} \qquad \text{(VI. 30)}$$

$$Z_0 = R_3 + \left(\frac{R_1R_2}{R_1 + R_2}\right), \text{ and } R_1C_1 = R_2C_3 \qquad \text{(VI. 31)}$$

The response is greatly improved. The arrangement shown in Figure. VI.38c is simple and gives the desired impedance matching.

(i) ***Low-Voltage Arms of the Measuring System Connected to Voltage Dividers*** The mode of connection and the layout arrangement of the secondary arm of the divider is very critical for the distortionless measurement of fast

transients. The LV arm of the divider itself introduces large distortions if not properly connected. Different corrections employed for connecting the LV arm to the measuring instrument via the signal cables are shown in Figs VI.38 and VI. 39. The signal cable Z_0 may be assumed to be loss-free so that the surge Z impedance $_0 = LC$, is independent of the fre quency and the travel time for the signal,

$T_0 = \sqrt{L/C}$ (refer to Chapter 8 for details). In the case of resistance dividers, the cable matching is achieved by having a pure resistance, $R_2 = Z_0$ at the end of the cable. The surge cable Z_0 and the resistance R_2 form an integral part of the cable system. Typically, Z_0 has values of 50 or 75 ohms. In actual practice, signal cables do have losses due to skin effect at high frequencies and hence Z_0 becomes a complex quantity. Thus, the matching of R_2 with Z_0 should be done at high frequencies or with a step input as indicated earlier. In the case of long cables, the cable resistance including that of the shield wire should be taken as a part of the matching resistance. The divider ratio in the case of the connection shown in Figure. VI.38 is

$$a = V_1/V_2 = 1 + R_1/R_2 + R_1/R'_2 \text{ and}$$
$$R'_2 = Z_0 \qquad \text{(VI. 32)}$$

For the capacitance dividers, the signal cable cannot be completely matched. A low ohmic resistance connected in parallel with C_2 would load the LV arm and hence, the output gets decreased. Connection of a resistance $R = Z_0$ at the input end (see Figs VI.38 and VI.39) will make the voltage across the CRO the same as that across C_2. The transient voltage ratio, at $t = 0$ is given as

$$a = V_1/V_2 = 1 + C_2/C_1 \text{ and}$$
$$\text{effective} = 1 + (C_2 + C_k)/C_1 \text{ for } t >> 2\ T_0 \qquad \text{(VI. 33)}$$

where C_k is the cable capacitance.

Thus, an initial overshoot of $\Delta V = C_k/(C_1 + C_2)$ will appear. This will be either small or negligible for medium and low cable lengths, and for high values of capacitance C_2. This error can be avoided and the response improved in the case of *R-C* dividers by using the arrangements shown in Figure. VI.39c.

Usually, the LV arms are made co-axial and are enclosed in metal boxes that are solidly grounded. The series resistors used in *R-C* divider forms an integral part of the divider's LV arm. Further, all the LV arm capacitors and resistors should have a very low inductance. A typical LV arm arrangement is shown in Figure. VI.40.

VI.2.8 Peak-Reading Voltmeters for Impulse Voltages

Sometimes it is enough if the peak of an impulse voltage wave is measured; its waveshape might already be known or fixed by the source itself. This is highly useful in routine impulse testing work. The methods are similar to those employed for ac voltage crest value measurements. The instrument is normally connected to the low voltage arms of the potential dividers described in Sec. VI.2.VI. The basic circuit along with its equivalent circuit and the response characteristic is shown in Figure. VI.41. The circuit consists of only rectifiers.

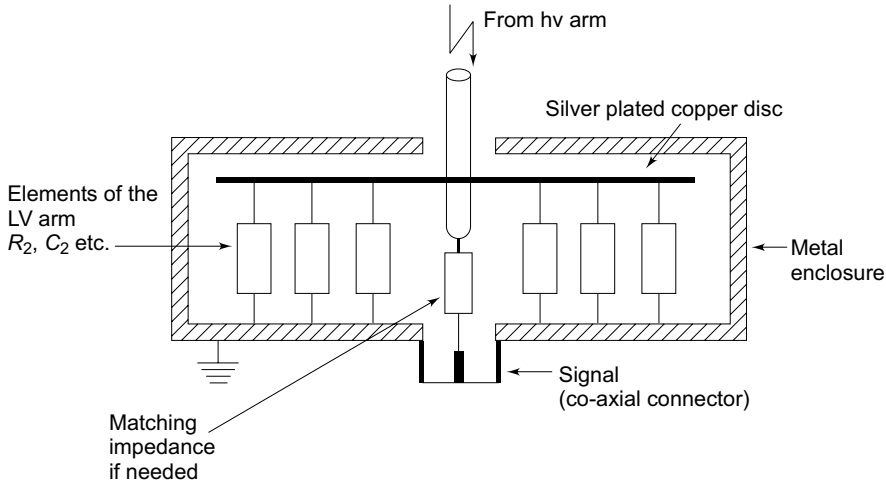

Figure. VI.40 *LV arm layout for voltage dividers*

Diode *D* conducts for positive voltages only. For negative pulses, the diode has to be connected in reverse. When a voltage impulse $v(t)$ appears across the low voltage arm of the potential divider, the capacitor C_m is charged to the peak value of the pulse. When the amplitude of the signal starts decreasing the diode becomes reverse biased and prevents the discharging of the capacitor C_m. The voltage developed across C_m is measured by a high impedance voltmeter (an electrostatic voltmeter or an electrometer). As the diode *D* has finite forward resistance, the voltage to which C_m is charged will be less than the actual peak of the signal, and is modified by the *R-C* network of the diode resistance and the measuring capacitance C_m. The error is shown in Figure. VI.41c. The error can be estimated if the waveform is known. The actual forward resistance of the diode *D* (dynamic value) is difficult to estimate, and hence the meter is calibrated using an oscillo scope. Peak voltmeters for either polarity employing resistance dividers and capacitance dividers are shown in Figure. VI.42. In this arrangement, the voltage of either polarity is transferred into a proportional positive measuring signal by a resistive or capacitive voltage divider and a diode circuit. An active network with feedback circuit is employed in commercial instruments, so that the fast rising pulses can also be measured. Instruments employing capacitor dividers require discharge resistance across the low-voltage arm to prevent the build-up of dc charge.

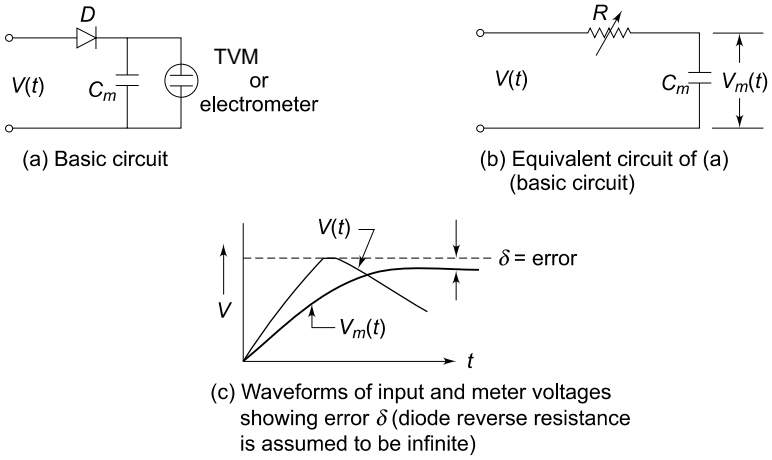

Figure. VI.**41** *A peak reading voltmeter and its equivalent cir cuit (R-C approximation)*

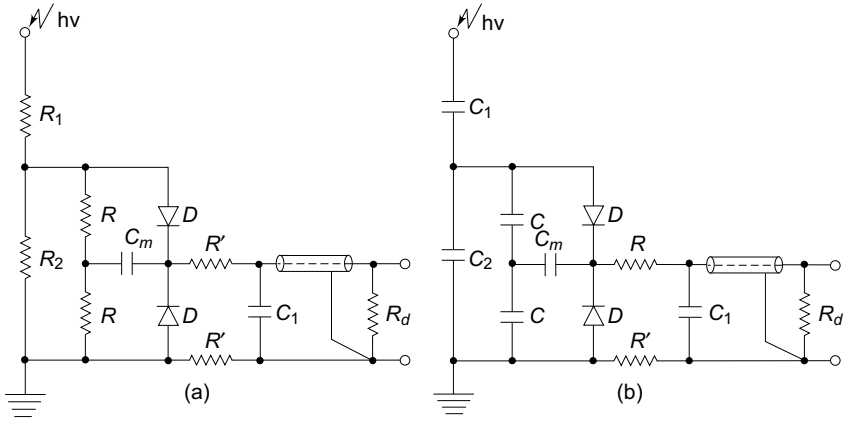

Figure. VI.**42** *Peak reading voltmeter for either polarity with (a) resistance divider, and (b) capacitance divider*

VI.3 MEASUREMENT OF HIGH CURRENTS—DIRECT, ALTERNATING, AND IMPULSE

In power systems, it is often necessary to measure high currents, arising due to short circuits. For conducting temperature rise and heat run tests on power equipments like conductors, cables, circuit breakers, etc., measurement of high currents is required. During lightning discharges and switching transients also, large magnitudes of impulse and switching surge currents occur, which require special measuring techniques at high potential levels.

VI.3.1 Measurement of High Direct Currents

High magnitude direct currents are measured using a resistive shunt of low ohmic value. The voltage drop across the resistance is measured with a millivoltmeter. The value of the resistance varies usually between 10 $\mu\Omega$ and 10 mΩ. This depends on the heating effect and the loading permitted in the circuit. High current resistors are usually oil immersed and are made as three or four terminal resistances (see Figure. VI.43). The voltage drop across the shunt is limited to a few millivolts (< 1 Volt) in power circuits.

Typical shunt used for measurement of current in HVDC transmission system is shown in Figure. VI.43c. The voltage drop across the shunt, which is an analog signal, is converted into a digital/optical signal and is sent via a fibre-optic cable to the ground-level instrument.

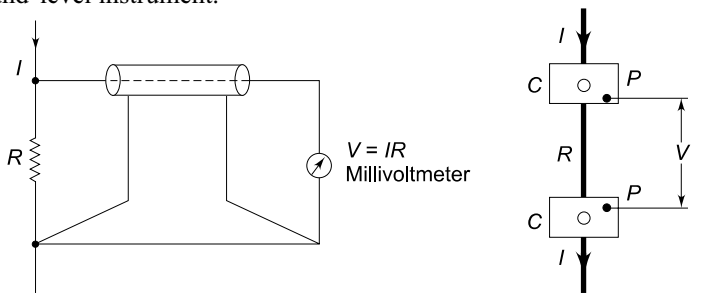

(a) Low ohmic shunt with a millivoltmeter for current measurement

(b) Four terminal shunt

CC — Current terminals
PP — Potential terminals
R — Ohmic element

(In 3 terminal construction bottom *C* and *P* terminals are made common)

Figure. VI.**43** *Calibrated ohmic shunt for dc current measurements*

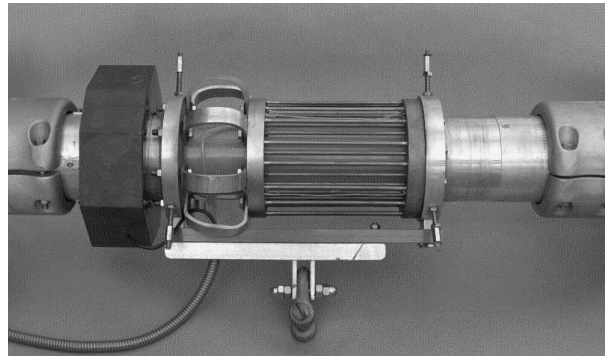

Figure VI.**43c** *HVDC shunt assembly*

(a) dc Current Transformer

Principle Transformer operates on the principle of ampere turn balance, i.e. the primary ampere turns ($N_1 I_1$) are balanced by the secondary ampere turns ($N_2 I_2$) where N_1 and N_2 are the turns in the primary and secondary windings and I_1 and I_2 are the respective currents in these windings. With dc current in the primary winding, core saturation occurs due to the non-linearity of the *B-H* curve of the core.

When a high-frequency excitation is given to the third or excitation winding located on the same core, the current through the secondary winding will have a distorted waveform containing a large-amplitude second harmonic. A fourth winding is added and a second harmonic current is injected in the opposite direction to make the harmonic current zero. The injected current will be proportional to the primary dc current and hence will give the measurement of dc current. Schematic diagram of a dc current transformer is shown in Figure. VI.44

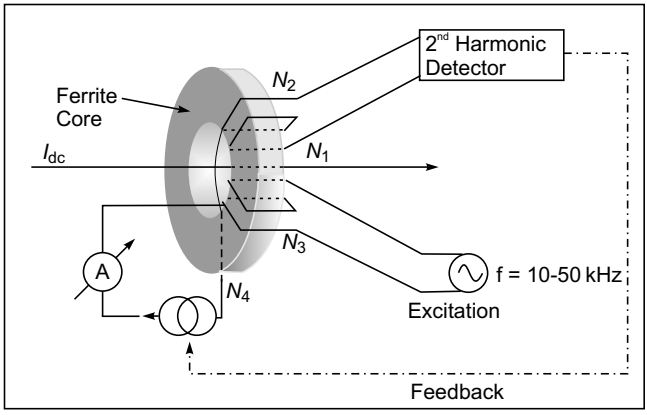

Figure. VI.**44** *DC CT schematic diagram*

The advantages of dc CT are the following:

- It gives isolation to high voltages.
- Power loss is much less compared to dc shunt, and the conductor through which the dc current flows need not be broken for connecting to the mains.

(b) Hall Generators for dc Measurements

The principle of the 'Hall effect' is made use of in measuring very high direct currents. If an electric current flows through a metal plate located in a magnetic field perpendicular to it, Lorenz forces will deflect the electrons in the metal structure in a direction normal to the direction of both the current and the magnetic field. The charge displacement generates an emf in the normal direction, called the "Hall voltage". The Hall voltage is proportional to the current *i*, the magnetic flux density *B*, and the reciprocal of the plate thickness *d*; the proportionality constant *R* is called the *Hall coefficient*

$$V_H = R\frac{B_i}{d} \qquad \text{(VI. 34)}$$

For metals, the Hall coefficient is very small, and hence semi-conductor materials are used for which the Hall coefficient is high.

In large current measurements, the current carrying conductor is surrounded by an iron cored magnetic circuit, so that the magnetic field intensity $H = (1/\delta)$ is produced in a small air gap in the core. The Hall elements is placed in the air gap (of thickness d), and a small constant dc current is passed through the element. The schematic arrangement is shown in Figure. VI.44a. The voltage developed across the Hall element in the normal direction is proportional to the dc current I. It may be noted that the Hall coefficient R depends on the temperature and the high mag netic field strengths, and suitable compensation has to be pro vided when used for measurement of very high currents.

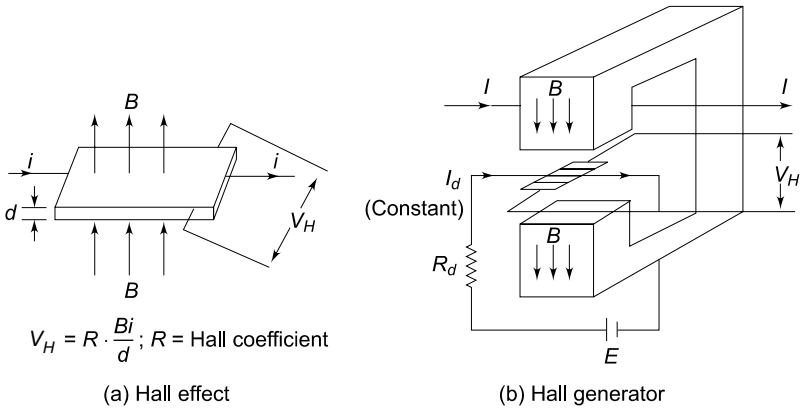

Figure. VI.**44a** *Hall generator for measuring high dc currents* Hall

generators can be used for measurement of unidirectional ac and impulse currents also. With proper design of Hall-element dimensions and addition of compensating circuits, the bandwidth of the Hall generator can be increased to about 50 MHz. As such, these generators can be used for the measurement of post arc currents and unidirectional impulse currents.

VI.3.2 Measurement of High-Power Frequency Alternating Currents

Measurement of power frequency currents are normally done using current transformers only, as use of current shunts involves unnecessary power loss. Also the current transformers provide electrical isolation from high voltage circuits in power systems. Current transformers used for extra high voltage (EHV) systems are quite different from the conventional designs as they have to be kept at very high voltages from the ground. A new scheme of current transformer measurements introducing electro -optical technique is described in Figure . VI.45. A voltage signal proportion al to the measuring current is generated and is transmitted to the ground through an electro-optical device. Light pulses proportional to the voltage signal are transmitted

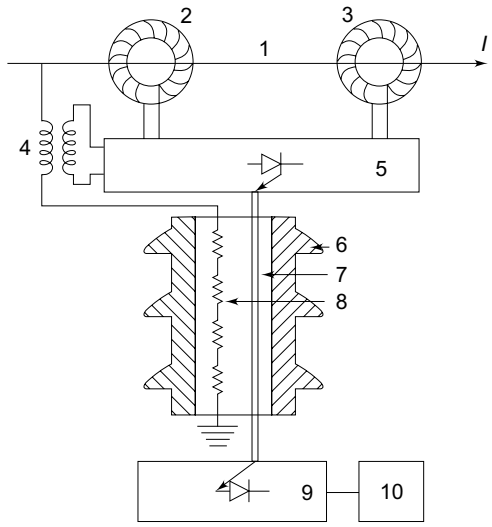

1. EHV conductor
2. Current sensing transformer
3. Power supply C.T.
4. Power supply P.T.
5. Analog-digital signal converter
6. Insulator for EHV

VI. Electro-optical glass fibre

8. Series high ohmic resistance
9. Digital-analog converter
10. Indicating or recording unit

Figure. VI.45 *Current transformer with electro-optical signal conver ter for EHV systems*

by a glass-optical fibre bundle to a photodetector and converted back into an analog voltage signal. Accuracies better than ±0.5% have been obtained at rated current as well as for high short circuit currents. The required power for the signal converter and optical device are obtained from suitable current and voltage transformers as shown in Figure. VI.45.

VI.3.3 Measurement of High Frequency and Impulse Currents

In power system applications as well as in other scientific and technical fields, it is often necessary to determine the ampli tude and waveforms of rapidly varying high currents. High impulse currents occur in lightning discharges, electrical arcs and post-arc phenomenon studies with circuit breakers, and with electric discharge studies in plasma physics. The current amplitudes may range from a few amperes to few hundred kiloamperes. The rate of rise for such currents can be as high as 10^6 to 10^{12} A/s, and rise times can vary from few microseconds to few nano seconds. In all such cases the sensing device should be capable of measuring the signal over a wide frequency band. The methods that are frequently employed are (i) resistive shunts, (ii) magnetic potentiometers or probes, and (iii) the Faraday and Hall effect devices.

The accuracy of measurement varies from 1 to 10%.

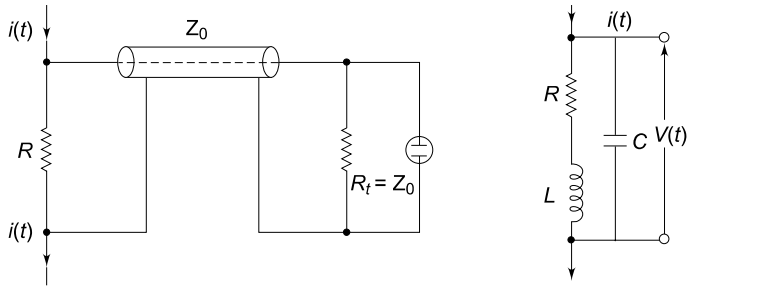

(a) Ohmic shunt (b) Equivalent circuit of the shunt

Figure . VI.46 *Calibrated low ohmic shunt and its equivalent circuit for impulse current measurements*

Resistive Shunts

The most common method employed for high impulse current measure ments is a low ohmic pure resistive shunt shown in Figure . VI.46. The equivalent circuit is shown in Figure. VI.46b. The current through the resistive element R produces a voltage drop $v(t) = i(t)R$. The voltage signal generated is transmitted to a CRO through a coax ial cable of surge impedance Z_0. The cable at the oscilloscope end is terminated by a resistance $R = Z_{i0}$ to avoid reflections. The resistance element, because of its large dimensions will have a residual inductance L and a terminal capacitance C. The induc tance L may be neglected at low frequencies (ω) , but becomes appreciable at higher frequencies (ω) when ωL is of the order of R. Similarly, the value of C has to be considered when the reactance $1/\omega C$ is of comparable values. Normally L and C become significant above a frequency of 1 MHz. The resistance value usually ranges from 10 $\mu\Omega$ to few milliohms, and the voltage drop is usually about a few volts. The value of the resistance is determined by the thermal capacity and heat dissipation of the shunt.

The voltage drop across the shunt in the complex frequency domain may be written as

$$V(s) = \frac{(R + Ls)}{(1 + RCs + LCs^2)} I(s) \qquad \text{(VI. 35)}$$

where s is the complex frequency or Laplace transform operator and $V(s)$ and $I(s)$ are the transformed quantities of the signals $v(t)$ and $i(t)$. With the value of C neglected it may be approximated as

$$V(s) = (R + Ls)\, I(s) \qquad \text{(VI. 36)}$$

It may be noted here that the stray inductance and capacitance should be made as small as possible for better frequency response of the shunt. The resistance shunt is usually designed in the following manner to reduce the stray effects.

(i) Bifilar flat strip design,
(ii) Coaxial tube or Park's shunt design, and
(iii) Coaxial squirrel cage design.

(i) *Bifilar Strip Shunt* The bifilar design (Figure. VI.47) consists of resistor elements wound in opposite directions and folded back, with both ends insulated by a teflon or other high quality insulation. The vol tage signal is picked up through a ultra high frequency (UHF) coaxial connector. The shunt suffers from stray inductance asso-ciated with the resistance element, and its potential leads are linked to a small part of the magnetic flux generated by the current that is measured. To overcome these problems, coaxial shunts are chosen.

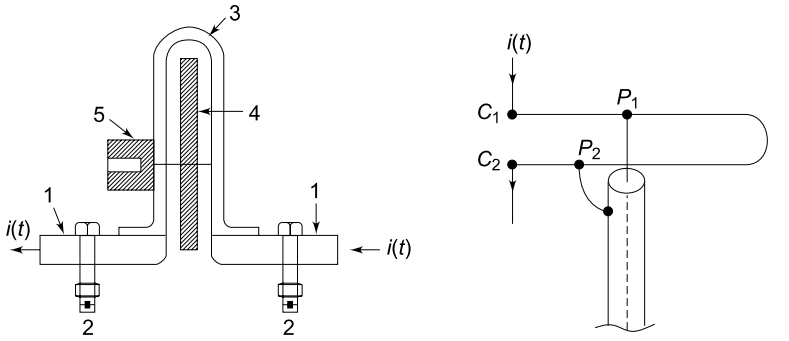

(a) Schematic arrangement

(b) Connection for potential and current terminals

1. Metal base
2. Current terminals (C_1 and C_2)
3. Bifilar resistance strip
4. Insulating spacer (teflon or bakelite)
5. Coaxial UHF connector

P_1, P_2 — Potential terminals

Figure. VI.**47** *Bifilar flat strip resistive shunt*

(ii) *Coaxial Tubular or Park's Shunt* In the coaxial design (Figure. VI. 48), the current is made to enter through an inner cylinder or resistive element and is made to return through an outer conducting cylinder of copper or brass. The voltage drop across the resistive element is measured between the potential pick-up point and the outer case. The space between the inner and the outer cylinder is air and hence acts like a pure insulator. With this construction, the maximum frequency limit is about 1000 MHz and the response time is a few nanosec onds. The upper frequency limits is governed by the skin effect in the resistive element. The equivalent circuit of the shunt is given in Figure. VI.49. The step response and Figure the . frequency VI.50. The response inductance are *L*shown shown in in Figure. VI.49 may be written as

$$L_0 = \frac{\mu dl}{2\pi r} \qquad \text{(VI.37)}$$

where, $\mu = \mu_0 \mu_r$; the magnetic permeability, $\mu_0 = 4\pi \times 10^{-7}$

d = thickness of the cylindrical tube,

l = length of the cylindrical tube, and

r = radius of the cylindrical tube

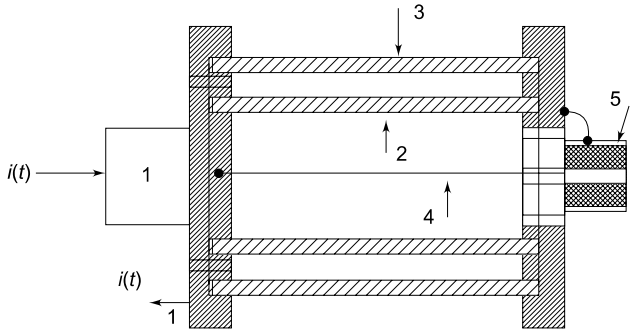

1. Current terminals
2. Coaxial cylindrical resistive element
3. Coaxial cylindrical return conductor (copper or brass tube)
4. Potential pick up lead
5. UHF coaxial connector

Figure. VI.**48** *Schematic arrangement of a coaxial ohmic shunt*

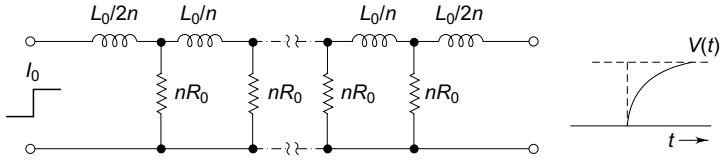

(a) Exact equivalent circuit

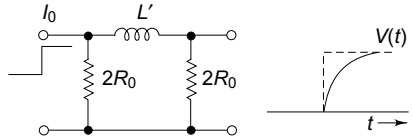

(b) Simplified circuit

L_0 — Inductance
R_0 — dc resistance
n — Number of sections per unit length
L' — 0.43 L_0

Figure. VI.**49** *Simplified and exact equivalent circuits of a coaxial tubular shunt*

The effective resistance is given by

$$R = \frac{V(t)}{I_0} = R_0 \theta(\omega t) \qquad \text{(VI. 38)}$$

where R_0 = the dc resistance; L_0 = inductance for dc currents and $\theta(\omega t)$ is the theta function of type 3 and is equal to

$$\left[1 + 2\sum_{n=1}^{\infty}(-1)^n \exp(-n^2 \omega t)\right]$$

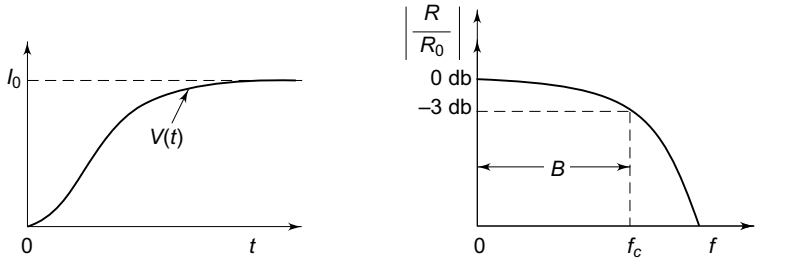

Figure. VI.50 *Step and frequency responses of a coaxial tubular shunt*

in which $\omega = \dfrac{(\pi^2 R_0)}{L_0}$

$V(t)$ = signal developed; and I_0 is the step current.

The effective impedance of the shunt for any frequency f according to Silsbee is given by

$$Z = \frac{R_0(1+j)\delta}{\sinh[(1+j)\delta]} \qquad \text{(VI.39)}$$

where, R_0 = dc resistance Ω,

$\delta = 2\,\pi\, d\sqrt{(f\mu)/\rho}$,

ρ = resistivity of the material, Ω-cm,
d = thickness of the tube, cm,
f = frequency, Hz, and
μ = permeability as defined earlier.

The simplified equivalent circuit shown in Figure. VI.49 is convenient to calculate the rise time of the shunt. The rise time accordingly is given by,

$$T = 0.237\,\frac{\mu d^2}{\rho}$$

and the bandwidth is given by

$$B = \frac{1.46R}{L_0} = \frac{1.46\rho}{\mu d^2} \qquad \text{(VI.40)}$$

The coaxial tubular shunts were constructed for current peaks up to 500 kA; shunts constructed for current peaks as high as 200 kA with di/dt of about 5×10^{10} A/s have induced voltages less than 50 V and the voltage drop across the shunt was about 100 V.

(iii) *Squirrel-Cage Shunts* In certain applications, such as post arc current measurements, high ohmic value shunts which can dissipate larger energy are required. In such cases tubular shunts are not suitable due to their limitations of heat dissipation, larger wall thickness, and the skin effect. To overcome these problems, the resistive cylinder is replaced by thick rods or strips, and the structure resembles the rotor construction of double squirrel-cage induction motor. The equivalent circuit for squirrel-cage construction is different, and complex. The shunts show peaky response for step input, and a compensating network has to be designed to get optimum response . In Figure. VI.51, the step response (Figure . VI.51a) and frequency response (Figure. VI.51b) characteristics are given. Rise times

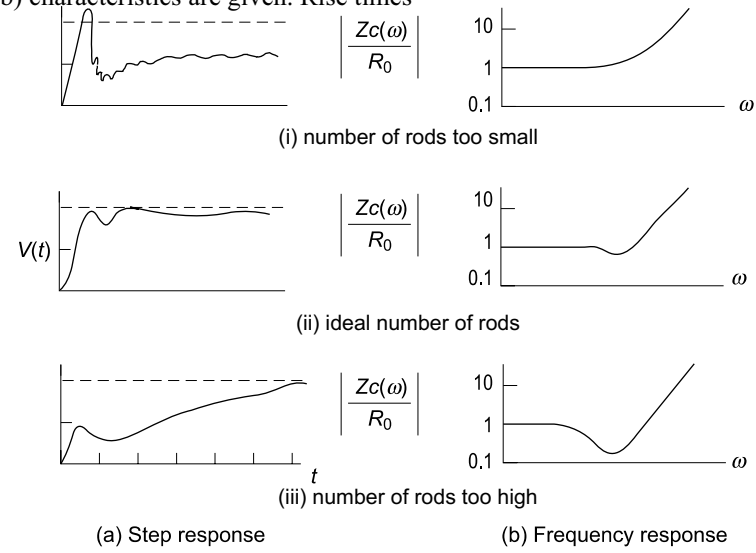

Figure. VI.**51** *Response of squirrel cage shunt for different number of rods*

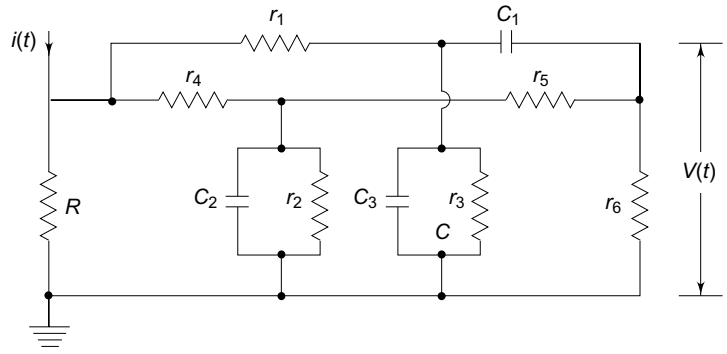

R—Shunt resistance

r_1–r_6—Resistance and capacitors in compensating double T network and C_1–C_3

Figure. VI.**52** *Compensating network for squirrel cage shunts*

of better than 8 ns with bandwidth more than 400 MHz were obtained for this type of shunts. A typical *R-C* compensat ing network used for these shunts is shown in Figure. VI.52.

(iv) *Material and Technical Data for the Current Shunts* The important factor for the materials of the shunts is the varia tion of the resistivity of the material with temperature. In Table VI.11 physical properties of some materials with tempera low ture coefficient, which can be used for shunt construction are given.

The importance of the skin effect has been pointed out in the coaxial shunt design. The skin depth d for a material of conduc tivity σ at any frequency f is given by

$$d = \frac{1}{\sqrt{\pi f \mu \sigma}} \qquad \text{(VI. 41)}$$

Skin depth, d, is defined as the distance or depth from the surface at which the magnetic field intensity is reduced to '1/e' (e = 2.718 ...) of the surface value for a given frequency f. Materials of low conductivity σ (high resistivity materials) have large skin depth and hence exhibit less skin effect.

It may be stated that low ohmic shunts of coaxial type or squirrel cage type construction permit measurements of high currents with response times less than 10 ns.

Table VI.11 *Properties of resistive materials*

Property	*Material*				
	Constantan	*Manganin*	*Nichrome*	*German silver*	*Ferro-alloy*
Resistivity ρ at 20°C (Ω-m)	0.49×10^{-6}	0.43×10^{-6}	1.33×10^{-6}	0.23×10^{-6}	0.49×10^{-6}
Temperature coefficient per °C (10^{-6})	30	20	20	≈ 50	40
Density at 20°C kg/litre	8.9	8.4	8.1	≈ VI.58	8.
Specific heat kilo calories/ kg°C	0.098	0.097	0.11	≈ 0.1	≈ 0.1

VI.3.4 Measurement of High Impulse Currents: Other Techniques (Rogowski Coils Current Transformers and Magnetic Links)

(a) Rogowski Coils If a coil is placed surrounding a current carrying conductor, the voltage signal induced in the coil is $v_i(t) = M\, dI(t)/dt$ where M is the mutual inductance between the conductor and the coil, and $I(t)$ is the current flowing in the conductor. Usually, the coil is wound on a nonmagnetic former of toroidal shape and

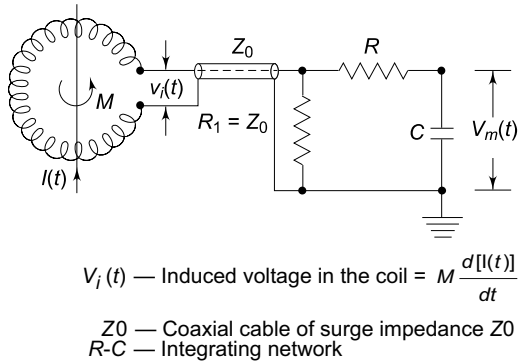

Figure. VI.53 *Rogowski coil for high impulse current measurements*

is coaxi ally placed surrounding the current-carrying conductor. The number of turns on the coil is chosen to be large, to get enough signal induced. The coil is wound cross-wise to reduce the leak age inductance. Usually, an integrating circuit (see Figure. VI.53) is employed to get the output signal voltage proportional to the be measured. The output voltage is given by current to

$$V_m(t) = \frac{1}{CR}\int_0^t v_i(t) = \frac{M}{CR} I(t) \qquad \text{(VI. 42)}$$

Rogowski coils with electronic or active integrator circuits have large bandwidths (about 100 MHz). At frequencies greater than 100 MHz the response is affected by the skin effect, the capacitance distributed per unit length along the coil, and due to the electromagnetic interferences. However, miniature probes having nanosecond response time are made using very few turns of copper strips for UHF measurements.

(b) Magnetic Links Magnetic links are short high retentivity steel strips arranged on a circular wheel or drum. These strips have the property that the remanent magnetism for a current pulse of 0.5/5 μs is same as that caused by a dc current of the same value. Hence, these can be used for measurement of peak value of impulse currents. The strips will be kept at a known distance from the current carrying conductor and parallel to it. The remanent magnetism is then measured in the laboratory from which the peak value of the current can be estimated. These are useful for field measurements, mainly for estimating the lightning currents on the transmission lines and towers. By using a number of links, accurate measurement of the peak value, polarity, and the percentage oscillations in lightning currents can be made.

The rate of rise of impulse currents can be measured using the magnetic links by placing them within the magnetic field of inductors which carry the main current to be measured. The inductors are connected in series with different values of resistances giving different time constants. Hence the magnetic links record the peak currents

whose values are different . Knowing the time constants of the resistance – inductance combination , the mean rate of rise of current in the main circuit is estimated.

VI.3.5 Other Techniques for Impulse Current Measurements

(i) *Hall Generators* Hall generators described earlier can be used for ac and im pulse current measurements also. The bandwidth of such devices was found to be about 50 MHz with suitable compensating devices and feedback. The saturation effect in magnetic core can be minimized, and these devices are successfully used for post arc and plasma current measurements.

(ii) *Faraday Generator or Ammeter* When a linearly polari zed light beam passes through a transparent crystal in the presence of a magnetic field, the plane or polarization of the light beam undergoes rotation.

The angle of rotation α is given by

$$\alpha = VBl \qquad \text{(VI. 43)}$$

where, V = a constant of the crystal which depends on the wavelength of the light,
B = magnetic flux density, and
l = length of the crystal.

To measure the waveform of a large current in an EHV system an arrangement shown in Figure. VI.54 may be employed. A beam of light from a stabilized light source

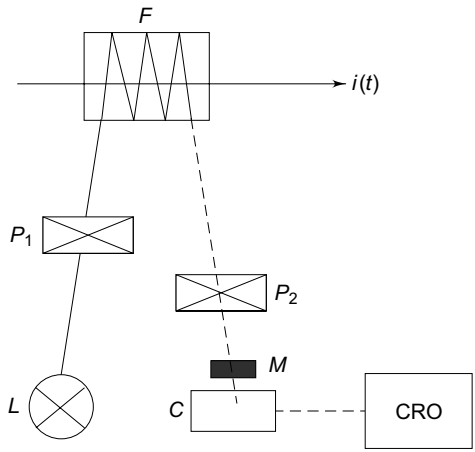

L — Light source
C — Photo-multiplier
CRO — Recording oscillograph
M — Filter
F — Crystal
P_1 — Polarizer
P_2 — Analyser

Figure. VI.**54** *Magneto-optical method of measuring impulse currents*

is passed through a polarizer P_1 to fall on a crystal F placed parallel to the magnetic field produced by the current I. The light beam undergoes rotation of its plane of polarization. After passing through the analyser, the beam is focused on a photomultiplier, the output of which is fed to a CRO. The output beam is filtered through a filter M, which allows only the monochromatic light. The relation between the oscillograph display and the current to be measured are complex but can be determined. The advantages of this method are that (i) there is no electric connection between the source and the device, (ii) no thermal problems even for large currents of several kiloamperes, and (iii) as the signal transmission is through an optical system, no insulation problems or difficulties arise for EHV systems. However, this device does not operate for dc currents.

(iii) *Current Transformers* Measurement of high frequency currents such as fault currents in power systems, switching current transients and impulse currents during impulse testing of transformers can be measured using current transformers with an air core or a ferrite core. The transformer will have a torroidal core with central bar primary or wound primary with single turn.

The secondary side of the current with N_1 primary and N_2 secondary turns is given by (with perfect ampere turn balance)

$$I_2(t) = \frac{N_1 I(t)}{N_2}$$

Usually, the secondary winding is terminated by a resistance R_2 and a CRO will be connected through a cable of surge impedance Z terminated by a resistance R equal to the surge impedance. The current I_3 through the cable and terminating resistance R is

$$I_3(t) = \frac{R_2}{R + R_2 + Z_0} I_2(t)$$

and the voltage across the resistance

$$R = V(t) = I_3(t)\, R = \left[\frac{RR_2}{R + R_2 + Z_0}\right] I_2(t)$$

$$\therefore \quad I_2(t) = \frac{N_1}{N_2} \frac{RR_2}{R + R_2 + Z_0} I_1(t)$$

Usually, R_2 is also made equal to Z_0 to avoid reflections in case of impulse currents.

The unit is usually made into an epoxy resin cast unit with primary and secondary terminals brought out on either side of the unit.

The advantages of the current transformer are electrical isolation and wide measuring range with tapped turns on secondary side from 10 A to 10 kA or more. The main limitations are limited bandwidth of less than 1 MHz, and distortion in the waveform.

Current Transformers Current transformers with either air cores or ferrite cores are used for measurement of high-impulse currents. Usually, they have a torroidal core with a central hole through which the primary or conductor in which the current is to measured will be inserted. The core can be of a split-type also. The secondary winding consists of a few turns (up to 500). The bandwidth of such transformers may be typically 40 Hz to 1 MHz for a peak current of 1000 A with an output voltage across the secondary between 0.5 to 5 V when terminated by 50 Ω. The typical insulation level provided between the primary and secondary windings is about 4 kV. Rf current transformers are typically designed for a peak current of 50 kA with a maximum rms current of 200 A. The rise time is about 0.1 μs and bandwidth 4 MHz with an output of 0.01 V/A with 50 Ω termination. The CTS have typical error of less than 2% with waveform distortion of less than 5% for standard impulse current waves. The VA rating can be from 0.5 VA to as high as 5 kVA. The bandwidth reduces as the VA ratings increase.

VI.4 CATHODE-RAY OSCILLOGRAPHS FOR IMPULSE VOLTAGE AND CURRENT MEASUREMENTS

When waveforms of rapidly varying signals (voltages or currents) have to be measured or recorded, certain difficulties arise. The peak values of the signals in high voltage measurements are too large, may be several kilovolts or kiloamperes. Therefore, direct measurement is not possible. The magnitudes of these signals are scaled down by voltage dividers or shunts to smaller voltage signals. The reduced signal $V_m(t)$ is normally proportional to the measured quantity. The procedure of transmitting the signal and displaying or recording it is very important. The associated electromagnetic fields with rapidly changing signals induce disturbing voltages, which have to be avoided. The problems associated in the above procedure are discussed in this section.

VI.4.1 Cathode-Ray Oscillographs for Impulse Measurements

Modern oscillographs are sealed tube, hot cathode oscilloscopes with photographic arrangement for recording the waveforms. The cathode ray oscilloscope for impulse work normally has input vol tage range from 5 m V/cm to about 20 V/cm. In addition, there are probes and attenuators to handle signals up to 600 V (peak to peak). The bandwidth and rise time of the oscilloscope should be adequate. Rise times of 5 ns and bandwidth as high as 500 MHz may be necessary.

Sometimes high-voltage surges test oscilloscopes do not have vertical amplifier and directly require an input voltage of 10 V. They can take a maximum signal of about 100 V (peak to peak) but require suitable attenuators for large signals.

Oscilloscopes are fitted with good cameras for recording purposes. Tektronix model 7094 is fitted with a lens of 1 : 1.2 polaroid camera which uses 10,000 ASA film which possesses a writing speed of 9 cm/ns.

With rapidly changing signals, it is necessary to initiate or start the oscilloscope time base before the signal reaches the oscilloscope deflecting plates, otherwise a portion of the signal may be missed. Such measurements require an accurate initiation

of the horizontal time base and is known as *triggering*. Oscilloscopes are normally provided with both internal and external triggering facility. When external triggering is used, as with recording of impulses, the signal is directly fed to actuate the time base and then applied to the vertical or *Y* deflecting plates through a delay line. The delay is usually 0.1 to 0.5 μs. The delay is obtained by the following:

1. A long interconnecting coaxial cable 20 to 50 m long. The required triggering is obtained from an antenna whose induced voltage is applied to the external trigger terminal.
2. The measuring signal is transmitted to the CRO by a normal coaxial cable. The delay is obtained by an externally connected coaxial long cable to give the necessary delay. This arrangement is shown in Figure. VI.55.
3. The impulse generator and the time base of the CRO are triggered from an electronic tripping device. A first pulse from the device starts the CRO time base and after a predetermined time a second pulse triggers the impulse generator.

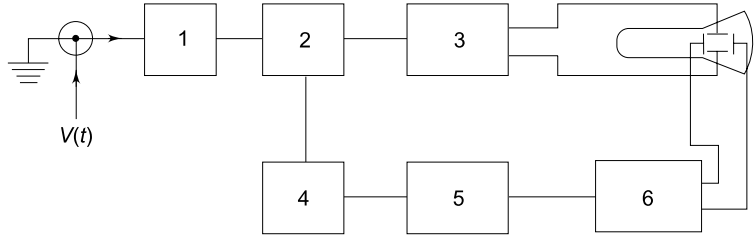

1. Plug-in amplifier
2. Y amplifier
3. Internal delay line
4. Trigger amplifier
5. Sweep generator
6. X amplifier

Figure. VI.55 *Simplified block diagram of surge test oscilloscopes*

VI.4.2 Instrument Leads and Arrangement of Test Circuits

It is essential that leads, layout, and connections from the signal sources to the CRO are to be arranged such that the induced voltages and stray pick-ups due to electromagnetic interference are avoided. For slowly varying signals, the connecting cables behave as either capacitive or inductive depending on the load a the end of the cable. For fast-rising signals, however, the cables have to be accounted as transmission lines with distributed parameters. A travelling wave or signal entering such a cable encounters the surge impedance of the cable. To avoid unnecessary reflections at the cable ends, it has to be terminated properly by connecting a resistance equal to the surge impedance of the cable. In cables, the signal travels with a velocity less than that of light which is given by

$$v = \frac{C}{\sqrt{\varepsilon_r \mu_r}}$$

where $C = 3 \times 10^8$ m/s and ε_r and μ_r are the relative permittivity and relative permeability respectively of the cable meateials. Therefore, the cable introduces a finite propagation time

$$t = \frac{1}{v} \times \text{length of the cable}$$

Measuring devices such as oscilloscopes have finite input impedance, usually about 1 to 10 MΩ resistance in parallel with a 10 to 50 pF capacitance. This impedance at high frequencies (f = 100 MHz) is about 80 Ω and thus acts as a load at the end of a surge cable. This load attenuates the signal at the CRO end.

Cables at high frequencies are not lossless transmission lines. Because of the ohmic resistance loss in the conductor and the dielectric loss in the cable material, they introduce attenuation and distortion to the signal. Cable distortion has to be eliminated as far as possible. Cable shields also generate noise, voltages due to ground loop currents and due to the electromagnetic coupling from other

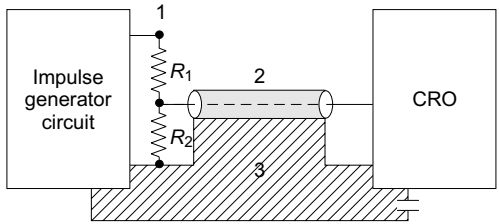

1. Potential divider 2. Coaxial signal cable 3. Ground loop

Figure. VI.56 *Ground loops in impulse measuring systems*

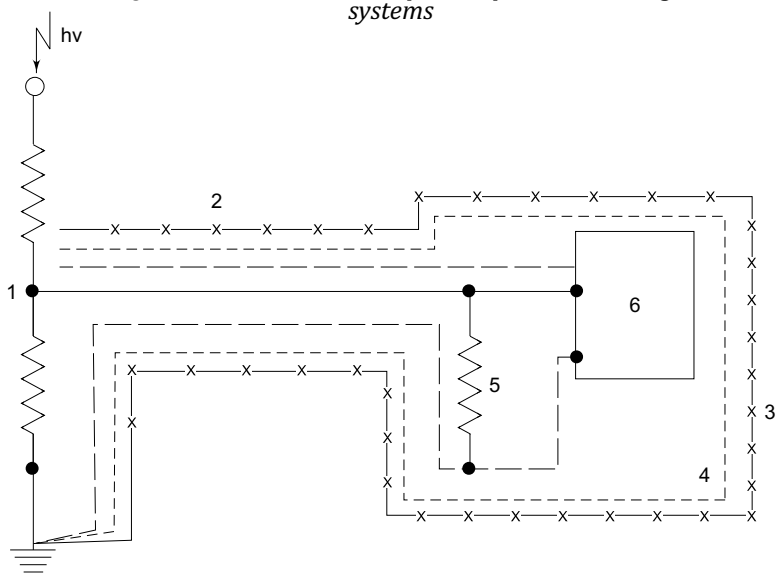

1. Potential divider
2. Triple shielded cable
3. Outer shield enclosure
4. Inner shielded enclosure
5. Terminating impedance
6. CRO

Figure. VI.57 *Impulse measurements using multiple shield enclosures and signal cable*

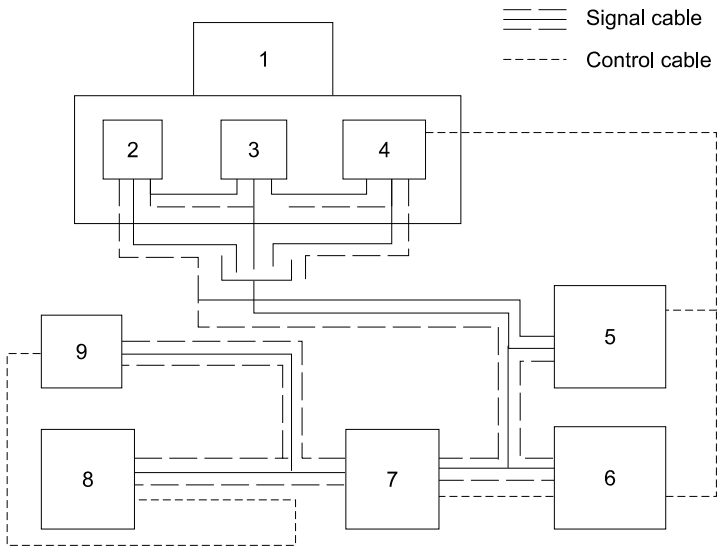

Figure. VI.58 *Layout of an impulse testing laboratory with control and signal cables*

conductors . In Figure . VI.56, the ground loop currents and their path is indicated. To eliminate these noise voltage multiple shielding arrangement as shown in Figure. VI.57 may have to be used.

Another important factor is the layout of power and signal cables in the impulse testing laboratories. Power and interconnecting cables should not be laid in a zig-zag manner and should not be cross-connected. All power cables and control cables have to be arranged through earthed and shielded conduits. A typical schematic layout is shown in Figure. VI.58. The arrangement should provide for branched writing from the cable tree and should not form loops. Where environmental conditions are so severe that true signal cannot be obtained with all countermeasures, electro-optical techniques for transmitting signal pulses may have to be used.

VI.4.3 The Impulse Test and Analysing System

It is extremely difficult to control and adjust the impulse wave shapes for different load conditions as in the case of large capacitive loads, very low inductors or coils, transformers with high inductance and capacitance. Further, whenever the tests require comparison of test records, the resolution and uncertainty in measurements will affect the test results and the recorders should be capable of detecting even small deviations or changes. Stringent conditions are imposed on the measuring systems, such as in the case of calibrations, diagnostic procedures, and transfer function analysis (e.g., as in transformer testing and fault diagnostics).

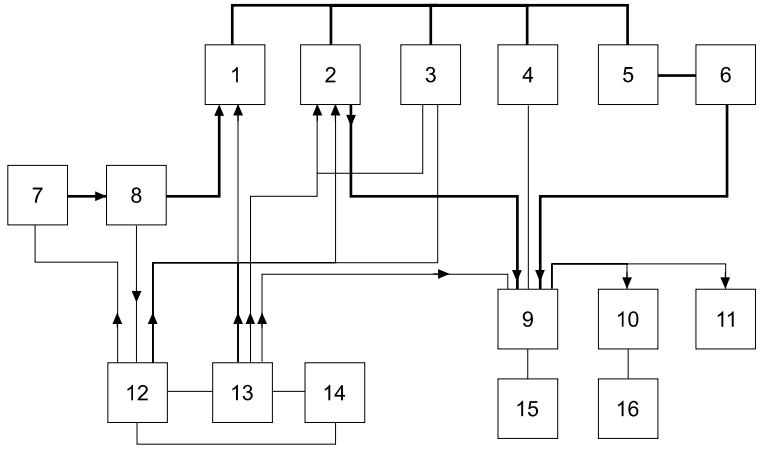

1. Impulse voltage generator
2. Chopping gap
3. Sphere gap
4. Impulse voltage divider
5. Test object
6. Shunt
VI. Solid state controller
8. Charging rectifier
9. Impulse oscilloscope
10. Impulse peak voltmeter
11. Time-to-breakdown meter
12. Control desk, control console
13. Trigatron trigger device
14. Program controller
15. Photographic equipment
16. Digital printer

Figure. VI.**59** *Block diagram of impulse voltage test system*

A modern impulse test measuring and analysing system consists of a multi-channel digital control and recording systems with 32 bit microprocessor controller recorder and analyser (Plate 6). The inputs from the measuring voltage dividers, current shunts, etc. are fed through a cable transmission system and *A-D* converter. The control signals are fed to the charging unit, the trigger gaps of impulse generator, to chopping gaps, etc. Preset operations can be performed from the controller. Variable memory depths up to or more than 128 kilo data points are available. Common impulse shapes can be analysed automatically for such computations, such as (i) getting difference function of two waves, (ii) the Fourier analysis and FFT depicting the original wave in time domain and its Fourier transform in frequency domain, (iii) Transfer function, i.e. the ratio of neutral current to test voltage ratio in frequency domain, and (iv) the coherence function such as comparison of impulse wave at reduced test level and at full voltage level, etc. The software is normally available in common PC operating systems such as MS WINDOWS. Typical schematic diagram of a test and analysing system is shown in Figure. VI.59.

This block diagram is provided for better comprehension of the system layout. All essential components are contained therein. Some components may be omitted, depending on the specific application. The connections indicated in the drawing are of a functional nature and do not necessarily correspond with system wiring.

KEY TERMS

- High-voltage and Current Measurements
- dc Voltage Measurements
- Potential Dividers
- Generating Voltmeters
- Electric Field Meters
- Measurement of Ripple Voltage
- ac Voltage Measurements
- Series Impedance Meters
- Potential Dividers
- CVTS
- Electrostatic Meters
- Peak Voltmeters
- Sphere Gap Measurements
- Impulse Voltage Measurements
- Potential Dividers
- Response Characteristics
- LV Arms
- Peak Voltmeters
- CRO
- Impulse Measuring Systems
- Impulse Current Measurements
- Shunts
- High Current Transformers

WORKED EXAMPLES

Example VI.1 *A generating voltmeter has to be designed so that it can have a range from 20 to 200 kV dc If the indicating meter reads a minimum current of 2μA and maximum current of 25 μA, what should the capacitance of the generating voltmeter be?*

Solution Assume that the driving motor has a synchronous speed of 1500 rpm.

$$I_{\text{rms}} = \frac{VC_m}{\sqrt{2}}\omega$$

where, V = applied voltage,
C_m = capacitance of the meter, and
ω = angular speed of the drive

Substituting, $2 \times 10^{-6} = \frac{20 \times 10^3 \times C_m}{\sqrt{2}} \times \frac{1500}{60} \times 2\pi$

$\therefore \quad C_m = 0.9$ p.F

At 200 kV, $I_{\text{rms}} = \frac{200 \times 10^3 \times 0.9 \times 10^{-12} \times 1500}{\sqrt{2} \times 60} 2\pi = 20.0\ \mu\text{A}$

The capacitance of the meter should be 0.9 pF. The meter will indicate 20 kV at a current 2 μA and 200 kV at a current of 20 μA.

Example VI.2 *Design a peak reading voltmeter along with a suitable micro-ammeter such that it will be able to read voltages, up to 100 kV (peak). The capacitance potential divider available is of the ratio 1000 : 1.*

Solution Let the peak reading voltmeter be of the Haefely type shown in Figure. VI.18b.

Let the micro-ammeter have the range 0–10 μA.

The voltage available at the C_2 arm = $100 \times 10^3 \times \frac{1}{1000} = 100$ V (peak)

The series resistance R in series with the micro-ammeter

$$= \frac{100}{10 \times 10^{-6}} = 10^7 \Omega$$

$$C_S R = 1 \text{ to } 10 \text{ s}$$

Taking the higher value of 10 s, $C_S = \frac{10}{10^7} = 1\ \mu\text{F}$

The values of C_S and R are 1 μF and $10^7 \Omega$.

Example VI.3 *Calculate the correction factors for atmospheric conditions, if the laboratory temperature is 37°C, the atmospheric pressure is 750 mmHg, and the wet bulb temperature is 27°C.*

Solution

Air density factor, $d = \frac{p}{760} \frac{293}{(273+t)}$

At $t = 37°C$ $d = \frac{750}{760} \frac{263}{310} = 0.9327$

From Table VI.6, air density correction factor $K = 0.9362$. From Figure. 10.1, the absolute humidity (by extrapolation) corresponding to the given temperature is 18 g/m^3. From Figure. 10.2, the humidity correction factor for 50 H z (curve(*Note: a* No humidity correction is needed for sphere gaps.)) is 0.925.

Example VI.4 *A resistance divider of 1400 kV (impulse) has a high-voltage arm of 16 kilo-ohms and a low-voltage arm consisting 16 members of 250 ohms, 2 watt resistors in parallel. The divider is connected to a CRO through a cable of surge impedance 75 ohms and is termi nated at the other end through a 75 ohm resistor. Calculate the exact divider ratio*

Solution hv arm resistance, $R_1 = 16{,}000$ ohms

lv arm resistance, $R_2 = \frac{250}{16}$ ohms

Terminating resistance, $R'_2 = 75$ ohms
hence, the divider ratio, $a = 1 + R_1/R_2 + R_1/R'_2$
$= 1 + 16{,}000 \times 16/250 + 16{,}000/75$
$= 1 + 1024 + 213.3 = 1238.3$

Example V.5 *The HV arm of an R-C, divider has 15 numbers of 120 ohms resistors with a 20 pF capacitor to ground from each of the junction points. The LV arm resistance is 5 ohms. Determine the capacitance needed in the LV arm for correct compensation.*

Solution

Ground capacitance per unit = $C'_g = 20$ pF
Effective ground capacitance = $C_e = (2/3)\ C_g$
$= 2/3\ (15 \times 20)$ (Refer Figure. VI.31)
$= 200$ pF

This capacitance is assumed to be between the centre tap of the hv arm and the ground as shown in Figs VI.31 and VI.29.

Here, $R_1/2 = 15 \times 120/2 = 900$ ohms
$R_2 = 5$ ohms

Then, the effective time constant of the divider,

$= (R_1/2 \cdot (2/3)\ C_g) = R_1\ C_e/2$
$= [(900 \times 200) \times 10^{-12}]/2 = 90$ ns

Making the LV arm time constant to be the same as that of the HV arm; the capacitance required for compensation is calculated as

$R_2C_2 = 90$ ns
$\therefore \quad C_2 = 90/5$ nF $= 18 \times 10^{-9}$ F

Example V.6 *A coaxial shunt is to be designed to measure an impulse current of 50 kA. If the bandwidth of the shunt is to be at least 10 MHz and if the voltage drop across the shunt should not exceed 50 V, find the ohmic value of the shunt and its dimensions.*

Solution

Resistance of the shunt (max) $R = \dfrac{50}{50 \times 10^2} = 1$ mΩ

Taking the simplified equivalent circuit of the shunt as given in Figure. VI.49b

Bandwidth $B = \dfrac{1.46R}{L_0} = 10$ MHz

or, $$L_0 = \frac{1.46R}{B} = \frac{1.46\times10^{-2}}{10\times10^{6}}$$

$$= 1.46\times10^{-10}\ \text{H} \quad \text{or} \quad 0.146\ \text{nH}$$

d, the thickness of the cylindrical resistive tube is taken from the consideration of the bandwidth as

$$B = \frac{1.46\rho}{\mu d^2}$$

where, r = resistivity of the material,

$\mu = \mu_0 = 4\pi\times10^{-7}$ H/m, and

d = thickness of the tube in metres

Let r = radius of the resistive tube,

l = length of the resistive tube,

d = thickness of the resistive tube, and

ρ = resistivity of the tube material.

Then the bandwidth $B = \frac{1.46\rho}{\mu d^2}$

where, $\mu = \mu_0\mu_r \approx \mu_0$

Substituting $B = 10^7$ Hz

$\rho = 30\times10^{-8}\ \Omega$m

$\mu_0 = 4\pi\times10^{-7}$

$$d = \frac{1.46\rho}{\mu B} = \sqrt{\frac{1.46\times30\times10^{-8}}{4\pi\times10^{-7}\times10^{7}}}$$

$$= 0.187\times10^{-3}\ \text{m} = 0.187\ \text{mm}$$

Let the length l be taken as 10 cm or 10^{-1} m;

then, $$R = \frac{\rho l}{A} = \frac{\rho l}{(2\pi r)d} = 1\ m\Omega$$

or, $$r = \frac{\rho l}{2\pi R d} = \frac{30\times10^{-8}\times10^{-1}}{2\pi\times10^{-3}\times0.187\times10^{-3}}$$

$$= 25.5\times10^{-3}\ \text{m or } 25.5\ \text{mm}.$$

For the return conductor the outer tube can be taken to have a length = 10 cm, radius = 30 mm, and thickness = 1 mm, and it can be made from copper or brass.

Example V.7 *A Rogowski coil is to be designed to measure impulse currents of 10 kA having a rate of change of current of 10^{11} A/s. The current is read by a TVM as a potential drop across the integrating circuit connected to the secondary. Estimate the values of mutual inductance, resistance, and capacitance to be connected, if the meter reading is to be 10 V for full-scale deflection.*

Solution

$$V_m(t) = \frac{M}{CR} I(t) \text{ for } \frac{1}{CR} << \omega \text{ (Eq. VI.42),}$$

taking the peak values

$$\frac{M}{CR} = \frac{V_m(t)}{I(t)} = \frac{10}{10^4} = 10^{-3}$$

The time interval of the change of current assuming sinusoidal variation is

$$\frac{10^4}{10^{11}} = 10^{-7} \text{ s} = \frac{1}{4} \text{ of a cycle}$$

$$\therefore \quad \text{frequency} = \frac{10^7}{4} \text{ Hz}$$

and,

$$\omega = 2\pi f = \frac{\pi}{2} \times 10^7$$

Taking

$$\frac{1}{CR} = \frac{\omega}{10\pi} = \frac{10^6}{2}$$

$$CR = \frac{2}{10^6}$$

$$M = 10^{-3}\, CR = 10^{-3}\, \frac{2}{10^6}$$

$$= 2 \times 10^{-9} \text{ H or 2 nH.}$$

Taking

$$R = 2 \times 10^3\ \Omega,$$

$$C = \frac{CR}{R} = 2 \times 10^{-6}/2 \times 10^3 = 10^{-9} \text{ F or 1000 pF}$$

(It should be noted that for a given frequency, $X_c << R$; otherwise the low frequency response will be poor. Here, X_c at $f = 10^7/4$ is 60 Ω only.)

Example V.8 *If the coil in Example VI.7 is to be used for measuring current of 8/20 impulse μs wave and of the same peak current, what should be the R-C integrating circuit*

Solution In this case, the lowest frequency to be read should be at least $\frac{1}{3}$ to $\frac{1}{5}$ of the lowest frequency component present in the waveform.

The frequency corresponding to the tail time is

$$\frac{1}{20\times10^{-6}} = 50 \text{ kHz}$$

$\therefore$ lowest frequency to be read is

$$50 \times \frac{1}{5} = 10 \text{ kHz} \quad \therefore \quad \omega = 2\pi \times 10^4 \text{ radians}$$

Taking $$\frac{1}{CR} = \frac{\omega}{10\pi}$$

$$= \frac{2\pi\times10^4}{10\pi} = 2\times10^3$$

$$M = 10^{-3} \times \frac{1}{2\times10^3} = 0.5 \times 10^{-6} \text{ H, or } 0.5\ \mu\text{H}$$

Taking $R = 2 \times 10^3\ \Omega$ as before,

$$C = \frac{0.5\times10^{-3}}{2\times10^3}$$

$$= 0.25\ \mu\text{F}$$

(X_c at a frequency of 10 kHz is about 60 Ω which is very much less than R.).

MULTIPLE-CHOICE QUESTIONS

1. A generating voltmeter is used to measure
   (a) impulse voltages (b) ac voltages
   (c) dc voltages (d) high-frequency ac voltages
2. A series capacitance voltmeter can measure
   (a) dc voltages (b) ac voltage (rms value)
   (c) ac voltage (peak value) (d) impulse voltages
3. CVT when tuned does not have
   (a) ratio error
   (b) phase angle error
   (c) both ratio and phase angle errors
   (d) temperature error
4. Electrostatic voltmeters can measure
   (a) only dc voltage
   (b) both dc and ac voltages up to high frequency
   (c) impulse voltages
   (d) ac, dc and impulse voltages

5. Sphere gaps are used to measure
   (a) dc voltages
   (b) ac peak voltages
   (c) dc, ac peak and impulse voltages
   (d) only dc and ac peak voltages.
6. Sphere gap measurement is linear and valid for gap spacing less than or equal to
   (a) radius of the sphere
   (b) diameter of the sphere
   (c) half the radius of sphere
   (d) two times diameter of the sphere
7. The main factors that affect the sparkover voltage of sphere gap are
   (a) humidity and waveform
   (b) nearby earthed objects and atmospheric conditions
   (c) diameter of the sphere
   (d) gap spacing, diameter and waveform
8. For an *RC* divider to be compensated, the condition is
   (a) $R_1 C_1 = R_2 C_2$ (b) $R_1 C_2 = R_2 C_1$
   (c) $R_1 C_1 = R_2 C_g$ (d) $(R_1 + R_2)(C_1 + C_2) < 1$ μs.
9. Compensated capacitance divider for high voltages (1 MV) generally has a bandwidth of
   (a) 10 MHz (b) 1 MHz
   (c) 100 MHz (d) 1000 MHz.
10. In a pure capacitance divider, the ground capacitance C_g is represented by adding additional capacitance from central point of hv capacitor to the ground and is equal to
   (a) C_g (b) $C_g/3$
   (c) $2\,C_g/3$ (d) $C_g/2$.
11. For an optimally damped *R*-*C* divider, the damping resistance R_1 connected in hv arm is equal to (L = high voltage lead inductance, and C_g = equivalent ground capacitance)
   (a) $4\sqrt{L/C_g}$ (b) $2\sqrt{L/C_g}$
   (c) $\sqrt{L/C_g}$ (d) $\frac{1}{2}\sqrt{L/C_g}$
12. The surge impedance of a measuring cable with its resistance neglected, C_g is (if L and C are inductance and capacitance of cable per unit lamp
   (a) $\sqrt{L/C}$ (b) $2\sqrt{L/C}$
   (c) $2\sqrt{LC}$ (d) $\sqrt{C/L}$

13. Hall generators are normally used to measure
    (a) impulse voltages (b) unidirectional impulse currents
    (c) any type of impulse currents (d) large ac currents
14. For measuring high impulse currents, the best type of shunt is
    (a) squirrel cage (b) bifilar strip
    (c) disc (d) coaxial tubular (Park type)
15. The skin depth for resistance material used for impulse shunts is given by
    (a) $(\pi f \mu\sigma)^{1/2}$ (b) $(\pi f \mu\sigma)^{-1/2}$
    (c) $2\sqrt{\pi f \mu\sigma}$ (d) $0.5\ (\pi f \mu\sigma)^{-1/2}$
16. Rogowski coils and high frequency current transformers have bandwidth of about
    (a) 100 KHz (b) 10 MHz
    (c) 1.0 MHz (d) 1100 Hz
17. An *R*-*C* voltage divider has hv an arm capacitance, C = 600 pF, resistance = 400 Ω and equivalent ground capacitance C_g = 240 pF. The effective time constant of the divider in nanoseconds is
    (a) 108 (b) 90
    (c) 69 (d) 32.
18. Shunts used for measuring impulse currents, in the range 10 kA–50 kA will have a resistance of the order of
    (a) 10 to 25 mΩ (b) 0.1 to 1 m Ω
    (c) 100 to 500 mΩ (d) 0.1 to 1.0 Ω.
19. The type of measuring device preferred for measurement of impulse currents of short duration is
    (a) Park's tubular shunt (b) current transformer
    (c) Hall generator (d) Faraday ammeter.
20. Secondary arm of a resistance impulse voltage divider consists of
    (a) a few resistors connected in series
    (b) a few resistors connected in parallel
    (c) a single wire wound resistor of very high power rating
    (d) a linear resistor in parallel with a non-linear resistor of high power rating
21. The resistivity of the materials used as shunts for high currents will be in the range (Ω - cm)
    (a) 1 to 5×10^{-5} (b) $\approx 10^{-3}$
    (c) 0.5×10^{-6} to 0.5×10^{-7} (d) 0.2×10^{-6} to 1.5×10^{-6}
22. In high frequency and *RF* current transformers, the secondary winding is terminated with a resistance of
    (a) 1 Ω (b) 10 Ω
    (c) 1 kΩ (d) 50 Ω or 75 Ω

23. To measure a high-voltage of peak value abut 150 kV, the suitable sphere gap would be (diameter in cm)
    (a) 5 or 10 (b) 10 or 15
    (c) 15 or 25 (d) 50 or 100
24. With a series capacitor voltmeter, a large error will result in when the
    (a) capacitance is larger
    (b) meter used is an electromechanical meter
    (c) voltage to be measured is non-sinusoidal and contains harmonics
    (d) none above
25. Sphere-gap measurement of peak voltage has an error of
    (a) $< \pm 1\%$ (b) 5 to 10%
    (c) 3 to 5% (d) $< 3\%$

Answers to Multiple-Choice Questions

1. (c)	2. (c)	3. (b)	4. (b)	5. (c)	6. (a)
VI. (b)	8. (a)	9. (c)	10. (c)	11. (a)	12. (a)
13. (b)	14. (d)	15. (a)	16. (b)	1VI. (d)	18. (a)
19. (a)	20. (b)	21. (d)	22. (d)	23. (c)	24. (c)
25. (d)					

REVIEW QUESTIONS

1. Discuss the different methods of measuring high dc voltages. What are the limitations in each method?
2. Describe the generating voltmeter used for measuring high dc voltages. How does it compare with a potential divider for measuring high dc voltages?
3. Compare the relative advantages and disadvantages of using a series resistance microammeter and a potential divider with an electrostatic voltmeter for measuring high dc voltages?
4. Why are capacitance voltage dividers preferred for high ac voltage measurements?
5. What is capacitance voltage transformer? Explain with phasor diagram how a tuned capacitance voltage transformer can be used for voltage measurements in power systems.
6. Explain the principle and construction of an electrostatic voltmeter for very high voltages. What are its merits and demerits for high-voltage ac measurements?
VI. Give the basic circuit for measuring the peak voltage of (a) ac voltage, and (b) impulse voltage. What is the difference in measurement technique in the above two cases?
8. Explain how a sphere gap can be used to measure the peak value of voltages. What are the parameters and factors that influence such voltage measurement?

9. Compare the use of uniform field electrode spark gap and sphere gap for measuring peak values of voltages.
10. What are the conditions to be satisfied by a potential divider to be used for impulse work?
11. Give the schematic arrangement of an impulse potential divider with an oscilloscope connected for measuring impulse voltages. Explain the arrangement used to minimize errors.
12. What is a mixed potential divider? How is it used for impulse voltage measurements?
13. Explain the different methods of high current measurements with their relative merits and demerits.
14. What are the different types of resistive shunts used for impulse current measurements? Discuss their characteristics and limitations.
15. What are the requirements of an oscillograph for impulse and high frequency measurements in high-voltage test circuits?
16. Explain the necessity of earthing and shielding arrangements in impulse measurements and in high-voltage laboratories. Give a sketch of the multiple shielding arrangements used for impulse voltage and current measurements.
17. Explain with schematic diagrams how dc current can be measured using dc current transformers.
18. How is a compensated dc potential divider used to measure the dc voltage in HVDC systems?

PROBLEMS

1. A generating voltmeter is to read 250 kV with an indicating meter having a range of (0–20) μA calibrated accordingly. Calculate the capacitance of the generating voltmeter when the driving motor rotates at a constant speed of 1500 r.p.m.
2. The effective diameter of the moving disc of an electrostatic voltmeter is 15 cm with an electrode separation of 1.5 cm. Find the weight in grams that is necessary to be added to balance the moving plate when measuring a voltage of 50 kV dc Derive the formula used. What is the force of attraction between the two plates when they are balanced?
3. A compensated resistance divider has its high-voltage arm consisting of a series of resistance whose total value is 25 kilo-ohms shunted by a capacitance of 400 pF. The LV arm has a resistance of 75 ohms. Calculate the capacitance needed for the compensation of this divider.
4. What are the usual sources of errors in measuring high impulse voltages by resistance potential dividers? How are they eliminated? An impulse resistance divider has a high-voltage arm with a 5000 ohm resistance and the LV arm with a 5 ohm resistance. If the oscilloscope is connected to the secondary arm through a cable of surge impedance 75 ohms, determine, (i) the terminating resistance, and (ii) the effective voltage ratio.

5. A mixed *R*-*C* divider has its hv arm consisting of a capacitance of 400 pF in series with a resistance of 100 ohms. The LV arm has a resistance of 0.175 ohm in series with a capacitance C_2. What should be the LV arm capacitance for correct compensation? The divider is connected to a CRO through a measuring cable of 75 ohms surge impedance. What should be the values of R_4 and C_4 (see Figure. VI.38b) in the matching im pedance? Determine the voltage ratio of the divider.
6. A bifilar strip shunt has a resistance of 100 mΩ and inductance of 0.1 μH with a parallel capacitance of 5 pF across its terminal. What will be its step response. Determine the rise time of the shunt.

VI. Determine the dimensions of a co-axial tubular shunt with nominal resistance of 1 mΩ and rise time of 10 ns. Take the resistivity of the material as 50×10^{-6} Ω-cm and length of the shunt not to exceed 15 cm.

8. A Rogowski coil is to measure 20 kA peak current with a maximum di/dt of 10^4 A/μs. A 0–10 V electronic voltmeter is connected across the integrating circuit of the coil. Estimate the mutual inductance of the coil and resistance and capacitance of the integrating circuit to be used.
9. An electrostatic voltmeter has an effective plate diameter of 50 cm with a gap separation of 30 cm. Find the force between the plates when measuring a dc voltage of 100 kV. What is the maximum voltage that can be measured if the electric field E is to be not more than 5 kV/cm.
10. A co-axial shunt has the following dimensions length = 10 cm, radius of resistive tube 2.5 cm, thickness = 0.2 mm and ρ = resisitivity = 50×10^{-6} Ω cm. Determine the resistance, inductance and band width of the shunt. What will be the voltage drop across the shunt if 10 kA peak current passes through it.

Answers to Problems

1. 0.72 pF
2. 88.57 g
3. 0.133 μF
4. R_3 = 70 ohms, R_4 = 75 ohms, Ratio = 1067
5. C_2 = 0.228 μF, C_4 = 533.3 pF, R_4 = 75 ohms
6. 0.02 ns
7. Radius of resistive tube = 2.54 cm
8. M = 0.22 μH, R = 10 kΩ, C = 4 nF
9. 15.02 g *wt*, 150 kV
10. R = 1.6 mΩ L = 0.16 μΩ, Band width = 14.5 MHz, V = 16 V

REFERENCES

REFERENCES

1. Anis, H., Trinh, N.G., and D. Train. «Generation of switching impulse using high voltage testing transformers.» «IEEE Transactions», PAS-94: 187, 1975.
2. Asner, A. «Equivalent circuit of the leads in high voltage measuring technique, particularly for measuring fast impulse voltages.» «Bulletin SEV», 52: 192–203, 1961.
3. Ayrton, H. «The Electric Arc», the Electrician series. New York: D. Van Nostrand Company, Inc., 1902, p. 120.
4. Baatz, H. «Overvoltages in Power Supply Networks». Springer-Verlag, Berlin, 1956. [In German.]
5. Becker, R. «Electromagnetic Fields and Interactions». New York: Dover Publications, 1964.
6. Bellaschi, P.L., and L.B. Rademacher. «Dielectric strength of station and line insulation to switching surges.» «AIEE Transactions», 65: 1047, 1946.
7. Bewley, L.V. «Traveling Waves on Transmission Systems». New York: Dover Publications, 1963.
8. Bleakney, W. «Physical Review», 35: 139, 1930.
9. Booker, J.R., Nichols, D.R., and W. Lazelere. «Design of a modular UHV AC outdoor test system.» «IEEE Transactions», PAS-102: 2501, 1983.
10. Boyd, H.A., Rohlfs, A.F., and L.E. Zaffanella. «Phase-to-ground and phase-to-phase switching-surge flashover of external insulation of UHV stations.» «IEEE Transactions on Power Apparatus and Systems», PAS-93(2): 518–528, 1974.
11. Burch, F.G. «On potential dividers for cathode ray oscillographs.» «Philosophical Magazine», Series 7, 13: 760, 1932.
12. Chubb, L.W., and C. Fortescue. «Calibration of the sphere gap voltmeter.» «AIEE Transactions», 32: 739, 1913.
13. CIGRE Task Force 33.03.03. «Switching impulse test procedure for phase-to-phase air insulation.» «Electra», 30: 55–69, 1973.
14. CIGRE Task Force 33.03.03. «The influence of non-standard conditions on the switching impulse strength of phase-to-phase insulation.» «Electra», 64: 211–236, 1979.
15. Cobine, J.D. «Gaseous Conductors—Theory and Engineering Applications». New York: Dover Publications Inc., 1958.
16. Compton, K.T. «Electrical discharges in gases—Part 1: Survey of fundamental processes.» «Review of Modern Physics», 2(2): 123–167, April 1930.
17. Compton, K.T., and I. Langmuir. «Review of Modern Physics», 2: 218, 1930.
18. Creed, F., and T. Collins. «The shaping circuit for high voltage impulses.» «IEEE Transactions», PAS-90: 2239, 1971.
19. Creed, F., and M.M.C. Collins. «Transient impedance of high voltage impulse generating systems.» «IEEE Transactions», PAS-89: 1387, 1970.
20. Crockcroft, J.D., and Walton, E.T.S. «Experiments with high velocity ions.» «Proceedings of the Royal Society of London, Series A», 136: 619, 1932.
21. Dawson, G.A. «A model for streamer propagation.» «Zeitschrift für Physik», 183: 159, 1965.
22. Dommel, H.W. «Digital computer solution of electromagnetic transients in single and multi-phase networks.» «IEEE Transactions on Power Apparatus and Systems», PAS-88: 388–399, April 1969.
23. Dommel, H.W., and W.S. Meyer. «Computation of electromagnetic transients.» «Proceedings of the IEEE», 62: 983–993, July 1974.

24. Elsner, R. «The measurement of fast high voltage impulse using voltage dividers.» «Archives fur Elektrotechnik», 33: 23–40, 1939.
25. Feser, K. «Transient behavior of damped capacitive voltage divider of some millions volts.» «IEEE Transactions», PAS-93: 116, 1974.
26. Freund, J.E., and R.E. Walpole. «Mathematical Statistics». Englewood Cliffs, NJ: Prentice Hall Inc., 1987.
27. Gallet, G., Hutzler, B., and J.-P. Riu. «Analysis of the switching impulse strength of phase-to-phase air gaps.» «IEEE Transactions on Power Apparatus and Systems», PAS-97(2): 485–494, 1978.
28. Hannakam, L. «Calculation of the transient current distribution in cylindrical massive conductor.» «ETZ-A», 91: 50–54, 1970. [In German.]
29. Hileman, A.R. «Insulation Coordination». New York: Marcel Dekker Inc., 1999.
30. Hyltén-Cavallius, N.R. «Impulse tests and measuring errors». ASEA Publications, 7551 E/ASEA Reg. 0977, 1957.
31. IEC Standard 60052. «Recommendations for Voltage Measurements by means of Sphere Gaps (One Sphere Earthed)». IEC, Geneva, Switzerland, 1960.
32. IEC Standard 60060-1. «High Voltage Test Techniques—Part 1: General Definitions and Test Requirements». IEC, Geneva, Switzerland, 1989.
33. IEC Standard 60060-2. «High Voltage Test Techniques—Part 2: Measuring Systems», 2nd edn. IEC, Geneva, Switzerland, 1994.
34. IEC Standard 60270. «Partial Discharge Measurement», 3rd edn. IEC, Geneva, Switzerland, 2000.
35. Kuffel, E., Zaengl, W.S., and J. Kuffel. «High Voltage Engineering—Fundamentals», 2nd edn. Pergamon Press, Oxford, 2000.
36. Lemke, E. «A critical review of partial discharge models.» «IEEE Electrical Insulation Magazine», 28(6): 11, 2012.
37. Malewski, R. «Digital techniques in high voltage measurements.» «IEEE Transactions», PAS-99: 4508, 1982.
38. Malewski, R., and N.R. Hyltén-Cavallius. «A low voltage arm for EHV impulse divider.» «IEEE Transactions», PAS-93: 1797, 1974.
39. Malewski, R., Nguyen, T.C., Feser, K., and N. Hyltén-Cavallius. «Elimination of the skin effect error in heavy current shunts.» «IEEE Transactions», PAS-100(3): 1333–1340, 1981.
40. Maruvada, P.S., and W. Janischewskyj. «Electrostatic field of a system of parallel cylindrical conductors.» «IEEE Transactions on Power Apparatus and Systems», 88: 1069, 1969.
41. Miyake, K., Watanabe, Y., and E. Ohsaki. «Effects of parameters on the phase-to-phase flashover characteristics of UHV transmission lines.» «IEEE Transactions on Power Delivery», PWRD-2(4): 1285–1291, 1987.
42. Peterson, O. «A self-balancing high-voltage capacitance bridge.» «IEEE Transactions», IM-13: 216–224, 1964.
43. Rizk, F.A.M. «Arc instability and time-constant in air-blast circuit-breakers.» «CIGRE», Paper No. 107, 1964.
44. Schwab, A., and J. Pagel. «Precision capacitive voltage divider for impulse voltage measurements.» «IEEE Transactions», PAS-91: 2376–2382, 1972.
45. Train, D., and P.E. Vohl. «Determination of ratio characteristics of cascade connected transformers.» «IEEE Transactions», PAS-95: 1911, 1976.

46. Zaengl, W.S. «A new voltage divider for fast impulse voltages.» «Bulletin SEV», 56: 232–240, 1965.
47. Zaengl, W.S. «High voltage measuring techniques», in «High Voltage Engineering», Springer-Verlag, 1986.